Sheffield Hallam University

A Sheffield Hallam University thesis

2/4
16:55
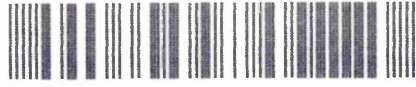
ProQuest Number: 10700880

ProQuest 10700880

HARDENABILITY, TRANSFORMATION AND PRECIPITATION EFFECTS

IN VANADIUM STEELS.

BY

GEOFFREY KEITH PLATTS BSc.

A THESIS SUBMITTED TO THE COUNCIL FOR NATIONAL ACADEMIC
AWARDS IN PARTIAL FULFILMENT FOR THE DEGREE OF

DOCTOR OF PHILOSOPHY

SPONSORING ESTABLISHMENT: COLLABORATING ESTABLISHMENT:

DEPARTMENT OF METALS   UNION CARBIDE CORPORATION

& MATERIALS ENGINEERING   PITTSBURGH

SHEFFIELD CITY POLYTECHNIC   U.S.A.

POND STREET

SHEFFIELD S1 1WB

JULY 1988.

DEDICATION

This thesis is dedicated to my wife, Julie, and my sons,
Michael and Andrew, for without their patience and support
the completion of this project would not have been
possible.

PREFACE

HARDENABILITY, TRANSFORMATION AND PRECIPITATION EFFECTS

IN VANADIUM STEELS.

The work reported in this thesis is based on an

investigation performed at the Sheffield City Polytechnic

during the period April 1981 to June 1984, under the

supervision of Dr. F.B. Pickering and Mr. G. Butterworth.

 The following lecture series, of the MSc course at the

Sheffield City Polytechnic, were attended:-

1. Heat Treatment and Transformation,

2. High Strength Steels,

3. Secondary Steel Making,

4. Numerical Analysis and Computer Programming.

The results presented in this thesis are to the best of my

knowledge, original except where reference is made to

other authors, and no part of it has been submitted for a

degree at any other University or College.

G.K. PLATTS.

(ii)

ACKNOWLEDGEMENTS

HARDENABILITY, TRANSFORMATION AND PRECIPITATION EFFECTS IN VANADIUM STEELS.

GEOFFREY KEITH PLATTS BSc.

ABSTRACT

Recent work has highlighted unusual effects of vanadium when used in conjunction with other microalloying additions on the hardenability of steels. Positive and negative synergistic effects have been observed, but studies into the mechanisms have been limited. To investigate the effects, vanadium interactions with aluminium, molybdenum, niobium and titanium were studied in low (0.1%) and medium (0.4%) carbon steels, containing normal (0.008%) and enhanced (0.020%) nitrogen. Utilising standard jominy test conditions of 950°C for one hour resulted in classical hardenability responses being obtained, where increasing quantities of microalloying additions in solution increase the hardenability. However, when the jominy test conditions were varied unexpected effects were observed. Extending the austenitising time to eight hours showed that the hardenability was dependent upon kinetic effects such as the rate of solution of the alloy carbides/nitrides and the rate at which the microalloying elements in solution segregated to the austenite grain boundaries. It was also observed that if the austenitising temperature was increased to 1200°C a decrease in hardenability could be obtained by increasing the quantity of vanadium, niobium or titanium. These effects were attributed to a combination of thermal dispersion of microalloying clusters from the austenite grain boundaries, preferrential transformation on large alloy carbides/nitrides and migration of the austenite grain boundaries. Therefore it was considered inadequate to explain hardenablity solely in terms of the carbon concentration, austenite grain size and amount of other alloying elements present. Additional factors such as cluster formation, grain boundary pinning etc., were identified and applied to the results to successfully explain the effects of the alloy interactions on hardenability.

Recent studies on vanadium alloyed pearlitic steels showed significant increases in strength could be obtained by precipitation within the pearlitic ferrite. Mechanical property investigations of two steels indicated that a maximum precipitation effect was obtained at an isothermal transformation temperature of 600°C.

CONTENTS

(vii)

(viii)

(ix)

1. INTRODUCTION

Vanadium carbide and nitride have very different solubilities in both austenite and ferrite and it has often been suggested that both phases may form either in the austenite or by an interphase precipitation mechanism during the austenite-ferrite transformation, depending upon the composition of the steel, the austenitising conditions, the thermo-mechanical processing and the cooling rate. It is also known that with a sufficiently rapid rate of cooling, interphase precipitation can be prevented and subsequent precipitation can then occur in the ferrite during a tempering treatment. A recent thermodynamic analysis of vanadium-carbon-nitrogen interactions has indicated that (1):

(i) theoretically the vanadium nitride is precipitated initially in the austenite but that as the nitrogen is consumed, the precipitate moves towards vanadium carbide.

(ii) due to carbon enrichment at the austenite-ferrite interface during the transformation, the interphase precipitate is predominantly vanadium carbide.

In addition it has been shown that precipitation directly from the ferrite after transformation is complete, is largely controlled by the

carbon (and/or nitrogen) dissolved in the ferrite (2).

Whether different rates of cooling are necessary for the suppression of interphase precipitation in steels of different carbon and nitrogen contents, because of the very different supersaturation for carbide and nitride, is not known. However, recent work has shown that a strengthening effect produced on continuous cooling occurs at slower cooling rates in high nitrogen steels compared with low nitrogen steels (3). The precise interpretation of this effect is not known, but could be due to the lower solubility of nitride giving a smaller supersaturation and thus a lower driving force for precipitation.

The major precipitation processes involved in vanadium steels may be briefly summarised as:-

(i) Precipitation from the austenite prior to transformation which is accelerated by strain inducement as in controlled rolling processes. This does not itself cause precipitation strengthening, and moreover decreases the amount of strengthening produced by precipitation during or after subsequent transformation of the austenite. Vanadium carbide precipitates at

2

somewhat lower temperatures than does vanadium nitride under these conditions (2).

(ii)   Precipitation at the austenite-ferrite interface during transformation, which can occur in two main forms:-

    (a)   Fibrous precipitation, which predominates when the transformation process occurs relatively slowly and at high transformation temperatures. The precipitates occur as fibres to give a structure similar to that of pearlite. However, for vanadium alloyed H.S.L.A. steels this mechanism is not very dominant.

    (b)   Interphase precipitation, which occurs as a banded dispersion due to the repeated nucleation at the low energy stepped austenite/ferrite transformation front. The banded structure closely follows the direction of the interface and the distances between the bands are determined by the successive positions occupied by the ferrite-austenite

3

interface.

(iii) Precipitation from supersaturated ferrite is produced when no precipitation occurs during the austenite to ferrite transformation due to the very rapid cooling rate. It is not until the material is tempered that precipitation is observed.

The exact nature and type of precipitate produced will substantially alter the mechanical properties of the material. For example, precipitation strengthening increases as the transformation temperature decreases because at higher temperatures the precipitates produced gradually coarsen during cooling and therefore become less effective as a strengthening mechanism. The depression of the transformation temperature, obtained by increasing the cooling rate or alloy concentration, would produce a finer and more effective precipitate dispersion, but the effects of the different types of precipitation on the toughness are at present not clearly established.

It has often been suggested that, because interphase precipitation occurs as planar arrays on the austenite-ferrite interface during transformation, it is detrimental to toughness and ductility. This seems to be

4

so, because when there is heavy interphase precipitation, the Impact Transition Temperature is high, but this might be due to both the large volume fraction of precipitate causing marked precipitation strengthening and to a relatively coarse ferrite grain size consequent upon the coarse austenite grain size produced by the high austenitising temperature which is usually employed to ensure complete solution of the vanadium carbides and nitrides. For example, a precipitation strengthening of 300 MPa would increase the Impact Transition Temperature by more than 100°C (4). On the other hand, when the vanadium carbide or nitride precipitates in the ferrite from supersaturated solid solution, there is a belief that the toughness is higher. Recent published work throws some doubt on this (5), but a careful analysis indicated that the interpretation of the results may be in doubt. Other recent work (6) also indicated that vanadium carbonitride precipitates on ferrite grain boundaries whereas vanadium nitride does not. The presence of vanadium carbonitride on the grain boundaries is reported to embrittle the steel, and this effect is worthy of further investigation. The conditions under which the different precipitate morphologies are produced require to be investigated, and in particular the effects of different precipitate morphologies require to be studied in terms of toughness effects.

Recent work has shown some unusual effects of vanadium in conjunction with other microalloying additions on the hardenability of steel. Synergistic interactions between microalloying elements have been shown to occur (7)(8). Utilisation of the positive alloy interactions could produce more efficient and economical use of the microalloying additions in the heat treated, quenched and tempered, engineering steels. However, not all the interactions are advantageous. Therefore, an extensive knowledge of the mechanisms involved is essential. Investigations into these mechanisms have been very limited due to their complexity. It has been shown that a 2 to 1 ratio of molybdenum to vanadium is required to produce an equivalent hardenability level (8)(9). If a similar effect is observed at the lower carbon level and no temper embrittlement problems are encountered the replacement of molybdenum by vanadium in many applications could become economically advantageous.

In pearlitic, higher carbon steels, which are used for forgings and railway products, vanadium is currently being used with advantage (10) to (15). Recent studies on these higher carbon steels have shown that vanadium carbide particles precipitate within the pearlitic ferrite. When this occurs it is accompanied by a large increase in the strength of the material. It has been suggested that the precipitation could be similar to the

interphase precipitation process observed in the low carbon alloys. The mechanisms of these precipitation effects are, however, little understood and require considerable study if effective use is to be made of them in industrially important steels.

In view of the questions posed in the above introduction, the aims of the present work can be summarised under two headings:-

(i)   Hardenability

To study how certain microalloying elements synergistically interact with vanadium in relation to hardenability. The areas where investigations will be performed are:-

(a)   the effects of vanadium interactions with Molybdenum, Niobium, Titanium and Aluminium, in alloys containing normal (0.008%) and enhanced (0.20%) nitrogen contents,

(b)   the possibility of replacing molybdenum by vanadium in low carbon alloys.

(ii)   Pearlitic Structures

To investigate the precipitation of carbides within the pearlitic ferrite and their effect upon the strength and toughness of the alloy.

2. LITERATURE REVIEW

2.1 General Introduction

Vanadium was first identified as a new element by Sefstrom, in 1831 from a black powder which formed on certain irons when treated with hydrochloric acid. However, the significance of the discovery was not appreciated until the turn of the century when Arnold, working at the University of Sheffield, proved that the addition of vanadium to tool steels improved the resistance to softening during high speed machining. At the same time, Henry Ford, in America, observed that the performances of crankshafts manufactured from Swedish iron were superior to those produced from irons of a different source. This improvement was directly related to the residual amounts of vanadium in the Swedish iron. These early applications were the genesis of today's vanadium industry.

Of the vanadium produced, the steel industry is substantially the major consumer with the remainder going to the titanium and chemical industries. In the steel industry over 50% of the vanadium used is added to carbon or High Strength Low Alloy steels as a microalloying addition, with vanadium contents of approximately 0.1%. Consequently, the low levels of alloying element present and the large quantity of vanadium used indicate the very

8

large tonnage of steel in this class. A further 25% of
the vanadium is used in heat-treatable steels, where the
alloy additions are required to increase the
hardenability and resistance to tempering, while the
remainder is used in tool and creep resistant steels.

The growth of H.S.L.A. steels is the result of increased
energy costs, mineral shortages and escalating prices of
many alloying additions. Therefore, the trends are
towards cost effective, high strength steels where weight
reductions are possible. The use of microalloying
elements in H.S.L.A. steels can produce significantly
higher strength levels than are possible from hot rolled
carbon steels. Consequently, the higher cost of the
microalloyed steel can be more than offset by the
possible reduction in the weight of the component. It
is, therefore, imperative that the optimum properties of
the H.S.L.A. steel are obtained. This can only be
achieved when the mechanisms by which vanadium influences
the transformations, hardenability and precipitation
processes are fully understood.

2.2   Phase Transformations

2.2.1 Phase Transformations in Plain Carbon Steels[16][17]

In the study of steels the iron-iron carbide equilibrium
diagram is very important since many of its basic
features are observed in even the most complex steels.

The iron-iron carbide diagram represents the metastable
system where Fe_3C (Cementite) forms in preference to
graphite in an iron-carbon system, due to the more
favourable kinetics of nucleation and growth of Fe_3C
which exist under normal cooling conditions. The most
dominant features of the diagram are the transformation
from austenite (γ) to ferrite (α), or cementite, and the
eutectoid transformation to pearlite.

In hypoeutectoid steels with below 0.8%C, the eutectoid
composition, austenite (γ), which is the high temperature
form of iron, will transform to ferrite (α), the low
temperature form of iron, during cooling. The
temperature at which this occurs is dependent upon the
carbon content of the steel, being $910°C$ for pure iron
and $723°C$ at 0.8%C. The austenite, which has a face-
centred cubic structure, can accomodate a far greater
quantity of carbon than the ferrite, with a body-centred
cubic structure. Therefore, upon cooling, carbon must be
rejected from the ferrite and accomodated by the
remaining austenite. Consequently, the remaining
austenite is continually enriched in carbon until the
eutectoid composition, 0.8%C, and the eutectoid
temperature, $723°C$, are reached, whereupon the remaining
austenite transforms to pearlite, a structure comprising
alternate lamellae of ferrite and cementite.

In hypereutectoid steels, with carbon contents in the range 0.8 to 2.06%C, cooling from the austenitic region causes cementite to form preferentially and depletes the austenite of carbon until once again eutectoid conditions are attained and the pearlitic transformation occurs.

The alloys which are to be investigated are hypoeutectoid steels with carbon contents ranging from 0.1 to 0.8% and therefore essentially consist, during slow cooling, of ferrite-pearlite structures. However, rapid cooling of hypoeutectoid steels can depress the transformation process to progressively lower temperatures and can result in the replacement of the ferrite-pearlite structures by non-equilibrium structures namely, martensite and bainite. These structures become especially significant in the consideration of hardenability studies and will therefore be dealt with in more detail along with the ferrite and pearlite structures in later sections.

2.2.1.1 The Austenite to Ferrite Transformation (18,19,20)

As previously mentioned, ferrite forms between 910°C and 723°C, under equilibrium conditions, in plain carbon steels, but can occur at much lower temperatures under non-equilibrium or continuous cooling conditions. Therefore, the exact nature of the ferrite morphology depends upon the temperature at which the transformation takes place.

(i)   <u>Grain Boundary Ferrite</u>

At high transformation temperatures the ferrite
nucleates at prior austenite grain boundaries
since they tend to be energetically favourable
nucleation sites and also paths for easy carbon
diffusion. The ferrite nucleates with a semi-
coherent interface with one parent austenite grain
and a non-coherent interface with the other. The
semi-coherent interface exhibits a Kurdjumov-Sachs
orientation relationship (21) with the austenite
grain, namely:-

$$\{111\}_\gamma \ /\!/ \ \{110\}_\alpha$$

$$\langle 110 \rangle_\gamma \ /\!/ \ \langle 111 \rangle_\alpha$$

Within a semi-coherent interface strain is produced, due
to the difference in lattice parameters of the two
phases, which is accomodated by an array of dislocations
at the interface. Consequently, the dislocation density
of the interface increases as the mismatch of the two
phases increases. Semi-coherent interfaces are generally
low energy boundaries and thus exhibit low mobility.
However, the incoherent interface which has a random
orientation relationship with the contiguous austenite is
a high energy boundary and will thus easily move under
thermal activation. The movement of the interface
proceeds normal to the boundary and forms polygonal

12

grains of ferrite at austenite grain boundaries. Under certain conditions the interfaces can develop growth facets where there is anisotropy of growth.

As the temperature of transformation is lowered the mobility of the incoherent interfaces decreases due to the reduction in the thermal energy. Consequently, the growth from the coherent interfaces become more dominant. This type of growth occurs as the result of the lateral movement of small non-coherent steps along the coherent interface. Therefore, growth of the ferrite proceeds, at these lower temperatures, in a direction normal to the coherent interface and into the austenite grain with which it has the Kurdjumov-Sachs orientation relationship, forming a saw-tooth ferrite morphology.

(ii)   Widmanstatten Ferrite

Widmanstatten ferrite forms at relatively low transformation temperatures where there is a high supersaturation of carbon and a high driving force for transformation. The characteristic laths, or plates, grow from either "clean" prior austenite grain boundaries or from pre-existing grain boundary ferrite. The lateral growth at the ferrite laths occurs by the movement of incoherent ledges along the low energy coherent interfaces. Therefore, the laths tend to obey a Kurdjumov-Sachs orientation relationship with the austenite

13

grain in which they grow, the broad faces being the habit planes.

(iii) Intragranular Ferrite

Intragranular ferrite occurs within the austenite grains either as equiaxed or lath type structures depending on the transformation temperature, the former structure being produced at the higher transformation temperatures and largely nucleating heterogeneously on inclusions or other second phase particles. The latter, or lath type ferrite, is basically the same as Widmanstatten ferrite, possibly nucleating from the activation of dislocation type nucleii.

2.2.1.2. The Austenite to Pearlite Transformation

Pearlite is formed by the co-precipitation of cementite and ferrite from austenite containing 0.8%C and transforming at a temperature below 723°C. In plain carbon and alloy steels there are two possible mechanisms of pearlite formation (22)(23).

(i) Direct transformation from austenite.

(ii) Branching of pro-eutectoid phase.

The former mechanism involves a duplex nucleus where both ferrite and cementite must be present (22). The nucleation generally occurs at the prior austenite grain boundaries with both the ferrite and the cementite forming a semi-coherent interface with one of the

adjoining austenite grains and a non-coherent interface
with the other. The semi-coherent interface of the
ferrite lamella obeys a Kurdjumov-Sachs orientation
relationship, with the austenite grain into which it is
not growing, while the cementite obeys a Pitsch
orientation relationship (24) with the austenite,
namely:-

$$(100)_{Fe_3C} \,/\!/\, (1\bar{1}1)_\gamma$$

$$(010)_{Fe_3C} \,/\!/\, (110)_\gamma$$

$$(001)_{Fe_3C} \,/\!/\, (\bar{1}12)_\gamma$$

Therefore, the combination of the two relationships give
a mutual orientation relationship between the ferrite and
the cementite. This is the Pitsch/Petch orientation
relationship (25):-

$$(001)_{Fe_3C} \,/\!/\, (215)_\alpha$$

$$[100]_{Fe_3C} \quad 2 \cdot 6° \,[311]_\alpha$$

$$[010]_{Fe_3C} \quad 2 \cdot 6° \,[131]_\alpha$$

NOTE :- THERE IS A SLIGHT VARIATION
OF 2·6° IN THE α/Fe_3C
DIRECTIONS .

The second mechanism results from the branching of the
pro-eutectoid phase (23). In hypereutectoid steels the
associated pearlite contains cementite which has the same
orientation relationship as the grain boundary film which
is the Pitsch relationship. Consequently, the pearlitic
ferrite has no relationship with the austenite but
conforms to a Bagaryatskii orientation relationship (26)

with the pearlitic cementite, i.e.

$$(100)_{Fe_3C} \,/\!/\, (0\bar{1}1)_\alpha$$

$$(010)_{Fe_3C} \,/\!/\, (1\bar{1}\bar{1})_\alpha$$

$$(001)_{Fe_3C} \,/\!/\, (211)_\alpha$$

Samuel et al (27) observed that branching of pro-eutectoid ferrite produced pearlite colonies which obeyed the Bagaryatskii orientation relationship despite the pro-eutectoid ferrite conforming to a Kurdjumov-Sachs orientation relationship with the austenite.

Once nucleation has occurred there is localised diffusion in the surrounding austenite matrix either towards the cementite phase creating a low carbon matrix allowing further ferrite nucleation, or away from the ferrite causing a build up of carbon in the matrix resulting in the nucleation of cementite. In this way it is possible to obtain side by side nucleation of α and Fe_3C.

Pearlitic growth occurs edge-wise into the austenite grain with the incoherent interface. However, for growth to occur carbon must diffuse away from in front of the ferritic phase and concentrate in front of the growing cementite interface. The diffusion could occur in the austenite, in the ferrite, or along the interface between the pearlite and the austenite. However, bulk diffusion in austenite would not occur fast enough to account for the high growth rates of pearlite observed. Diffusion through the ferrite could explain the growth rates

16

observed but it would cause barrelling of the carbide
lamellae. Therefore, it is considered that the carbon
diffuses along the interface between the pearlite and
austenite and the general consensus seems to support this
view.

The pearlitic lamellae grow in colonies until they
impinge with other pearlite colonies. The lamellae
within a single colony are approximately parallel but
they may branch. However, different colonies exhibit
different growth directions and therefore cause
variations in the direction of the pearlitic lamellae.

The spacing of the pearlite lamellae is very sensitive to
the change in transformation temperature (28). At lower
transformation temperatures there is slower carbon
diffusion which results in a smaller interlamellar
spacing, i.e.

$$S \propto \frac{1}{T_e - T} \qquad - - - - - - - (1).$$

where:-   S = interlamellar spacing

Te = equilibrium eutectoid temperature

T = transformation temperature

In steels there is a definite relationship between the
thickness of the ferrite and cementite lamellae, where:-

$$t = \frac{S}{\left(\dfrac{f_p}{0.15(\%C)} - 1\right)} \qquad - - - - -(2).$$

17

where:- 　t = thickness of cementite lamellae

S = interlamellar spacing

fp = fraction of pearlite

%C = carbon content of steel

In a eutectoid steel the relationship between thickness of the cementite and the interparticle spacing is approximately 1 to 7. For hypoeutectoid steels it is possible to obtain 100% pearlite structures at the lower transformation temperatures but the pearlite is then diluted, resulting in a thinner cementite lamella for a given interlamellar spacing. Gladman et al, defined a dilution factor which could be incorporated into equation 2 (28), where:-

$$D = \frac{0.8 \times f_p}{(\% C)} \quad \text{------} \quad (3).$$

and

$$t = \frac{0.12 S}{(D - 0.12)} \quad \text{------} \quad (4).$$

The morphology of pearlite is a very important parameter since the inter-lamellar spacing, colony size and prior austenite grain size have significant effects on the mechanical properties of pearlitic steels.

2.2.1.3　The Austenite to Martensite Transformation
(18) (20) (29) (30)

Martensite is formed at very low transformation

18

temperatures where the cooling rate is sufficient to suppress the higher transformation temperature processes of ferrite, pearlite and bainite. The transformation reaction occurs by a diffusionless shear mechanism forming a body-centred tetragonal structure. The formation of martensite is largely an athermal transformation in that the extent of the transformation is independent of the time at temperature. This is the result of the very rapid rate of reaction; the rate of movement of the martensite/austenite interface can reach the speed of sound. Lowering the temperature of transformation does not result in the existing martensite growing but causes new martensite laths to nucleate. The morphology of the martensite nucleated is dependent upon the carbon content of the alloy, being lath like in low carbon alloys and lenticular in higher carbon alloys.

(i)   Lath Martensite (31)

Lath martensite occurs in plain carbon steels with up to $\simeq$0.4% carbon. The laths tend to form in sheaves due to sympathetic nucleation and have low angle boundaries between each lath. However, they form high angle boundaries on contact with other martensite sheaves. The long straight interfaces of the laths are semi-coherent and conform to the habit plane of a Kurdjumov-Sachs type relationship, adopting the $\{111\}_\gamma$ habit plane. The

internal structure of the laths consists of a high density of dislocations which form tangled arrays but can, if the transformation temperature is high enough, form dislocation substructures. The structure of the lath martensite is only slightly tetragonal and is often regarded as body-centred cubic.

(ii)   Lenticular Martensite (32)

This type of martensitic structure appears as individual lens-shaped plates rather than lath type sheaves. The plates often touch at their tips in a zig-zag array, resulting from a burst phenomenon. In the carbon range 0.5 to 1.4%C the martensite obeys the Kurdjumov-Sachs relationship, adopting the $\{225\}_\gamma$ habit plane. It is the adoption of the several variants of this habit plane, within a small volume, automatically nucleated, that results in the burst phenomenon. Internally the plates normally contain micro-twins which form due to the lower martensite start (M_s) temperature caused by the increased carbon content. Lenticular martensite is truly a body-centred tetragonal structure due to the martensite inheriting all the carbon from the austenite during the transformation. The exact nature of the transformation is complex and has been studied by various authors (31-33).

20

In steels with greater than 1.4% carbon the orientation
relationship between the austenite and martensite changes
from the Kurdjumov-Sachs to the Nishiyama-Wassermann
relationship and the $\{225\}_\gamma$ habit plane changes to the $\{259\}_\gamma$
plane. The Nishiyama (34)-Wassermann relationship (35)
is:-

$$\{111\}_\gamma // \{110\}_{\alpha'}$$

$$\langle 112 \rangle_\gamma // \langle 011 \rangle_{\alpha'}$$

The martensite remains lenticular, forming by the burst
mechanism and is generally accompanied by an audible
click. However, the plates tend to be far more heavily
twinned in nature than at lower carbon concentrations.

2.2.1.4   The Austenite to Bainite Transformation

Bainite is formed by the transformation of austenite at a
temperature between that for the ferrite-pearlite
transformation and the martensite transformation. The
transformation process is essentially a shear
transformation (36) but is also dependent upon the
diffusion of carbon. The bainite transformation is
generally regarded as a duplex transformation process,
similar to pearlite, in that the resulting microstructure
contains ferrite and cementite. However, two different

bainite structures have been observed:-

(i)   Upper bainite

(ii)   Lower bainite

(i)   Upper Bainite

Upper bainite tends to occur at the higher
temperatures in the bainitic transformation range
and forms as elongated ferrite laths with
cementite forming between the laths. The
formation of the ferrite laths is the result of a
shear transformation similar to that observed in
martensitic structures (36). The laths form in
packets due to sympathetic nucleation, which are
only slightly misoriented and therefore form low
angle boundaries. However, a number of different
packets may be nucleated within the same austenite
grain resulting in high angle boundaries between
the different packets.

It is considered that the bainitic carbide results
from the partitioning of carbon from the bainitic
ferrite to the austenite, during the
transformation causing a build up of carbon at the
austenite/ferrite interface. Consequently a stage
is reached where the cementite precipitates
directly from the austenite.

The ferritic laths have been shown to be stepped

along their broad faces, similar to Widmanstatten ferrite. It would therefore be expected that the interfaces would be semi-coherent and thus have an orientation relationship with the austenite from which the bainitic ferrite formed. It is found that within the accuracy of electron diffraction, upper bainite obeys either the Kurdjumov-Sachs or the Nishiyama-Wassermann orientation relationship.

The orientation relationship between austenite and cementite has been shown to conform to the Pitsch relationship. Therefore, it would be expected that an orientation relationship between the bainitic ferrite and cementite would exist. However, no unique relationship has been observed.

(ii)   Lower Bainite

Lower bainite tends to form at lower transformation temperatures than experienced in the formation of upper bainite. Once again the bainitic ferrite forms as laths by a shear process. However, because of the lower transformation temperature the laths are more frequently nucleated within the austenite grains than for upper bainite. The sympathetic nucleation observed in upper bainite is not so apparent in the lower bainite structure.

The bainitic carbide in lower bainite does not precipitate at the ferrite lath boundaries but rather within the laths. The carbides form as parallel arrays of plates which adopt a specific angle of approximately 55° to the axis of the ferrite laths. There has been two alternative theories proposed for the occurrence of this carbide morphology. The first theory involves precipitation of cementite from supersaturated (37) ferrite while the second involves precipitation at the austenite/bainitic ferrite interface, during the transformation, by an interphase precipitation mechanism (38).

The former mechanism is due to the lower diffusion rate of carbon causing supersaturation of the ferrite laths. Consequently, a high driving force is required for the ferritic growth to continue and so the transformation process relies upon the precipitation of carbides within the laths to lower the supersaturation. However, this type of mechanism does not explain the unique orientation at which the carbides form within the ferrite laths.

The interphase precipitation mechanism involves the precipitation of the cementite at small ledges

24

which have been observed on the broad faces of the ferrite laths. It has been suggested that the carbides obey a Bagaryatskii orientation relationship with the bainitic ferrite, which is the relationship generally found in the tempering of martensite. However, in contrast to tempered martensite, the carbides in lower bainite exhibit only one variant of the relationship such that the precipitates form parallel arrays at one angle of 55° to the axis of the banite laths. The occurrence of the single variant strongly suggests a ledge type mechanism at the austenite/ferrite interface (38). However, Ohmori (39) suggested that the precipitates obeyed the Isaichev relationship, namely:-

$$(010)_{Fe_3C} \,/\!/ \, (1\bar{1}\bar{1})_{\alpha}$$
$$(103)_{Fe_3C} \,/\!/ \, (101)_{\alpha}$$

which is the relationship produced when cementite is formed on the ferrite surface, once again inferring a ledge type mechanism.

However, Bhadeshia (40) examined the austenite/ferrite interface and found that contrary to the expectations of interphase precipitation theory, the cementite was essentially confined to the ferrite, suggesting cementite nucleation within supersaturated ferrite. Therefore, it is very clear that much further work is required before the

exact nature of the bainite transformations can be conclusively determined.

2.2.2   The Effect of Alloying Additions
        on Phase Transformations

The addition of alloying elements to steels greatly influences their mechanical properties by altering the conditions of the decomposition of austenite. The normal alloying elements can be classified into one of two distinct groups. The first group are ferrite stabilisers, consisting of such elements as vanadium, chromium, titanium, niobium, molybdenum etc., which encourage the formation of the body-centred cubic ferrite structure and therefore reduce the size of the austenite phase field in the binary equilibrium diagram.

The second group are austenite stabilisers and consist of such elements as manganese and nickel. Austenite stabilisers extend the austenite phase field and thus depress the decomposition of austenite to lower transformation temperatures under equilibrium conditions. It is possible that if a sufficient amount of alloying addition is present austenite can remain untransformed even at room temperature.

All alloying elements except cobalt decrease the rate of

austenite decomposition irrespective of the final
transformed structure.

In the case of the ferrite transformation two growth
mechanisms have been observed for alloyed carbon steels.
The first mechanism occurs when the alloying elements
partition between the ferrite and the austenite phases.
When this situation arises the rate of reaction is
retarded due to the reaction being dependent upon the
rate of diffusion of the alloying element in austenite.
The second and more common type of growth occurs when
there is no partitioning of the alloying elements.
However, the growth of the ferrite is still retarded.
Kinsman and Aaronson (41) proposed that the retardation
was caused by the interface collecting atoms of the
alloying elements during the transformation, resulting in
an impurity drag. The movement of the interface would
then be dependent upon the diffusivity of the interfacial
solute atoms.

Also two modes of growth have been observed for the
austenite to pearlite transformation. The first type of
growth occurs when the alloying additions partition
between the pearlitic ferrite and cementite. The
alloying elements which partition to the cementite tend
to be carbide stabilisers which are often also ferrite
stabilisers, while the elements which partition to the
ferrite tend to be non-carbide formers and often are

27

austenite stabilisers. At high transformation temperatures the driving force for transformation is small but can be increased by the partitioning of the alloying elements. Consequently, the transformation becomes dependent upon the diffusivity of the alloying elements. However, at lower transformation temperatures the driving force for transformation is higher so that partitioning is not required for the reaction to proceed. Consequently, there is a temperature at which the reaction will just proceed without the aid of partitioning of alloying elements. This is called the 'Nil Partitioning Temperature'. The growth of pearlite in this case is probably controlled by the carbon diffusion in austenite. However, it must be remembered that the diffusivity of carbon will be reduced due to the presence of the alloying additions.

The effect of alloying elements upon the interlamellar spacing of pearlite under continuous cooling conditions depends upon its effect on the transformation temperature. Elements which raise the transformation temperature can, under specific conditions increase the interlamellar spacing of pearlite due to the higher diffusion rates which are possible. Conversely, elements that decrease the transformation temperature tend to decrease the interlamellar spacing. However, under these conditions the intrinsic nature of the alloying elements are not exhibited because when using isothermal

transformation conditions at a constant under-cooling, all the alloying elements with the exception of cobalt, increase the interlamellar spacing. The increase under these conditions results from the alloying elements decreasing the growth rate of pearlite, and it has been shown that the pearlite growth rate is inversely proportional to the interlamellar spacing.

The addition of alloying elements, such as V, Nb, Ti, Al, etc., also influence the thickness of the pearlitic cementite lamellae, t, since as previously mentioned in section 2.2.1.2, a depression of the transformation temperature will produce a 'dilute' pearlite structure where the cementite lamella is thinner.

Alloy additions tend to refine the pearlite colony size despite the retardation of both the nucleation and growth rates. Although fewer pearlite colonies form they grow more slowly which allows further colonies to nucleate and thus refine the overall pearlite structure.

It has been shown that the addition of strong carbide-forming elements can cause partial or complete replacement of cementite by the appropriate alloy carbide, for example, vanadium (42), molybdenum (43), niobium (44) etc. The resulting microstructures are dominated by the austenite to ferrite transformation and

29

the precipitation of alloy carbides. Consequently, to
obtain pearlitic structures, higher carbon concentrations
are required in the presence of micro-alloying additions.

The effect of alloying elements upon the martensitic
transformation, with the exception of cobalt, is to
decrease the martensite start temperature (M_s). The
relative effects of some alloying elements are indicated
in the following empirical relationship due to Andrews
(45).

$$M_s(^\circ C) = 539 - 423(\% \, C) - 30 \cdot 4(\% Mn) - 17 \cdot 7(\% \, Ni)$$
$$- 12 \cdot 1 (\% \, Cr) - 7 \cdot 5 (\% \, Mo) - - - - - - - - (5).$$

It should be noted from the above relationship the very
high depression of the M_s by carbon relative to the other
alloying additions. It is generally considered that the
depression of the M_s temperature is caused by the solute
atoms increasing the strain energy of the system and
therefore requiring a higher driving force before the
transformation will proceed.

Finally, the effect of alloy additions on the bainite
transformation is to depress the reaction to lower
transformation temperatures and to longer time. The
temperature below which bainite is formed, B_s, can be
described in terms of alloy content by empirical linear
equations (46).

$$B_s(^\circ C) = 830 - 270(\% \, C) - 90(\% Mn) - 37(\% Ni) - 70(\% \, Cr)$$
$$- 83(\% \, Mo) - - - - - - - - - (6).$$

30

However, since the alloying elements also influence the ferrite/pearlite transformations there tends to be a greater separation of the transformation C-curves. Consequently, by selection of the appropriate alloying addition, the ferrite-pearlite reaction could be delayed to such an extent that fully bainitic steels could be obtained over a wide range of cooling rates.

2.2.3   The Effect of Vanadium on the Phase Transformations

(a)   Effect of Vanadium on A_1 and A_3 temperatures

The A_1 temperature defines the maximum temperature at which pearlite can form, and despite the fact that vanadium is a powerful ferrite former, recent data (47) indicates that it has no effect on the A_1. This is surprising but could be due to there being insufficient variation in vanadium content, in the published results, for a trend to be established, or due to the fact that up to about 0.2% vanadium in pure Fe-V alloys there is little change, or even a slight depression in the $\alpha \rightleftharpoons \gamma$ transformation temperature (48). In this latter respect, vanadium is not unlike chromium in showing a minimum temperature in the gamma loop, and if it is inferred that on this basis vanadium would be expected to raise A_1 in a manner similar to chromium, then it would be suggested that the increase in A_1 temperature per unit weight percent

31

vanadium would be $\simeq 50^{\circ}$C.

The A_3 temperature defines the maximum temperature for pro-eutectoid ferrite formation, and vanadium increases A_3 by 104°C per weight percent (47). This means that pro-eutectoid ferrite can form at higher temperatures in vanadium steels than in vanadium free steels. This has a bearing on the continuous cooling transformation characteristics, in that at the slower cooling rates, vanadium may actually increase the transformation temperature. This effect may be misinterpreted as indicating that vanadium actually decreases the hardenability, when in actual terms of martensitic hardenability, the reverse is the case.

(b)   Isothermal Transformation Characteristics

Despite there being T.T.T. diagrams for many steels containing vanadium, there seems to have been little or no systematic research into the effect of vanadium on the T.T.T. diagram. Most of the data refers to either the higher carbon tool steels, or to steels containing appreciable quantities of other alloying elements such as chromium and molybdenum. Moreover, variations in the austenite grain size and/or austenitising temperature renders comparisons almost impossible.

Nevertheless, certain features of the T.T.T.
diagram are able to be defined:-

(i)   For a 0.12%C, 1.6%Mn, 0.010%N_2 steel,
            the effect of 0.13%V on the 0% pro-
            eutectoid ferrite, 0% bainitic ferrite
            and 0% pearlite lines is shown in Fig. 1
            (49). The steels were austenitised at
            1250°C, but had different austenite
            grain sizes, that of the vanadium steel
            being about half that of the vanadium
            free steel. The presence of vanadium
            raised both A_1 and A_3 so that at
            transformation temperatures above ≏ 810
            °C the vanadium free steel did not
            transform whilst the 0.13%V steel
            partially transformed at temperatures up
            to 850°C. Due to the finer austenite
            grain size in the 0.13%V steel, it
            formed pro-eutectoid ferrite slightly
            more rapidly, as expected due to an
            austenite grain boundary surface area
            for ferrite nucleation of about 8 times
            that of the vanadium free steel. There
            can be little doubt that for the same
            grain size, 0.13%V retards the pro-
            eutectoid ferrite transformation. The

pro-eutectoid ferrite was observed to

contain interphase ˄precipitates of vanadium

carbide/nitride, and recent ˄work has

indicated that increasing the nitrogen

content increases the amount of

interphase precipitation (50).

(ii)   As can be seen from Figure 1, despite

the difference in prior austenite grain

size, 0.13%V retards bainitic ferrite

formation particularly at the lower

transformation temperatures towards the

M_s , where austenite grain boundary

nucleation of bainitic ferrite is much

less prevalent. Again there can be

little doubt that vanadium retards

bainite formation. There seems to be no

quantitative data available for the

effect of vanadium on the B_s temperature

(47) although it might be expected that

vanadium would be equally as effective

as molybdenum in depressing B_s , if not

actually more so. In fact it might be

expected that vanadium would depress B_s

by≈100°C per weight percent (47), and

recent work on the continuous cooling

transformation characteristics tends to

confirm this because 0.45%V seems to

lower B_S by $\simeq$ 50°C (50). An
interesting feature is shown by Figure
1, namely that when bainitic ferrite is
preceded by pro-eutectoid ferrite, the B_S
increases. A possible explanation for
this is that the interphase
precipitation in the pro-eutectoid
ferrite so depletes the remaining
austenite in vanadium, carbon and
nitrogen that the B_S is raised. This
emphasises the importance of solute
concentration changes in the austenite
throughout the progress of
transformation on the way in which the
transformation progresses in the
remaining austenite. This can be
important in the evolution of the
microstructure during continuous
cooling.

(iii)   Figure 1, shows that, when the ferrite
contains large amounts of interphase
precipitation, as occurs in the 0.13%V
steel transformed just below A_1,
pearlite formation is greatly retarded.
This is possibly due to the withdrawal
of carbon from the untransformed

35

austenite.

(iv)   Recent work has shown (51) that at very high temperatures in the pro-eutectoid ferrite transformation range, above $\approx$ 810°C in a 0.05%C, 0.28%V steel, there is no interphase precipitation and the vanadium partitions strongly to the ferrite. This is also accompanied by a discontinuity in the 0% pro-eutectoid ferrite transformation curve. Between 810°C and 760°C the major precipitation is by the interphase mechanism and increasing the nitrogen content leads to a finer form of interphase precipitate, a smaller inter-sheet spacing, a suppression of the fibrous type of precipitate, and an increase in the temperature range over which interphase precipitation occurs. This latter effect is due to nitrogen depressing the temperature for the start of Widmanstatten ferrite formation, i.e. the B_s for bainitic ferrite, as might be expected. Moreover, nitrogen inhibits the pro-eutectoid ferrite reaction (51) but once initiated increases the rate of the reaction.

36

STACK MATERIAL REQUEST FORM

READER'S NAME: .... GLYNN HEWITT ....

DATE(S) REQUIRED: .... 27-3-93 ....

****

THESES/DISSERTATIONS

Number: ..... 6745 ....

Author: ..... G.K.Platts ......

Title: ..... Hardenability, transformation and precipitation
..... effects in Vanadium steels. ....

JOURNALS

Title: ....

....

Volume/Part/Date/Pages: ....

....

****

LIBRARY USE

Ticket Number: .... 554556 ....

Date(s) of Issue: ....

....

Staff Initials on Return: ....

Decreasing the transformation
temperature below 760°C causes, together
with the normal interphase precipitate,
an additional precipitation of vanadium
carbide on dislocations generated in the
ferrite by the lower transformation
temperature. These effects are
important with regard to the hardness
changes which occur in jominy
hardenability specimens at the slower
cooling rates remote from the quenched
end.

(v)   In higher carbon steels in which
pearlite is the predominant high
temperature transformation product of
austenite, it has been shown that
vanadium carbide can form in the ferrite
between the cementite lamellae in the
pearlite (10). This apparently can
strengthen, but the mechanism by which
it forms prior to, during, or
after the pearlite transformation, is by
no means understood.

(vi)   There is little data available on the
effect of vanadium on the M_s

temperature, the published equations giving no coefficient for vanadium (47) (52 - 58). There is no reason to believe that vanadium behaves any differently from other similar alloying elements, and thus it undoubtedly depresses M_S . From very recent thermodynamic data (59), it seems most likely that its effect lies between those of molybdenum and chromium for which there is data (50). Averaging the effects for molybdenum and chromium from the published data, would lead to the conclusion that vanadium depressed M_S by $\simeq 20^{\circ}$C per weight per cent.

(c)   Continuous Cooling Transformation
       Characteristics

As in the case of T.T.T. diagrams, there is little or no systematic data reported on the effect of vanadium on C.C.T. diagrams. Recent work, however, (50) has investigated the effects of high vanadium contents of $\simeq 0.45\%$ on the C.C.T. diagrams of 0.06/0.08%C, 1.8/2.0%Mn steels with 0.008%N_2 or 0.014%N_2 . The effect of vanadium is shown in Figure 2. In this particular

case the vanadium does not appear to increase the martensitic hardness, probably due to the refinement of the austenite grain size. However, there are a number of effects of interest:-

(i) Vanadium increases the ferrite transformation start temperature, F_S , probably because it will raise A_3 by about $50^\circ C$.

(ii) There is a discontinuity in the F_S temperature in the presence of vanadium, as noted by Ballinger and Honeycombe (60) and said to be due to the partitioning of vanadium at the higher F_S temperature

(iii) When vanadium partitioned ferrite forms, there is no interphase precipitation of vanadium carbide and the transformation of the remaining austenite is depressed to form martensite-bainite aggregates (M/B) and possibly retained austenite. This effect does not apparently occur in vanadium free steel. Carbon may also help in this respect by partitioning to the untransformed

39

austenite.

(iv)   Vanadium markedly depresses the B_s
temperature, as has been
indicated earlier.

A study of the effect of increased nitrogen
(to 0.013% (50)) showed that nitrogen increased
the martensitic hardenability, which confirmed
results reported by Vassiliou (49), and also
showed that nitrogen depressed the ferrite and the
bainite transformation temperature. It was also
inferred that nitrogen increased the amount of
interphase precipitate.

Although considerable analyses have been carried
out on the effects of alloying elements on C.C.T.
diagrams (47) (60-64), none of this work has shown
any effect of vanadium on the critical cooling
velocity for martensite, bainite or ferrite-
pearlite formation, possibly because of
insufficient systematic variation in the vanadium
content and due to randomisation introduced by
varying austenite grain sizes and undissolved
vanadium carbide/nitride. Also, statistical
analyses of the effects of alloying additions and
the cooling rate on the hardness of martensite and
bainite shows no effect of vanadium (47). This

might be expected as the solid solution hardening effect of vanadium is small especially at the relatively low levels investigated, and even when there is undissolved vanadium carbide or nitride the carbon and nitrogen content of the martensite or bainite will be little affected. However, it has been shown that vanadium increases the hardness of the ferrite-pearlite structure at a constant cooling rate (47), the effect being described by the equation:-

$$HV = 42 + 223(C) + 53(Si) + 30(Mn) + 7(Cr)$$
$$+ 19(Mo) + 12.6(Ni) + \log(CR) \cdot \left\{ 10 - 19(Si) \right.$$
$$\left. + 8(Cr) + 4(Ni) + 130(V) \right\} \quad \ldots \ldots \quad (7)$$

where (CR) is the cooling rate in $^{\circ}$C/hour.

This effect undoubtedly reflects the influence of vanadium on interphase precipitation at slow cooling rates, but it should also be influenced by the V:C ratio of the steel, the austenitising temperature and the actual transformation temperature. This latter effect of transformation temperature, by altering the dislocation density of the transformed ferrite can also influence both the rate of precipitation of vanadium carbide and the distribution and morphology of the precipitates. Thus the situation may not be so simple as described by the equation (7).

2.3 Precipitation Processes

As previously mentioned, it is the difference in the
solubility of carbon in austenite and ferrite which
produces the familiar ferrite-cementite aggregates
observed in plain carbon steels. Similarly, the alloy
carbides obtained in alloy steels, are much more soluble
in austenite than ferrite and will also tend to
precipitate upon cooling. The conditions under which
these precipitates form significantly affect the
resulting mechanical properties of the alloy. The
precipitation processes which are generally involved
are:-

    (i)   Precipitation in austenite prior to
                 transformation.

    (ii)   Precipitation at the austenite-ferrite
                 interface during the transformation
                 process,

and   (iii)   Precipitation from supersaturated
                 ferrite by tempering or ageing
                 subsequent to transformation.

Alloy carbides can also be produced from bainitic and
martensitic structures by tempering, and is considered as
an acceptable method of obtaining high strength levels,
despite the need for a second heat treatment process.
Consequently extensive reviews on the tempering processes
are readily available (65-69). However, it is not

envisaged that tempering of such structures will be
investigated in the present study and therefore the
precipitation processes involved will not be considered
in this review.

2.3.1   Precipitation in Ferritic Structures

2.3.1.1. Precipitation in Austenite prior to Transformation

At high heat treatment temperatures the austenite can
accomodate a significant amount of microalloying element
in solution. However, as the temperature decreases, the
solubility of the alloy carbides/nitrides decreases
causing precipitation to occur within the austenite phase
(70). Although this phenomenon readily occurs in the
absence of deformation, it is accelerated by strain
inducement caused by certain controlled rolling processes
(2). This type of precipitation does not cause an
increase in strength by precipitation hardening and in
the majority of cases reduces the overall strength of the
alloy. This situation is caused by the rapid coarsening
of the precipitates due to the high temperatures at which
they form. Consequently, they are relatively ineffective
as a strengthening mechanism. Also, precipitation in
austenite reduces the amount of alloying element in
solution and thus reduces the potential strengthening due
to interphase precipitation during the subsequent
transformation of the austenite.

However, it has been shown that precipitates formed in

43

austenite influence the tendency of the material to recrystallise during controlled rolling. The precipitates pin the grain and sub-grain boundaries and therefore delay recrystallisation to higher strain conditions. Consequently, when recrystallisation occurs the resulting microstructure contains a much finer grain size (71).

Davenport et al (72) reported that niobium, titanium and vanadium carbides that precipitated in austenite conformed to an orientation relationship with the parent austenite, namely:-

$$(100)_{M(C,N)} \parallel (100)_\gamma$$
$$(010)_{M(C,N)} \parallel (010)_\gamma$$

WHERE :- M = MICROALLOYING ELEMENT.

Therefore, the precipitates preserve a record of the austenite orientation but the precipitates will show no fixed orientation relationship with respect to the final ferrite matrix. This is due either to the subsequent changes in austenite orientation due to recrystallisation or by the change in orientation obtained during the austenite to ferrite transformation.

2.3.1.2   Precipitation at the Austenite/Ferrite
           Interface During Transformation

Although the precipitation processes occurring at the

44

austenite-ferrite interface during transformation are
complex, three different morphologies have been
established.

        (i)   Fibrous Precipitation

        (ii)   Coherent Interphase Precipitation

        (iii)   Incoherent Interphase Precipitation

2.3.1.2.1   Fibrous Precipitation

Fibrous precipitation forms with a morphology similar to
that of pearlite consisting of fibres of alloy carbides
associated with ferrite. However, the structures are
generally an order of magnitude finer than those of
pearlite. This refinement of the structure results from
the partitioning of the alloying element which is
required to allow the growth to continue. Consequently,
the slower diffusion rates of the alloying elements
results in the finer structure.

The precipitation process is similar to particulate
interphase precipitation in that nucleation occurs at the
austenite/ferrite interface during the transformation
(43). However, fibrous precipitation tends to grow in a
direction normal to the interface and in the direction of
movement of the interface. There is a close association
between fibrous and particulate precipitation in that
both types have been observed even within the same grain
(51) and along the same austenite/ferrite interface (70).
Therefore, the formation of fibrous precipitation depends

45

upon the nature of the transformation interface. Fibrous
precipitation does not normally occur at semi-coherent
planar interfaces but rather at higher energy curved
incoherent interfaces which move by atomic diffusion
(73). Consequently, growth must proceed by boundary
migration forming fibrous precipitation until a ledge
type growth mechanism can be established. Alternatively,
a change in the type of precipitation can occur simply by
a change in orientation of the austenite grain causing a
change in the nature of the interface from a semi-
coherent type to a non-coherent interface, or vice versa
(74).

It is generally accepted that any factors which slow down
the rate of transformation, causing the reaction to
approach equilibrium conditions, will increase the amount
of fibrous precipitation (75). Consequently fibrous
precipitation is favoured at high temperatures, where the
driving force for transformation is low, and by the
presence of microalloying additions. It has also been
observed that an increase in the amount of fibrous
precipitation, at the expense of particulate
precipitation, can be achieved by deformation during
controlled rolling. Walker et al (76) explained this in
terms of the moving transformation front sweeping up the
dislocations in the austenite and therefore altering the
structure of the austenite/ferrite interface.

Fibrous precipitation occurs at the austenite/ferrite interface, and therefore there would be expected to be an orientation relationship between the precipitates, ferrite and the austenite. Investigations on Fe-C-Cr alloys (73) have shown that the fibrous precipitate is related to the ferrite in which it occurs by Kurdjumov-Sachs orientation relationship. However, in any one ferrite grain, the fibrous precipitates adopt a single variant of the orientation relationship.

2.3.1.2.2 <u>Coherent Interphase Precipitation</u>

Interphase precipitation is the most important of the precipitation processes due to the significant strengthening properties of the very fine particulate alloy carbides. The precipitation forms a characteristic banded structure in which the carbide particles are arranged in regularly spaced bands which run almost parallel to the austenite/ferrite interface and tend to follow any change in the direction of the boundary.

Nucleation of coherent interphase precipitation occurs at the austenite/ferrite interface on planar coherent or semi-coherent interfaces (72) rather than on dislocations as was previously surmised (77). It is now well established that precipitation occurs during the stepwise movement of the austenite/ferrite interface. However, the precipitates do not form on the disordered riser of

the ledge but rather upon the planar interface (20)(78).
Although precipitation upon the riser is energetically
more favourable its high mobility makes nucleation
impossible. Cocks et al (79) determined that the
mobility of the riser was at least an order of magnitude
greater than the broad faces of the ledges.
Consequently, nucleation must occur on the lower energy,
low mobility planar faces (78). As a result the sheet
spacing is dependent upon the height of the multiple
steps and of the distance between positions at which the
interface is pinned. Therefore, if the transformation
temperature was lowered the height of the steps and the
distance between pinned interface positions would be
reduced which would produce a finer band spacing.

The precipitates within the sheets are randomly arranged.
Consequently the appearance of interphase precipitation
can be altered from a series of well defined bands into a
random distribution simply by tilting the sample (72).
This could cause difficulty in distinguishing between a
random distribution caused by interphase precipitation or
a random distribution resulting from supersaturated
ferrite precipitation. However, the two different
morphologies can be easily distinguished using electron
diffraction methods (72). Analysis of their diffraction
patterns confirmed that both types of precipitate in
vanadium steels conformed to the Baker-Nutting

orientation relationship (80) with the ferrite, which is normally observed in tempered vanadium steels, namely:-

$$\{100\}_{V_4C_3} \; // \; \{100\}_\alpha$$

$$\langle 110 \rangle_{V_4C_3} \; // \; \langle 100 \rangle_\alpha$$

However, coherent interphase precipitation was found to nucleate on only one of the three possible ferrite cube planes. They tend to adopt the habit plane which brings the relationship most closely parallel to the austenite/ferrite interface. Consequently, the appearance of at least two different Baker-Nutting variants identify precipitation from supersaturated ferrite.

The adoption of a single variant of the Baker-Nutting orientation relationship which is most parallel to the interface can be very important when dark field examination of a sample is being employed. A change in the direction of the interface can result in the precipitate switching to one of the other two available habit planes in order to maintain the orientation most parallel to the interface. Under dark field conditions this would result in the disappearance of the precipitates (81).

Recently Howell et al (73) have determined an orientation relationship of interphase precipitation in a 12%Cr steel, namely:-

$$(111)_\gamma \parallel (011)_\alpha \parallel (111)_{M_{23}C_6}$$
$$[10\bar{1}]_\gamma \parallel [111]_\alpha \parallel [10\bar{1}]_{M_{23}C_6}$$

This relationship shows that the ferrite is related to the austenite by the Kurdjumov-Sachs relationship and it is therefore implied that the austenite/ferrite interface must have been coherent or semi-coherent. Also since the carbide phase is related to both the austenite and ferrite phases the carbide must have nucleated at the austenite/ferrite interface and not within one of the phases.

Interphase precipitation has also been observed in association with Widmanstatten type ferrite (82) occurring as planar sheets parallel to the broad faces of the ferrite plates. As was reported in section 2.2.1.1, it is generally accepted that Widmanstatten ferrite undergoes lateral growth by the movement of small ledges along its low energy boundary. Consequently, interphase precipitation occurs in a similar way to that encountered at high transformation temperatures. However, this type of structure is dominated by the precipitation from supersaturated ferrite and its extent is determined by the kinetics of the transformation process (83).

2.3.1.2.3   Incoherent Interphase Precipitation

Recent studies (83) have provided evidence for a third type of interphase precipitation which occurs at high transformation temperatures and is associated with high energy boundaries. This type of precipitation has been termed incoherent interphase precipitation since it is considered that the precipitation occurs as discrete particles at incoherent austenite/ferrite interfaces.

Incoherent interphase precipitation has been shown to occur at high transformation temperatures when fibrous precipitation gives way to interphase precipitation (57). Ricks et al (83) reported that the addition of nickel totally eliminated fibrous precipitation and that interphase precipitation occurred even on high energy interfaces. The resulting microstructures have been shown to have two distinct morphologies:-

    (i)   Coarse random dispersions (60)

    (ii)   Regularly spaced curved sheets which follow the interface boundary (74)(84)

Study of the austenite/ferrite interface (74)(83) showed that the boundary could be very irregular and have little tendency to form facets. The interfaces contained bowed sections where the boundary was pinned by carbides nucleated at the interface (85). Consequently it was concluded that incoherent interphase precipitation could be formed by an interface bowing mechanism (78)(85), as

suggested by Heikkinen (86). It was also shown that abrupt changes in the interface could occur and that these changes were associated with a curved sheet type precipitation. The regular spacings of these sheets suggested a ledge type mechanism of precipitation on high energy incoherent interfaces. Therefore, Ricks et al (84) proposed a "quasi-ledge" mechanism where the disordered bowing interface is stopped by copious precipitation upon it. The interface is immobilised because the spacing between the carbide particles becomes too small to allow bowing between them to occur even under the high driving force condition of the $\gamma \rightarrow \alpha$ transformation. Under these conditions the interface requires a ledge type mechanism to continue migration, see Figures 3 and 4.

Incoherent precipitation was shown to have a three phase orientation relationship similar to that encountered in coherent interphase precipitation, namely:-

$$(111)_\gamma // (011)_\alpha // (111)_{M_{23}C_6}$$
$$[10\bar{1}]_\gamma // [11\bar{1}]_\alpha // [10\bar{1}]_{M_{23}C_6}$$
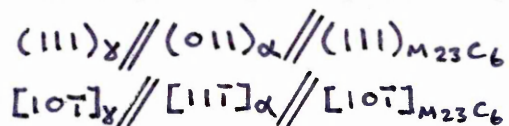
The carbides were also observed to have only one variant of the orientation relationship allowing a cube-cube relation for $M_{23}C_6$ with the austenite. However, in vanadium steels this would be the variant most parallel to the austenite/ferrite interface and obeying a Baker-Nutting relationship.

52

2.3.1.3   <u>Precipitation from Supersaturated Ferrite</u>

Supersaturated ferrite is produced when there is no precipitation during the austenite to ferrite transformation. It is not until the ferrite is aged, or tempered, that precipitation proceeds. This situation is produced when the austenite to ferrite transformation occurs at a relatively low temperature, generally resulting from rapid cooling rates. Consequently, supersaturated ferrite is normally observed in association with Widmanstatten or bainitic type ferrite (20)(70), and is aided by the higher dislocation density in such ferrite.

It is considered that there are two types of precipitates formed from supersaturated ferrite (87), namely:-

       (i)   Randomly oriented precipitation.

      (ii)   Multivariant precipitation.

2.3.1.3.1   <u>Randomly Oriented Precipitation</u>

Randomly oriented precipitation is thought to occur at transformation temperatures just low enough to form supersaturated ferrite. Consequently, there is a low driving force for precipitation and therefore precipitation must occur at preferred nucleation sites. These are normally dislocations, but can in some circumstances be grain boundaries (20), which are formed as a result of the Widmanstatten ferrite transformation.

The high dislocation densities, resulting from the volume
change which takes place during the transformation, are
ideal for nucleation of the precipitates. Once
precipitation has occurred, the low driving force and
pipe diffusion result in the growth of incoherent
boundaries and thus the formation of globular particles.

2.3.1.3.2   Multivariant Precipitation

Multivariant precipitation is more common than randomly
oriented precipitation and occurs in ferrite formed at
even lower transformation temperatures, where the driving
force for precipitation is higher due to the lower
solubility of the alloy carbides (70)(87). Precipitation
occurs uniformaly throughout the structure, forming
clusters of very fine particles. Smith et al (87)
observed that in some cases the precipitates formed along
lines of dislocations. Holding the material at the
transformation temperature caused prefer ential
coarsening to occur when the initially coherent particles
tended to form a plate type morphology. The plate type
structure arises due to the growth along preferred
ferrite planes and in vanadium steels this plane will be
one of the three variants of the Baker-Nutting
orientation relationship. However, all three variants
are possible within the same area since there is no
dependency upon the austenite/ferrite interface.

Precipitation from supersaturated ferrite is considered
to be especially important during the coiling of strip
that had previously been hot rolled. The slow cooling in
the coiled condition can lead to the formation of small,
finely dispersed precipitates. These precipitates can
provide a very effective strengthening mechanism but can
easily over age and result in variable mechanical
properties.

2.3.2   Precipitation Processes in Pearlitic Structures
In predominantly pearlitic steels it has been shown that
alloy carbides not only precipitate in the pro-eutectoid
ferrite but also within the ferrite lamellae of the
pearlite (11-13)(88-93). It, therefore, seems possible
that like precipitation in ferrite, the precipitation in
pearlitic steels can occur under various conditions,
namely:-

    (i)   Precipitation in austenite.

    (ii)   Precipitation during the transformation.

    (iii)   Precipitation from the supersaturated
               condition.

2.3.2.1   Precipitation in Austenite Prior to Transformation
In order to obtain pearlitic structures in the presence
of carbide forming micro-alloying elements it is
necessary to increase the carbon content of the steel.
This in turn suppresses the pro-eutectoid ferrite reaction

allowing the austenite structure to be maintained at lower heat treatment temperatures. Also, an increase in carbon content reduces the amount of alloying element that can be accommodated in solution in the austenite and tends to leave undissolved carbides. Consequently, there is less potential for precipitation in austenite upon cooling. However, this type of precipitation has been observed in the pearlitic ferrite after transformation, as fairly coarse randomly oriented particles.

2.3.2.2. Precipitation During the Austenite to Pearlite Transformation

Although fibrous precipitation has not been observed in pearlitic ferrite, evidence has been produced for the presence of interphase precipitation (91-93). Dunlop et al (93) studied the precipitation of vanadium carbides in pearlitic ferrite and observed that although less distinguishable than in pro-eutectoid ferrite, several areas of banded dispersions could be isolated. Analysis of their diffraction patterns showed that all the areas obeyed a Baker-Nutting oriented relationship and that only one variant of the three possible ferrite planes was adopted. This behaviour is typical of interphase precipitation but the exact nature of the precipitation process is not fully understood. This is because it is normally considered that the growth of pearlite occurs by the migration of high energy

56

incoherent interfaces and not by a ledge mechanism associated with coherent interfaces. Consequently, it would be expected that an incoherent interphase precipitation mechanism would be adopted. A bowing type mechanism would explain why banded dispersions were only occasionally observed. Also, it is possible that the apparent planar banding could in fact be slightly curved due to a 'quasi' ledge mechanism. The occurrence of precipitates at the pearlite/austenite interface could prevent the movement of the interface and thus explain the observed refinement of the pearlite colony size in alloy steels.

Dunlop et al (93) also observed that rapid cooling rates caused considerable precipitation at the interface between the cementite lamella and the pearlitic ferrite. Therefore he suggested that the intersection of the cementite/pearlitic ferrite and the pearlite/austenite transformation front must be a good heterogeneous nucleation site. It was also observed that in slowly cooled samples, and to a lesser extent in rapidly cooled samples, that a precipitate free zone formed around the cementite lamellae suggesting that the vanadium partitioned to, and dissolved to some extent in the cementite during the transformation. It is known that up to 10%V can dissolve in cementite (94).

2.3.2.3 <u>Precipitation from Supersaturated Ferrite</u>

If rapid cooling rates are employed the interphase
precipitation in pearlite can be suppressed in a similar
way to that observed in ferritic structures. Ageing of
vanadium alloys (93) revealed that nucleation and growth
occurred on dislocations and the resulting precipitates
obeyed a Baker-Nutting orientation relationship in which
all three possible variants were operational.

2.3.3 <u>Precipitation Processes in Vanadium Alloys</u>

It is well known that the precipitation of vanadium
carbides and nitrides in ferrite produces precipitation
strengthening (95) and that its effectiveness depends
upon the composition of the steel, the austenitising
conditions, the thermo-mechanical processes and the
cooling rate.

It has been generally accepted that both vanadium carbide
and nitride have a cubic 'NaCl' type structure and that
the nitride forms with a composition close to VN while
the carbide can vary between $VC_{0.75}$ and VC. Also, it is
normally considered that the two precipitates are
completely miscible. However, recent work (1) has shown,
thermodynamically, that it would be expected that
vanadium nitride would precipitate first in the austenite
but that as the nitrogen was consumed the precipitate
would move toward vanadium carbide. It was also

suggested that due to carbon enrichment at the austenite-ferrite interface during transformation, the interphase precipitate would be predominantly vanadium carbide.

Vanadium is added to steels to produce both ferrite grain refinement and precipitation strengthening. Consequently the size of the particles and their distribution are very critical. Various studies (2)(96)(97) have shown that precipitation of vanadium nitride in austenite does occur in vanadium steels and detracts from the precipitation strengthening in ferrite. This results from the precipitates produced at these high temperatures rapidly coarsening and becoming ineffective as a strengthening mechanism. Also the amount of potential vanadium which could precipitate during the transformation, as interphase precipitation and thus produce effective strengthening, is reduced. However, precipitation in austenite can retard the recrystallisation of the austenite and therefore produce a finer grain size. Consequently, to obtain maximum precipitation strengthening it is important to ensure all the alloying element is in solution, so that it can be precipitated as interphase precipitation, but for a fine grain size it is advantageous to have precipiates present in the austenite to inhibit both grain growth and the recrystallisation process during rolling. Therefore, the conditions under which the alloys are heat treated are very important.

The interphase precipitation processes observed in
vanadium alloys are dominated by the coherent interphase
precipitation mechanism (20)(42). Fibrous precipitation
is only very rarely observed, if at all, unless the rate
of the transformation is reduced by the addition of
chromium (73)(74) or manganese (20). However, equally
spaced non-planar sheets of precipitates, indicative of
incoherent interphase precipitation, have been observed
(51)(78)(84). Ricks et al (84) concluded that the
interparticle spacings observed for the interphase
precipitation were too small to allow a bowing type
mechanism to occur and therefore suggested a 'quasi-
ledge' type mechanism. Interphase precipitation has also
been observed in association with Widmanstatten type
ferrite structures, occurring by a ledge type mechanism
(82).

Precipitation from supersaturated ferrite has been shown
to occur (20)(70)(87) and has aroused particular interest
during the coiling of vanadium steels subsequent to hot
deformation, since it can have a direct effect upon the
resulting mechanical properties.

The addition of small quantities of vanadium to higher
carbon steels, where the major microstructural component
is pearlite, has also been shown to markedly increase the
strength of the steel (10)(98). This is considered to

occur due to precipitation of vanadium carbides within the ferritic lamellae of pearlite as well as in the pro-eutectoid ferrite (11-13)(88-93). The occurrence of the precipitates within the ferritic lamellae is thought to be due to an interphase type mechanism, since several areas of banded precipitates have been observed (91-93) together with a single variant of the Baker-Nutting orientation relationship. It has been suggested that because of the banded areas a ledge type mechanism for precipitation is involved despite the fact that pearlite growth is generally regarded as a movement of incoherent rather than coherent interfaces. Therefore, it is possible that the bands may be slightly curved and thus produced by a 'quasi'-ledge mechanism, as was recently proposed for incoherent interphase precipitation in ferritic alloy steels (84). It is clear that further work in this area is required before the situation is fully understood. However, the potential use for precipitation within the ferritic lamellae of pearlite, as a strengthening mechanism has been quickly realised, especially for railway applications due to the increased loads modern rails have to withstand (10)(99).

2.4   Hardenability

2.4.1   Hardenability Concepts
The hardenability of steels has been of much interest for more than 50 years during which time the metallurgical

61

significances of the processes involved have been developed (100-102).

Hardenability has been defined in a number of different ways but is usually considered to be "the capability of the steel to transform partially or completely from austenite to some percentage of martensite at a given depth when cooled under given conditions". Consequently, hardenability is primarily concerned with the rates of decomposition of austenite to form ferrite, pearlite, bainite and martensite. Therefore, it depends upon such factors as alloy composition, prior austenite grain size, austenitisation temperature and rate of cooling. As a result it is very difficult to predict hardenability from basic principles and therefore tend to rely upon practical tests.

2.4.2   Hardenability Testing

2.4.2.1   The Grossmann Test

Much of the early work on hardenability was conducted by Grossmann (103-105) who developed a quantitative test to determine the hardenability of various steels. The method involved quenching several bars of different diameters, but from the same alloy, into a particular cooling medium. Once quenched the bars were sectioned and a hardness traverse performed along the diameter of the bar. Also the bars were examined microscopically to determine which bar had a 50% martensite structure at its

centre. The diameter of this bar would then be classified as the critical diameter, D_0 . However, this value had no absolute significance since it was dependent upon the quenching medium employed in the test. Consequently, the variations in D_0 caused by the various quenchants used were determined and rationalised with respect to a standard condition. This was achieved by referring to H coefficients where the value for quenching in still water was standardised as 1. It was then possible to determine a value for hardenability in an ideal quenchant where the surface would be instantly cooled to the temperature of the quenchant, i.e. $H = \infty$. Under these conditions the diameter of the alloy bar which produced 50% martensite at its centre would be called the ideal critical diameter, D_i .

Grossmann investigated a large number of alloy steels and systematically determined the effects of various alloying elements upon a base steel. From this work he devised a method for calculating hardenability from the composition of the steel (104). The method was based upon the consideration that the steel had a base hardenability due to its carbon content alone and that this value of the ideal critical diameter was multiplied by a factor for each element present. The effects for variations in grain size were incorporated into the base hardenability factors. In the ensuing period numerous investigations

were undertaken in an attempt to clarify and modify the Grossmann principles (106-109). However, despite the fact that the practical situations were found to be more complex than described in the Grossmann model, the principles involved are still widely used in the steel industry.

2.4.2.2   The Jominy End Quench Test

Despite the high reliability of the Grossmann test, other types of test have been perfected, the most important of which is the jominy end quench test (110). The test requires that a standard round bar 4 ins (102 mm) long and 1 ins (25.4 mm) diameter is produced. The sample is heated to the required austenitising temperature in an environment which protects it from scaling and decarburisation and then rapidly transferred to a jig where one end of the bar is quenched by a standard jet of water. The quenching of one end results in a range of cooling rates along the length of the bar and a corresponding variation in the microstructure. To obtain quantitative results from the test, the quenched bars have two flat surfaces carefully ground on opposite sides to a depth of 0.015 ins. Hardness measurements are then made at 1/16 ins intervals along the centre line of the two flats. A graph of hardness versus distance along the jominy bar is then produced, from which it is easy to determine the 50% martensite hardness position. However hardenability data is still expressed in terms of the

ideal critical diameter; consequently standard conversion factors of the type devised by Grossmann et al (104) have to be applied to the jominy data.

The advantage of the jominy test is that it is a simple, but reliable test that produces a whole range of cooling rates along the length of the bar and thus allows the hardenability to be determined from a single sample. However, certain classes of steels, for example shallow-hardening steels, are unsuitable for the jominy test and therefore other less common, and more specialised, tests have been devised.

2.4.3   Factors Which Influence Hardenability

When formulating the critical equations to predict the hardenability of a steel from its chemical composition it is normally accepted that the ideal critical diameter depends upon the following three factors:-

(i)   the carbon content of the steel

(ii)   the prior austenite grain size

(iii)   the quantity of other alloying elements present.

However, the situation can easily be complicated by other factors such as the austenitising temperature, the austenitising time, the presence of undissolved precipitates etc. Consequently, it is not surprising

that variable hardenability effects have been observed.

2.4.3.1   The Effect of Carbon

Carbon is a very important element in the study of
hardenability since it determines the maximum hardness of
the martensitic phase of the alloy. This in turn
determines the 50% martensite hardness value which is
used to calculate the hardenability of the alloy from
standard jominy curves. Therefore, since the 50%
martensite hardness varies with carbon composition the
correct value for each alloy must be calculated using
standard conversion curves of the type produced by
Grossmann et al (104), see Figure 5.

In addition, from its effect on the continuous cooling
transformation diagrams it can be seen that carbon has a
characteristically strong hardenability effect in its own
right. Increasing the carbon content of the steel
retards the non-martensitic transformation reactions and
causes the 'C' curves of the bainite and ferrite/pearlite
transformations to become more distinct. To allow the
transformation of austenite to a non-martensitic
transformation product carbon must diffuse away from the
nucleating phase. Consequently, as the carbon content is
increased diffusion away from the non-martensitic phase
is more difficult. This results in a tendency to form
bainitic rather than ferritic/pearlitic structures. A
change in the non-martensitic structure formed will have

a direct effect on the position of the 50% martensite

hardness value. For example, a 50% martensite, 50% lower

bainite structure will have a higher hardness than a 50%

martensite, 50% upper bainite structure. Therefore, not

only must the carbon content of the martensite be

considered but also the strucure obtained at the

theoretical 50% martensite hardness position of the

jominy specimen.

The dependence of hardenability on the carbon content of

the steel has been studied by various authors over

different carbon ranges. The most significant studies

have been by Grange (109), for essentially alloy free

carbon steels, Kramer et al (108) for low alloy medium

carbon sheets, and Jatczak (111), for carburising and

high alloy steels. However, no work has been reported on

steels typical of high strength low alloy steels with

carbon concentrations below 0.2%. Consequently, carbon

figures for these low carbon situations had to be

extrapolated from the values quoted for steels in the

medium carbon range.

2.4.3.2   The Effect of Austenite Grain Size

It has been shown that the austenite grain size can have

a direct effect upon the hardenability of a steel if all

other factors remain constant (103)(104)(112), Figure 5.

An increase in the prior austenite grain size causes an

increase in hardenability due to the reduction of the grain boundary area. This causes a corresponding reduction in the number of nucleation sites for the transformation of the non-martensitic transformation product. Consequently, the transformation processes are retarded and the hardenability increased.

Grossmann (103) noticed that the effect of the austenite grain size varied depending upon the non-martensitic phase produced during quenching. The austenite grain size had less effect on the hardenability when the transformation produced a bainitic rather than a ferritic/pearlitic structure. This probably results from the fact that the ferritic/pearlitic structures are principally nucleated at prior austenite grain boundaries while the bainitic structure nucleates more throughout the austenite grain.

It is also possible that the effectiveness of the microalloying elements present in the alloy could be enhanced by the increase in the austenite grain size. This would result from there being the same quantity of microalloying elements in solution but a reduced number of grain boundary nucleation sites at which the microalloying elements could retard the transformation.

2.4.3.3   The Effect of Alloying Additions

All alloying elements except cobalt decrease the rate of

austenite decomposition irrespective of the final transformation structure and will therefore be expected to increase the hardenability of steel. It is generally accepted that to influence the hardenability the microalloying elements must be dissolved in the austenite and should, if all other factors remain constant, progressively increase the hardenability as the quantity of microalloying element in solution is increased. However, much of the published data is presented in terms of the total microalloying element content rather than the amount dissolved in the austenite at the austenitising temperature. This could account for some of the variable effects reported in different studies. Over the past 30 years or more the effects of alloying elements upon the hardenability of steels have been extensively investigated, providing multiplication factors for individual elements, see Figure 6, which could be used in empirical equations to predict the hardenability of a steel from its chemical composition (109)(111)(113). Such equations have been successfully used for many years in medium and high carbon steels. However, with the development of high strength low alloy steels new multiplication factors were not determined for the low carbon situation. Consequently, carbon figures had to be extrapolated from the medium carbon range and the standard effects of the alloying elements, in the medium carbon range, applied. It is obvious that this

situation is unsatisfactory and that the carbon and
alloying element multiplication factors need to be
determined for low carbon steels. As previously stated
in section 2.4.3.1 as the carbon content of the steel is
lowered the individual 'C' curves of the bainite and
ferrite/pearlite transformations become less distinct.
Consequently a stage will be reached where the
hardenability becomes dependent upon the ferrite/pearlite
transformation rather than the bainite reaction.
Similarly, the effects of the microalloying elements may
vary as the carbon content of the steel is reduced, since
in medium carbon steels it is their effect upon the
bainite reaction which influences the hardenability,
whereas in a low carbon alloy it could be their ability
to retard the ferrite/pearlite and the bainite reaction
which determines the hardenability (114).

Recently it has been shown that synergistic effects
between different alloying elements occur in microalloyed
steels (7-9) (114). This effect has renewed much
interest in hardenability since the utilisation of the
positive alloy interactions could produce more efficient
and economical use of microalloying elements. However,
negative interactions have also been observed which could
decrease the hardenability. Consequently, the mechanisms
of the interactions need to be studied before their
advantages can be used commercially. Once the
synergistic effects between different alloying additions

have been quantified it is envisaged that further
modifications to the equations for predicting
hardenability will be possible.

2.4.3.4 The Effect of Austenitising Conditions

Although not included in standard equations for the
prediction of hardenability, the austenitising conditions
can have a significant affect upon the hardenability of
steel. The austenitising temperature is important since
it determines the quantity of microalloying elements
dissolved in the austenite prior to end quenching the
jominy specimen. The temperature is normally selected to
allow maximum solution of any microalloying additions
whilst maintaining the smallest possible austenite grain
size. If the temperature is too low any undissolved
alloy carbides/nitrides would result in a lower value of
hardenability since less microalloying element would be
in solution and therefore available to influence the
hardenability of the steel. In addition the precipitates
could have a two fold effect on the hardenability.
Firstly, they could act as grain boundary pinning agents
and result in a small prior austenite grain size, thus
causing a smaller ideal critical diameter than expected.
Secondly, the precipitates could act as preferred sites
for the nucleation and growth of the non-martensitic
transformation products and again results in a reduction
in the hardenability.

In contrast if the temperature selected is too high the prior austenite grain size will rapidly increase. This effect, as stated in 2.4.3.2, would increase the observed hardenability of the alloy due to the reduction in the grain boundary area. It has also been reported (101) that at higher austenitising temperatures, a more homogenous austenite is formed, which reduces the number of nucleation sites for high temperature transformation and therefore increases the hardenability.

The time at austenitising temperature also influences the hardenability of the alloy by determining the quantities of alloy carbides/nitrides taken into solution. Due to the kinetics of the solution process, extended periods at temperature could cause an increase in the microalloying elements in solution and a corresponding increase in the hardenability. However, increasing the time at the austenitising temperature could result in grain growth and a subsequent increase in the hardenability observed. Consequently, it is clear that the processes involved are more complex than was first imagined and need to be treated carefully. This is especially the situation when using multiplication factors, since the conditions under which they were determined could be significantly different to those under which they are to be applied.

2.4.4   The Effects of Vanadium on Hardenability

Vanadium, like the majority of alloying elements, can significantly increase the hardenability of steel, figures 7 and 8. Data collated from various sources show vanadium to be slightly more effective in promoting hardenability than Mo, Cr, W or Ni, see figure 9 (101). Since vanadium is a relatively inexpensive addition, compared with some of the other elements, the potential replacement of molybdenum by vanadium to achieve at least an equivalent hardenability at a lower cost is exciting much current interest (8)(9). However, the precise quantitative effects of vanadium on hardenability and the mechanisms involved are not fully understood. This is especially true as synergistic effects between it and other microalloying elements have been reported (7)(114). These synergistic effects could have either a positive or negative influence on the hardenability. Consequently, the potential for improved effectiveness of the microalloying elements, by certain combinations of elements, makes it essential that a comprehensive understanding of the hardenability mechanisms involved is obtained.

2.4.4.1   The Basic Effects of Vanadium on Hardenability

It is generally agreed that it is the amount of vanadium dissolved in the austenite at the austenitising temperature, rather than the total vanadium content of

73

the alloy, that influences the hardenability. Increasing
the amount of vanadium dissolved in austenite increases
the hardenability, providing all other factors which
control hardenability remain unaltered, i.e. the
austenite grain size, and the volume fraction and
particle size of any undissolved vanadium carbide/nitride
precipitates. The beneficial effect on hardenability is
because the vanadium in solid solution decreases the
rates of both nucleation and growth of the various
transformation products of austenite. The predominant
effect is probably on the nucleation stage and since the
austenite grain boundaries are preferred nucleation sites
for the non-martensitic transformation products, the
effectiveness of the vanadium in solution not only
depends upon the amount of vanadium in solution but also
its ability to segregate to the austenite grain
boundaries (116). The fact that vanadium is very
effective at low concentrations whilst its beneficial
effect decreases, and may even be detrimental at high
concentrations, would tend to support the proposed
segregation to the austenite grain boundaries. However,
it must be considered that if vanadium does segregate to
the austenite grain boundaries then there may be an
austenitising temperature at which the microalloying
elements in solution are thermally dispersed and a
decrease in hardenability observed (116).

In addition it is probable that the ability of the vanadium to influence the ideal critical diameter will be very dependent upon the austenite grain size. For a fixed quantity of vanadium in solution it would be expected that as the austenite grain size was increased the vanadium would become more effective in increasing the hardenability since there would be fewer grain boundary nucleation sites for the transformation to be eliminated. Consequently, the possibility of grain boundary segregation of vanadium and its ability to effectively eliminate grain boundary nucleation sites needs further investigation.

2.4.4.2   The Carbon·Effect in Vanadium Steels

In vanadium steels the vanadium readily reacts with the carbon and nitrogen present to form vanadium carbide and nitride precipitates. If these precipitates are not completely taken into solution at the austenitising temperature a decrease in hardenability will be observed. Not only would the reduced quantities of vanadium, nitrogen and carbon in solution decrease the hardenability, but would also reduce the martensitic hardness value required for the calculation of the ideal critical diameter value. In the majority of cases the austenitising temperature selected is sufficient to ensure all the alloy carbide precipitates are taken into solution prior to quenching. However, the alloy-carbon

solubility limit at the selected austenitising
temperature must be considered prior to calculating the
hardenability of the alloy.

2.4.4.3   The Effect of Vanadium on the Austenite
           Grain Size

Vanadium nitride/carbide precipitates, present in
vanadium steels, act as grain boundary pinning agents and
allow finer austenite grain sizes to be maintained at
higher austenitising temperatures than for corresponding
vanadium free steels. A small grain size increases the
grain boundary area of the alloy and therefore, increases
the number of possible nucleation sites for the
transformation from austenite. This could cause an
apparent reduction in the effectiveness of the vanadium
to increase the hardenability. Consequently, for steels
containing precipitates, especially nitrides, and refined
grain sizes the results obtained must be carefully
corrected to a standard austenite grain size prior to the
assessment of the influences of the individual
microalloying elements on the hardenability.

Similarly, the effect of austenitising temperature on the
hardenability can appear to be greater than in reality.
This is due to the combined effects of grain coarsening
and the extra solution of the vanadium carbide/nitride
precipitates which results in more vanadium in solution
to increase the hardenability. Although the possible

76

relationships between hardenability, and the austenitising temperature are complex they can be expressed schematically as in figure 10. At low austenitising temperatures the vanadium carbide and nitride precipitates are stable ensuring a fine austenite grain size and small quantities of microalloying elements in solution to influence the hardenability. Therefore, at low temperature relatively low ideal critical diameter values are observed. However, as the temperature is increased both the vanadium carbides and nitrides begin to dissolve. This initially does not allow grain growth to occur but does allow extra vanadium, carbon and nitrogen to enter solution and thus increases the hardenability. The rate of solution of the carbides is significantly higher than the nitrides and would tend to control the increase in hardenability. This gradual increase in the ideal critical diameter would continue until the temperature at which all the vanadium carbides were taken into solution. At this point the rate of increase in hardenability might be expected to reduce since it is now dependent upon the rate of solution of the more stable vanadium nitride precipitates. However, as the austenitising temperature is further increased a situation will be reached where the vanadium nitrides are no longer effective in maintaining a small austenite grain size. As the grain size grows an additional positive influence on the hardenability will be observed.

77

Consequently, the increase in ideal critical diameter is dependent upon the combined effect of grain coarsening and the solution of vanadium nitride precipitates. When the temperature at which all the vanadium nitrides are taken into solution is reached no further increase in vanadium is available to further increase the hardenability which is subsequently solely dependent upon the coarsening of the prior austenite grain size.

2.4.4.4. Microstructures Associated with Jominy Specimens from Vanadium Steels

In general the microstructure along a jominy test specimen for a vanadium steel may be schematically interpreted as shown in figure 11. The initial high hardness martensite quickly changes through lower bainite, to upper bainite and then to polygonal ferrite. Despite the high dislocation density in the ferrite the cooling rate is sufficiently rapid to prevent the precipitation of the vanadium carbides and nitrides taken into solution at the austenitising temperature (117). At slower rates of cooling, further from the quenched end, an effect particularly associated with vanadium steels may be observed. Under certain conditions a secondary increase in hardness may occur due to strengthening caused by interphase precipitation in the pro-eutectoid ferrite, see figure 12 (49). However, at even slower cooling rates the austenite transformation temperature is so high that interphase precipitation does not occur and

78

the hardness correspondingly decreases.

For the two vanadium alloys presented in figure 12, the strengthening associated with the interphase precipitation occurred at the same position on the jominy curves, i.e. at the same cooling rates. This indicated that the effect could be associated with the two alloys having a similar nitrogen concentration. This was supported by the fact that as the nitrogen concentration was increased to 0.020% the resulting increase in hardness due to interphase precipitation occurred at slower cooling rates, and could be associated to the nitrogen retarding the pro-eutectoid ferrite reaction.

Recent work (49) on the tempering of jominy quenched specimens has shown that further increases in hardness may be obtained. This is due to the varying degrees of supersaturation and dislocation densities. Tempering at 550° C produced a hardness peak where the supersaturation was high and the nucleation of vanadium precipitates was aided by high dislocation densities, see figure 13. However, by increasing the tempering temperature to 650°C it was possible to cause a general increase in hardness due to precipitation even where the nucleation process was not aided by the low dislocation density present at the slowly cooled end of the jominy specimen.

2.4.4.5   The Interaction of Vanadium with Other

          Alloying Elements

An alloying element does not have a unique effect upon

hardenability but is dependent upon the precise

combination of other microalloying elements in the steel.

Consequently, failure to appreciate the changing

influence of the elements, for different combinations of

elements, could explain the wide variation in the

hardenability factors reported for a given alloying

element. However, it is only recently that clear

evidence of significant interactions between

microalloying additions has been available. Both

positive and negative interactions have been observed

depending upon the specific combination of alloying

elements in the steel (7)(8)(114). These interactions

have often been termed synergistic interactions since the

combined effect of the elements have a greater influence

on the hardenability than can be explained by the

summation of their individual effects.

It has been shown that individually vanadium can be

substituted for molybdenum on a one for two basis to

achieve an equivalent hardenability (8)(9)(114). However

when both vanadium and molybdenum are added to the steel

the resultant hardenability is greater than expected.

The calculated Grossmann multiplying factors when added

singly were 1.34 and 1.12 respectively, but when in

combination were increased to 1.44 and 1.22

respectively (9).

A large increase in hardenability, which could not be
explained by the conventional Grossmann approach, was
observed by Sandberg et al when molybdenum, vanadium and
titanium additions were all present in a 0.4%C, 1%Cr,
0.015%N$_2$ steel (114). However, this effect disappeared
when the steel contained only molybdenum and vanadium
additions. It was suggested that the strong affinity of
the titanium for the nitrogen resulted in titanium
nitride precipitation and therefore allowing more
vanadium to be available in solution to influence the
hardenability of the alloy.

In addition recent work by Eldis et al into the effects
of various microalloying elements when added as
individual elements and in certain combinations has been
reported (7). The investigations were performed at both
950 and 1200°C austenitising temperatures, tables 1 and
2. It can be seen that austenitising at 1200°C has a
much more significant influence on the microalloying
interactions than at 950°C. The hardenability at the
1200°C austenitising temperature was markedly increased
when the vanadium was in combination with molybdenum, or
titanium, or molybdenum plus niobium, or especially
molybdenum plus titanium. However, no mechanistic
explanations for the observed effects were presented.

3.   <u>Materials for Investigation</u>

The steels used were air melted in an Induction furnace
and silicon killed. Silicon was used in preference to
aluminium in order to prevent any aluminium – vanadium –
nitrogen interactions. 'U-vac' samples were taken prior
to casting so that the actual alloy compositions could be
determined. The alloys were then cast into 15kg ingots.

Ingots of the correct analyses were then surface dressed
and forged into 33 mm diameter bars suitable for the
machining of standard jominy samples. The chemical
analyses of the alloys are presented in table 3.

4. Experimental Procedures

4.1 Preliminary Studies

4.1.1 Homogenisation Studies

To obtain reliable and reproducible results it was necessary to produce a standard initial condition, in which the material was as homogeneous as possible. During the casting of the experimental alloys microscopic segregation of the microalloying additions could have occurred and resulted in variations in properties and transformation behaviour. To determine the level of homogeneity, samples were taken from a low carbon - low vanadium steel, (alloy 613), and isothermally transformed. The regions of preferred nucleation and growth of ferrite were then determined. The procedure adopted for this isothermal transformation study was as follows:-

a) Austenitise at 1250° C for 30 minutes

b) Quench into a salt bath pre-set at 750° C

c) Hold at 750° C for 24 hours

d) Quench into iced brine solution.

Even after holding for 24 hours at 750° C the transformation process was still incomplete due to the temperature being above the A_1 temperature. Therefore, quenching the samples resulted in the untransformed austenite being converted into martensite. Consequently the resultant microstructure showed a mixed ferritic/martensitic structure where the ferritic areas

defined the regions of preferential nucleation.

Specimens from the 'as forged' bar produced a banded
isothermal microstructure, shown in figure 15, which
extended radially from the centre, and longitudinally
along the length of the bar. The banded nature of the
samples indicated that the forged bars were
inhomogeneous. Observation of samples taken from the 'as
cast' ingot showed that the inhomogeneity was associated
with interdendritic segregation, see figure 16. Point
analysis using the EDAX system of the Scanning Electron
Microscope was used to investigate the microsegregation.
Areas of ferrite and the adjacent areas of martensite
were analysed for vanadium, silicon, manganese and iron.
The results were statistically analysed, see tables 4 to
7, and when standard 'T-tests' were performed a
significant difference at the 5% level was obtained for
silicon only. Consequently, it was suggested that the
inhomogenity was caused by the segregation of silicon to
the interdendritic martensitic regions. Silicon is known
to be an element which tends to retard the transformation
from austenite and therefore areas of high silicon would
be more likely to form martensite upon quenching.

In an attempt to eliminate the effects of segregation, a
series of heat treatment trials were performed which
showed that an acceptable level of homogenisation could

be obtained if the 'as forged' material was heat treated at 1250°C for 4 hours. Isothermal transformation studies showed an even distribution of the alloying elements in the ferrite and martensite and a non-banded microstructure was developed, as shown in figure 17. EDAX analysis could not detect any significant difference in the levels of any of the elements investigated.

4.1.2 Determination of the Solubility Temperatures of Vanadium Carbide and Nitride Precipitates for Low and Medium Carbon Steels

The theoretical temperatures required to take all the vanadium carbide and nitride precipitates into solution were determined by using standard solubility equations of the following types (1):-

a)   for vanadium carbides

$$Log_{10} [V][C] = \frac{-9500}{T} + 6.72 \quad - - - -(8)$$

b)   for vanadium nitrides

$$Log_{10} [V][N] = \frac{-7840}{T} + 3.02 \quad - - - -(9)$$

where: T = Temperature in degrees Kelvin
[ ] = Mass %

From the results, presented in table 8, it was decided that the austenitising temperatures for the hardenability investigations should be:-

i)   950°C; where for the low carbon alloys all the vanadium carbides would be taken

85

into solution but the vanadium nitrides
would remain partially undissolved.

ii)   1200°C; where for the low carbon alloys
the vanadium carbide and nitride
precipitates would be completely taken
into solution.

4.1.3   Grain Refinement Studies

The adoption of a homogenisation treatment of 1250°C for
4 hours resulted in rapid austenite grain growth.
Therefore the extent to which this grain growth occurred
was investigated using a method devised by Vassiliou
(49).   Test specimens from the low carbon, low vanadium
alloy (613) were homogenised and then quenched into iced
brine.   A fully martensitic structure was produced which
was subsequently tempered at 500°C for 8 hours to allow
carbide precipitation to outline the prior austenite
grain boundaries.   Electrolytic etching for several
minutes in 'Struers' solution, see Appendix A, allowed
the prior austenite grain size to be clearly observed.

To allow direct comparison of the hardenability results
obtained in the present study with those of other authors
using similar vanadium alloys (7-9), it was necessary to
obtain a common grain size by refining the homogenised
grain size, see table 9.   The method used was to
thermally cycle the material through the transformation

region. Grain refinement was achieved because each time there was a phase change each grain produced a number of nucleation sites which resulted in a larger number of grains for the same volume of material. The test specimens were only maintained at the heat treatment temperature for a period of 30 minutes prior to quenching. This procedure restricted grain growth of the new grains and thus maintained a fine grain size. A series of heat treatment routes were investigated, as detailed in table 10, from which the two following methods of grain refinement were selected.

a)   Method (vi) of table 10, one heat treatment cycle to 950°C followed by one cycle to 1200°C.

b)   Method (viii) of table 10, two heat treatment cycles to 950°C.

These heat treatment routes were selected since in addition to achieving the required grain sizes they consisted of a common initial treatment followed by a second treatment equivalent to the austenitising conditions to be used in the hardenability investigations.

4.1.4   Determination of the Method to Refine the Precipitate Morphology during Rolling

The size and distribution of the alloy carbides and nitrides present in an alloy may influence the hardenability of the material, therefore, a method to

refine the precipitates was investigated. It was considered that accelerated cooling between 1050 and 600 °C at a rate of approximately 15°C/sec would suppress the vanadium nitride precipitates formed in the austenitic region (118). The resultant precipitation would be much finer and more widely distributed.

The method of accelerated cooling adopted was to quench the material from 1050°C into a suitable unagitated quenching medium which would allow the bar to cool at the required rate. A suitable quenching medium was determined by implanting a thermocouple at the mid-position along the central axis of a forged bar and using a 'Datalog' recording system the cooling rates from 1050 °C for various quenchants were obtained, see figure 18. It was observed that an average cooling rate of 12.7°C per second could be achieved, by immersion in the standard quenching oil RDN 175 supplied by B.P. International Limited, which was considered acceptable for the purposes of the present study. Consequently, the heat treatment route adopted to refine the alloy precipitates was as follows:-

     i)   Reheat the dressed cast ingot to 1250°C,

     ii)   finish roll into bar at 1050°C,

     iii)   accelerate cool by quenching in oil to 600°C,

     iv)   allow bar to cool in air to room temperature.

4.2   Hardenability Investigations

4.2.1   General Jominy Test Requirements

Standard jominy end quench test specimens (110) were, unless stated otherwise, machined from forged bars which had previously been homogenised at 1250°C for 4 hours and subsequently grain refined by heat treating at 950°C for 30 minutes. The specimens were then austenitised for one hour at treatment temperatures of 950°C or 1200°C under non-oxidising conditions. The required heat treatment conditions for the 950°C austenitising temperature were achieved by inserting the specimens into protective sheaths containing small carbon blocks, in accordance with the British Standard 4437 (119). At the higher austentising temperature of 1200°C the carbon sheath method could not be used due to the diffusion of carbon into the wall of the sheath, thus lowering the melting point to below the jominy test temperature. Consequently, the 1200°C austentising temperatures were achieved using a high temperature inert argon atmosphere furnace.

After one hour at the austenitising temperature the samples were rapidly transferred to a standard jominy rig and end quenched by a jet of water, pre-set at a constant flow rate of 1.7 litres per minute.

Flat surfaces were then carefully ground on opposite sides of the samples and standard Vickers hardness

measurements were taken using a 30 kg load. An average reading from the two flats was used to determine the hardenability of the alloy. The hardenability criterion used was to determine the 50% martensite hardness from the amount of carbon dissolved in the austenite prior to quenching (104). The jominy distance was then taken as the distance from the quenched end of the jominy specimen to the 50% martensite hardness position. This method of assessment effectively eliminated any fluctuations in the carbon contents of the alloys. The resultant jominy distances were then converted into ideal critical diameter values in accordance with the work of Grossmann et al (120). The prior austenite grain size was then determined by examination of the microstructure of the alloys at the quenched end of the jominy specimen. The ideal critical diameter values were subsequently corrected for variations in the prior austenite grain size using the correction factors of Kramer et al (108). For the 950°C austenitising temperature the results were converted to a standard austenite grain size of A.S.T.M. 10 (0.01 mm) while the results from the 1200°C austenitising temperature were converted to a standard austenite grain size of A.S.T.M. 2 (0.16 mm). No corrections to the hardenability results were made for variations in the cooling rate from the two austenitising temperatures, since the effect was expected to be small.

4.2.2 Rates of Heating and Cooling during Jominy testing

To assess the significance of the variation in cooling rate from the two austenitising temperatures, 950 and 1200°C, a series of investigations were performed with jominy specimens implanted with thermocouples. Three standard jominy test specimens from a low carbon low vanadium steel (alloy 613) had thermocouples implanted at fixed positions along the central axes of the bars and were connected to a 'Datalog' recording system. This allowed the temperature along the bars to be continuously monitored during the jominy tests.

A single specimen was used for each of the following investigations:-

i)   to determine the heating and cooling curves associated with jominy end quench test performed at austenitising temperature of 950°C.

ii)   to determine the heating and cooling curves associated with a jominy end quench test performed at an austenitising temperature of 1200°C.

iii)   to record the temperature profiles produced when a standard jominy specimen was austenitised at 1200°C but end quenched from 950°C. The detailed heat treatment route adopted for this trial

was to austenitise the specimen at 1200
° C for one hour, remove the specimen from
the furnace and allow to cool to 950°C
in still air. When at 950° G the
specimen was placed into a second
furnace pre-set at 950°C and allowed to
stabilise for a few minutes prior to
jominy end quench testing.

4.2.3   The Hardenability of Low Carbon Steels
4.2.3.1   Vanadium Base Alloys
4.2.3.1.1   The Effect of Vanadium and Nitrogen
Concentrations

To evaluate the effects of variations in the vanadium and
nitrogen concentrations of a low carbon steel, standard
jominy end quench tests were performed using
austenitising temperatures of 950 and 1200°C for each of
the following alloys:-

i)   Alloy 612; a low vanadium - low nitrogen alloy

ii)   Alloy 617; a high vanadium - low nitrogen alloy

iii)   Alloy 619; a low vanadium - high nitrogen alloy

iv)   Alloy 622; a high vanadium - high nitrogen alloy

In addition a single jominy specimen from a low vanadium
- low nitrogen alloy (No. 613) was austenitised at 1200°C
but quenched from 950°C, in accordance with the procedure
outlined in section 4.2.2. This test was performed to
determine whether the differences in the hardenability

effects at the two austenitising temperature were caused by the variation of the austenitisation temperature in its own right or by its indirect effect upon the rate of cooling during the quenching procedure.

4.2.3.1.2   The Effect of Austenitising Temperature

To assess the effect of the austenitising temperature on the hardenability one specimen from a low vanadium - low nitrogen alloy (No. 613) was jominy tested at each of the following temperatures:-

      i)   1050° C

      ii)   1125° C

      iii)   1275° C

4.2.3.1.3   The Effect of Extended Periods at the
Austenitising Temperature

To investigate the effect of extended time at the austenitising temperature one specimen from each of the alloys 612, 619 and 622 was jominy tested after austenitising at 950° C for the following time periods:-

      i)   4 hours

      ii)   8 hours

4.2.3.1.4   The Effect of Precipitate Morphology
on Hardenability

To investigate the effects of precipitate morphology on hardenability, a low carbon, low vanadium, high nitrogen alloy ingot was manufactured, (No. 777). Half of the

ingot was rolled to bar using the accelerated cooling method, detailed in section 4.1.4, while the second half was processed by the conventional method of air cooling from the final rolling temperature.

Jominy specimens were then machined from the rolled bar and tested in the following ways:-

i)   Two specimens from the conventionally cooled material, in the unhomogenised condition, were tested after austenitising at 950° C for 1 and 8 hours respectively.

ii)   Three specimens from the accelerated cooled material, in the unhomogenised condition, were tested after austenitising at 950°C for 1, 4 and 8 hours.

4.2.3.2   Vanadium-Aluminium Alloys

To evaluate the interactions between vanadium and aluminium, at two nitrogen levels, the ideal critical diameter values were determined after austenitising at both 950 and 1200°C for each of the following alloys:-

i)   Alloy 638; a low vanadium, low nitrogen, aluminium steel.

ii)   Alloy 639; a low vanadium, high

nitrogen, aluminium steel.

In addition the effects of extended austenitising times at 950°C were investigated by performing jominy tests using specimens from alloy 639 austenitised for the following times:-

    i)   4 hours

    ii)   8 hours.

4.2.3.3   Vanadium-Molybdenum Alloys

To determine the hardenability interactions between vanadium and molybdenum, at two nitrogen levels, jominy end quench tests were performed using austenitising temperatures of 950 and 1200°C for both of the following alloys:-

    i)   Alloy 640 - a low vanadium, low nitrogen, molybdenum steel.

    ii)   Alloy 641 - a low vanadium, high nitrogen, molybdenum steel.

Also the effects of extended austenitising times at 950°C on the alloy 641 were determined by jominy testing after the following austenitising times:-

    i)   4 hours

    ii)   8 hours.

4.2.3.4   Vanadium-Niobium Alloys

The vanadium-niobium hardenability interactions, at two nitrogen levels, were determined at austenitising temperatures of 950 and 1200°C respectively, using the

following alloys:-

    i)   Alloy 642; a low vanadium, low nitrogen, niobium steel

    ii)   Alloy 643; a low vanadium, high nitrogen, niobium steel.

4.2.3.5   Vanadium-Titanium Alloys

To evaluate the hardenability interactions between vanadium and titanium, at two nitrogen levels, standard jominy tests were performed using austenitising temperatures of 950 and 1200°C for each of the following alloys:-

    i)   Alloy 644; a low vanadium, low nitrogen, titanium steel

    ii)   Alloy 645; a low vanadium, high nitrogen, titanium steel.

4.2.4   Medium Carbon Steels

4.2.4.1   Vanadium Base Alloys

To determine the effect of the vanadium-nitrogen ratio on the hardenability of a medium carbon steel, jominy end quench tests were performed using austenitising temperatures of 950 and 1200°C for each of the following alloys:-

    i)   Alloy 623 - a low vanadium, low nitrogen steel

    ii)   Alloy 624 - a low vanadium, high

96

nitrogen steel.

4.2.4.2   Vanadium-Aluminium Alloys

To investigate the hardenability interactions between
vanadium and aluminium, at two nitrogen levels, specimens
were jominy tested from austenitising temperatures of 950
and 1200°C for each of the following alloys:-

    i)   Alloy 662; a low vanadium, low nitrogen,
              aluminium steel

    ii)   Alloy 663; a low vanadium, high
              nitrogen, aluminium steel.

4.2.4.3   Vanadium-Molybdenum Alloys

The hardenability interactions between vanadium and
molybdenum were investigated, at two nitrogen levels, by
jominy end quenching specimens from each of the following
alloys using austenitising temperatures of 950 and 1200°C

    i)   Alloy 664; a low vanadium, low nitrogen,
              molybdenum steel

    ii)   Alloy 665; a low vanadium, high
              nitrogen, molybdenum steel.

4.2.4.4   Vanadium-Niobium Alloys

The vanadium-niobium hardenability interactions, at two
nitrogen levels, were determined using austenitising
temperatures of 950 and 1200°C for each of the following
alloys:-

i)   Alloy 671; a low vanadium, low nitrogen, niobium steel

ii)   Alloy 668; a low vanadium, high nitrogen, niobium steel.

4.2.4.5   Vanadium-Titanium Alloys

To determine the effect of vanadium-titanium interactions on the hardenability, at two nitrogen levels, the following alloys were jominy tested using austenitising temperatures of 950 and 1200°C.

i)   Alloy 669; a low vanadium, low nitrogen, titanium steel

ii)   Alloy 672; a low vanadium, high nitrogen, titanium steel.

4.3   High Carbon Vanadium Alloys

4.3.1   Construction of T.T.T. Diagrams

The isothermal transformation characteristics in the transformation temperature range 500 to 650°C, the temperature range that the alloys were expected to exhibit interphase precipitation, were investigated using the following high carbon alloys:-

i)   Alloy 626; a low vanadium, low nitrogen, eutectoid steel

ii)   Alloy 695; a low vanadium, high nitrogen, eutectoid steel.

Specimens from both alloys were heat treated in an inert

atmosphere for 1 hour at 1250°C, to ensure complete solution of the microalloying additions and were then quenched into a salt bath that had previously been pre-set at the required transformation temperature. The specimens were allowed to isothermally transform for various times before quenching in water at approximately 20°C. The specimens were then sectioned and metallographically examined. Where only partial transformation had occurred the structures were examined by quantitative metallography, using the 'Optimax' system, for the proportion of the structure remaining untransformed. From these results the Time-Temperature-Transformation (T.T.T.) diagrams for the two alloys were constructed.

Specimens that exhibited fully transformed structures were hardness tested using a standard Vickers hardness testing machine with a 30 kg load.

4.3.2   S.E.M. and T.E.M. Examinations
The specimens used for the construction of the T.T.T. diagrams were examined to investigate the precipitation of vanadium carbides within the ferritic lamellae of the pearlitic structure. An initial examination was performed using Scanning Electron Microscopy (S.E.M.) techniques.

In addition carbon replicas and thin foil specimens were

studied using Transmission Electron Microscopy (T.E.M.)
techniques.

4.3.3   Mechanical Properties Evaluation

The mechanical properties of the two eutectoid alloys
(626 and 695) were determined at each of the isothermal
transformation temperatures. Standard Charpy and tensile
specimens were produced using a two stage machining
process, see figures 19 and 20. The specimens were rough
machined prior to solution treatment at 1250°C for 1 hour
in an inert atmosphere and then quenched into a salt
bath, pre-set at the isothermal transformation
temperature. The specimens were allowed to transform
fully prior to water quenching. Final machining of the
specimens to size was performed and the specimens
subsequently tested. A two stage manufacturing process
was adopted so that during quenching, from the solution
treatment temperature to the isothermal transformation
temperature, the specimens could reach the required
temperature as quickly as possible, but still allow any
surface contamination, or decarburisation caused by the
heat treatment process, to be removed during the final
stage machining.

Standard Charpy impact tests for specimens isothermally
transformed at 550, 575, 600, 625 and 650°C were
performed at each of the following test temperatures.

> i)   room temperature

ii)   100°C

iii)   200°C

iv)   250°C

In addition standard tensile specimens were tested, from the same isothermal transformation temperatures, at room temperature using an Instron type 1200 series tensile testing machine.

5.   Experimental Results and Preliminary Discussion

5.1   Hardenability Results

In the presentation of the hardenability results it was considered necessary, due to the complexity of the alloying interactions, that a preliminary qualitative interpretation of the observations was included in this section.   The method adopted was to take a base alloy with a base hardenability value and observe changes in the ideal critical diameter value as the alloying elements in the steel varied from that of the base steel. Typical factors that were considered for the interpretation were:-

i)   the quantity of microalloying elements in solution.

ii)   the ability of the elements in solution to segregate to, or desegregate from, the prior austenite grain boundaries.

iii)   the ability of the elements to form clusters or complexes which exhibit different influences on the hardenability.

iv)   the quantity, particle size and distribution of undissolved alloy carbide/nitride precipitates.

v)   the ability of undissolved precipitates to act as preferred sites for the transformation from austenite.

vi)   the ability of the undissolved
precipitates to act as grain boundary
pinning agents and maintain immobilised
austenite grain boundaries.

5.1.1   Jominy Heat Treatment Curves

Utilising thermocouples implanted at various positions
along the central axis of standard jominy specimens it
was possible to construct heating and cooling curves for
tests performed at both $950°C$ and $1200°C$ austenitising
temperatures. The temperature along the length of the
bars increased uniformly during the heating cycle and
could therefore be expressed as a single curve for each
of the austenitising temperatures, as shown in figure 21.
The results obtained show that despite the different
rates of heating the final austenitising temperature was
achieved after similar time periods, approximately 25
minutes. However, the cooling curves from the two
temperatures not only varied due to the initial
temperature but also as a function of the position of the
thermocouple from the quenched end.

Consequently, the resultant cooling curves were expressed
isometrically in figures 22 and 23 respectively. This
variation in the cooling rates of the two specimens must
have a direct influence on the hardenability but was
considered to be small compared with the other
hardenability factors which were being investigated.

103

However, to confirm this assumption a third implanted specimen was used to record the temperature profiles produced when a jominy specimen was austenitised at 1200 °C, cooled in still air to 950°C, allowed to stabilise and subsequently end quenched from a 950°C austenitising temperature, see figure 24. Having confirmed that the heat treatment route successfully represented a situation where the specimen was austenitised at 1200°C but quenched using the cooling rates associated with a 950°C austenitising temperature, it was possible to determine if the change in austenitising temperature or the rate of cooling of the jominy bar was the most significant on the hardenability. Results to be presented in detail in section 5.1.2.2.1 confirm that the austenitising temperature is a more dominant factor on the hardenability than the rate of cooling. Consequently, no correction for variation in cooling rate was attempted.

5.1.2 Hardenability of Low Carbon Steels

5.1.2.1 Low Carbon-Vanadium Alloys

5.1.2.1.1 Hardenability Results Using 950 and
1200°C Austenitising Temperatures

Standard jominy test specimens from each of the four vanadium alloys, (Alloys 612, 617, 619 and 622), were jominy end quench tested after soaking for one hour at the austenitising temperatures. The ideal critical diameter values calculated from the jominy tests, corrected to a common grain size of ASTM 10 for the 950°C

austenitising temperature and ASTM 2 for the 1200°C austenitising temperature, are presented in tables 11 and 12 respectively.

In vanadium steels it is generally accepted that increasing the vanadium content of an alloy increases the hardenability, providing that the vanadium is dissolved in the austenite at the austenitising temperature. Therefore, the theoretical quantities of microalloying elements present in solution were calculated, using standard solubility data (1), for 950°C and 1200°C, and are presented in tables 13 and 14 respectively. Consequently, the hardenability results were expressed in terms of vanadium in solution, see figures 25 and 26.

At the lower austenitising temperature of 950°C the classical hardenability relationship was observed where increasing the vanadium in solution increased the hardenability of the alloy.
At the 1200°C austenitising temperature increasing the vanadium in solution resulted in a slight decrease in the hardenability of the alloy. Therefore the mechanisms which were dominant at the lower austenitising temperature were not dominant at the higher austenitising temperature. Although published hardenability data using an austenitising temperature of 1200°C, is very limited, Eldis et al (7) reported that the carbide-nitride

formers, such as vanadium, niobium and titanium, initially increased the hardenability at 1200°C but then caused a decrease in hardenability at higher alloy concentrations, see figure 14. Eldis proposed that the decrease in hardenability was caused by the alloys exceeding the vanadium-carbon solubility limit and therefore removing both vanadium and carbon from solution. However, from standard solubility equations all the vanadium and carbon present in the alloys studied by Eldis would have been taken into solution at a temperature as low as 850°C, see Appendix B. Although no viable explanation of the results was presented in the work by Eldis, it did confirm the results obtained in the present study. Consequently, the relationships between vanadium and hardenability are more complicated than were initially believed and appear to be austenitising temperature dependent.

When formulating standard equations to describe the hardenability of an alloy it is normally accepted that the ideal critical diameter value depends upon the carbon content of the steel, the grain size and the amount of other alloying elements in solution at the austenitising temperature. In the present study, the hardenabilities were calculated using the distance from the quenched end of the jominy bar to the 50% martensite hardness position. Therefore, to eliminate the effect of variations in the carbon content of the alloys, the 50%

martensite hardness value was calculated for each individual alloy. Consequently, by converting all the ideal critical diameter values for the vanadium alloys, austenitised at both 950 and 1200°C, to a single grain size, ASTM 4, it was possible to observe the individual effects of the microalloying additions, see table 15 and figure 27. If the hardenability was only due to the vanadium in solution and was independent of the austenitising temperature, the plot of the corrected ideal critical diameter value against vanadium in solution would have resulted in all the data lying on a single curve. However, it can be seen from figure 27 that the corrected ideal critical diameter values for the 1200°C austenitising temperature were significantly lower than those obtained at the 950°C austenitising temperature. This confirmed the earlier observed austenitising temperature dependance of the vanadium hardenability effects. Since the 1200°C results were lower than the 950°C results for equivalent vanadium concentrations in solution, the effectiveness of vanadium, with respect to increasing the hardenability, must be reduced as the austenitising temperature is increased. However, as the quenching rates from the two austenitising temperatures were different, the observed variation in hardenability results could have been caused by the quenching process rather than by the variation in the austenitising temperature. Therefore, a further

jominy specimen was austenitised at 1200°C, rapidly
cooled to 950°C in air and then end quenched at a rate
similar to that observed during the 950°C jominy tests.
The result from this test, which is included in table 15
and figure 27, was similar to the 1200°C austenitising
temperature results rather than the 950°C austenitising
temperature results. Therefore, the observed differences
in hardenability for the two sets of results must be
associated with the austenitising temperature rather than
the jominy specimen quench rate.

5.1.2.1.2   The Effect of Austenitising Temperature
             on Hardenability

To evaluate the effect of austenitising temperature on
the hardenability, a series of low carbon-low vanadium
alloys were tested at various austenitising temperatures
between 950 and 1275°C. The ideal critical diameter
values obtained were corrected to a single austenite
grain size, ASTM 4, and are presented in table 16 and
figure 28. It can be seen that increasing the
austenitising temperature resulted in a progressive
decrease in the hardenability of the alloy.

Above an austenitising temperature of 1090°C all the
vanadium nitride precipitates would be taken into
solution resulting in the maximum amounts of vanadium and
nitrogen being available to influence the hardenability.
Therefore, the observed decrease in the ideal critical

diameter value was not associated with a change in the quantity of microalloying additions in solution or by the presence of precipitation. Consequently, the decrease in hardenability must be related to the increase in temperature. It has been proposed that hardenability is dependent not only upon the quantity of microalloying elements in solution but also only their ability to segregate to the grain boundaries (121). The greater quantity of microalloying elements segregated to the grain boundaries the more nucleation sites for the transformation from austenite are eliminated. In addition according to the work by Garbarz and Pickering (122), the effectiveness of the microalloying additions is dependent upon the rate of segregation, of the elements in solution to the grain boundaries, in relation to the rate at which the grain boundaries are moving during grain growth. The slower the rate of segregation, or faster the rate of grain growth, the lower will be the resulting effectiveness of the microalloying elements in solution. Therefore, at the higher temperatures where the grain boundaries are unpinned and the grains grow rapidly the microalloying elements become less effective and result in a decrease in hardenability.

In addition as the austenitising temperature is increased the microalloying elements present in solution possess greater thermal energy and are therefore more easily

displaced from the prior austenite grain boundaries. This reduction in the level of segregation to the grain boundaries results in an additional decrease in the hardenability of the alloy.

Below an austenitising temperature of 1090°C the situation is further complicated by the presence of undissolved vanadium nitride precipitates. The influence of the precipitates depends upon three factors, namely their effect as preferential nucleation sites for the transformation from austenite, the effect of reducing the available microalloying elements in solution and the effect of pinning the prior austenite grain boundaries and refining the austenite grain size.

As the temperature is raised from 950 to 1090°C the amount of precipitation would be reduced as extra vanadium and nitrogen would be taken into solution. Therefore, if the precipitates act as nucleation sites for the transformation from austenite the decrease in the volume fraction of precipitates with increasing temperature would be expected to increase the ideal critical diameter of the alloy. However, the precipitates which would be expected to influence the hardenability are those formed at high temperatures in the austenite and grow to a large size. Therefore, since these precipitates would be the slowest to be taken into solution the increase in hardenability due to the

110

reduction in the precipitation would be expected to be small.

In addition the extra vanadium and nitrogen taken into solution as the temperature was increased would also have been expected to have increased the hardenability of the alloy. However, as the temperature is increased the driving force for segregation is reduced and could therefore result in a decrease in hardenability despite an increase in the microalloying elements in solution.

As previously mentioned pinning of the grain boundaries by precipitates can be an important factor in the promotion of increased hardenability. However, as the temperature was raised from 950 to 1090°C there was only a very small increase in the prior austenite grain size, see table 16 indicating that the boundaries were still being effectively pinned despite the reduction in the quantity of undissolved vanadium nitride. Therefore, the grain boundary pinning effects of the precipitates could be ignored over this temperature range.

Consequently, the observed decrease in hardenability observed between 950°C and 1090°C must be directly associated with the increase in the thermal energy of the microalloying elements in solution and therefore reducing the driving force for the segregation process to the

111

prior austenite grain boundaries, i.e. thermal dispersion
of the alloying elements away from the grain boundaries.

5.1.2.1.3   The Effect of Extended Times at an
             Austenitising Temperature of 950°C

It was considered possible that at an austenitising
temperature of 950°C the hardenability of the alloy could
be dependent upon the rate at which the vanadium
carbide/nitride precipitates were taken into solution.
Consequently, a series of low carbon-vanadium steels were
jominy end quench tested after austenitising at a
temperature of 950°C for periods of one, four and eight
hours respectively. The results, corrected to a constant
grain size of ASTM 10 , presented in table 17 and figure
29, show that the ideal critical diameter value for each
of the alloys progressively increased with increasing
time at the solution treatment temperature. The observed
increase in hardenability could have been caused by two
factors. Firstly, the extended time at the austenitising
temperature could allow more vanadium carbide/nitride
precipitates to dissolve allowing greater quantities of
both vanadium and nitrogen to be in solution and thus
influence the hardenability of the alloy. At the longer
times a maximum hardenability value was obtained which
could coincide with the situation where the equilibrium
quantities of vanadium, carbon and nitrogen are in
solution. The temperatures at which vanadium nitrides
are dissolved are much higher than those for vanadium

carbides. Therefore it must be considered that the dominant effect would be the rate of solution of the vanadium nitride precipitates. If the hardenability is due to the rate of solution of the precipitates their morphology and distribution throughout the alloy must be important. A fine dispersion of precipitates, such as produced by interphase precipitation (20), would be expected to dissolve at a faster rate than a coarse dispersion and would therefore reach a maximum hardenability after a shorter austenitising period.

Alternatively, the increase in the hardenability with increasing austenitising time could be caused by the rate of segregation of the microalloying elements in solution to the grain boundaries. The longer the time the specimen is held at the austenitising temperature the more established will the segregation phenomenon become until at the longer time periods the equilibrium segregation conditions are obtained where a maximum ideal critical diameter value is observed.

The kinetic effects encountered at the 950°C austenitising temperature result in a more complicated evaluation of the hardenability processes occurring since after one hour a meta-stable situation is obtained where the full influence of the microalloying elements is not observed. Ideally, to eliminate the kinetic effects on

113

the assessment of steels with sparingly soluble
precipitates, the hardenability investigations should be
performed after extended austenitising periods.

It can be seen from figure 30, that the relationship
between the corrected ideal critical diameter values and
the theoretical quantitives of vanadium in solution are
significantly different after austentising for one and
eight hours respectively. The generally accepted
progressive increase in hardenability for an increase in
the amount of vanadium in solution is only observed after
a one hour austenitising period. The results obtained
after an eight hours at the austenitising temperature
show that the two high nitrogen alloys exhibit higher
hardenabilities than the low nitrogen alloy irrespective
of the quantity of vanadium in solution. Consequently,
it must be assumed that the hardenability is determined
by a number of contributing factors. In addition to
being dependent upon the quantities of microalloying
elements in solution, the hardenability may also be
dependent upon the rate at which the precipitates are
dissolved, and the alloying elements are taken into
solution. Also for the microalloying elements to be
effective they must segregate to the prior austenite
grain boundaries. Therefore, the ideal critical diameter
value will also be dependent upon the rate of segregation
of the microalloying additions. However, the presence of
any remaining precipitates will also have an influence on

114

the hardenability. The undissolved precipitates can act as preferential nucleation sites for the transformation from austenite and they can also act as grain boundary pinning agents.

If the rates at which the alloy precipitates are dissolved are considered, the difference in the hardenability trends observed for one and eight hours respectively, see figure 30, can be explained. Vanadium nitride precipitates are significantly more stable than vanadium carbide precipitates at a temperature of 950°C. Consequently, for short austenitising periods the hardenability of the alloy is essentially controlled by the rate of solution of the vanadium carbides, since little time is available for the slower dissolving vanadium nitrides to enter solution. However, as the austenitising times are extended more time is available for the vanadium nitrides to be dissolved and influence the hardenability of the alloy.

5.1.2.1.4   The Effect of Precipitate Morphology on
             Hardenability at an Austenitising
             Temperature of 950°C

To evaluate the effect of precipitate morphology on the hardenability, a series of jominy end quench tests were performed on a low carbon-low vanadium steel (cast number 777). Half the cast ingot was conventionally rolled into

bar and allowed to air cool from the final rolling
temperature of 1050°C. The second half of the ingot was
rolled into bar using a modified technique in order to
refine the precipitate morphology of the alloy, as
described in section 4.1.4. A portion of the bar
produced by the modified route was subsequently
homogenised and grain refined. This material was
homogenised in order to assess the effect of the
homogenisation process, adopted in the the earlier
hardenability investigations, to eliminate the effect of
silicon segregation. In addition it was considered that
the homogenisation process would eliminate any beneficial
effects of the refinement treatment by dissolving the
precipitates at 1250°C and producing larger precipitates
in the austenitic temperature range upon cooling

From the results presented in table 18 and figure 31, it
can be seen that after austenitising at 950°C for one
hour the ideal critical diameter value, corrected to a
standard grain size of ASTM 10, the unhomogenised
accelerated cooled specimen was only slightly higher than
the unhomogenised conventionally cooled specimen.
However, after four hours a significant difference
between the two types of specimens was observed. This
indicated that as expected the finer vanadium nitride
precipitates produced by the accelerated cooling
technique were being dissolved more rapidly than the

coarse precipitates produced by the conventional rolling
technique. In addition, after eight hours at the
austenitising temperature all the effects due to the
precipitate morphologies were eliminated since the
equilibrium quantities of microalloying elements in
solution were achieved and equivalent hardenability
values obtained.

Homogenisation of the material produced by the
accelerated cooling method resulted in a hardenability
curve that was significantly different from the
unhomogenised curve, see figure 31. The initial ideal
critical diameter value was lower, than for the
unhomogenised specimen, but the rate of increase in
hardenability with time was greater. The difference in
the results obtained after austenitising for one hour was
thought to be due to the grain refinement treatment
employed after homogenisation. Thermally cycling the
material through the transformation region caused the
formation of new grain boundaries where the segregation
of the microalloying elements was kept to a minimum by
the short time period .These new low segregation level
grain boundaries would be less effective in retarding the
transformation and would therefore result in a reduced
ideal critical diameter value. However, the rate at
which the hardenability increases with time is dependent
upon the rate of solution of the microalloying elements
and the rate at which they segregate to the prior

austenite grain boundaries. Considering, the
unhomogenised specimens the rate of increase in
hardenability is additionally influenced by the amount of
silicon segregation. As observed in section 4.1.1
silicon segregation, present in the unhomogenised
specimens, resulted in preferential nucleation of the
transformation products of austenite and was only
eliminated after 4 hours at 1250° C. Therefore at an
austenitising temperature of 950° C only at periods
greatly in excess of 4 hours would the preferential
nucleation phenomenon be eliminated.

5.1.2.2   Low Carbon-Vanadium-Aluminium Alloys

5.1.2.2.1   Hardenability Results Using a 950° C
Austenitising Temperature

The addition of aluminium to a low carbon-low vanadium
steel (alloy 638) increased the ideal critical diameter
value, see table 19 and figure 32. Aluminium is a strong
nitride forming element and would be expected to
preferentially combine with the nitrogen present to form
aluminium nitride. This would result in less nitrogen
being available to form vanadium nitrides and therefore
allow more vanadium to influence the hardenability. In
addition a small quantity of aluminium was taken into
solution as shown in table 20. At an austenitising
temperature of 950°C, an increase in vanadium and
aluminium in solution would be expected to increase the

hardenability while a reduction in nitrogen in solution would be expected to reduce the hardenability. Consequently, from consideration of the quantities of microalloying elements in solution the observed increase in hardenability could be explained in terms of the combined positive effects of the vanadium and aluminium in solution dominating the negative effect of the reduced nitrogen in solution. However, the effect of the precipitation present must also be considered. As previously stated the quantity of vanadium nitride precipitates would be reduced and would therefore be expected to cause an increase in hardenability due to the removal of the precipitates as preferred nucleation sites for the transformation from austenite. Similarly, the increase in aluminium nitride precipitates would be expected to increase the number of possible nucleation sites and thus reduce the hardenability.

The addition of aluminium and extra nitrogen to the base vanadium steel (alloy 639) resulted in an increase in the ideal critical diameter value when compared with the base alloy (612) but no change when compared with the vanadium-aluminium-low nitrogen alloy (638), see table 19 and figure 32. The equivalent hardenability values obtained when the two aluminium containing alloys were compared must be due to a balance in the individual hardenability effects. Considering the theoretical quantities of the microalloying elements in solution it

can be seen from table 20 that the nitrogen in solution is increased whilst the vanadium and aluminium in solution is decreased. Additionally the extra nitrogen in the alloy resulted in significantly more aluminium and vanadium nitride precipitation which could act as preferred nucleation sites for the transformation from austenite and thus reduce the hardenability. Consequently the positive effect of the extra nitrogen in solution under these conditions must be equal to the combined effects of the reduced vanadium and aluminium in solution and the increased amount of precipitation.

5.1.2.2.2   The Effect of Extended Times at a 950°C
             Austenitising Temperature

In section 5.1.2.1.3 it was stated that after one hour at an austenitising temperature of 950°C the equilibrium conditions were not obtained. Therefore, further jominy tests were performed after four and eight hours at the austenitising temperature for the vanadium-aluminium-high nitrogen alloy (639). The ideal critical diameter values presented in table 21 and figure 29, show that compared with the vanadium-high nitrogen alloy (619) the initial hardenability values obtained were higher but the rate at which the hardenability increased with increasing time at 950°C was lower. The significant increases in hardenability at the shorter austenitising intervals, when aluminium is added to a vanadium alloy, is due to

the aluminium nitride precipitation allowing more
vanadium to enter solution and influence the
hardenability of the alloy. However, the rate at which
the hardenability increases with increasing time at the
austenitising temperature is dependent upon the rate at
which the alloy nitride precipitates dissolve.
Therefore, the rate of increase in hardenability for the
vanadium alloy is dependent upon the rate of solution of
vanadium nitride precipitate whereas in the vanadium-
aluminium alloy it is dependent upon the rate of solution
of the aluminium nitrides. Also the hardenability is
dependent upon the rate at which the microalloying
elements from the dissolving precipitates segregate to
the prior austenite grain boundaries. Consequently,
since aluminium nitrides are more stable than vanadium
nitrides the observed slower rate of increase in
hardenability was expected in the alloy containing
aluminium.

5.1.2.2.3   Hardenability Results Using a 1200°C
            Austenitising Temperature

The effect of adding aluminium to a low carbon-low
vanadium steel (alloy 638) was to increase the ideal
critical diameter value obtained, see table 22 and figure
34. At an austenitising temperature of 1200°C all the
vanadium and the majority of the aluminium and nitrogen
in the alloy would be taken into solution, see table 23.
Therefore, considering the theoretical quantities of

121

microalloying elements in solution, it can be seen that
in the aluminium containing steel the quantities of
vanadium and nitrogen in solution were decreased whereas
an additional amount of aluminium was present in
solution. At 1200°C a reduction in vanadium and nitrogen
in solution would result in the formation of vanadium-
carbon-nitrogen clusters which would diffuse more easily.
Therefore, the clusters would be expected to be easier to
thermally disperse from the prior austenite grain
boundaries and result in a reduction in hardenability.
The aluminium in solution however, would be expected to
form aluminium-nitrogen clusters which, due to the size
of the aluminium atom, would be slower to diffuse but
once established at the grain boundary would tend to be
more difficult to thermally disperse and thus increase
the ideal critical diameter. If the grain boundaries
migrated the slow diffusing clusters would find it more
difficult to move with the grain boundaries. Therefore,
if the rate of grain boundary movement exceeded the rate
of diffusion of the cluster desegregation would occur
with an associated decrease in the hardenability.
Consequently, the role of the precipitates remaining at
the austenitising temperature could be significant. Due
to the wide dispersion of the aluminium nitrides at 1200
°C they would tend to be ineffective at pinning the
austenite grain boundaries but would tend to act as
preferred nucleation sites for transformation and

therefore be expected to reduce the hardenability.

The addition of aluminium and extra nitrogen (alloy 639) resulted in a decrease in the ideal critical diameter value when compared with both the base vanadium alloy (612) and the aluminium, low nitrogen steel (638), see table 22 and figure 34. It can be seen from table 23 that the nitrogen in solution, for the base vanadium alloy and the aluminium, high nitrogen alloy, was approximately equal and could therefore be ignored. But the vanadium in solution decreased while the aluminium in solution increased. The effect that these changes in microalloying elements in solution had on the hardenability would be dependent upon whether the austenite grain boundaries were effectively pinned. Although the addition of extra nitrogen resulted in an increase in the amount of aluminium nitride precipitation present it was not considered adequate to successfully pin the grain boundaries. Therefore, the decrease in vanadium in solution would be expected to increase the hardenability by producing a cluster that could more easily diffuse with the migrating grain boundaries, whereas, the increase in aluminium would result in clusters which would diffuse more slowly and be less able to move with the boundaries, and cause a decrease in ideal critical diameter. In addition the extra aluminium nitrides would act as preferred nucleation sites for the austenite transformation and therefore tend to decrease

the hardenability.

The decrease in hardenability when comparing the two aluminium containing alloys was associated with the changes in microalloying elements in solution. It can be seen from table 23 that both the vanadium and aluminium in solution were increased, while the quantity of nitrogen in solution was decreased. Again assuming the grain boundaries were not adequately pinned the increase in both vanadium and aluminium in solution would be expected to form clusters which were more difficult to diffuse and could therefore be unable to move with the migrating grain boundaries. This would cause an associated decrease in the ideal critical diameter of the steel. However, the reduction in nitrogen in solution would cause the clusters to diffuse more easily and tend to increase the hardenability. In addition, the extra aluminium nitrides present in the high nitrogen alloy would tend to act as preferred sites for transformation and contribute to the observed decrease in the ideal critical diameter value of the steel.

5.1.2.3   Low Carbon-Vanadium-Molybdenum Alloys

5.1.2.3.1   Hardenability Results Using a 950° C
            Austenitising Temperature

The addition of molybdenum to a base vanadium steel (alloy 640) resulted in an increase in the ideal critical

diameter value, see table 19 and figure 32. Considering the amounts of microalloying elements in solution, see table 20, the vanadium and nitrogen in solution for the two alloys were very similar and could be ignored. Consequently, the increase in hardenability must have been directly related to the amount of molybdenum in solution. Calculation of the hardenability multiplying factor for molybdenum resulted in a figure of 1.15 for a 0.10% molybdenum addition. The average factor for molybdenum, according to Mangonon (9) is 1.12 when added singly but increases to 1.22 for a 0.10% molybdenum addition when in combination with vanadium. Therefore, there is good agreement between the present study and other published work.

The addition of molybdenum and extra nitrogen to a base vanadium steel (alloy 641) resulted in an increase in the ideal critical diameter value when compared with the base vanadium alloy (612) but a decrease when compared with the molybdenum-low nitrogen alloy (640), see table 19 and figure 32. Considering the microalloying elements in solution the observed increase in hardenability when compared with the base vanadium alloy must be associated with the molybdenum in solution at the austenitising temperature. It can be seen that all the molybdenum was taken into solution and was therefore available to increase the hardenability of the alloy. However, the extra nitrogen caused increased vanadium nitride

precipitation and thus less vanadium in solution to influence the ideal critical diameter value. Both the increased precipitation and the reduction in the vanadium in solution would tend to reduce the hardenability rather than cause the observed increase.

The decrease in the ideal critical diameter when compared with the molybdenum-low nitrogen alloy was associated with the combined effect of a reduced quantity of vanadium in solution and an increase in the amount of precipitation. It can be seen from table 20 that there was no change in the amount of molybdenum in solution, and only a slight increase in nitrogen in solution, which could therefore be ignored.

5.1.2.3.2 The Effect of Extended Times at a 950°C Austenitising Temperature

To investigate the kinetic effects in vanadium-molybdenum alloys, additional jominy end quench tests were performed on the vanadium-molybdenum-high nitrogen alloy (641) after austenitising at 950°C for 4 and 8 hours respectively. The results presented in table 21 and figure 33 show a high initial hardenability at short austenitising periods which gradually increased with extended times at temperature until a maximum hardenability was achieved. The high hardenability observed at the short austenitising periods was caused by

the molybdenum rapidly entering solution and therefore being available to inhibit the transformation. Also it has been suggested (123) that the presence of molybdenum increases the solubility of vanadium in an alloy. The resulting extra microalloying elements in solution would also tend to increase the hardenability of the alloy.

The gradual increase in the ideal critical diameter value with extended austenitising times was believed to be due to the kinetics of solution of the vanadium nitride precipitates. Comparison of the curves for the vanadium-molybdenum-high nitrogen (641) and the vanadium-high nitrogen alloy (619) shows that the rate of increase of hardenability of the molybdenum alloy was higher than that of the base alloy. This indicates that the solubility of the vanadium nitride precipitates, or possibly the rate of segregation of the microalloying elements to the grain boundaries, is enhanced by the presence of molybdenum in solution and would therefore support the observations of Watanabe (123).

5.1.2.3.3   Hardenability Results Using a 1200°C
            Austenitising Temperature

The addition of molybdenum to a base vanadium steel (alloy 640) caused an increase in the ideal critical diameter value obtained, see table 22 and figure 34. At an austenitising temperature of 1200°C all the microalloying elements were taken into solution and were

127

available to influence the hardenability of the alloy.
It can be seen from table 23 that compared with the base
vanadium alloy there was a slight reduction in the
amounts of both vanadium and nitrogen in solution but a
significant additional quantity of molybdenum in
solution. The reduction in vanadium in solution would
tend to form a vanadium-carbon-nitrogen cluster that was
able to diffuse more readily and would therefore be more
easily thermally dispersed from the grain boundaries.
However, if the grain boundaries migrated the clusters
would more easily move with the boundaries and maintain a
high hardenability. Similarly, a reduction in nitrogen
in solution would also form vanadium-carbon-nitrogen
clusters which could diffuse more easily and therefore
increase the hardenability. However, it is considered
that the dominant effect would be the large quantity of
molybdenum taken into solution, which indicates that even
at 1200°C the presence of molybdenum increases the ideal
critical diameter.

The addition of molybdenum and extra nitrogen to a base
vanadium steel (alloy 641) resulted in an increase in the
ideal critical diameter when compared with both the base
vanadium alloy (612) and the molybdenum-low nitrogen
alloy (640), see table 22 and figure 34. The increase in
hardenability when compared with the base vanadium alloy
was associated with the combined effects of the decreased

vanadium in solution, the increased nitrogen and the additional molybdenum in solution, see table 23. However, again it would be expected that the dominant factor on the hardenability would be the large quantity of molybdenum.

Comparing the theoretical quantities of microalloying elements in solution for the two molybdenum alloys, it can be seen from table 23 that the steels contained equivalent quantities of molybdenum in solution, which could therefore be ignored. Consequently, the observed increase in hardenability was associated with the decrease in vanadium in solution and the increase in nitrogen in solution. Since no precipitates were retained at the austenitising temperature of 1200°C the grain boundaries would be free to migrate. Therefore a decrease in vanadium in solution would form a vanadium-carbon-nitrogen cluster which could diffuse more easily. These clusters would be more able to migrate with the moving grain boundaries and would therefore be expected to increase the hardenability, whereas, the increase in the nitrogen in solution would slow down the diffusion rate of the vanadium-carbon-nitrogen clusters and would tend to decrease the ideal critical diameter.

5.1.2.4   Low Carbon-Vanadium-Niobium Alloys

5.1.2.4.1   Hardenability Results Using a 950°C
            Austenitising Temperature

The addition of niobium to a base vanadium steel (alloy

642) resulted in an increase in the ideal critical diameter, see table 19 and figure 32. Niobium is a strong carbide/nitride forming element and would result in the precipitation of niobium carbides/nitrides in preference to vanadium carbides/nitrides. Consequently, more vanadium would be available in solution to segregate to the prior austenite grain boundaries and enhance the hardenability, see table 20. In addition, niobium would also be taken into solution and would be expected to increase the hardenability. However, the quantity of niobium in solution was small due to the precipitation of both niobium nitride and niobium carbide. The removal of carbon from solution was very small and was considered insufficient to alter the 50% martensite hardness and therefore the calculated hardenability value. However, the change in the type and dispersion of the precipitates would be expected to have an influence on the hardenability by changing the effectiveness of the precipitates in reducing grain boundary movement and the extent to which they might act as nucleation sites for the transformation.

The addition of niobium plus extra nitrogen to the base steel (alloy 643) resulted in an increase in hardenability when compared with both the base vanadium alloy (612) and the vanadium-niobium-low nitrogen alloy (642), see table 19 and figure 32. Comparing the

theoretical quantities of microalloying elements in solution with the base vanadium alloy, it can be seen from table 20 that the vanadium in solution was decreased but both the niobium and nitrogen in solution slightly increased. Therefore, the observed increase in hardenability was unexpected since the result suggests that the positive effect of the slight increase in niobium and nitrogen in solution more than offset the much larger reduction of vanadium in solution. However, it should be mentioned that niobium has been reported to be a powerful hardenability agent (2)(124). It is also possible that the increase in hardenability could be caused by the different precipitation effects present. The addition of extra nitrogen resulted in approximately the same amount of vanadium nitride precipitation but also extensive additional niobium nitride precipitation. If this extra niobium nitride precipitation more effectively pinned the prior austenite grain boundaries, and did not significantly act as preferred sites for the transformation from austenite, then the segregation of the microalloying elements to the grain boundaries could more easily be achieved and therefore result in the observed increase in the hardenability of the alloy.

Comparing the microalloying elements in solution for the two niobium alloys, it can be seen from table 20 that the vanadium and niobium in solution were decreased, whereas

the nitrogen in solution was increased. Therefore, to increase the hardenability the effect of the nitrogen in solution must have been greater than the combined effect of the reduction in vanadium and niobium in solution. However, the precipitates present at the austenitising temperature could also enhance the hardenability by more effectively pinning the austenite grain boundaries and thus allowing segregation to the grain boundaries to be more easily established. In the low nitrogen steel (642) niobium carbides and niobium nitrides are present at 950 °C but no vanadium carbides or nitrides. However, in the high nitrogen steel (643) vanadium nitride and an increased amount of niobium nitride was present but no vanadium or niobium carbides. Consequently, the combination of precipitates present in the high nitrogen steel would be expected to increase the hardenability since the increased quantity of niobium nitrides and the vanadium nitrides would more effectively pin the austenite grain boundaries. In addition the elimination of the larger niobium carbides would result in a reduction in the amount of preferential nucleation occurring during transformation and a corresponding increase in hardenability.

5.1.2.4.2 Hardenability Results Using a 1200°C Austenitising Temperature

The addition of niobium to the base vanadium steel (alloy

642) resulted in a decrease in the ideal critical diameter, see table 22 and figure 34. Comparing the theoretical quantities of microalloying elements in solution it can be seen, from table 23, that the niobium alloy contained slightly less vanadium and nitrogen in solution but an additional quantity of niobium in solution. Consequently, since the changes in vanadium and nitrogen in solution were very small, compared to the niobium in solution, it is suggested that under these conditions increasing niobium in solution decreased the hardenability of the alloy. The work of Eldis et al (7), figure 14, showed that the addition of niobium, at an austenitising temperature of 1200°C, initially increased the hardenability of the alloy but resulted in a subsequent decrease in hardenability at higher concentrations. It is possible that at low niobium levels the niobium in solution combines with the nitrogen and/or carbon to form grain boundary clusters which increase the hardenability. However, at higher niobium concentrations the niobium in solution could compete with the vanadium in solution to form clusters with the available nitrogen and carbon in solution. A niobium rich cluster rather than a vanadium cluster would be more difficult to thermally disperse from the austenite grain boundaries and/therefore increase the hardenability. Howver, its rate of diffusion will be slower than a vanadium cluster and therefore if the grain boundaries migrate it will be more difficult for the niobium rich

133

clusters to move with the grain boundaries.
Consequently, when the rate of grain boundary movement
exceeds the rate of diffusion of the nitrogen rich
cluster an associated decrease in hardenability would
occur, as was observed.

The addition of niobium plus extra nitrogen to the base
vanadium steel (alloy 643) resulted in a large increase
in hardenability when compared with both the base
vanadium alloy (612) and the vanadium-niobium-low
nitrogen alloy (642), see table 22 and figure 34. In the
niobium-high nitrogen alloy some niobium nitride
precipitates were not taken into solution even at the
1200° C austenitising temperature. The effect of these
precipitates would be to decrease the hardenability since
they would act as preferred nucleation sites for the
transformation but increase the hardenability by pinning
the prior austenite grain boundaries allowing segregation
of the microalloying elements in solution to be
established. Comparing the calculated quantities of
microalloying elements in solution for the niobium-high
nitrogen alloy and the base vanadium alloy it can be
seen, from table 23, that there was a slight decrease in
vanadium in solution but a significant increase in both
the niobium and nitrogen in solution. Therefore, it
would appear that if the correct niobium and nitrogen
combinations can be achieved significant increases in

hardenability can be obtained. The extra niobium nitride precipitates would significantly contribute to the increase in the ideal critical diameter by more effectively pinning the prior austenite grain boundaries. Therefore, the segregation phenomenon could be maintained even at the higher austenitising temperature and result in a higher hardenability.

Comparing the microalloying elements in solution for the two niobium containing alloys it can be seen from table 23 that the increase in hardenability was associated with a slight decrease in niobium but a significant increase in nitrogen in solution. Although nitrogen in solution would be expected to increase the hardenability the dominant influence would be expected to be the increased quantity of vanadium and niobium nitrides. Again the grain boundaries would be more effectively pinned allowing the segregated microalloying elements in solution to eliminate the nucleation sites for the transformation and consequently increase the hardenability.

5.1.2.5   Low Carbon-Vanadium-Titanium Alloys
5.1.2.5.1   Hardenability Results Using a 950°C
Austenitising Temperature

The addition of titanium to a base vanadium steel (alloy 644) resulted in a large increase in the ideal critical diameter value obtained, see table 19 and figure 32.

135

Titanium is a very strong carbide/nitride former and would therefore preferentially combine with the carbon and nitrogen in the alloy to form titanium carbide and nitride precipitates. Therefore more vanadium would remain in solution and be available to increase the hardenability of the alloy. Consequently, it can be seen from table 20 that the hardenability was increased by the combined positive effects of the increased quantities of both vanadium and titanium in solution and despite the decreased quantity of nitrogen in solution. However, the addition of titanium resulted in no vanadium nitrides being present at the 950°C austenitising temperature but rather a combination of both titanium carbide and titanium nitride precipitates. The change in the type and extent of precipitation would also have an effect on the hardenability of the alloy. The titanium carbide precipitates would remove both titanium and carbon from solution but the amount of carbon removed was considered too small to alter the hardenability value of the alloy. These carbides could however act as preferred nucleation sites for the transformation from austenite and thus reduce the hardenability. In contrast the titanium nitride precipitates would be expected to strongly pin the prior austenite grain boundaries and result in a marked increase in the hardenability by allowing the microalloying elements in solution to segregate to the heavily pinned grain boundaries.

136

The addition of titanium and extra nitrogen to a base vanadium steel (alloy 645) resulted in a further increase in the ideal critical diameter when compared with both the base vanadium alloy (612) and the vanadium titanium-low nitrogen alloy (644), see table 19 and figure 32. Comparing the theoretical quantities of microalloying elements in solution with those in the base vanadium alloy it can be seen from table 20, that again the increase in the hardenability was caused by the combined effects of the titanium and vanadium in solution. Comparing the precipitates present at the austenitising temperature the addition of titanium and extra nitrogen resulted in the elimination of any vanadium nitrides but extensive precipitation of titanium nitrides. Consequently, these very efficient grain boundary pinning precipitates could also result in an increase in the hardenability of the alloy by allowing the microalloying elements in solution to segregate to the austenite grain boundaries.

Comparing the microalloying elements in solution for the two titanium alloys, it can be seen from table 20 that the increase in hardenability was directly associated with a decrease in the amount of titanium in solution. This observation was unexpected but is similar to the trends observed for the niobium alloys in section 5.1.2.4.1. However, it is possible that the dominant

hardenability factors are type and dispersion of precipitates present in the alloy at the 950°C austenitising temperature. In the low nitrogen steel both titanium carbides and nitrides were present whereas in the high nitrogen steel no titanium carbides were present but there was significantly more titanium nitride precipitates. The elimination of the titanium carbides would be expected to increase the hardenability since such large precipitates would have acted as preferred nucleation sites for the transformation from austenite. Similarly, the increase in quantity of fine titanium nitride precipitates would be expected to increase the hardenability by more effectively pinning the austenite grain boundaries allowing the segregation of the microalloying elements in solution to be more easily achieved.

5.1.2.5.2   Hardenability Results Using a 1200°C Austenitising Temperature

The addition of titanium to a base vanadium steel (alloy 644) caused an increase in the ideal critical diameter of the alloy, see table 22 and figure 34. It can be seen from table 23 that the observed increase in hardenability was associated with a slight decrease in both the vanadium and nitrogen in solution but a significant increase in the amount of titanium in solution. Therefore it must be considered that the titanium in

solution was the predominant factor. A titanium rich

cluster would, due to the large size of the titanium

atom, diffuse to the grain boundaries more slowly.

However once established at the boundaries they would be

more difficult to thermally disperse from the boundary

and would therefore be expected to increase the

hardenability of the steel. If the grain boundaries were

allowed to migrate the influence would be expected to

decrease since the clusters would find it more difficult

to diffuse with the moving boundaries. Consequently, the

titanium nitrides remaining at the austenitising

temperature must have a significant influence on the

ideal critical diameter. These precipitates would act as

both preferred nucleation sites for transformation and as

grain boundary pinning agents. Due to the observed

increase in hardenability it is suggested that the grain

boundary pinning effect of the precipitates dominates the

nucleating effect and allows segregation of the

microalloying elements in solution to be established.

The addition of titanium and extra nitrogen to a base

vanadium steel (alloy 645) resulted in an increase in the

observed ideal critical diameter value, see table 22 and

figure 34. The increase in hardenability when compared

with the base vanadium alloy can again be explained in

terms of the increased titanium in solution and the

presence of undissolved titanium nitride precipitates.

The grain boundaries would be pinned by the precipitates

and therefore allow the vanadium and titanium to segregate to the grain boundaries and increase the ideal critical diameter.

Comparing the results from the two titanium containing steels the increase in hardenability was associated with a decrease in the titanium in solution but a slight increase in the nitrogen in solution. A slight increase in hardenability due to the extra nitrogen in solution would be expected, but this effect would not be sufficient to explain the large increase in the hardenability observed. Similarly, it is unlikely that the increased hardenability is caused by the variation in the amount of titanium in solution. Therefore, it must be concluded that the dominant factor is the presence of the extra fine titanium nitride precipitates present in the high nitrogen steel. To influence the hardenability the microalloying elements in solution must be present at the prior austenite grain boundaries. However, if the grain boundaries migrate it is more difficult to establish the segregation phenomenon. Consequently, in the high nitrogen steel the austenite grain boundaries are more effectively pinned by the extra precipitates allowing a greater level of segregation and a corresponding increase in the hardenability of the steel.

140

5.1.3   Hardenability of Medium Carbon Steels

5.1.3.1   Medium Carbon-Vanadium Alloys

5.1.3.1.1   Hardenability Results Using a 950°C Austenitising Temperature

The addition of extra nitrogen to the medium carbon-low vanadium steel (alloy 624) resulted in a decrease in the ideal critical diameter when compared with the base vanadium alloy (623), see table 24 and figure 35. The extra nitrogen would be expected to combine with the vanadium in solution and result in further precipitation of vanadium nitride. Therefore, it can be seen from table 25 that the quantity of vanadium in solution was reduced whereas the quantity of nitrogen in solution was increased. Consequently, since a decrease in vanadium in solution would be expected to decrease the hardenability, as explained by classical hardenability theories, while an increase in nitrogen would be expected to increase the hardenability, it would appear that the vanadium effect was the dominant factor. In addition, the effects of the extra vanadium nitride precipitates must also be considered. The increased quantity of precipitates would be expected to more effectively pin the prior austenite grain boundaries and therefore result in an increase in hardenability. However, due to the higher nitrogen content the size of the vanadium nitrides would be expected to increase and therefore become less effective at pinning grain boundaries and also have an increased

potential for preferential nucleation of the transformation products. Both these effects would be expected to decrease the hardenability and could therefore contribute to the observed decrease in the hardenability.

5.1.3.1.2 Hardenability Results Using a 1200° C Austenitising Temperature

At the higher austenitising temperature of 1200° C the addition of extra nitrogen (as in alloy 624) again decreased the ideal critical diameter of the alloy when compared with the base vanadium steel (alloy 623), see table 26 ;and figure 36. Comparing the theoretical quantities of microalloying elements in solution, see table 27 the observed decrease in hardenability could be directly related to the increased quantity of nitrogen in solution. Therefore, it suggests that under certain conditions, especially at 1200° C, the presence of extra nitrogen can exhibit a slight negative influence on the hardenability of a steel. The extra nitrogen in solution would have been expected to have formed a modified vanadium-carbon-nitrogen cluster with a higher nitrogen concentration. This modified cluster would be more difficult to thermally disperse and would therefore tend to increase the hardenability rather than decrease it as observed. Therefore there must be a more dominant factor influencing the ideal critical diameter. At 1200° C all the alloy precipitates would have been taken into

solution and therefore the grain boundaries would be able to migrate and the austenite grains to grow. Consequently, since a high nitrogen cluster would be expected to exhibit a slower rate of diffusion it is possible that the modified clusters cannot adequately migrate with the austenite grain boundaries resulting in less grain boundary segregation and thus a corresponding decrease in the hardenability.

5.1.3.2   Medium Carbon-Vanadium-Aluminium Alloys

5.1.3.2.1   Hardenability Results Using a 950°C Austenitising Temperature

The addition of aluminium to the base vanadium steel (alloy 662) resulted in an increase in the ideal critical diameter, see table 24 and figure 35. The aluminium preferentially combined with the nitrogen present to form aluminium nitride precipitates. Consequently, it can be seen from table 25, that all the vanadium in the alloy was taken into solution and was available to influence the hardenability.

In addition there was an increase in the quantity of aluminium in solution, but a reduction in the quantity of nitrogen in solution. The increase in vanadium and aluminium in solution would be expected to combine to increase the hardenability and dominate the negative effect of the reduced nitrogen in solution. However, again it must be remembered that the precipitates present at the austenitising temperature will influence the

143

hardenability of the alloy.

The addition of aluminium and extra nitrogen to the base vanadium steel (alloy 663) resulted in only a slight increase in hardenability when compared with the base vanadium alloy (623) and a decrease in hardenability when compared with the vanadium-aluminium-low nitrogen alloy (662), see table 24 and figure 35. From the quantities of microalloying elements in solution, presented in table 25, a significant increase in hardenability would have been expected when compared with the base vanadium alloy. The increased quantities of both vanadium and aluminium in solution should have easily dominated the effect of the reduced nitrogen in solution. Therefore, it may be suggested that since the aluminium nitrides formed will be relatively large, compared with vanadium nitrides, the grain boundary pinning effects could be reduced and the potential for the precipitates to act as preferred nucleation sites for the transformation could be increased. Consequently, under these conditions the aluminium nitride precipitates tend to reduce the hardenability and offset to some extent the positive influence of the increased quantities of vanadium and aluminium in solution.

The observed decrease in the ideal critical diameter value, when comparing the two aluminium alloys, suggests that the reduction in aluminium in solution was more

144

significant than the combined increase in the quantities

of both vanadium and nitrogen in solution, see table 25.

However, the aluminium in solution effect would also be

aided by the extra large aluminium nitride precipitates,

formed in the high nitrogen alloy, providing extra

nucleation sites for the transformation and a

corresponding tendency to decrease the hardenability.

5.1.3.2.2   Hardenability Results Using a 1200°C

             Austenitising Temperature

The effect of adding aluminium to a medium carbon-low

vanadium steel (as in alloy 662) was to decrease the

observed ideal critical diameter value, see table 26 and

figure 36. According to the calculated quantities of

microalloying elements in solution, shown in table 27,

the vanadium and aluminium in solution were increased,

whereas the nitrogen in solution was decreased.

Consequently at 1200°C the increase in vanadium and the

decrease in nitrogen in solution would tend to decrease

the hardenability of the alloy. Whereas, the increase in

aluminium would be expected to increase the

hardenability. Aluminium in solution would tend to form

aluminium-nitrogen clusters and would therefore compete

with the vanadium to form their respective clusters. The

interaction between aluminium and nitrogen would be

expected to be greater than for vanadium and nitrogen.

Therefore, aluminium-nitrogen clusters would be expected

to form preferentially and consequently reduce the nitrogen concentrations of the vanadium-carbon-nitrogen clusters. Due to the larger atomic radius of aluminium, when compared with vanadium, the driving force for grain boundary segregation would be increased but the rate at which the cluster would diffuse would be reduced. Consequently, if the grain boundaries are stationary it is possible that the vanadium clusters more rapidly segregate to the grain boundaries but are also more easily thermally dispersed and could therefore be relatively ineffective at increasing the hardenability. On the other hand, the aluminium-nitrogen clusters would take longer to segregate to the grain boundaries but would be more difficult to thermally disperse from the boundaries and therefore could be more significant, especially at high austenitising temperatures. However, if the grain boundaries migrate it would be the ability of the cluster to diffuse with the moving boundary that would determine its relative effect. Consequently, in this respect the higher diffusion rates of the vanadium-carbon-nitrogen clusters could be more significant.

It must also be remembered that large aluminium nitride precipitates are still present even at $1200^{o}C$ and will therefore influence the hardenability. Since the precipitates will be large and widely spaced their effect upon grain boundary movement would be expected to be minimal and they would tend to act as preferred

nucleation sites for transformation. Consequently, the precipitates would be expected to contribute to the observed decrease in the hardenability.

The addition of aluminium and extra nitrogen to the base vanadium steel (as in alloy 663) resulted in a decrease in the hardenability when compared with both the base vanadium alloy (623) and the vanadium-aluminium-low nitrogen alloy (662), see table 26 and figure 36. The decrease in hardenability when compared with the base vanadium alloy (623) was associated with an increase in both the vanadium and aluminium in solution, see table 27. Again the increase in vanadium in solution would tend to cause a decrease in the hardenability by forming a cluster that is larger in size and therefore diffuses more slowly. Consequently, its ability to diffuse with a migrating austenite grain boundary is also reduced. Despite the increased aluminium nitride precipitation, it would be expected that the precipitate dispersion would be inadequate at $1200°C$ to pin the grain boundaries and restrict grain growth. Therefore, as the vanadium concentration was increased the vanadium clusters would not be able to diffuse at the same rate as the moving boundaries and thus would not be able to increase the hardenability. Similarly, as the aluminium concentration in solution is increased the rate of diffusion of the aluminium-nitrogen clusters would be

147

reduced and again would result in a decrease in the hardenability. In addition the extra, large aluminium nitrides would act as preferred nucleation sites for the transformation and contribute to a decrease in the ideal critical diameter.

Considering the microalloying elements in solution for the two aluminium alloys, it can be seen from table 27 that the decrease in hardenability was associated with an increase in both the vanadium and nitrogen in solution but a decrease in the amount of aluminium in solution. The increase in vanadium and nitrogen in solution would tend to decrease the hardenability by decreasing the rate at which the vanadium-carbon-nitrogen clusters could diffuse. However, the decrease in aluminium in solution would also result in the aluminium-nitrogen clusters being able to diffuse more quickly and improve the possibility of migration with the moving grain boundaries. In addition, it would appear that the precipitates remaining at the austenitising temperature have a significant effect upon the hardenability of the alloy. The large aluminium nitrides present in the high nitrogen steel would still be inadequate to successfully pin the grain boundaries and would act as preferred nucleation sites for the austenite transformation, and decrease the hardenability.

5.1.3.3 Medium Carbon-Vanadium-Molybdenum Alloys

5.1.3.3.1 Hardenability Results Using a 950°C Austenitising Temperature

The addition of molybdenum to the base vanadium steel (alloy 664) caused an increase in the ideal critical diameter value, see table 24 and figure 35. This increase in the hardenability must be directly related to the large quantity of molybdenum taken into solution, see table 25.

The addition of molybdenum and extra nitrogen to the base vanadium steel (alloy 665) also resulted in a similar increase in hardenability when compared with the base vanadium alloy (623) but resulted in a decrease in hardenability when compared with the vanadium-molybdenum-low nitrogen alloy (664), see table 24 and figure 35. It can be seen that when the molybdenum-vanadium-high nitrogen alloy is compared with the base vanadium alloy, the increase in hardenability was caused by the combined positive effects of increased vanadium and molybdenum in solution dominating the slight reduction of nitrogen in solution, see table 25. In addition the extra nitrogen in the alloy resulted in an increased quantity of vanadium nitride precipitation. Although the vanadium nitrides would be larger in size the wider dispersion of the precipitates could still more effectively pin the austenite grain boundaries and increase the hardenability by allowing the segregation of the microalloying elements

149

to the grain boundaries to become established. However, the larger vanadium nitride precipitates would increase the potential for transformation by acting as preferred nucleation sites and consequently could tend to reduce the hardenability.

From the theoretical quantities of microalloying elements in solution the slight decrease in hardenability when comparing the two molybdenum alloys was unexpected. It can be seen from table 25, that the increased quantities of vanadium and molybdenum in solution should have dominated the slight decrease in the amount of nitrogen in solution and resulted in an increase in hardenability. Therefore, it must be concluded that the observed decrease in hardenability, in the higher nitrogen alloy, was caused by the additional vanadium nitride precipitation. The combined effect of the larger vanadium nitrides being less effective in pinning the austenite grain boundaries while increasing the potential for preferred nucleation must have more than offset the effect of increased grain boundary pinning due to the wider dispersion, and resulted in the observed decrease in the hardenability of the high nitrogen alloy.

5.1.3.3.2   Hardenability Results Using a 1200°C
            Austenitising Temperature

The addition of molybdenum to the medium carbon-low

vanadium steel (alloy 664) resulted in an increase in the ideal critical diameter, see table 26 and figure 36. At the 1200° C austenitising temperature all the microalloying elements were in solution and available to influence the hardenability. It can be seen from table 27 that the increase in hardenability was accompanied by a decrease in vanadium and nitrogen in solution but an increase in the molybdenum in solution. The decrease in the vanadium in solution would be expected to slightly increase the hardenability by reducing the vanadium concentration of the vanadium-carbon-nitrogen clusters. The resulting increase in the rate of diffusion of the clusters would enable them to diffuse as the grain boundaries migrate. In addition molybdenum in solution would be expected to increase the hardenability whereas the reduction in the amount of nitrogen in solution would slightly reduce the hardenability. Consequently, the observed increase in hardenability must have been caused by the combined effects of the vanadium and molybdenum more than offsetting the effect of the nitrogen.

The addition of molybdenum and extra nitrogen to the base vanadium steel (alloy 665) resulted in the same hardenability when compared with the base vanadium alloy (623) but a decrease in the hardenability when compared with the vanadium-molybdenum-low nitrogen alloy (664), see table 26 and figure 36. Since there was no change in the hardenability when compared with the base vanadium

alloy the factors influencing the ideal critical diameter value must have been balanced. Consequently, it can be seen from table 27, that the positive influences of increased molybdenum and nitrogen in solution must have been equal to the negative influence of the increased vanadium in solution.

Similarly, the decrease in the hardenability of the high nitrogen alloy compared with the low nitrogen alloy was associated with the increased quantities of vanadium, molybdenum and nitrogen in solution, see table 27. However, in this instance the negative effect of the increased vanadium in solution was greater than the combined positive effects of increased molybdenum and nitrogen in solution.

5.1.3.4   Medium Carbon-Vanadium-Niobium Alloys

5.1.3.4.1   Hardenability Results Using a 950°C Austenitising Temperature

The addition of niobium to the base vanadium steel (alloy 671) resulted in a slight increase in the ideal critical diameter, see table 24 and figure 35. The niobium, being a strong carbide/nitride former, preferentially combined with the carbon and nitrogen to precipitate niobium carbide and niobium nitride. Consequently, more vanadium was taken into solution and influenced the hardenability, see table 25. The increased vanadium in solution

together with the additional niobium in solution would be expected to increase the hardenability despite the reduced quantity of nitrogen in solution. However, the increase in hardenability was small due to the change in the precipitates present at the 950°C austenitising temperature. The addition of niobium reduced the amount of vanadium nitride to a very low level but caused additional amounts of both niobium carbide and niobium nitride. The removal of the grain boundary pinning effects of the vanadium nitride precipitates would be to some extent compensated by the presence of niobium nitride precipitates. However, the niobium carbide precipitates, being coarser, could act as preferred nucleation sites for the transformation (2) and therefore result in a lower hardenability than expected.

The addition of niobium and extra nitrogen to the base vanadium steel (alloy 668) resulted in a slight decrease in the hardenability when compared with both the base vanadium alloy (623) and the vanadium-niobium-low nitrogen alloy (671), see table 24 and figure 35. The decrease in hardenability when compared with the base vanadium alloy was unexpected if the microalloying elements in solution are considered, see table 25. It would have been expected that the positive effects of the increased vanadium and niobium in solution would have more than offset the negative effects of the reduced quantity of nitrogen in solution. Consequently, the

153

observed slight reduction in hardenability could be associated with the precipitates present at the austenitising temperature. The addition of niobium and extra nitrogen resulted in approximately the same quantity of vanadium nitrides present but additional quantities of both niobium nitride and niobium carbide. The extra precipitation would have been expected to help pin the austenite grain boundaries and increase the hardenability by allowing segregation of the microalloying elements to the grain boundaries to become more effective. However, the larger precipitates, especially the niobium carbides, would be expected to be less effective at pinning grain boundaries but more effective at providing preferred nucleation sites for the transformation and could be responsible for the observed slight decrease in hardenability.

The decrease in hardenability at the higher nitrogen content when comparing the two niobium alloys can be explained in terms of the negative effect of the reduced vanadium in solution offsetting the positive effect of the slight increase in the nitrogen in solution, see table 25. However, the hardenability must also have been effected by the change in the combination of precipitates present at the austenitising temperature. The extra nitrogen in the vanadium-niobium-high nitrogen alloy (669) resulted in increased quantities of both vanadium

and niobium nitrides but a reduced quantity of niobium
carbides. The wider dispersion of the precipitates would
be expected to more effectively pin the austenite grain
boundaries and increase the hardenability while the
reduction in the number of large niobium carbide
precipitates present would tend to reduce the number of
preferred nucleation sites for the transformation and
also cause an increase in the hardenability. However,
the vanadium and niobium nitrides would be larger in the
high nitrogen alloy and would therefore be less effective
at pinning grain boundaries and could therefore
contribute to the observed decrease in the ideal critical
diameter.

5.1.3.4.2   Hardenability Results Using a 1200°C
             Austenitising Temperature

At the higher austenitising temperature of 1200°C the
addition of niobium to the base vanadium steel (alloy
671) resulted in a decrease in the ideal critical
diameter, see table 26 and figure 36. Comparing the
theoretical quantities of microalloying elements in
solution it can be seen from table 27 that the niobium
alloy contained an increased amount of both vanadium and
niobium in solution but a decreased quantity of nitrogen
in solution. At 1200°C an increase in vanadium would be
expected to decrease the hardenability of the alloy by
forming a vanadium cluster with a reduced rate of
diffusion and therefore will be less able to migrate with

the moving austenite grain boundaries.

From the work of Eldis et al (7), and the results obtained in section 5.1.2.4.2, it is possible that at low niobium levels the niobium in solution combines with the nitrogen and/or carbon to form extra grain boundary clusters which increase the hardenability. However, at higher niobium concentrations the niobium clusters would diffuse at a slower rate, and may not be able to move with the migrating austenite grain boundaries resulting in a reduced effect on the ideal critical diameter of the steel. The reduction in the quantity of nitrogen in solution would tend to form clusters which were more carbon concentrated and would therefore result in the clusters having a higher rate of diffusion. Consequently the reduction in nitrogen would be expected to increase the hardenability of the alloy. However, even at 1200°C some precipitates would still be present and influence the ideal critical diameter. The precipitates present in the niobium steel (671) would mainly consist of large niobium carbides which would be relatively ineffective as a grain boundary pinning agent but would act as preferred nucleation sites for transformation and would therefore be expected to reduce the hardenability.

The addition of niobium and extra nitrogen to a base vanadium steel (alloy 668) resulted in a very slight

156

decrease in hardenability when compared with the base
alloy (623) but an increase when compared with the
vanadium-niobium-low nitrogen alloy (671), see table 26
and figure 36. The decrease in hardenability when
compared with the base vanadium alloy was associated with
an increase in the quantities of all the microalloying
elements vanadium, niobium and nitrogen in solution, see
table 27. Consequently, it would be expected that the
increase in all the three microalloying elements would
have caused a decrease in the hardenability since each
would have resulted in an decrease in the rate of
diffusion of the clusters. However, the niobium alloy
(668) contained undissolved niobium carbide and nitride
precipitates even at the 1200°C austenitising
temperature. The finer niobium nitrides would tend to
pin the grain boundaries but due to their wide dispersion
they would be expected to be relatively ineffective.
Also the larger niobium carbides would tend to act as
preferred sites for the nucleation of the transformation
and could therefore contribute to the decrease in the
ideal critical diameter.

Considering the two niobium alloys it can be seen from
table 27, that the only change in the microalloying
elements in solution was an increase in the quantity of
nitrogen. Since, the extra nitrogen would be expected to
form clusters which would diffuse more slowly it would be
more difficult to migrate with the austenite grain

boundaries and would therefore be expected to result in a decrease in the hardenability. However, it must also be noted that the extra nitrogen produced an additional small quantity of niobium nitride. These precipitates would be smaller than the niobium carbides and therefore be more effective at pinning grain boundaries. Thus they could contribute to the observed increase in the hardenability by allowing more clusters to segregate to the boundaries.

5.1.3.5   Medium Carbon-Vanadium-Titanium Alloys

5.1.3.5.1   Hardenability Results Using a 950°C
Austenitising Temperature

The addition of titanium to the base vanadium steel (alloy 669) resulted in an increase in the ideal critical diameter, see table 24 and figure 35. Titanium, being a strong carbide/nitride forming element would tend to combine with the carbon and nitrogen in preference to the vanadium. Consequently, all the vanadium in the alloy would be in solution at 950°C, and available to increase the hardenability, see table 25. Also a very small quantity of titanium was taken into solution which would be expected to cause a further slight increase the hardenability. However, the titanium effectively removed all the nitrogen from solution, which would therefore result in a corresponding reduction in hardenability. In addition the change in the type and dispersion of the

precipitates present at 950°C would also influence the hardenability of the alloy. The titanium alloy would contain large volume fractions of both titanium carbide and nitride. The titanium carbides would be larger in size and therefore not be so effective in pinning the austenite grain boundaries but due to the large volume fraction they could cause a degree of grain boundary pinning and thus contribute to a slight increase in hardenability. However, due to their large size the titanium carbides would be expected to be very good sites for preferred nucleation for the transformation and thus contribute a negative influence on the hardenability. The titanium nitrides on the other hand, would be much finer than the titanium carbides and would be much more effective at pinning grain boundaries. Consequently, the titanium nitrides would be expected to produce significant grain boundary pinning that would be the dominant effect and result in a significant increase in the hardenability.

The addition of titanium and extra nitrogen to base vanadium steel (alloy 672) resulted in a very large increase in hardenability when compared with both the base alloy (623) and the vanadium-titanium-low nitrogen alloy (669), see table 24 and figure 35. Comparing the dissolved microalloying contents with the base alloy, it can be seen from table 25 that again the increase in hardenability can be explained in terms of the combined

positive influence of the increased quantities of vanadium and titanium in solution more than offsetting the negative influence of the reduced nitrogen in solution. However, both titanium carbide and nitride precipitates would be present and contribute to the hardenability obtained. The larger titanium carbides would tend to be ineffective in pinning the grain boundaries and would act as nucleation sites for transformation; therefore they would tend to lower the hardenability. Conversely, the heavy dispersion of finer titanium nitrides would be expected to be extremely good at pinning the austenite grain boundaries and thus increase the hardenability by allowing the segregation of the microalloying elements to the grain boundaries to be more easily established. The very effective grain boundary pinning effect is considered to be a significant factor in the observed large increase in the hardenability.

Comparing the microalloying elements in solution for the two titanium containing alloys, it can be seen from table 25 that the large increase in hardenability was accompanied by a reduction in the amount of dissolved vanadium. This observation was unexpected but similar to the trends observed in the low carbon titanium alloys, section 5.1.2.5.1. Consequently, it is possible that at higher dissolved vanadium concentrations the titanium and

vanadium in solution could compete with each other to form modified clusters which are less effective as a hardenability factor. Alternatively, it is more likely that the dominant hardenability factors are the type and distribution of the precipitates present at the austenitising temperature. In the high nitrogen alloy (672) the amount of titanium nitride is increased whereas the amount of titanium carbide is decreased. The reduction in the large titanium carbides would mean less sites for preferential nucleation and therefore an increase in the hardenability. In addition the significant increase in the volume fraction of titanium nitride precipitates would be extremely effective at pinning the austenite grain boundaries and must therefore be largely responsible for the observed increase in the ideal critical diameter.

5.1.3.5.2 Hardenability Results Using a 1200°C Austenitising Temperatue

The addition of titanium to the base vanadium steel (alloy 669) resulted in a decrease in the ideal critical diameter, see table 26 and figure 36. Comparing the microalloying elements in solution, it can be seen from table 27 that vanadium and titanium in solution were increased whereas the nitrogen in solution was decreased. At 1200°C the increase in vanadium and titanium in solution would be expected to behave in a similar way by forming clusters with the carbon and nitrogen in

solution. Consequently, as the vanadium or titanium in solution is increased, the rate of diffusion of the clusters would tend to be reduced. Therefore, their rate of segregation and their ability to diffuse with migrating grain boundaries would also be reduced. Consequently, a decrease in the hardenability would be expected. But, the decrease in nitrogen in solution would tend to increase the rate of diffusion of the clusters and therefore increase the ideal critical diameter. However, considering the precipitates present in the titanium containing steel (669) at 1200° C, both titanium carbides and nitrides remained undissolved. The large titanium carbides would be ineffective in pinning the austenite grain boundaries but would readily act as preferred nucleation sites for the transformation and therefore decrease the hardenability. The much finer titanium nitrides would not tend to act as readily as preferred nucleation sites but would be much more effective in pinning the austenite grain boundaries and therefore contribute a positive influence on the hardenability. Since the observed change in the ideal critical diameter value was negative it is suggested that the titanium carbide precipitation was the dominant factor.

The addition of titanium and extra nitrogen to the base vanadium steel (alloy 672) resulted in a very large

increase in hardenability when compared with both the
base vanadium alloy (623) and the vanadium-titanium-low
nitrogen alloy (669), see table 26 and figure 36.
Comparing the microalloying elements in solution with the
base alloy, it can be seen from table 27 that again the
vanadium and titanium in solution were increased whereas
the nitrogen in solution was decreased. Therefore, the
vanadium and titanium in solution would have been
expected to decrease the hardenability whereas the
reduction in nitrogen would cause an increase in the
ideal critical diameter. Consequently for the
microalloying elements in solution to cause the observed
large increase in hardenability the nitrogen in solution
would need to have exhibited a very large positive
influence. It is rather suggested that the hardenability
was associated with the precipitates. At 1200°C only
titanium nitride precipitates are present in the
vanadium, titanium, high nitrogen steel (672). This fine
and widespread dispersion of titanium nitrides would not
act as significantly as preferred sites for the
transformation but would very effectively pin the
austenite grain boundaries. The restriction of grain
boundary movement would allow segregation to the
boundaries to be established and result in the observed
significant increase in the ideal critical diameter. If
the grain boundaries were immobilised the effect of
increasing the vanadium and titanium in solution would be
altered. The titanium/vanadium concentrated clusters

163

would diffuse more slowly than for clusters with lower concentrations, but once established at the grain boundaries would be more difficult to thermally disperse from the austenite grain boundaries. Consequently, when the grain boundaries are adequately pinned the relationship that increasing the microalloying element in solution increases the hardenability is restored.

Comparing the microalloying elements in solution for the two titanium alloys, it can be seen from table 27, that there was only a slight decrease in vanadium and titanium in solution and a slight increase in nitrogen in solution, for the high nitrogen alloy (672). Since these variations in the amount of microalloying elements in solution were small it is unlikely that they could have resulted in the observed large increase in the hardenability of the steel. Consequently, it is again suggested that the dominant factor for the increase in hardenability was the distribution of the precipitates present at the austenitising temperature. The addition of the extra nitrogen meant that large quantities of extra titanium nitrides were formed which lowered the amount of titanium in solution to a level where the titanium-carbon solubility limit was not exceeded. The absence of the large titanium carbides, which could act as preferred nucleation sites for the transformation, and the extra titanium nitride precipitation more effectively

pinning the grain boundaries, were probably the reasons for the observed large increase in the hardenability of the high nitrogen alloy.

5.2 Precipitation Processes in Vanadium Alloy Pearlitic Steels

5.2.1 Time-Temperature-Transformation Diagrams

To investigate the precipitation and transformation processes in high carbon, vanadium steels, Time-Temperature-Transformation (T.T.T.) diagrams were determined for two steels, between the temperatures 500°C and 650°C. The steels used were a high carbon, vanadium, low nitrogen steel (626), and a high carbon, vanadium, high nitrogen steel (695). From the T.T.T. diagrams presented in figure 37, it can be seen that the increased vanadium and nitrogen in steel 695 slightly raised the temperature of the nose of the pearlite transformation, whilst also increasing the rate of transformation.

Hardness values were determined from samples which had been fully transformed by isothermally treating for twenty-four hours, and are presented in table 28 and figure 38. As the isothermal transformation temperature was increased the hardness decreased, due to the formation of a coarser pearlitic microstructure. In addition it was observed that the low nitrogen steel (626) exhibited a higher hardness value, compared with the high nitrogen steel (695), irrespective of the transformation temperature studied.

165

5.2.2   Microstructural Examination

5.2.2.1   Scanning Electron Microscopy (S.E.M.)

S.E.M. examination of the fully transformed

microstructure from the vanadium high nitrogen alloy 695

revealed that as the transformation temperature was

decreased the pearlite lamellae were refined, see figures

39 to 42. It was also observed that at the higher

transformation temperatures a small proportion of pro-

eutectoid ferrite was present which had nucleated at

either prior austenite grain boundaries, figure 43, or at

manganese sulphide inclusions, figure 44. However, since

the specimens had been held at the transformation

temperature for twenty-four hours, the cementite lamellae

of the pearlite had started to spheroidise, figure 45,

but there was no significant effect upon the pearlite

hardness.

Examination of the vanadium, low carbon steel 626, showed

that the pearlite lamellae were refined when compared

with the high nitrogen alloy transformed under identical

conditions, see figures 46 and 47 compared with figures

39 and 42.

5.2.2.2   Transmission Electron Microscopy (T.E.M.)

It has recently been reported that in vanadium steels

precipitation can occur by an interphase mechanism (11-

13) (88-93) and that there is a corresponding increase in

the strength of the steel. Consequently, it was decided to investigate such a phenomenon. However, due to the relatively short time period available, only one alloy and one transformation temperature could be studied. Therefore, the high nitrogen alloy (695) at a transformation temperature of 650°C was selected.

Examination of thin foils from a specimen transformed for 24 hours did reveal precipitation within the pearlitic ferrite as described by Dunlop (93), see figures 48 to 52, however, no dark field images or electron diffraction patterns were obtained to identify the interphase precipitates. There was no obvious precipitate row formation but there was evidence of a precipitate free zone adjacent to the cementite lamellae, see figures 48 and 49. It was also observed that spheroidisation of the cementite lamellae had commenced and the distribution of precipitates marked the original position of the cementite lamellae, see figure 52. As a result of the spheroidisation it was considered necessary to examine specimens transformed at shorter time intervals.

A specimen transformed at 650°C for three minutes forty seconds resulted in the formation of a partially transformed structure containing both areas of pearlite and martensite as shown in figures 53 and 54. However, examination of the pearlitic regions did not show any precipitation within the ferritic lamellae. This suggested that the precipitates were either too fine to

be resolved or that the precipitates nucleated after, rather than during, the transformation process. However, an area of pro-eutectoid ferrite was observed which contained significant precipitation, see figures 55 and 56.

In a recent paper by Mottishaw and Smith (125) it was suggested that a precipitation peak occurred within three minutes of ageing. Therefore, since the steel was fully transformed after approximately eight minutes, further specimens were prepared after holding at temperature for eleven and sixteen minutes respectively. Again the extensive distribution of precipitates associated with interphase precipitation was not observed. However, rows of precipitates were observed in both series of specimens, as shown in figures 57 to 62. These precipitates were relatively coarse compared with those observed in the specimen transformed for twenty-four hours, and were thought to be due to the presence of dislocations. Whether the dislocations resulted in the coarsening of very fine pre-existing precipitates, or the nucleation of new precipitates on the dislocations is uncertain. However, a large proportion of the precipitates appeared to line up at approximately 50 degrees to the direction of the cementite lamellae. This suggested that very fine interphase precipitation could have been present which was beyond the resolution of the microscope until the precipitates were associated with a

dislocation which allowed them to preferrentially grow.

5.2.3   Mechanical Properties of High Carbon,

Vanadium Steels

5.2.3.1 Tensile Properties

To investigate the tensile properties of the two high
carbon, vanadium steels, 626 and 695, specimens were
isothermally transformed at a series of transformation
temperatures between 550° C and 650°C. The transformed
specimens were subsequently tested at room temperature
using an Instron 1200 tensile testing machine. From
these tests the ultimate tensile stress, 0.2% proof
stress and the percentage elongation to failure were
recorded. It was expected that as the temperature of
transformation decreased a corresponding increase in the
strength of the steel would be observed, due to the
refinement of the pearlitic microstructure. However, the
results presented in tables 29 and 30, and figures 63 and
64, showed a tendency for a peak in strength at an
isothermal transformation temperature of approximately
600°C. This increase in strength is indicative of
precipitation within the specimens, which accounts for
the more marked increase observed in the high nitrogen
alloy 695.

5.2.3.2   Impact Properties
Specimens to investigate the impact properties of the

high steels were also isothermally transformed at a series of transformation temperatures between 550°C and 650°C. Charpy Impact specimens machined from the transformed material were subsequently tested at a series of test temperatures ranging from room temperature to 250 °C. The results presented in tables 31 and 32, and figures 65 to 68, showed that both alloys tended to exhibit a decrease in toughness at an isothermal transformation temperature of approximately 600°C. This decrease in impact value confirmed the strengthening peaks observed during tensile testing and therefore supported the suggestion that precipitation occurred in the specimens transformed at 600°C.

6   Discussion

6.1   Hardenability Results

It has been shown that the addition of microalloying

elements to a vanadium H.S.L.A. steel can cause

significant variations in the hardenability after

austenitising at both 950 and 1200°C. A simplified

thermodynamic approach was applied to rationalise the

effects of the microalloying additions, assuming that it

was the quantities of microalloying elements in solution

which determined the hardenability. Using this approach

the majority of the experimental results could be

satisfactorily explained. However, it was clear from the

investigations that the situation was more complex than

was originally believed. Consequently, it was considered

necessary that other factors that could influence the

ideal critical diameter should be assessed in order to

more fully understand the mechanisms which were

controlling the hardenability. A preliminary

interpretation of the results was presented in Section

5.1 which considered the following factors:-

        i)   the quantity of microalloying elements in

                    solution

        ii)   the ability of the elements in solution

                    to segregate to, or desegregate from,

                    the prior austenite grain boundaries.

        iii)   the ability of the microalloying

                    elements in solution to form clusters or

                    complexes which exhibit different

influences on the hardenability.

iv)   the quantity, particle size and distribution of undissolved alloy precipitates.

v)   the ability of undissolved precipitates to act as preferred sites for the transformation from austenite.

vi)   the ability of the undissolved precipitates to act as grain boundary pinning agents and maintain a small austenite grain size.

Section 5.1 proposed explanations for the individual experimental results obtained, and consequently the present section will tend not to discuss the individual results, but will rather deal in general with the theories of the mechanisms which are occurring and their inter-relationships within the different alloy systems.

6.1.1 Vanadium Steels

In vanadium steels it is generally accepted that the hardenability is dependent upon the amount of vanadium in solution at the austenitising temperature and it has been suggested (118) that its beneficial effect is associated with its ability to segregate to the austenite grain boundaries and eliminate the the grain boundary nucleation sites for the transformation. When vanadium carbides and nitrides are taken into solution the carbon

and nitrogen enter solution as interstitial solute atoms.
In contrast, vanadium having a larger atomic radius than
carbon or nitrogen, nearer to the size of iron,

enters solution as a substitutional solute atom.
Introducing a solute atom into the matrix lattice, be it
interstitial or substitutional, causes a localised strain
energy associated with the distortion of the matrix
lattice. Therefore, there is a driving force for the
microalloying elements to reduce the strain energy. This
is achieved by diffusion to either a grain boundary, a
free surface or a vacancy site. In addition the grain
boundaries also exhibit an interfacial strain energy,
resulting from the mis-orientation of the matrix lattices
of the two adjacent grains which form the boundary.
Consequently, segregation of microalloying elements to
the grain boundaries can also reduce the interfacial
boundary energy by decreasing the energy associated with
the lattice misfit. Therefore, since it is the high
energy grain boundary sites which are the preferred
nucleation sites for the phase transformation, a
reduction in the grain boundary energy would retard the
transformation and thus increase the hardenability. It
would therefore seem possible to rationalise the
hardenability results with respect to the quantities of
microalloying elements in solution per austenite grain
boundary area. However, analysing the results from the
present study in this way proved inconclusive. This could
have been a direct consequence of different boundaries

173

exhibiting different interfacial energies and a corresponding uneven distribution of the microalloying elements segregating to the grain boundaries. Therefore, since grain boundaries with a high degree of misfit exhibit the greater interfacial energies a preference for the microalloying elements to segregate to this type of boundary would be expected. Therefore, if the hardenability results could be related to the quantities of microalloying elements in solution at these high energy austenite grain boundaries per unit area, a more precise interpretation of the hardenability effects may have been possible.

The earliest and simplest quantitative model for grain boundary segregation, as a function of temperature and solute concentration, was developed by McLean (126) and may be expressed as follows:-

$$\frac{Xb}{Xbo - Xb} = \frac{Xc}{1 - Xc} \exp\left[\frac{E_1}{RT}\right] \quad \text{--------} \quad (10)$$

where

    Xb = grain boundary concentration

    Xbo = saturation grain boundary concentration

    Xc = bulk solute concentration

    E_1 = free energy of absorption at the grain boundary

    R   = the gas constant

    T   = temperature in degrees Kelvin

McLean's model shows that, as expected, the segregation increases as the solute content rises or as the temperature falls. However, the model assumes that there are a fixed number of sites at the boundary which attract solute atoms which have a single binding energy and that any interactions between segregating solute atoms can be ignored. Consequently, the model could only be applied to simple cases of extremely dilute systems and in the absence of strong preferential interactions. In recent years more general models have been evolved to incorporate more complex features such as:-

i) the existence of grain boundaries with a range of interfacial energies and therefore a range of solution atom binding energies. This results in preferential segregation to certain high energy grain boundaries.

ii) significant interactions between segregating atoms of the same type.

iii) segregation site competition and significant interactions between segregating atoms of different types. The solute interactions could be either positive or negative with respect to their influence on segregation.

These more complex models for segregation have been reviewed by other authors (127 - 129) and will not

therefore be dealt with in details in the present study.

In a vanadium steel, at a constant austenitising temperature at which both vanadium carbides and nitrides are taken into solution, the microalloying elements could act as individual elements or collect together to form microalloying clusters. If they remained as individual elements the carbon and nitrogen being interstitial elements would quickly segregate to the grain boundaries and have an almost instantaneous effect upon the hardenability. Whereas, the vanadium, being a substitutional element, would require a longer time to diffuse to the grain boundaries before its effect upon the hardenability could be realised. McLean (126) expressed this time dependance as:-

$$\frac{Cgbt - Cgbo}{Cgb\infty - Cgbo} = 1 - \exp\left(\frac{4Dt}{\alpha^2 d^2}\right) \operatorname{erfc}\left(2\sqrt{\frac{Dt}{\alpha d^2}}\right) \quad --(11)$$

where Cgbo = initial grain boundary concentration

   Cgbt = grain boundary concentration after time t
           at lower temperature

   Cgb∞ = equilibrium grain boundary concentration
           after infinite time at the lower
           temperature

   D   = solute diffusion co-efficient

   α = ratio of solute concentration in boundary
           to that of the matrix at equilibrium

176

d   = grain boundary thickness

From this expression the time for 50% completion of segregation is:-

$$t_{50} = 0.591 \frac{\alpha^2 d^2}{4D} \quad ----------- \quad (12)$$

However, if the microalloying elements combined to form vanadium-carbon-nitrogen clusters it would be the ability of the individual cluster to segregate to the grain boundaries which would determine its influence upon the hardenability of the alloy. These clusters could range from vanadium-carbon rich clusters to vanadium-nitrogen rich clusters and therefore would be expected to exhibit different rates of diffusion. As the clusters become more nitrogen concentrated the rate of diffusion would be expected to be reduced. Therefore, a nitrogen rich cluster would be less effective in retarding the nucleation stage of the transformation unless adequate time was allowed for equilibrium segregation conditions to be established.

Formation of vanadium-carbon-nitrogen clusters could also have an effect upon the hardenability by influencing the rate of growth, rather than the nucleation, of the non martensitic transformation product. The growth of

177

bainite, ferrite or pearlite requires the diffusion of carbon. If the carbon is associated with a vanadium-carbon-nitrogen cluster its rate of diffusion would be much slower than if the carbon was as individual interstitial atoms, which would consequently reduce the rate of growth of the non-martensitic phase and cause an associated increase in the hardenability. The extent to which cluster formation affects the hardenability during the growth stage of transformation is beyond the scope of the present study but its possible significance should be noted.

Increasing the quantity of vanadium taken into solution and segregating to the grain boundary should cause a progressive increase in the hardenability. This classical response was observed at an austenitising temperature of $950^{\circ}C$ for a holding period of one hour, but was not observed after four and eight hours respectively, see figure 30. Therefore, at the lower austenitising temperature the effects of the microalloying elements are complicated by kinetic effects such as the rate of solution of the alloy carbides/nitrides and the rate of segregation of the microalloying elements to the grain boundaries. Allowing extended times at the austenitising temperature enables the kinetic effects to be minimised and allows the effects of the microalloying elements to be more precisely determined. The results presented in figure 30

178

are important since the two high nitrogen alloys exhibit the higher hardenabilities and consequently highlight the interdependence of vanadium and nitrogen in solution. The alloy with 0.075% vanadium in solution (Alloy 619) had a higher hardenability than the alloy containing a 0.124% vanadium in solution (Alloy 612) which could be explained by the higher nitrogen in solution of the low vanadium alloy, contributing a significant influence in its own right. However, the results suggest that this influence is not significant after one hour, at the austenitising temperature, and depends on the kinetics of solution of the vanadium nitrides or the rate of its segregation to the grain boundaries. If the latter proposal is considered the extra nitrogen in solution in alloy 619 would be expected to quickly migrate to the grain boundaries if the nitrogen was present as an interstitial element. However, if the nitrogen forms nitrogen rich vanadium-carbon-nitrogen clusters extended periods at temperature would be required before the extra influence of nitrogen in solution could be realised. Consequently, cluster formation could explain the significant different between the one and eight hour ideal critical diameter values for the low vanadium, high nitrogen alloy (619). If the low vanadium, low nitrogen alloy (612) and the high vanadium, high nitrogen alloy (622) are considered, it can be seen from table 13 that they contain approximately the same nitrogen in solution.

Therefore, if the increase in hardenability between one and eight hours is only due to the diffusion of nitrogen rich clusters, the increase for alloys 612 and 622 should be similar. As can be seen from figure 30, alloy 622 shows a much greater increase in hardenability than alloy 612 and therefore the diffusion of nitrogen rich clusters does not fully explain the observed effects. But as the quantity of vanadium in solution is increased the number of vanadium atoms in a cluster could also be increased. This may subsequently decrease the rate at which the cluster could diffuse to the grain boundaries. Consequently, the increase in the ideal critical diameter value for the alloy 622 by extending the austenitising time from one to eight hours could be associated with the extra time required for the vanadium rich cluster to reach the grain boundaries.

In addition, the increase in hardenability with extended austenitising time could be associated with the rate of solution of the precipitates. At $950^{\circ}C$ not all the vanadium nitrides would be expected to be in solution, therefore, if only the volume fraction of precipitates dissolved is considered, a larger volume fraction would be expected to require a longer time at the austenitising temperature to achieve equilibrium. However, since the high vanadium, high nitrogen alloy 622 takes longer to reach equilibrium conditions, than the low vanadium, low nitrogen alloy, despite a smaller volume fraction of

precipitates being dissolved, this indicates that the size and distribution of the precipitates are also important. It was shown in section 5.1.2.1.4 that a dispersion of fine precipitates, such as produced by interphase precipitation (20 (72) would go into solution faster than a coarse dispersion produced by precipitation within the austenite (70), and would therefore reach a maximum hardness after a shorter austenitising time. However, once equilibrium conditions are reached equivalent hardenabilities are achieved. Consequently, in order to assess the increases in ideal critical diameter values, by extending the holding period from one to eight hours, the precipitate morphologies of the alloys would need to be studied.

Due to the kinetic effects occurring at $950^{\circ}C$ explanations of the alloy interactions at this temperature must be treated with caution. In the past the majority of hardenability investigations have employed an austenitising period of one hour which would have produced results obtained from a transient state rather than equilibrium conditions. Consequently, this would have tended to provide an under estimation of the hardenability of the steel. However, commercially it is not practical to use long austenitising times and so treatments must be devised which would accelerate the alloy nitride/carbide solution process in order to obtain

reliable hardenability data for relatively short austenitisation periods, even at 950°C.

Kinetic effects could explain why Eldis (7) observed very little influence on the hardenability from the addition of microalloying elements at an austenitising temperature of 950°C. A treatment period of 20 minutes, as used by Eldis, would only be sufficient to raise the temperature of the sample to the required test temperature but would allow virtually no time for the solution of the precipitates and the diffusion of the microalloying elements to the prior austenite grain boundaries.

At an austenitising temperature of 1200°C, the alloy interactions are less likely to be complicated by kinetic effects and austenitising times of one hour are probably adequate. However, performing hardenability tests after austenitising at 1200°C is undesirable due to the large prior austenite grain size produced. In a commercial steel this would cause a corresponding reduction in the ductility and toughness of the steel. In addition increasing the austenitising temperature decreases the driving force for segregation to the grain boundaries. Increasing the temperature increases the vibrational energy of the lattice and allows a greater level of elastic strain energy, due to the solute in solution, to be accommodated. The progressive reduction in the effectiveness of the vanadium to influence the

hardenability with increasing temperature is shown in figure 28. It is also considered probable that a temperature could be reached where the microalloying elements in solution are thermally dispersed from the grain boundaries. It was observed that at the $1200^{\circ}C$ austenitising temperature a decrease in the ideal critical diameter was obtained as the vanadium in solution was increased, see figure 26. This was unexpected since even if the vanadium was being dispersed from the grain boundaries an increase in vanadium in solution would still have been expected to increase the hardenability. Therefore, it must be assumed that the extra vanadium in solution increases the vanadium concentration of the vanadium-carbon-nitrogen clusters and thus increases the lattice strain energy. If the distortion of the lattice is sufficient the cluster could act as a preferred nucleation site allowing the transformation from austenite to occur more easily. The increased strain associated with the cluster would also decrease their rate of diffusion. This could be significant if it is considered that at these high temperature grain boundaries may migrate and the austenite grains grow. For grain boundary nucleation sites to be eliminated the microalloying elements must be segregated to the grain boundaries. Therefore, if the grain boundaries migrate the associated microalloying elements must diffuse with the moving grain boundaries.

Consequently, if the austenite grain boundaries move too rapidly for the rate of diffusion of the microalloying elements in solution there will be a reduction in the elements at the grain boundaries and a corresponding reduction in the hardenability of the steel. If, as suggested earlier, increasing the amount of vanadium in solution causes a reduction in the rate of diffusion at the vanadium-carbon-nitrogen clusters a decrease in the hardenability could occur due to the clusters inability to diffuse with the migrating austenite grain boundaries, there being no grain boundary pinning particles at these high austenitising temperatures.

Austenite grain growth will also have a direct influence on the hardenability of the steel due to the reduction in the grain boundary area. This results in a decrease in the number of nucleation sites for the transformation. Therefore, less microalloying elements in solution would be required to affect an equivalent increase in the hardenability of the steel. In this way the effectiveness of the vanadium in solution could be increased despite the lower driving force for segregation to the grain boundaries at the higher temperatures where grain growth is likely to occur.

To ensure an adequate level of hardenability it has been suggested to be essential to limit grain boundary movement and thus allow the microalloying elements in

184

solution to segregate to the austenite grain boundaries (122). This can be achieved by pinning the grain boundaries with carbide/nitride precipitates. In vanadium steels, depending upon the austenitising temperature vanadium carbides and/or nitrides may be present and will be available to pin the grain boundaries. However, their effectiveness as grain boundary pinning agents will depend upon their size and distribution within the alloy. Austenite grain coarsening occurs at temperatures lower than the temperature at which the vanadium carbide or nitride is completely dissolved. Consequently, using appropriate assumptions it is possible to estimate the grain coarsening temperature (131), using the value of r crit for the size of the undissolved carbides/nitrides above which grain growth of the austenite can occur.

The value of r crit is given by (130):-

$$r\ crit = \frac{6\ R_0\ f}{\pi}\left\{\frac{3}{2} - \frac{2}{z}\right\}^{-1} - - - - - (13)$$

where; f = volume fraction of undissolved precipitates

R_0 = matrix grain size

z = R/Ro, where R is the radius of the growing grain so that z is a grain size hetrogeneity factor

The volume fraction is readily calculated from the solubility equations (8) and (9) and will decrease as the

185

austenitising temperature is increased.

$$Log \ [v][c] = \frac{-9500}{T(°K)} + 6.72 \quad - - - - - - (8)$$

$$Log \ [v][N] = \frac{-7840}{T(°K)} + 3.02 \quad - - - - - (9)$$

Hence r crit will decrease as the austenising temperature increases because, all other factors being equal, r crit is proportional to the volume fraction of precipitates undissolved, see figure 69. However, the actual particle size, r, of the undissolved precipitates will increase with increasing austenitising temperature due to Ostwald Ripening and r can be shown to depend upon temperature (T °K) and time (t) by an equation of the type (131):-

$$Log \ r = \frac{-A}{T(°K)} + B + \frac{Log \ t}{3} \quad - - - - - - - - - - - - (14)$$

where A and B are constants.

The variation of r with temperature is also shown in figure 69, and the temperature at which r crit equals r is the grain coarsening temperature. Consequently, the finer the precipitates and the wider the dispersion the more effective will be the grain boundary pinning. Therefore, it would be expected that the much finer vanadium nitrides would be significantly more efficient than the vanadium carbides in restricting grain boundary

movement. However, it must also be remembered that any vanadium carbides/nitrides undissolved will result in less vanadium being in solution to segregate to the grain boundaries and influence the hardenability. In addition if the precipitates are large, especially the vanadium carbides, they may act as preferred nucleation sites for the transformation from austenite and thus cause a reduction in the ideal critical diameter value.

6.1.2   Vanadium-Aluminium Steels

The addition of aluminium to a vanadium steel results in the aluminium preferentially combining with the nitrogen present to form aluminium nitride. This results in less vanadium nitrides forming. Therefore, more vanadium is dissolved and is available to influence the hardenability of the alloy. The larger quantity of vanadium in solution would be expected to increase the hardenability at the lower austenitising temperatures where the vanadium segregates to the grain boundaries but decrease the hardenability at higher temperatures where thermal dispersion of the vanadium and grain boundary migration occurs. Also an additional quantity of aluminium would remain in solution which would be expected to segregate to the prior austenite grain boundaries and increase the ideal critical diameter value. Since aluminium does not form a carbide it is unlikely that it would form vanadium-aluminium-carbon-nitrogen clusters, and it is

187

more probable that separate aluminium-nitrogen and vanadium-carbon-nitrogen clusters are formed. Since the vanadium-carbon-nitrogen clusters would be depleted of nitrogen they would tend more towards a carbon rich cluster which would consequently result in an increase in the rate of diffusion of the clusters. This would allow an increased rate of diffusion to the grain boundaries and thus a corresponding increase in hardenability, especially at the lower austenitising temperatures where kinetic effects need to be considered, see figure 33.

Aluminium-nitrogen clusters, due to the larger size of the aluminium atom compared with vanadium, would be expected to diffuse at a slower rate than a nitrogen rich vanadium-carbon-nitrogen cluster. Consequently, at low temperatures the hardenability effect of the aluminium in solution may not be realised until longer austenitising times. This is supported by the curves presented in figure 33 since the rate of increase in hardenability with time for the aluminium containing alloy (639) is slower than that for the vanadium alloy (619). However, the curves could also be explained in terms of the respective rates of solution of the vanadium and aluminium nitrides. Since the aluminium nitride is more stable its rate of solution would be slower than that for vanadium nitride.

A change in the precipitates present could also influence

the hardenability values obtained. The reduction in the volume fraction of vanadium nitride present would result in the grain boundary pinning being less effective, despite the increased volume fraction of aluminium nitride. This is the result of the aluminium nitrides being larger than the vanadium nitrides and therefore less effective as a grain boundary pinning agent. Therefore, if the number of vanadium nitrides is reduced below a certain level and there is not sufficient aluminium nitride to pin the boundaries, migration of the grain boundaries could occur and cause a decrease in the ideal critical diameter.

6.1.3 Vanadium-Molybdenum Steels

Molybdenum, in the amounts added in the present study, is readily taken into solution at the austenitising temperature and therefore would not be expected to be present in the form of precipitates. Also, since the molybdenum does not readily form carbides or nitrides, the association of the molybdenum in solution with the carbon or nitrogen in solution would be expected to be insignificant. Therefore, molybdenum would tend to either remain as individual solute atoms or form molybdenum clusters which would segregate to the grain boundaries and increase the ideal critical diameter value of the steel. Consideration of the base vanadium alloy and the vanadium, molybdenum, low nitrogen alloy showed

189

that the quantities of vanadium and nitrogen were similar

for both steels, see table 20 (c.f. steels 612 and 640).

Therefore, the increase in hardenability must have been

directly related to the amount of molybdenum in solution,

i.e. 0.21% Mo in solution resulted in an increase in the

ideal critical diameter of 10.9 mm. Converting this

result into a multiplying factor, which is normally used

to express the effectiveness of an alloying addition (8)

(9) (104) (109), gave a factor of 1.15 for a 0.10% Mo

addition. The average factor for molybdenum when added

singly, according to Mangonon (8) (9) is 1.12 whilst in

combination with vanadium the factor increases to 1.22

for a 0.10% Mo addition; therefore there is good

agreement with other published work.

In addition the kinetic effects discussed in section

5.1.2.3.2 support the observations of Watanabe (123) that

the presence of molybdenum increases the solubility of

vanadium. Such an effect would result in an additional

increase in the ideal critical diameter not exhibited in

a molybdenum free steel.

6.1.4   Vanadium-Niobium Steels

When niobium is added to a vanadium steel it readily

combines with the carbon and nitrogen to form niobium

carbide and nitride precipitates. These

carbides/nitrides are more stable than the vanadium

carbides/nitrides and would therefore be expected to form

190

in preference to the vanadium precipitates. The subsequent decrease in the carbon and nitrogen available to combine with the vanadium would result in more vanadium remaining in solution to influence the hardenability of the steel. Also an additional small quantity of niobium would remain in solution which would be expected to behave in a similar way to the vanadium in solution. Therefore, at low temperatures the niobium in solution would segregate, together with the vanadium, to the grain boundaries and cause an increase in hardenability, while at higher temperatures, where thermal dispersion and grain boundary migration could occur, a decrease in the ideal critical diameter would be expected.

Since niobium forms both carbides and nitrides the niobium in solution would be expected to associate with the carbon and nitrogen in solution to form niobium-carbon-nitrogen clusters. It is also possible that vanadium-niobium-carbon-nitrogen clusters could be formed. Due to the larger atomic radius of niobium, compared with vanadium, the niobium-carbon-nitrogen clusters would be expected to have a slower rate of diffusion than the corresponding vanadium-carbon-nitrogen clusters. In addition the presence of the larger niobium atoms in the vanadium-niobium-carbon-nitrogen clusters would cause an increase in the strain energy of the

cluster and thus tend to reduce the rate of diffusion of the cluster. Consequently, niobium would be expected to be an element which exhibits variable hardenability effects, since longer periods at the austenitising temperature would be required to produce its full influence and would therefore be very dependent upon the kinetics of the systems.

The reduction in the rate of diffusion of the niobium clusters could explain the results of Eldis (7), where at 1200°C niobium initially increased the hardenability but subsequently decreases it at higher concentrations. At the lower niobium concentrations the rate of diffusion of the clusters could be sufficient to move with the migrating austenite grain boundaries while at higher concentrations where the clusters would become more niobium rich the corresponding decrease in the rate of diffusion could result in the clusters not being able to move with the grain boundaries and cause a reduction in the hardenability.

The influence of niobium on the ideal critical diameter is also dependent upon the precipitation occurring in the steel. It has been stated previously that the microalloying elements in solution need to segregate to the grain boundaries in order to effectively eliminate the grain boundary nucleation sites. Consequently, if the grain boundaries are successfully pinned the

segregation phenomenon can more easily be established. Since niobium forms very stable nitrides and carbides the potential for grain boundary pinning is high. Also it should be noted that it is not simply the volume fraction of the precipitates which is important but their morphology and distribution. In a steel containing niobium, but no vanadium, a balance between niobium as precipitates, to pin the grain boundaries, and niobium in solution, to segregate to the grain boundaries, must be reached in order to successfully increase the hardenability. In a vanadium-niobium steel the major role of the niobium is to pin the austenite boundaries while the vanadium is allowed to enter solution, segregate to the boundaries and promote hardenability. However, it is possible that large niobium precipitates, especially carbides, could act as additional preferred nucleation sites for the transformation and thus could decrease the ideal critical diameter, this effect has been observed by Amin et al (2). Therefore, since niobium nitrides are often smaller than niobium carbides, they would not only be more successful at restricting grain growth but would also be less likely to act as preferred nucleation sites.

6.1.5 Vanadium-Titanium Steels

Titanium is a very strong carbide/nitride former and would therefore combine with the carbon and nitrogen

present in preference to the vanadium. Therefore, the extent of vanadium precipitation would be reduced, resulting in an increase in the vanadium in solution. Since only a very small quantity of titanium enters solution it is probable that the significant increases in hardenability are due to the precipitates produced rather than the quantity of titanium in solution. Therefore it is proposed that titanium influences the hardenability in a similar way to niobium, namely, to very effectively pin the prior austenite grain boundaries, allowing the vanadium in solution to segregate to the grain boundaries, and increase the ideal critical diameter value.

Although the quantity of titanium in solution is small it would be expected to form titanium-carbon-nitrogen, or vanadium-titanium-carbon-nitrogen clusters. Therefore, due to the large atomic radius of titanium these clusters would be expected to exhibit higher strain energies and thus a slower rate of diffusion. Consequently longer times at the austenitising temperature would be required before the segregation phenomenon associated with titanium containing clusters could be established.

Titanium is a very effective grain boundary pinning agent due to the formation of a widespread distribution of very fine titanium nitrides. Therefore, to achieve a large increase in the hardenability, the steel must contain a

reasonably high level of nitrogen. As the concentration of the nitrogen in the steel is increased the volume fraction of the titanium nitrides are also increased which, despite the larger size of the precipitates, would more effectively pin the austenite grain boundaries, thereby allowing the hardenability to be enhanced by the vanadium clusters segregating to the boundaries. In addition the increased titanium nitride precipitation would result in less titanium available to form titanium carbide. The subsequent reduction in the number of the much larger titanium carbides would also have a positive influence on the hardenability, by removing possible preferred sites for the nucleation of the austenite transformation. The very positive effect of increasing the nitrogen concentration in the steel can clearly be observed in figures 32, 34, 35 and 36.

The titanium nitrides being more thermally stable than vanadium nitrides are taken into solution at higher temperatures and would therefore result in the grain boundary pinning being more effective at higher temperatures. Thus the decrease in hardenability with increasing temperature, associated with the initiation of grain boundary movement, would be delayed to much higher austenitising temperatures. Hence, the very large advantage of adding titanium to the steel during the 1200°C austenitisation investigations, shown in figures 34 and 36.

6.1.6 Effect of Carbon on the Influence of Microalloying Elements on the Hardenability of Vanadium Steels

The carbon concentration in steels is important when considering the hardenability associated with microalloying additions. Slight variations in composition can be corrected for by using standard curves of the type produced by Grossmann et al (104), figure 5. However, the change in carbon concentrations studied within the present research programme varied by approximately 0.3 mass % and therefore could not be compensated for by applying correction factors. Consequently, the effect of increasing the carbon from 0.1% to 0.4% should be considered in relation to the following:-

i)   the effect of carbon in solution on the martensite hardness value

ii)   the effect of carbon on the type of non martensitic transformation product

iii)   the effect of carbon in solution on the formation and rate of diffusion of microalloy clusters

iv)   the effect of carbon on the precipitation processes.

As previously stated in section 2.4.3.1, increasing the carbon content increases the as quenched martensite hardness. This has a direct influence on the 50%

martensite hardness value used to determine the ideal critical diameter value of the steel. This effect was identified prior to testing and allowed the steels to be corrected for variations in hardness. However, no data was available for the conversion to the 50% martensite hardness for the low carbon steels, therefore relationships from the medium carbon range were extrapolated to the low carbon levels. Nevertheless, the corrections were considered adequate to render the effect of carbon on the martensite hardness insignificant.

It has also been stated that carbon had a strong influence on the hardenability in its own right (108) (109). The effect of increasing the carbon content of the steel is to retard the non martensitic transformations. The 'C' curves of the bainite and the ferrite/pearlite transformations were also made more distinct. Consequently, in low carbon steels it would be expected that it is the ability of the microalloying elements to retard the upper bainite and ferrite transformations which determines their effect on hardenability, whereas in medium carbon steels it is their ability to retard the lower bainite transformation which determines the hardenability. Optical microscopy of the jominy bars at the calculated 50% martensite positions confirmed this effect, see figures 70 to 85. The low carbon steel 619, quenched from 950°C, showed a structure consisting of grain boundary pro-eutectoid

ferrite, upper bainite and martensite, figures 70 and 71, whereas, the equivalent medium carbon steel 624 consisted of lower bainite and martensite, figures 72 and 73. The significance of this observation is that, since the curves to calculate the 50% martensite hardness were derived from medium carbon steels, the ideal critical diameter values for the low carbon steels will be under estimated. Lower bainite has a higher hardness than pro-eutectoid ferrite or upper bainite. Consequently, if at the theoretical 50% martensite hardness position a ferrite/upper bainite structure was present an increase in the quantity of martensite would be expected, to compensate for the lower hardness of the non martensitic phase. However, for specimens quenched from 950°C the effect was not very noticeable. Examination of the corresponding specimens quenched from 1200°C also showed that pro-eutectoid ferrite and upper bainite were the non martensitic phases for the low carbon steel while lower bainite was the non martensitic phase for the medium carbon steel. However, it was also observed that the non martensitic phases in both steels essentially occurred at the prior austenite grain boundaries, and appear to be less than 50% at the calculated 50% martensite position. Therefore detailed analysis of the specimens at the theoretical 50% martensite positions was performed. The medium carbon alloy showed good agreement with the theoretical value with a martensite level of 54% whereas

the low carbon alloy 619 had a martensite level of 78%. The proportions of non martensitic phases for the low carbon steel were 3% pro-eutectoid ferrite, 1% lower bainite and 18% upper bainite. These figures confirmed the earlier suggestion that the hardenabilities of the low carbon steels were under estimated. However, despite the doubt concerning the precise level of the ideal critical diameter values obtained for the low carbon steels, the relative effects of the microalloying additions would be the same, i.e. an 80% hardenability criterion being used rather than the calculated 50%.

Increasing the quantity of carbon in solution also effects both the formation of the microalloying clusters and the rate at which they segregate to the austenite grain boundaries. As the carbon concentration is increased more carbon atoms are accommodated in the clusters and therefore increase the strain on the matrix lattice. This extra strain results in a slower rate of diffusion to the prior austenite grain boundaries. However, despite the clusters taking longer to reach the boundaries, and eliminate the grain boundary nucleation sites, once established at the boundaries they would be more difficult to disperse. Also, since the growth of the non martensitic phases requires diffusion of carbon away from the transformation front a high carbon cluster would be less able to diffuse away from the interface and would therefore reduce the rate of growth of the new

phase. As mentioned earlier, in the higher carbon steels, it is the inability of the carbon to diffuse away from the non martensitic phase which results in the formation of lower bainite rather than upper bainite.

The effect of increasing carbon on ideal critical diameter value, resulting from alloy carbide precipitation, must also be considered. In the majority of jominy tests the temperature from which the steels are quenched was selected so that all the carbon was in solution at the austenitising temperature. However, as the carbon concentration increased the required austenitising temperature increased and can under certain conditions result in undissolved alloy carbides. The presence of alloy carbides causes a reduction in both the microalloying element and carbon being available in solution to influence the hardenability. The removal of carbon from solution would also effect the martensite hardness and therefore influence the theoretical 50% martensite hardness position. In addition the precipitates themselves would tend to be coarser than the corresponding alloy nitrides and would therefore be less effective at pinning the prior austenite grain boundaries and could even act as preferred nucleation sites for the transformation from austenite and thus contribute to a decrease in the hardenability. Using standard solubility equations it was calculated that niobium carbides would

be present, at both 950°C and 1200°C, for both the medium

carbon niobium steels, 671 and 668. Also titanium

carbides would be present in both the medium carbon,

titanium steels, 669 and 672, at 950°C but only present

in the low nitrogen alloy 669 at 1200°C.

When the possible effects caused by the difference in the

carbon concentrations of the two series of steels studied

are considered, it can be seen, by comparing figures 32

and 34 with figures 35 and 36, that there was generally

good agreement on the effects of the various

microalloying additions, especially at 950°C where grain

boundary migration does not occur. It was therefore

considered reasonable to propose similar explanations for

both the low and medium carbon hardenability results.

6.1.7   Quantitative Effects of the Microalloying

Elements at a 1200°C Austenitising Temperature

It has already been stated that in recent years it has

been accepted that the hardenability of an alloy was

dependent upon the quantity of microalloying elements in

solution. Consequently, the results presented in table

23 should enable the effects due to the individual

microalloying elements to be quantified. However,

observation of the vanadium alloys showed that as the

vanadium in solution varied, so did the nitrogen in

solution. Therefore, to obtain the individual effects the four low carbon vanadium results, obtained at 1200°C, were used to formulate three simultaneous equations with two unknown values. These equations were solved and three values for the effects of vanadium and nitrogen in solution on the ideal critical diameter were obtained, see table 33. An average of these values was taken so that it was possible to correct the hardenability results for the other alloys for variations in the vanadium and nitrogen concentrations. This then allowed the individual effects of the other microalloying elements in solution to be isolated. The results expressed in terms of the multiplying factors for a 0.1% addition are presented in table 33 and figure 85. It can be seen that aluminium, niobium and titanium caused an increase in hardenability whilst vanadium caused a decrease as the alloying element in solution was increased. It is interesting to note that the general trend is for the multiplying factor to increase with increasing atomic radius of the microalloying addition. The larger the atom size the greater would be the binding energy between the grain boundary and the solute atom. Consequently, large atoms, such as titanium, would be more difficult to thermally disperse from the prior austenite grain boundaries and therefore maintain a high ideal critical diameter value for the steel to higher austenitising temperatures. However, if the results for aluminium,

202

niobium and titanium are considered, it is observed that the hardenability multiplying factor increased as the potential for grain boundary pinning increased. Titanium would be expected to be more effective at pinning grain boundaries than niobium which in turn would be more effective than aluminium. Consequently, if the grain boundaries are more effectively pinned the grain boundary segregation can more easily be established and result in an increase in the hardenability.

The multiplying factor of 1.026 for a 0.10% addition of molybdenum at a 1200°C austenitising temperature, is slightly lower than the value of 1.15 calculated in section 6.1.3, for molybdenum at a 950°C austenitising temperature, and the values of 1.12 and 1.22 reported by Managanon [8] [9]. This result could be associated with either a reduction in the driving force for segregation to the austenite grain boundaries or the migration of the grain boundaries and the need for the segregated molybdenum to diffuse with the migrating boundaries in order to influence the hardenability.

A similar treatment of the 950°C results was not possible due to the large variations in the vanadium and nitrogen values obtained. This was caused by the presence of undissolved precipitates and their kinetics of solution encountered at the lower solution treatment temperature of 950°C.

203

6.2 Precipitation Processes in Vanadium Alloyed Pearlitic Steels

In pearlitic steels the mechanical properties can be markedly increased by means of microalloying additions. It has been reported that small vanadium additions could increase the 0.2% proof stress by 90 to 200 MPa (10) (125) (132 to 135). This increase in strength, observed under continuous cooling conditions, is thought to be due to two distinct effects. Firstly, the vanadium depresses the austenite to pearlite transformation temperature which results in a reduction in the interlamellar spacing of the pearlite. The refinement of the pearlitic structure has a significant influence on the strength of the steel, and is expressed by Gladman et al (135) by the following relationships:-

$$\text{Yield stress (MPa)} = 15.4 \left\{ f_\alpha^{1/3} \left[2.3 + 3.8(Mn) + 1.13d^{-1/2} \right] + (1 - f_\alpha^{1/3}) \left[11.6 + 0.25 S_o^{-1/2} \right] + 4.1(Si) + 27.6\sqrt{(N)} \right\} ----(15).$$

and
$$\text{Tensile strength (MPa)} = 15.4 \left\{ f_\alpha^{1/3} \left[16 + 74.2\sqrt{(N)} + 1.18d^{-1/2} \right] + (1 - f_\alpha^{1/3}) \left[46.7 + 0.23 S_o^{-1/2} \right] + 6.3(Si) \right\} ---------(16).$$

where f_α = volume fraction of ferrite

d = grain diameter of ferrite in millimeters

So = interlamellar spacing of pearlite in
     millimeters

( ) = Alloy concentration in mass %

In fully pearlitic steels the equations can be reduced
to:-

$$Y.S.(MPa) = 15.4 \left\{ \left[11.6 + 0.25 S_o^{-1/2} \right] + 4.1 (Si) + 27.6 \sqrt{(N)} \right\} \quad ---(17)$$

and

$$T.S.(MPa) = 15.4 \left\{ \left[46.7 + 0.23 S_o^{-1/2} \right] + 6.3 (Si) \right\} \quad ------(18)$$

The second effect that increases the strength of a
vanadium containing pearlitic steel is the precipitation
of vanadium carbide particles within the pearlitic
ferrite. It has been suggested that the large increase
in strength could be associated with an interphase
precipitation process similar to that observed in low
carbon steels (20) (72) (73) (78) (79). To study the
precipitation effects two high carbon vanadium steels
(626 and 695) were isothermally transformed in the
temperature range 550°C to 650°C. Hardness measurements
were performed on the fully transformed structures which
showed that as the transformation temperature was
increased the hardness of the specimens decreased, table
28 and figure 38. The decrease in hardness was caused by
the formation of a coarser pearlitic microstructure,
figures 39 to 42. It was also observed that the low
nitrogen steel (626) exhibited a higher hardness value
than the high nitrogen steel (695) irrespective of the

transformation temperature studied. Examination of the microstructures from the two steels, transformed at the same temperatures, revealed that the high nitrogen steel (695) produced a coarser pearlitic structure, see figures 46 and 47 compared with 39 and 42, and therefore a decreased hardness value. When isothermally transforming steels, with a constant undercooling, all alloying elements, except cobalt, increase the interlamellar spacing of the pearlite. Therefore, it is considered that the extra nitrogen, in alloy 695, decreased the growth rate of the pearlite, and since pearlite growth rate is inversely related to interlamellar spacing, resulted in the observed increase in the interlamellar spacing.

Transmission Electron Microscopy (T.E.M.) studies were performed on the high nitrogen steel (695) transformed at a temperature of 650 °C. Alloy 695 was selected due to the increased potential for precipitation of vanadium carbonitrides at the different transformation temperatures. The highest transformation temperature was selected since this would give the largest pearlite interlamellar spacing. This was considered important since various microstructural studies (93) (125) (134) revealed that the precipitates occur mainly in the centre of the pearlitic ferrite lamellae, with precipitate free zones close to the cementite lamellae. Structures

206

similar to those observed by Dunlop (93) were obtained in the specimens held at the transformation temperature for 24 hours, see figures 48 to 52. The formation of the precipitate free zone indicated that the microalloying elements had re-distributed in the ferrite during or after the transformation. It is suggested that the vanadium partitions to, and to some extent dissolves in the cementite lamellae. It is known that up to 10% of vanadium can dissolve in cementite (94). However, no dark field images or electron diffraction patterns were obtained to identify the interphase precipitates.

Observation of specimens which were partially transformed did not show any precipitation within the ferritic lamellae, suggesting that the precipitates were either too fine to resolve or were precipitated after the transformation was complete, see figure 53. However, significant precipitation was observed in the pro-eutectoid ferrite present, figures 55 and 56.

Specimens held at the transformation for 3 and 8 minutes after the completion of the transformation did show precipitation which was thought to be due to the presence of dislocations, see figures 57 to 62. Whether the dislocations caused pre-existing precipitates to coarsen, or resulted in nucleation of new precipitates is unknown. However, a large proportion of the precipitates appeared to line up at approximately 50 degrees to the direction

of the cementite lamellae. Ridley et al (134) also observed short rows of precipitates oriented at an angle of approximately 60° to the longitudinal axes of the cementite lamellae, in a 0.2% vanadium containing eutectoid steel. It was shown by Ridley that most of the precipitates were present on only one of the possible habit planes of the Baker-Nutting relationship. The precipitates showing only one of the three possible variants suggests that the precipitates were formed by an interphase type mechanism rather than by homogeneous nucleation in the ferrite after transformation, or by heterogeneous nucleation on dislocations or sub-boundaries. Consequently, it is possible that the precipitates observed in the present study were also formed by an interphase precipitation mechanism and were coarsened by their interaction with dislocations.

Mottishaw et al (125) and Cordon et al (132) observed that marked increases in strength of pearlite were obtained by the addition of vanadium. However, no conclusive evidence for the presence of precipitates could be obtained using conventional electron microscopy. Consequently, Atom Probe Ion Microscopy studies were performed which successfully observed precipitates within the pearlitic ferrite. It was calculated that the precipitates were 3 to 4 nm in diameter and were essentially vanadium rich carbonitrides. However, even

when chromium was present as a residual element
noticeable levels were present in the vanadium
carbonitrides.

Recent work by Garbarz et al (122) on the thermo-
mechanical processing of austenite in vanadium containing
eutectoid steels, transformed at 600°C, also found no
indications of vanadium carbonitride precipitation using
conventional electron microscopy techniques. However,
ageing of the specimens produced fine precipitates which
occurred randomly and only in areas of pro-eutectoid
ferrite and in lamellar or non lamellar pearlite where
the diffusion distance within the ferritic phase was
comparatively large. In the pearlitic ferrite with
interlamellar spacing characteristic of transformation at
600°C, precipitation was only observed on dislocations
and therefore confirmed the observations of the present
study.

The mechanical properties of the two vanadium steels 626
and 695 were evaluated for a series of isothermal
transformation temperatures between 550°C and 650°C. The
tensile results presented in table 29 and 30, and figures
63 and 64, showed a maximum strength at an isothermal
transformation of 600°C. To assess the extent of
strengthening due to precipitation the experimental
results were compared with the theoretical tensile and
yield strengths for precipitate free pearlite calculated

209

using the relationships of Gladman et al (136) presented earlier in equations 17 and 18. The interlamellar spacing of the pearlite (So) was calculated using a Zener (137) type relationship where there is a linear relationship between the reciprocal of the mean interlamellar spacing and the transformation temperature. From the results presented in table 34 and figure 87, it can be seen that the experimental results did not show the gradual decrease in strength, with increasing transformation temperature predicted by the theoretical calculations, but exhibited a well defined precipitation peak at approximately 600°C. For the low nitrogen alloy 626 the increase in strength at 600°C was 155 MPa for the yield stress and 70 MPa for the tensile strength, while for the high nitrogen alloy 695 the increases were 245 MPa and 155 MPa respectively. The larger rise in strength of the high nitrogen steel 695 suggested that the increase was due to the precipitation of vanadium carbonitrides rather than vanadium carbides.

The Charpy Impact test results also showed a tendency to exhibit a precipitation related effect at approximately 600°C. The results presented in tables 31 and 32, and figures 65 and 66, show a slight decrease in toughness for both steels. The relationships between the toughness properties and the pearlite structure are more complex than for the tensile properties, however Gladman et al

(136) expressed the temperature at which an impact energy of 27J is obtained by the equation:-

$$I^{\circ}C = f_{\alpha}\left[-46 - 11.5\, d^{-1/2}\right] + (1 - f_{\alpha})\left[-335 + 5.6\, So^{-1/2} -13.3p^{-1/2} + 3.48 \times 10^{6}\, t\right] + 48.7\,(Si) + 762\sqrt{(Nf)} \quad ---(19)$$

where:- So = interlamellar spacing in millimeters

        p = pearlite colony size in millimeters

        t = cementite lamellae thickness in millimeters

      Nf = free interstitially dissolved nitrogen

         (Mass %)

For fully pearlitic steels the equation can be simplified to:-

$$I^{\circ}C = \left[-335 + 5.6\, So^{-1/2} - 13.3p^{-1/2} + 3.48 \times 10^{6}\, t\right] + 48.7\,(Si) + 762\sqrt{(Nf)} \quad ----------\ (20)$$

Test temperatures required to achieve an impact energy of 27J were calculated for a precipitate free fully pearlitic steel using the Gladman relationship and were compared with the temperatures observed for the low nitrogen, vanadium steel 626, see table 35 and figure 88. The expected gradual reduction in the Charpy test temperature with increasing transformation temperature was not realised for alloy 626. Instead the 27J temperature increased up to a transformation temperature of 600°C before gradually decreasing again at higher transformation temperatures. This loss of toughness must be associated with the precipitation effects observed in

211

the tensile results. A similar curve produced from the experimental results for the steel 695 was not possible since only one test result exceeded the 27J impact energy value. However, if a similar curve was constructed at a 17J impact energy level, again a loss in toughness around the 600°C isothermal transformation temperature was observed, figure 88.

Both the tensile and impact data indicated that the maximum precipitation effects were occurring at approximately 600°C. Consequently, microscopical examination of the specimens transformed at 600°C, rather than 650°C, could have identified more direct evidence for the presence of interphase precipitation. However, as stated previously, work by Garbarz et al (122) performed on vanadium steels transformed at 600°C did not show interphase precipitation using conventional electron microscopy. Therefore, it is believed that to determine the presence and mechanisms involved with interphase precipitation of vanadium carbonitrides in pearlite, a more detailed examination of specimens transformed at 600 °C is required, and that more specialised equipment able to resolve very fine precipitates, or even pre-precipitation clusters, would be necessary.

7.   Conclusions

7.1   Hardenability Investigations

The addition of microalloying elements to both low and medium carbon, vanadium steels has been shown to significantly influence the hardenability after austenitising at both $950^{\circ}C$ and $1200^{\circ}C$. Applying the accepted theories, that the ideal critical diameter was dependent solely upon the carbon concentration, the prior austenite grain size and the quantities of microalloying elements present in solution, the majority of the results could be successfully explained. However, when jominy test conditions were varied the classical response, of increasing microalloying concentrations causing a corresponding increase in hardenability, was not observed.

Extending the time that the steels were austenitised, at $950^{\circ}C$, prior to jominy end quenching produced results which indicated that the ideal critical diameter was dependent upon kinetic effects. In particular it was shown that the hardenability depended upon such factors as the rate of solution of the microalloying carbides/nitrides and the rate at which the microalloying elements formed clusters and segregated to the austenite grain boundaries. This effect was confirmed when specimens which had a refined precipitate morphology, which would therefore be expected to enter solution more

rapidly, reached a maximum hardenability after a shorter time interval.

Increasing the austenitising temperature to 1200°C also showed that non-standard hardenability behaviour could be obtained, even though kinetic effects would be less likely at this high temperature. It was observed that the hardenability could be reduced by the addition of such elements as vanadium, niobium and titanium. These inconsistencies were attributed to a number of effects such as thermal dispersion of the grain boundary microalloying clusters, large undissolved precipitates acting as preferred nucleation sites for the transformation and the migration of the austenite grain boundaries.

To successfully interpret the hardenability interactions it was necessary to assess the individual contributions of the following factors:-

i)   the quantity of microalloying elements in solution

ii)   the ability of the elements in solution to segregate to, or desegregate from, the prior austenite grain boundaries

iii)   the ability of the microalloying elements in solution to form clusters, or complexes, which exhibit different influences on the hardenability

iv)   the volume fraction, particle size and distribution of undissolved alloy

carbides/nitrides

v)   the ability of the undissolved precipitates to act
        as preferred nucleation sites for the
        transformation from austenite

vi)   the ability of the undissolved precipitates to act
        as grain boundary pinning agents and restrict
        austenite grain boundary migration

The analysis of the results identified two situations
where the effects of the microalloying additions could be
significantly different. When movement of grain
boundaries is adequately restricted, either by using a
low austenitising temperature or the presence of
extensive grain boundary pinning agents, the classical
hardenability responses were observed. It is suggested
that the microalloying elements in solution form clusters
of elements which exert strain on the matrix lattice.
Therefore, to reduce this strain energy the clusters
segregate to the high energy austenite grain boundaries,
which also reduces the energy of the boundaries. If the
boundaries are stationary the segregation phenomenon is
readily established. Therefore, when increased
quantities of microalloying elements are added, and taken
into solution, more segregation to the grain boundaries
occurs and causes an increase in the hardenability of the
steel.

However, a second situation exists, at high temperatures,

where grain boundary pinning is inadequate to prevent the migration of the prior austenite grain boundaries. At these temperatures more of the lattice strain energy of the clusters can be accommodated by the matrix and therefore the driving force for segregation to the grain boundaries is reduced, and in certain circumstances could result in the thermal dispersion of the microalloying clusters away from the boundaries. Under moving boundary conditions it is not only the ability of the clusters to segregate to the grain boundaries which determine the hardenability but also their ability to diffuse with the migrating grain boundaries. Increasing the quantity of microalloying elements in solution increases the size of the clusters, increases their strain energy but reduces their rate of diffusion. Consequently, at low concentrations the clusters may adequately diffuse with the grain boundaries and increase the hardenability of the steel. Whereas, at higher concentrations the rate of diffusion could be reduced to an extent that the clusters could not diffuse with the grain boundaries and therefore result in a decrease in the observed ideal critical diameter.

The addition of niobium to a vanadium steel caused the formation of niobium carbides and nitrides in preference to vanadium carbides and nitrides. Therefore, extra vanadium was available in solution to segregate to the prior austenite grain boundaries and increase the ideal

critical diameter. Consequently, the pinning of the austenite grain boundaries were controlled by the niobium precipitates. However, these precipitates being larger than the vanadium precipitates would be less effective at pinning the austenite grain boundaries, for equivalent volume fractions, and would also be more likely to act as preferred sites for the transformation from austenite.

The addition of titanium to a vanadium steel produced the largest increases in hardenability especially at the higher nitrogen concentrations. Titanium like niobium is a very strong carbide/nitride forming element which resulted in the formation of titanium carbides and nitrides in preference to those of vanadium. Again more vanadium is maintained in solution to increase the hardenability. However, titanium nitrides are very fine and therefore are very effective at pinning the austenite grain boundaries. The precipitates are also more thermally stable and would therefore maintain their grain boundary pinning properties to higher austenitising temperatures. The effect of increased nitrogen in the steels was shown to have significant influences upon the ideal critical diameter. Nitrogen entering solution segregated to the austenite grain boundary and had a direct influence on the hardenability. However, the most significant effect was the increase in the volume fraction of the alloy nitrides. The increased

precipitation more effectively pinned the grain boundaries allowing the segregation of the microalloying elements in solution to be more easily established and thus increase the hardenability.

The effect of increased carbon in the steel resulted in much larger ideal critical diameters. However, unlike nitrogen it was the microalloying elements effect in solution, rather than the precipitation of alloy carbides, that was the dominant influence. The carbon in solution increased the hardenability by delaying the nucleation and growth of the transformation products. Because of the increased concentration it was more difficult for the carbon to diffuse away from the transformation front and resulted in a change in the non-martensitic transformation phases obtained. In low carbon steels ferrite/upper bainite structures were observed, whereas in medium carbon steels lower bainite was observed. This led to an under estimation of the low carbon hardenability results but the effects of the addition of microalloying effects were relatively the same.

The quantitative effects of the alloying elements on a base vanadium steel were determined for the low carbon alloys at an austenitising temperature of 1200°C. It was observed that as a general trend the hardenability multiplying factors increased with increasing atomic

radius of the microalloying addition and is therefore an indication of the greater binding energies between the solute atoms and the grain boundaries. However, the aluminium, niobium and titanium results showed that as the multiplying factor increased, the potential for effective grain boundary pinning of the austenite was increased. The multiplying factor for molybdenum was calculated as 1.026 for a 0.10% addition compared with 1.15 calculated at 950°C for the same steel. It is suggested that the reduction in multiplying factor at 1200°C is due to a reduction in the driving force for segregation to the grain boundaries or by the migration of the austenite grain boundaries. A similar quantitative examination of the results for the 950°C austenitising temperature on the medium carbon steels was not possible due to the presence of undissolved precipitates and the kinetic effects associated with their solution.

7.2 Precipitation Processes in Vanadium Alloyed Pearlitic Steels

Construction of the T.T.T. diagrams for the two vanadium alloyed pearlitic steels showed that the extra nitrogen in the high nitrogen alloy raised the temperature of the nose of the pearlite transformation and also increased the rate of the transformation.

Microstructural examination of the high nitrogen steel transformed at an isothermal transformation temperature of 650°C showed that after 24 hours extensive precipitation within the pearlitic ferrite was present, with a precipitate free zone observed adjacent to the cementite lamellae. However, specimens which were held at the transformation temperature for up to 8 minutes after the completion of the transformation did not show extensive precipitation typical of interphase type precipitation. However, a large proportion of the precipitates observed did line up at approximately 50 degrees to the direction of the cementite lamellae. It was therefore suggested that interphase precipitation could be present which was beyond the resolution of the microscope used for the examination of the specimens and that the precipitates observed were those which had been preferentially coarsened by interaction with dislocations.

Mechanical property data obtained by isothermally transforming tensile and Charpy test specimens indicated that the maximum precipitation effects, of both steels, occurred at approximately 600°C. The tensile results showed that in the low nitrogen steel the increase in strength at the 600°C isothermal transformation temperature was 155 MPa for the yield stress and 70 MPa for the tensile stress, while for the high nitrogen steels the increases were 245 MPa and 155 MPa

respectively. Electron microscopy of specimens transformed at $600^\circ C$ could have provided more direct evidence for interphase precipitation. However, it was considered that to determine the presence and the nature of the precipitation mechanisms involved would require more specialised equipment such as an Atom Probe Ion Microscope to resolve the very fine precipitates or pre-precipitation clusters.

8.   Suggestions for Further Work

8.1   Hardenability Investigations

The ideal critical diameters determined in this study were calculated from the distance from the quenched end of the jominy test bar to the 50% martensite hardness value position. Consequently, since no data was available for the martensite hardness typical of the low carbon steels, the relationships from the medium carbon range were extrapolated to the low carbon levels. Similarly, no conversion of jominy distance to ideal critical diameter was available for the distances typical of the low carbon steels. Consequently these relationships had also to be extrapolated to those typical of the low carbon steels. Examination of the theoretical 50% martensite conditions to check if the calculations were valid showed that the low carbon steels contained approximately 80% martensite. The major reason for this observation was the change in non martensitic structure from lower bainite to pro-eutectoid ferrite and upper bainite. Consequently, it is considered essential that the correct factors for low carbon steels be determined, so that the same criteria for hardenability can be applied at both low and medium carbon levels.

To eliminate variables which were present from an 'as cast' structure, such as the interdendritic segregation of silicon observed in the present study, the bars were

homogenised and grain refined prior to jominy testing. Consequently, relating the individual hardenability values back to an industrial situation would be tenuous, however the observed trends would be expected to occur for both the homogenised and unhomogenised situations. It is therefore recommended that the more complex situation of hardenability of unhomogenised steels is studied and related to the effects observed for homogenised and grain refined material. This could have an effect on the precipitate morphologies and therefore a direct influence on the ideal critical diameter.

It has been suggested that an important part of the hardenability process is the formation of microalloying clusters in solution and their effectiveness at segregating to the prior austenite grain boundaries. Consequently, it is necessary to study this phenomenon to fully understand the mechanisms of hardenability. However, such an investigation would require specialised high resolution equipment and techniques such as Auger spectography, Atom Probe Ion Microscopy etc.

The presence of undissolved microalloy carbides/nitrides have also been identified as an important factor in the determination of the hardenability. The precipitates can either act as preferred nucleation sites for the transformation, and cause a decrease in hardenability or could act as grain boundary pinning agents, and

contribute to an increase in hardenability. Therefore the effects of volume fraction, size and distribution of the precipitates on hardenability require study. The control of the precipitate morphology could have industrial implications, since the thermomechanical treatment of the steels could produce a more beneficial morphology which could allow more effective utilisation of the microalloying elements.

Jominy end quench test specimens have been successfully used to determine hardenability for many years. However, it has been shown that once the standard jominy conditions are altered unusual and unexpected hardenability effects have been observed. Since the actual conditions used in industrial applications will almost certainly be different from the standard jominy conditions the hardenability effects would also be different. It is therefore suggested that the time-temperature-hardenability relationships are studied in more detail to assess how sensitive the hardenability is to variations in processing parameters.

In the present study only vanadium interactions with one other microalloying addition were investigated and explanations for the results proposed. Therefore, it would be interesting to see if the theories could be extended to multi-interaction situations and to see if

more quantitative effects could be determined so that more accurate methods for determining the hardenability from the chemical composition of the steel could be devised.

8.2 Precipitation in Vanadium Alloyed Pearlitic Steels

Mechanical property data from the two vanadium alloyed pearlitic steels indicated that the maximum precipitation effects were obtained at a transformation temperature of approximately 600°C. Consequently, it is suggested that to determine the presence and mechanisms involved in the precipitation strengthening that a more detailed examination of specimens isothermally transformed at 600°C be performed using equipment able to resolve very fine precipitates, or even pre-precipitation clusters.

REFERENCES

1.   W Roberts and A Sandberg; Swedish Institute for
      Metals Research, Report No. IM.1489. October, 1980.

2.   R K Amin, M Korchynsky and F B Pickering; Metals
      Technology, 1981. 8 (7), p.250.

3.   A D Vassiliou; PhD Thesis, Sheffield City
      Polytechnic, 1987.

4.   F B Pickering; "The Optimisation of Microstructures
      in Steel and their Relationship to Mechanical
      Properties" in "Hardenability Concepts with
      Applications to Steel". AIME, 1977, p.179.

5.   J P Benson; Metal Science, 1979, 13 (6), p.366.

6.   V N Kopernikova et al; Metalloved. Term. Obrab.
      Met., 1979, 11, p.43.

7.   G T Eldis and W C Hagel; in "Hardenability Concepts
      with Applications to Steel", AIME Seminar, Chicago,
      1977, p.397.

8.   P L Mangonon; Journal of Metals,1981, June, p.18.

9.   P L Mangonon; Met. Trans. A. 1982, 13(A), p.319.

10.   "Vanadium in Rail Steels"; Vanitec Seminar, Chicago,
      1979, published by Vanitec.

11.   S Engineer et al; H F F Berickt, 1980, 6, p.911.

12.   D Whittaker; Metallurgia, 1979, 46 (4), p.275.

13.   S Engineer et al; Thyssen. Edelst. Techn. Berickt,
      1980, 6 (2), p.85.

14.   G Thewlis and D J Naylor; Metals and Materials,
      1981, Dec., p.21.

15.   S Engineer et al; Thyssen Edelst. Tech. Berickt,
      1981, 7 (1), p.3.

16.   R E Reed-Hill; "Physical Metallurgy Principles".

17.   R W K Honeycombe; "Steels:-Microstructure and
      Properties". Edward Arnold (Publishers) Ltd.,
      London, 1981.

18.   G A Chadwick; "Metallography of Phase
      Transformations". Butterworth Press.

19. H I Aaronson; "Decomposition of Austenite by
     Diffusional Processes", Interscience, New York,
     1962.

20. R W K Honeycombe; "Ferrite", Metal Science, June
     1980, p.201.

21. G Kurdjumov and G Sachs; Z. Physik, 64, 1930, p.325.

22. R F Mehl and W C Hagel; "The Austenite-Pearlite
     Reaction", Prog. Met. Physics, 6, ed. B Chalmers and
     R King, Pergamon Press, 1956.

23. R J Dippenaar and R W K Honeycombe; Proc. Roy. Soc.,
     1973, Series A., p.455.

24. W Pitsch; Acta. Met., 10, 1962, p.897.

25. N J Petch; Acta. Crystallogr., 1953, 6, p.96.

26. A Bagaryatskii; Dokl. Akad. Nauk., SSSR, 73, 1950,
     p.1161.

27. F H Samuel and A A Hussein; Trans. ISIJ., Vol.23,
     1983, p.65.

28. T Gladman, I D McIvor and F B Pickering; JISI.,
     1972, 210, p.916.

29. C M Wayman; J. of Sheffield Uni. Met. Soc., 1983, 7
     p.19.

30. E R Petty; "Martensite, Fundamentals and
     Technology", Longmans, 1970.

31. P H Chang, P G Winchell and G L Liedl; Met. Trans.,
     A., Vol.14A, Feb. 1983, p.163.

32. B P J Sandvik and C M Wayman; Met. Trans., A.,
     Vol.14A, May 1983, p.809-845.

33. G V Kurdjumov; Met. Trans., A., Vol.7A, July 1976,
     p.999.

34. Z Nishiyama; Sci. Rep. Tohuku Univ., 23, 1934,
     p.637.

35. G Wassermann; Archs. Eisenhutt., 16, 1933, p.647.

36. B P J Sandvik; Met. Trans., A., Vol.13A, May 1982,
     p.779.

37.   F B Pickering; "Transformation and Hardenability in Steels". Symposium by Climax Molybdenum Co., Ann Arbor, 1967, p.109.

38.   R W K Honeycombe and F B Pickering; Met. Trans., A., Vol.3A, May 1972, p.1099.

39.   Y Ohmori; Trans. ISIJ., 1971, Vol.11, p.95-101, p.250.

40.   H K D H Bhadeshia; Acta. Metall., Vol.28, 1980, p.1103.

41.   K R Kinsman and H I Aaronson; Met. Trans., A., Vol.13A, May 1982, p.39.

42.   A T Davenport, F G Berry and R W K Honeycombe; Met. Sci. J., 1968, Vol.2, p.104.

43.   F G Berry and R W K Honeycombe; Met. Trans., 1970, Vol.1, p.3279.

44.   J M Gray and R B S Yeo; Trans. ASM., 1968, Vol.61, p.255.

45.   K W Andrews; J. Iron Steel Inst., Vol.203, 1965, p.721.

46.   W Steven and A G Haynes; J Iron Steel Inst., 1956, 183, p.349.

47.   "Atlas of Continuous Cooling Transformation Diagrams for Engineering Steels"; British Steel Corporation, 1977, p.227.

48.   M Hanson; "Constitution of Binary Alloys", McGraw-Hill, 1958, p.730.

49.   A D Vassiliou; Progress Report to Union Carbide, Sept., 1980.

50.   R D Cochrane; Private Communication via F B Pickering.

51.   N K Balliger; PhD thesis, Cambridge University, 1977.

52.   W Steven and A G Haynes; JISI, 1956, 183, p.349.

53.   P Payson and C H Savage; Trans. ASM, 1944, 33, p.261.

54.   L A Carapella; Met. Prog. 1944, 46, p.108.

55.   E S Rowland and S R Lyle; Trans. ASM, 1946, 37, p.27.

56.   A E Wehrenberg; Trans. AIMME, 1946, 167, p.494.

57.   R A Grange and H M Stewart; Trans. AIMME, 1946, 167, p.467.

58.   G H Eichelman and F C Hull; Trans. ASM, 1953, 45, p.77.

59.   H K D H Bhadeshia; Private Communication via F B Pickering.

60.   N K Balliger and R W K Honeycombe; Met. Trans., 11A, 1980, p.421.

61.   T Kunitake and H Ohtani; Sumitomo Search 1969 (2), Nov., p.18.

62.   P Maynier et al; Rev. de Met., 1972, 62, p.505.

63.   R Blondeau et al; Rev. de Met., 1973, 70, p.883.

64.   R Blondeau et al; Rev. de Met., 1975, 72, p.759.

65.   M G H Wells; Acta. Met., 1964, 12, p.389.

66.   F B Pickering; ISI., Special Report, No.64, 1959, p.23.

67.   A R Cox; Iron and Steel, December, 1968, p.539.

68.   J H Woodhead and A G Quarrell; JISI., 1965, 203, p.605.

69.   R W K Honeycombe; "Structure and Strength of Alloy Steels", Climax Molybdenum Publication, 1975.

70.   R W K Honeycombe; Scand. J. of Met., 8, 1979, p.21.

71.   T Tanaka et al; "Microalloying '75"., Session 1, Vanitec, London, 1975, p.88.

72.   A T Davenport, L C Brossard and R E Miner; Journal of Metals, June, 1975, p.21.

73.   P R Howell, J V Bee and R W K Honeycombe; Met. Trans., A., Vol.10A, Sept., 1979, p.1213.

74.   K Campbell and R W K Honeycombe; Met. Sci. J., 1974, Vol.8, p.197.

75.   A D Batte and R W K Honeycombe; J. Iron Steel Inst., 1973, Vol.211, p.284.

76. D J Walker and R W K Honeycombe; Met. Sci., May 1980, p.184.

77. M Tannino and K Aoki; Trans. ISIJ., 8, 1968, p.337.

78. R W K Honeycombe; Met. Trans. A., Vol.7(A), July 1976, p.915.

79. G J Cocks, R A Legge and D R Minor; Met. Sci., Oct. 1980.

80. R G Baker and J Nutting; "Precipitation Processes in Steels", ISI Report No.64, (1959), p.1.

81. A T Davenport and R W K Honeycombe; Proc. Roy. Soc., 1971, Vol.322, p.191.

82. P R Howell, R A Ricks and R W K Honeycombe; J. of Met. Sci., 15, 1980, p.376.

83. R A Ricks, P R Howell and R W K Honeycombe; Met. Trans. A., Vol.10(A), August 1979, p.1049.

84. R A Ricks and P R Howell; Acta. Metall., Vol.31, No.6, 1983, p.853.

85. R A Ricks and P R Howell, Met. Sci., Vol.16, June 1982, p.317.

86. V K Heikkinen; Scand. J. Metall., 109, (1973), p.112.

87. R M Smith, J G Williams and D P Dunne; Met. Forum, Vol.5, No.2 1982, p.109.

88. D Frodl et al; Harterei, Techn. Mit., 1974, 29(3), p.169.

89. V I Syneishchikova et al; Steel in the USSR, 1980, 11, p.1010.

90. J Dilewijns, L Schetky and A M Sage; "Vanadium in Rail Steels", Vanitec Seminar, Chicago, 1979, Paper E.

91. A M Sage, W Hodgson and D H Stone; ibid-paper B.

92. M T Lewis, W B Morrison and N Ridley; "Advances in the Physical Metallurgy and Applications of Steels", Metals Society Conference, Liverpool, Sept. 1971.

93. G L Dunlop, C J Carlsson and G Frimodig; Met. Trans. A., Vol.9(A), Feb. 1978, p.261.

94. S K W Shaw and A G Quarrell; JISI, 1957, 185, 10.

95. F Schmidt, L Meyer and G Strassburger; Bander-Bleche-Rohre, 1968, 9, (11), p.676.

96. M J Crooks et al; Met. Trans. A., Vol.12(A), Dec. 1981, p.1991.

97. M J White; MSc Thesis, Massachusetts Institute of Technology, Dec., 1977.

98. W Heller, R Schweitzer and L Weber; Can. Met. Quart., Vol.21, No.1, Jan-March 1982, p.3.

99. Canadian Metals Quarterly, Vol.21, No.1, Jan-March 1982.

100. W Crafts and J L Lamont; "Hardenability and Steel Selection"., Pitman, London, 1949,.

101. C A Siebert, D V Doane and D H Breen; "The Hardenability of Steels". ASM., 1977.

102. "Hardenability Concepts with Applications to Steel". AIME Seminar, Chicago, 1977.

103. M A Grossmann and R L Stephenson; Trans. ASM, Vol.29, 1941.

104. M A Grossmann; Trans. Am. Inst. Min. Met. Eng., Vol.150, 1942, p.227.

105. M A Grossmann; "Elements of Hardenability" ASM, 1952.

106. W Crafts and J L Lamont; Trans. Am. Inst. Min. Met. Eng., Vol.158, 1944, p.157.

107. H E Hostetter; Trans. AIME, Vol.167, 1946, p.643.

108. I R Kramer, S Siegel and J G Brooks; Trans AIME, Vol.167, 1946, p.670.

109. R A Grange; Met. Trans. A., Vol.4(A), Oct. 1973, p.2231.

110. W E Jominy; Met. Prog., Dec. 1941, p.911.

111. C F Jatczak; Met. Prog., Sept. 1971, p.60.

112. R V Fostini and F J Schoen; Met. Trans. A., Vol.13(A), May 1982, p.195.

113. A F DeRetana and D V Doane; Met. Prog., Sept., 1971.

114. O Sandberg, P Westerhult and W Roberts; Swedish Institute for Metals Research - Report No.I.M.1687, Aug., 1982.

115. W Roberts; Reported at discussion organised by Vanitec, Sheffield 1981.

116. F B Pickering; Proceedings of an International Conference on H.S.L.A. Steels 1985, China, 1985, p.305.

117. J H Butcher and J D Grozier; ASM Met. Eng. Quart. 1965, Nov., p.1.

118. M Korchynski; Private Communication.

119. British Standard Method for the End Quench Hardenability Test for Steel (Jominy Test); B.S.4437:1969.

120. M A Grossmann, M Asimow and W F Craig; SAE Trans., Vol.49, 1941, p.283.

121. C J McMahon; Met. Trans. A., Vol.11(A), March 1980, p.531.

122. B Garbarz and F B Pickering; Unpublished research.

123. H Watenabe; Private Communication via F B Pickering.

124. J S Kirkaldy; Discussion to ref.7.

125. T D Mottishaw and G D W Smith; in "HSLA Steels - Technology and Applications", ed. M Korchynsky, Metals Park, Ohio, ASM, 1984, p.163.

126. D McLean; "Grain Boundaries in Metals", Oxford University Press, 1957, Chapter 1.

127. E D Hondros; in "Grain Boundary Structure and Properties", ed. by G A Chadwick and D A Smith, Academic Press, New York, 1976, p.265.

128. E D Hondros and M P Seah; International Metals Reviews, Dec. 1977, p.262.

129. M Guttmann; Met. Trans. A., Vol.8(A), 1977, p.1383.

130. T Gladman; Proc. Roy. Soc. Series A, 1966, 294, p.298.

131. T Gladman and F B Pickering; JISI, 1967, 205, p.653.

132. B W Cordon, P Timney, T D Mottishaw and G D W Smith;
      in "Developments in the Drawing of Metals, The
      Metals Society, London, 1983, p.288.

133. D E Parsons, D A Munro and J Ng-Yelim; Can. Met.
      Quart., Vol.22, No.4, 1983, p.475.

134. N Ridley, N T Lewis and W B Morrison; in "Advances
      in the Physical Metallurgy and Applications of
      Steels", The Metals Society, London, 1982, p.199.

135. E E Laufer and D M Fegredo; Can. Met. Quart.,
      Vol.22, No.2, 1983, p.193.

136. T Gladman, I D McIvor and F B Pickering; JISI, 1972,
      210, p.916.

137. C Zener; Trans. AIME, 167, 1946, p.550.

TABLE 1   Effect of Microalloying Additions on

the Hardenability of Steels

Element	ΔDi^* mm per wt % austenitised at:	
	925°C	1200°C
V	+19.53	+25.11
Mo	+ 5.09	+30.56
Nb	-30.50	+110.80
Ti	-35.10	-35.29

TABLE 2   The Synergistic Effects of Vanadium With Other
Microalloying Elements

Effect	ΔDi^* mm per wt % austenitised at:	
	925°C	1200°C
With no Mo	-	+ 8.05
With 0.3% Mo	-	+42.16
With no Ti	-	- 6.35
With 0.088% Ti	-	+56.56
With no Mo and no Nb	+ 3.69	+14.08
With 0.3% Mo and 0.038% Nb	+ 2.81	+67.34
With no Mo and no Ti	+ 9.01	- 9.30
With 0.3% Mo and 0.088% Ti	-10.78	+87.72

TABLE 3   Analyses of Experimental Steels

Cast No.	Chemical analysis mass %								
	C	Si	Mn	V	N$_2$	Al	Mo	Nb	Ti
612	0.080	0.30	1.54	0.145	0.0083	-	-	-	-
613	0.113	0.21	1.41	0.140	0.0079	-	-	-	-
619	0.085	0.29	1.42	0.125	0.0170	-	-	-	-
617	0.093	0.26	1.50	0.220	0.0089	-	-	-	-
622	0.095	0.43	1.58	0.220	0.0200	-	-	-	-
638	0.091	0.43	1.64	0.140	0.0091	0.058	-	-	-
639	0.095	0.33	1.65	0.135	0.0165	0.050	-	-	-
640	0.083	0.30	1.65	0.140	0.0071	-	0.21	-	-
641	0.087	0.36	1.60	0.135	0.0151	-	0.21	-	-
642	0.085	0.21	1.45	0.135	0.0070	-	-	0.065	-
643	0.090	0.41	1.60	0.135	0.0185	-	-	0.065	-
644	0.085	0.36	1.52	0.140	0.0078	-	-	-	0.055
645	0.088	0.42	1.52	0.140	0.0168	-	-	-	0.060
623	0.365	0.36	1.47	0.130	0.0100	-	-	-	-
624	0.390	0.43	1.57	0.130	0.0200	-	-	-	-
662	0.365	0.37	1.54	0.140	0.0060	0.070	-	-	-
663	0.390	0.28	1.50	0.120	0.0160	0.040	-	-	-
664	0.390	0.33	1.41	0.120	0.0070	-	0.17	-	-
665	0.400	0.28	1.45	0.180	0.0160	-	0.20	-	-
671	0.340	0.28	1.50	0.145	0.0075	-	-	0.060	-
668	0.380	0.37	1.61	0.145	0.0170	-	-	0.060	-
669	0.340	0.30	1.64	0.150	0.0070	-	-	-	0.075
672	0.380	0.31	1.55	0.145	0.0170	-	-	-	0.082
626	0.735	0.35	1.55	0.140	0.0100	-	-	-	-
695	0.710	0.32	1.57	0.170	0.0150	-	-	-	-
777	0.090	0.40	1.59	0.130	0.0180	-	-	-	-

TABLE 4   S.E.M. Analyses for Unhomogenised Material

Ferrite				Martensite			
Si%	V%	Mn%	Fe%	Si%	V%	Mn%	Fe%
0.199	0.037	0.187	98.575	0.329	0.098	0.936	98.638
0.203	0.075	1.134	98.586	0.307	0.110	1.024	98.558
0.236	0.063	1.070	98.629	0.248	0.096	1.088	98.566
0.229	0.067	1.057	98.644	0.305	0.013	1.058	98.622
0.194	0.037	1.278	98.489	0.342	0.054	1.214	98.388
0.294	0.044	1.001	98.659	0.402	0.076	1.202	98.318
0.194	0.021	0.978	98.807	0.381	0.087	1.065	98.465
0.176	0.051	1.131	98.640	0.361	0.101	1.242	98.294
0.255	0.109	0.999	98.635	0.242	0.108	1.169	98.479
0.199	0.063	1.056	98.680	0.351	0.110	1.117	98.480

TABLE 5   T-Test Results for Unhomogenised Material

Element in Ferrite	Element in Martensite	Degrees of Freedom	T-Test Value	5% Level of Significance
Si	Si	18	5.42212	5.07
V	V	18	2.28868	5.07
Mn	Mn	18	0.52659	5.07
Fe	Fe	18	3.36196	5.07

TABLE 6   S.E.M. Analyses for Homogenised Material

Ferrite				Martensite			
Si%	V%	Mn%	Fe%	Si%	V%	Mn%	Fe%
0.494	0.149	0.945	98.411	0.499	0.096	1.226	98.177
0.331	0.071	1.140	98.456	0.413	0.083	1.272	98.230
0.471	0.045	1.143	98.339	0.296	0.088	1.169	98.446
0.400	0.116	1.012	98.470	0.374	0.068	1.247	98.310
0.365	0.155	1.214	98.264	0.379	0.138	1.196	98.285
0.301	0.133	1.019	98.545	0.355	0.016	1.195	98.387
0.353	0.090	1.109	98.446	0.457	0.056	1.174	98.312
0.319	0.118	1.219	98.343	0.526	0.076	1.250	98.146
0.505	0.071	1.127	98.294	0.560	0.114	1.136	98.188
0.267	0.089	1.063	98.580	0.488	0.112	1.087	98.311

TABLE 7   T-Test Results for Homogenised Material

Element in Ferrite	Element in Martensite	Degrees of Freedom	T-Test Value	5% Level of Significance
Si	Si	18	1.43600	5.07
V	V	18	1.02503	5.07
Mn	Mn	18	2.88316	5.07
Fe	Fe	18	3.02743	5.07

TABLE 8   Calculated Solubility Temperatures

Cast No.	T (°K) For VC	T (°C) For VC	T (°K) For VN	T (°C) For VN
612	1097	824	1320	1047
613	1115	842	1312	1039
619	1092	819	1377	1104
617	1129	856	1368	1095
622	1131	858	1458	1185
638	1103	830	1325	1052
639	1103	830	1382	1109
640	1097	824	1301	1028
641	1098	825	1372	1099
642	1097	824	1297	1024
643	1100	827	1394	1121
644	1099	826	1310	1037
645	1100	827	1388	1115
623	1181	908	1327	1054
624	1185	912	1399	1126
662	1186	913	1286	1013
663	1195	922	1390	1117
664	1180	907	1286	1013
665	1208	935	1410	1137
671	1183	910	1310	1037
668	1191	918	1393	1120
669	1186	913	1307	1034
672	1191	918	1393	1120
626	1233	960	1335	1062
695	1244	971	1397	1124
777	1098	825	1387	1114

Values Calculated Using Equations (1):-

i)   For VC: $\log_{10} [V][C] = \dfrac{-9500}{T(°K)} + 6.72$ ...... (8)

ii)   For VN: $\log_{10} [V][N] = \dfrac{-7840}{T(°K)} + 3.02$ ...... (9)

TABLE 9   Standard Grain Sizes Used By Other Authors

Author	Treatment Temperature	Grain Size (mm)	A.S.T.M. No.
Eldis	1200°C	0.160	2.0
Eldis	950°C	0.007	11.0
Mangonon	954°C	0.0076	10.0

TABLE 10   Grain Size Measurements

Condition of Sample	Grain Size (mm)	A.S.T.M. No.
(i) Original bar treated at 1250°C	0.1578	2.05
(ii) Homogenised bar	0.3025	0.18
(iii) Homogenised + 1 cycle to 1250°C	0.2738	0.49
(iv) Homogenised + 1 cycle to 1200°C	0.1880	1.58
(v) Homogenised + 2 cycles to 1200°C	0.1691	1.86
(vi) Homogenised + 1 cycle to 950°C 1 cycle to 1200°C	0.1542	2.28
(vii) Homogenised + 1 cycle to 950°C	0.0095	10.17
(viii) Homogenised + 2 cycles to 950°C	0.0048	12.00
(ix) Homogenised + 1 cycle to 1200°C 1 cycle to 950°C	0.0088	10.40

TABLE 11   Hardenability of a Low Carbon Vanadium Steel
             Austenitised at 950°C

Cast No.	Composition (Mass %)	Grain Size (mm)	Di (mm) Uncorrected	Di* (mm) Corrected	ΔDi* (mm)
612	0.08C, 0.30Si 1.54Mn, 0.145V 0.0083N$_2$	0.0155	37	34	-
619	0.085C, 0.29Si 1.42Mn, 0.125V 0.017N$_2$	0.0141	33	31	-3
617	0.093C, 0.26Si 1.50Mn, 0.22V 0.0089N$_2$	0.115	37	36	+2
622	0.095C, 0.43Si 1.58Mn, 0.22V 0.0200N$_2$	0.0110	36	35	+1

All Di* values corrected to ASTM grain size No. 10

TABLE 12   Hardenability of a Low Carbon Vanadium Steel
             Austenitised at 1200°C

Cast No.	Composition (Mass %)	Grain Size (mm)	Di (mm) Uncorrected	Di* (mm) Corrected	ΔDi* (mm)
612	0.08C, 0.30Si 1.54Mn, 0.145V 0.0083N$_2$	0.218	49	45	-
619	0.085C, 0.29Si 1.42Mn, 0.125V 0.017N$_2$	0.139	43	45	-
617	0.093C, 0.26Si 1.50Mn, 0.22V 0.0089N$_2$	0.173	45	44	-1
622	0.095C, 0.43Si 1.58Mn, 0.22V 0.0200N$_2$	0.151	43	42	-3

All Di* values corrected to ASTM grain size No. 2

TABLE 13   Solute Dissolved in the Austenite for Low Carbon,
Vanadium Steels Austenitised at 950°C

Cast No.	% V	% N_2	% Al	% Mo	% Nb	% Ti	Di* (mm) corrected
612	0.124	0.0025	-	-	-	-	34
619	0.075	0.0042	-	-	-	-	31
617	0.194	0.0016	-	-	-	-	36
622	0.145	0.0021	-	-	-	-	35

All Di* values corrected to ASTM grain size No. 10

TABLE 14   Solute Dissolved in the Austenite for Low Carbon,
Vanadium Steels Austenitised at 1200°C

Cast No.	% V	% N_2	% Al	% Mo	% Nb	% Ti	Di* (mm) corrected
612	0.145	0.0083	-	-	-	-	45
619	0.125	0.0170	-	-	-	-	45
617	0.220	0.0089	-	-	-	-	44
622	0.215	0.0146	-	-	-	-	42

All Di* values corrected to the ASTM grain size No. 2

TABLE 15   Hardenability Results for Low Carbon, Vanadium Steels
            Corrected to a Single Grain Size

Cast No.	Austenitising Temp (°C)	Grain Size (mm)	Di (mm) Uncorrected	Di* (mm) Corrected	V in Solution (%)
612	950	0.0155	37	52	0.124
617	950	0.0115	37	55	0.194
619	950	0.1410	35	47	0.075
622	950	0.0110	36	54	0.145
612	1200	0.2180	49	38	0.145
617	1200	0.1730	45	37	0.125
619	1200	0.1390	43	37	0.220
622	1200	0.1510	43	35	0.215
612	1200/950	0.1619	37	31	0.145

All Di* values corrected to ASTM grain size No. 4

TABLE 16   Effect of Austenitising Temperature on the Hardenability
            of a Low Carbon, Vanadium Steel

Cast No.	Composition (Mass %)	Austenitising Temperature (°C)	Grain Size (mm)	Di (mm) Uncorrected	Di* (mm) Corrected
612	0.08C, 0.30Si 1.54Mn, 0.145V 0.0083N_2	950	0.016	37	51
613	0.113C, 0.21Si 1.41Mn, 0.140V 0.0079N_2	1050	0.020	33	44
613	"	1125	0.114	39	35
612	0.08C, 0.30Si 1.54Mn, 0.145V 0.0083N_2	1200	0.218	49	37
613	0.113C, 0.21Si 1.41Mn, 0.140V 0.0079N_2	1275	0.291	30	21

All Di* values corrected to ASTM grain size No. 4

TABLE 17   Effect Of Austenitising Time on the Hardenability of a
             Series of Low Carbon, Vanadium Steels

Cast No.	Composition (Mass %)	Time at Austenitising Temperature	Grain Size (mm)	Di (mm) Uncorrected	Di* (mm) Corrected
612	0.08C, 0.30Si 1.54Mn, 0.145V 0.0083N$_2$	1 hour	0.0155	37	34
		4 hours	0.0145	40	38
		8 hours	0.0148	40	38
619	0.085C, 0.29Si 1.42Mn, 0.125V 0.017N$_2$	1 hour	0.0141	33	31
		4 hours	0.0131	39	37
		8 hours	0.0141	44	41
622	0.095C, 0.435Si 1.58Mn, 0.220V 0.020N$_2$	1 hour	0.0110	36	35
		4 hours	0.0105	42	42
		8 hours	0.0101	44	44

All Di* values corrected to ASTM grain size No. 10

TABLE 18   Effect of Precipitate Morphology on Hardenability at an Austenitising Temperature of 950°C

Cast No.	Heat Treatment Condition	Time at Austenitising Temperature	Grain Size (mm)	Di (mm) Uncorrected	Di* (mm) Corrected
777	Air cooled from the forging temperature	1 hour	0.0096	35	35
		8 hours	0.0115	45	43
777	Oil quenched from the forging temperature	1 hour	0.0096	35	36
		4 hours	0.0117	38	37
		8 hours	0.0116	45	43
777	Oil quenched from the forging temperature and homogenised	1 hour	0.0106	33	32
		4 hours	0.0110	42	41
		8 hours	0.0110	42	40

All Di* values corrected to ASTM grain size No. 10

244

TABLE 19   Effects of Alloying Elements on the Hardenability of a Low Carbon, Vanadium Steel Austenitised at 950°C

Cast No.	Composition	Grain Size (mm)	Di (mm) Uncorrected	Di* (mm) Corrected	ΔDi* (mm)
612	0.08C, 0.30Si, 1.54Mn 0.145V, 0.0083N$_2$	0.0155	37	34	-
619	0.085C, 0.29Si, 1.42Mn 0.125V, 0.0171N$_2$	0.0141	33	31	-3
617	0.093C, 0.26Si, 1.50Mn 0.22V, 0.0089N$_2$	0.0115	37	36	+2
622	0.095C, 0.43Si, 1.58Mn 0.22V, 0.0200N$_2$	0.0110	36	35	+1
638	0.091C, 0.43Si, 1.64Mn 0.14V, 0.0091N$_2$, 0.058Al	0.0133	46	43	+9
639	0.095C, 0.33Si, 1.65Mn 0.135V, 0.0165N$_2$, 0.050Al	0.0117	45	43	+9
640	0.083C, 0.30Si, 1.65Mn 0.14V, 0.0071N$_2$, 0.21Mo	0.0129	47	45	+11
641	0.087C, 0.36Si, 1.60Mn 0.135V, 0.0151N$_2$, 0.21Mo	0.0125	45	43	+9
642	0.085C, 0.21Si, 1.45Mn 0.135V, 0.007N$_2$, 0.065Nb	0.0099	35	35	+1
643	0.09C, 0.41Si, 1.60Mn 0.135V, 0.0185N$_2$, 0.065Nb	0.0099	36	36	+2
644	0.085C, 0.36Si, 1.52Mn 0.14V, 0.0078N$_2$, 0.055Ti	0.0119	40	39	+5
645	0.088C, 0.42Si, 1.52Mn 0.14V, 0.0168N$_2$, 0.060Ti	0.0128	47	45	+11

All Di* values corrected to ASTM grain size No. 10

TABLE 20   Solute Dissolved in the Austenite, and DI* (Corrected)
Values for Low Carbon Steels Austenitised at 950°C

Cast No.	%V	%N$_2$	%Al	%Mo	%Nb	%Ti	Di*(mm) Corrected
612	0.124	0.0025	-	-	-	-	34
619	0.075	0.0042	-	-	-	-	31
617	0.194	0.0016	-	-	-	-	36
622	0.145	0.0021	-	-	-	-	35
638	0.140	0.0008	0.042	-	-	-	43
639	0.135	0.0016	0.021	-	-	-	43
640	0.123	0.0025	-	0.21	-	-	45
641	0.092	0.0033	-	0.21	-	-	43
642	0.135	0.0019	-	-	0.031	-	35
643	0.109	0.0028	-	-	0.006	-	36
644	0.140	-	-	-	-	0.029	39
645	0.140	-	-	-	-	0.003	45

All Di* values corrected to ASTM grain size No. 10

TABLE 21   The Effect of Time at an Austenitising Temperature of 950°C

Cast No.	Composition (Mass %)	Time at austenitising temperature	Grain Size (mm)	Di (mm) Uncorrected	Di* (mm) Corrected
619	0.085C, 0.029Si 1.42Mn, 0.125V 0.017N$_2$	1 hour	0.0141	33	31
		4 hours	0.0131	39	37
		8 hours	0.0141	44	41
639	0.95C, 0.33Si 1.61Mn, 0.135V 0.0165N$_2$, 0.050Al	1 hour	0.0117	45	43
		4 hours	0.0115	45	44
		8 hours	0.0117	49	47
641	0.087C, 0.36Si 1.60Mn, 0.135V 0.0151N$_2$, 0.21Mo	1 hour	0.0125	45	43
		4 hours	0.0148	54	50
		8 hours	0.0152	54	50

All Di* values corrected to ASTM grain size No. 10

TABLE 22   Effects of Alloying Element on the Hardenability of a
             Low Carbon, Vanadium Steel Austenitised at 1200°C

Cast No.	Composition (Mass %)	Grain Size (mm)	Di (mm) Uncorrected	Di* (mm) Corrected	ΔDi* (mm)
612	0.08C,0.3Si,1.54Mn 0.145V,0.0083N₂	0.218	49	45	--
619	0.085C,0.29Si,1.42Mn 0.125V,0.017N₂	0.139	43	45	-
617	0.093C,0.26Si,1.50Mn 0.22V,0.0089N₂	0.173	45	44	-1
622	0.095C,0.43Si,1.58Mn 0.22V,0.020N₂	0.151	43	42	-3
638	0.091C,0.43Si,1.64Mn 0.14V,0.0091N₂,0.058Al	0.199	54	51	+6
639	0.095C,0.33Si,1.65Mn 0.135V,0.0165N₂,0.050Al	0.185	45	43	-2
640	0.083C,0.30Si,1.65Mn 0.14V,0.0071N₂,0.21Mo	0.138	57	59	+14
641	0.087C,0.36Si,1.60Mn 0.135V,0.0151N₂,0.21Mo	0.072	57	69	+24
642	0.085C,0.21Si,1.4Mn 0.135V,0.007N₂,0.065Nb	0.186	46	44	-1
643	0.09C,0.41Si,1.60Mn 0.135V,0.0185N₂,0.065Nb	0.184	63	61	+16
644	0.085C,0.36Si,1.52Mn 0.14V,0.0078N₂,0.055Ti	0.071	50	62	+17
645	0.088C,0.42Si,1.52Mn 0.14V,0.0168N₂,0.06Ti	0.049	52	70	+25

All Di* values corrected to ASTM grain size No. 2

TABLE 23: <u>Solute Dissolved in the Austenite, and Di*(Corrected)</u>
<u>Values for Low Carbon Steels Austenitised at 1200°C</u>

Cast No.	%V	%N$_2$	%Al	%Mo	%Nb	%Ti	Di* (mm) corrected
612	0.145	0.0083	-	-	-	-	45
619	0.125	0.0170	-	-	-	-	45
617	0.220	0.0089	-	-	-	-	44
622	0.215	0.0146	-	-	-	-	42
638	0.140	0.0053	0.051	-	-	-	51
639	0.135	0.0081	0.033	-	-	-	43
640	0.140	0.0071	-	0.21	-	-	59
641	0.135	0.0151	-	0.21	-	-	69
642	0.135	0.0070	-	-	0.065	-	44
643	0.135	0.0170	-	-	0.057	-	61
644	0.140	0.0010	-	-	-	0.031	62
645	0.140	0.0020	-	-	-	0.010	70

All Di* values corrected to ASTM grain size No.2.

TABLE 24: Effects of Alloying Elements on the Hardenability of
a Medium Carbon, Vanadium Steel Austenitised at 950°C

Cast No.	Composition	Grain Size (mm)	Di (mm)	Di* (mm) Corrected	ΔDi* (mm)
623	0.365C, 0.36Si, 1.47Mn, 0.130V, 0.0100N_2	0.0107	55	54	-
624	0.390C, 0.43Si, 1.57Mn, 0.130V, 0.0200N_2	0.0092	51	52	-2
662	0.365C, 0.37Si, 1.54Mn, 0.140V, 0.0060N_2, 0.070Al	0.0137	74	70	+16
663	0.390C, 0.28Si, 1.50Mn, 0.120V, 0.0160N_2, 0.040Al	0.0106	58	58	+4
664	0.390C, 0.33Si, 1.41Mn, 0.120V, 0.0070N_2, 0.17Mo	0.0111	75	74	+20
665	0.400C, 0.28Si, 1.45Mn, 0.180V, 0.0160N_2, 0.20Mo	0.0102	71	71	+17
671	0.340C, 0.28Si, 1.50Mn, 0.145V, 0.0075N_2, 0.060Nb	0.0109	56	55	+1
668	0.380C, 0.37Si, 1.61Mn, 0.145V, 0.0170N_2, 0.060Nb	0.0130	56	53	-1
669	0.340C, 0.30Si, 1.64Mn, 0.150V, 0.0070N_2, 0.075Ti	0.0103	61	61	+7
672	0.380C, 0.31Si, 1.55Mn, 0.145V, 0.0170N_2, 0.082Ti	0.0085	108	110	+56

All Di* values corrected to ASTM grain size No.10.

TABLE 25: Solute Dissolved in the Austenite, and Di*(Corrected)
Values for Medium Carbon Steels Austenitised at 950°C

Cast No.	%V	%N$_2$	%Al	%Mo	%Nb	%Ti	Di* (mm) corrected
623	0.104	0.0029	-	-	-	-	54
624	0.072	0.0042	-	-	-	-	52
662	0.140	0.0006	0.060	-	-	-	70
663	0.150	0.0020	0.014	-	-	-	58
664	0.105	0.0029	-	0.17	-	-	74
665	0.131	0.0024	-	0.20	-	-	71
671	0.144	0.0021	-	-	0.027 (0.003)*	-	55
668	0.123	0.0023	-	-	0.007 (0.003)*	-	53
669	0.150	-	-	-	-	0.051 (0.003)*	61
672	0.145	-	-	-	-	0.024 (0.003)*	110

All Di* values corrected to ASTM grain size No.10.

( )* denotes solute dissolved in Austenite after considering alloy-carbon solubility limit.

TABLE 26: <u>Effects of Alloying Elements on the Hardenability of</u>
<u>a Medium Carbon, Vanadium Steel Austenitised at 1200°C</u>

Cast No.	Composition	Grain Size (mm)	Di (mm)	Di* (mm) Corrected	ΔDi* (mm)
623	0.365C, 0.36Si, 1.47Mn, 0.130V, 0.0100N_2	0.238	104	92	-
624	0.390C, 0.43Si, 1.57Mn, 0.130V, 0.0200N_2	0.280	100	76	-16
662	0.365C, 0.37Si, 1.54Mn, 0.140V, 0.0060N_2, 0.070Al	0.222	83	75	-17
663	0.390C, 0.28Si, 1.50Mn, 0.120V, 0.0160N_2, 0.040Al	0.194	72	68	-24
664	0.390C, 0.33Si, 1.41Mn, 0.120V, 0.0070N_2, 0.17Mo	0.200	106	103	+11
665	0.400C, 0.28Si, 1.45Mn, 0.180V, 0.0160N_2, 0.20Mo	0.205	98	92	0
671	0.340C, 0.28Si, 1.50Mn, 0.145V, 0.0075N_2, 0.060Nb	0.215	85	79	-13
668	0.380C, 0.37Si, 1.61Mn, 0.145V, 0.0170N_2, 0.060Nb	0.222	100	91	-1
669	0.340C, 0.30Si, 1.64Mn, 0.150V, 0.0070N_2, 0.075Ti	0.103	55	61	-31
672	0.380C, 0.31Si, 1.55Mn, 0.145V, 0.0170N_2, 0.082Ti	0.110	121	134	+42

All Di* values corrected to ASTM grain size No.2.

TABLE 27: <u>Solute Dissolved in the Austenite, and Di*(Corrected)
Values for Medium Carbon Steels Austenitised at 1200°C</u>

Cast No.	%V	%N$_2$	%Al	%Mo	%Nb	%Ti	Di* (mm) corrected
623	0.130	0.0100	-	-	-	-	92
624	0.130	0.0200	-	-	-	-	76
662	0.140	0.0041	0.067	-	-	-	75
663	0.150	0.0097	0.026	-	-	-	68
664	0.120	0.0070	-	0.17	-	-	103
665	0.180	0.0160	-	0.20	-	-	92
671	0.145	0.0075	-	-	0.060 (0.030)^x	-	79
668	0.145	0.0168	-	-	0.058 (0.030)^x	-	91
669	0.150	0.0003	-	-	-	0.052 (0.030)^x	61
672	0.145	0.0006	-	-	-	0.026 (0.030)^x	134

All Di* values corrected to ASTM grain size No.2.

( )^x denotes solute dissolved in Austenite after considering alloy-carbon solubility limit.

TABLE 28: **Effect of Transformation Temperature on the Hardness of High Carbon Vanadium Steels**

Isothermal Transformation Temperature (°C)	Hardness (Hv 30)	
	Steel 626	Steel 695
550	372	350
600	320	310
650	253	244

TABLE 29: **Mechanical Properties of High Carbon Vanadium Steel 626**

Isothermal Transformation Temperature (°C)	Yield Stress (N/mm^2)	0.2% Proof Stress (N/mm^2)	Tensile Strength (N/mm^2)	% Elongation
550	735.8	824.0	1128.2	6.34
575	735.8	801.5	1116.4	6.61
600	716.1	794.6	1116.4	7.70
625	686.7	747.5	1074.2	6.05
650	598.4	654.3	966.3	5.03

TABLE 30: **Mechanical Properties of High Carbon Vanadium Steel 695**

Isothermal Transformation Temperature (°C)	Yield Stress (N/mm^2)	0.2% Proof Stress (N/mm^2)	Tensile Strength (N/mm^2)	% Elongation
550	755.4	825.9	1098.7	5.31
575	784.8	873.1	1167.4	6.10
600	804.4	868.2	1196.8	6.16
625	735.8	806.4	1113.4	5.39
650	657.3	725.9	1015.3	5.09

TABLE 31: Charpy Impact Data of High Carbon Vanadium Steel 626

Isothermal Transformation Temperature (°C)	Charpy Test Temperature (°C)			
	20	100	200	250
550	9.8 J	10.2 J	32.6 J	-
575	10.1 J	14.7 J	27.7 J	-
600	8.8 J	11.9 J	22.8 J	31.5 J
625	8.8 J	11.6 J	23.8 J	32.6 J
650	9.0 J	12.6 J	24.2 J	33.3 J

TABLE 32: Charpy Impact Data of High Carbon Vanadium Steel 695

Isothermal Transformation Temperature (°C)	Charpy Test Temperature (°C)			
	20	100	200	250
550	8.4 J	8.8 J	19.6 J	-
575	6.7 J	8.8 J	18.9 J	-
600	5.3 J	8.8 J	16.5 J	23.8 J
625	7.4 J	9.1 J	16.8 J	23.5 J
650	7.4 J	9.8 J	19.3 J	29.8 J

TABLE 33: Quantitative Effects of Alloying Elements in Solution on Multiplying Factor (Austenitised at 1200°C)

Cast No.	Element	Multiplying Factor for 0.01% Addition	Average Multiplying Factor
-	V	0.998	
-	V	0.998	0.996
-	V	0.993	
-	N	0.919	
-	N	0.990	0.963
-	N	0.980	
638	Al	1.025	1.006
639	Al	0.987	
640	Mo	1.026	1.026
641	Mo	1.027	
642	Nb	0.998	1.012
643	Nb	1.056	
644	Ti	1.237	1.426
645	Ti	1.615	

TABLE 34: __Mechanical Properties of High Carbon Vanadium Steels__

Isothermal Transformation Temperature (°C)	Steel 626		Steel 695		Plain Carbon Steel	
	Tensile Strength (N/mm^2)	Yield Stress (N/mm^2)	Tensile Strength (N/mm^2)	Yield Stress (N/mm^2)	Tensile Strength (N/mm^2)	Yield Stress (N/mm^2)
550	1128.2	735.8	1098.7	755.4	1102.1	627.6
575	1116.4	735.8	1167.4	784.8	1076.5	594.7
600	1116.4	716.1	1196.8	804.4	1049.3	565.2
625	1074.2	686.7	1113.4	735.8	1020.1	533.4
650	966.3	598.4	1015.3	657.3	986.2	496.6

TABLE 35: __Charpy Impact Data for High Carbon Vanadium Steels__

Isothermal Transformation Temperature (°C)	Charpy Test Temperature to Achieve 27 J Impact Energy (°C)	
	Steel 626	Theoretical Steel
550	176	240
575	200	214
600	228	194
625	222	183
650	218	168

FIG 1;EFFECT OF 0.13% V ON T.T.T. DIAGRAM OF A 0.12%C,1.6%Mn,0.01%N STEEL.

FIG 1A; 0% V : AUSTENITE GRAIN SIZE 141 μm

FIG 1B; 0.13% V : AUSTENITE GRAIN SIZE 71 μm.

258
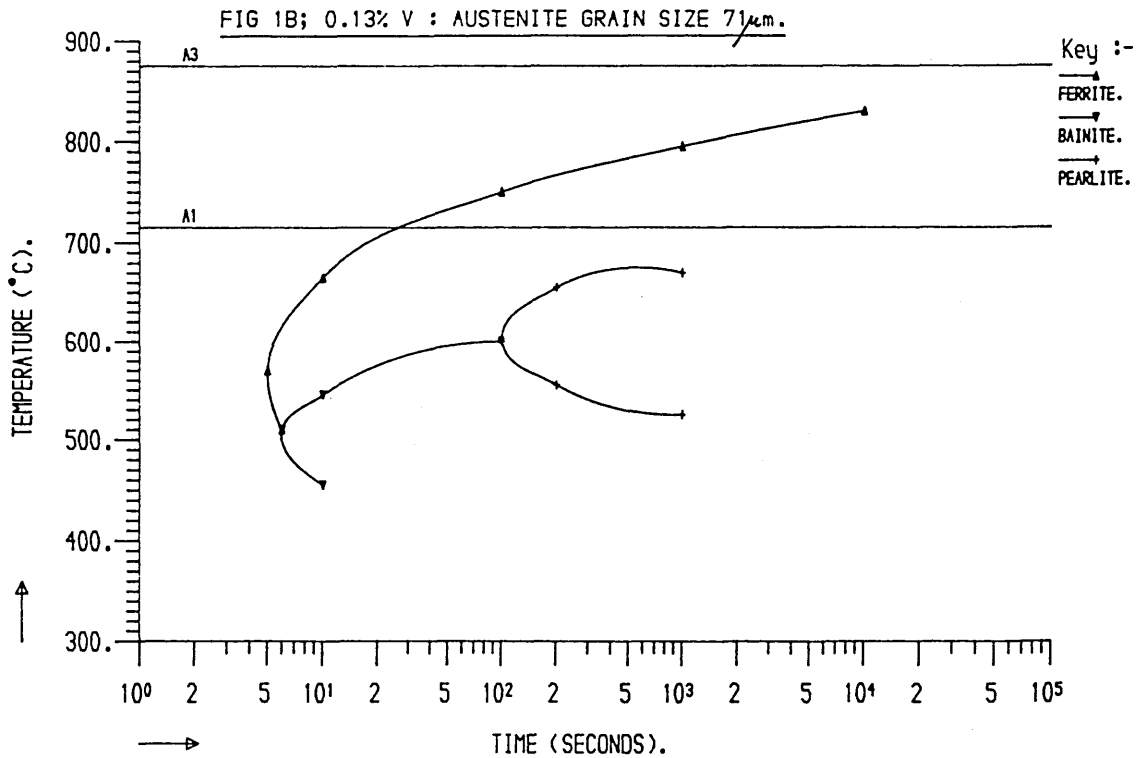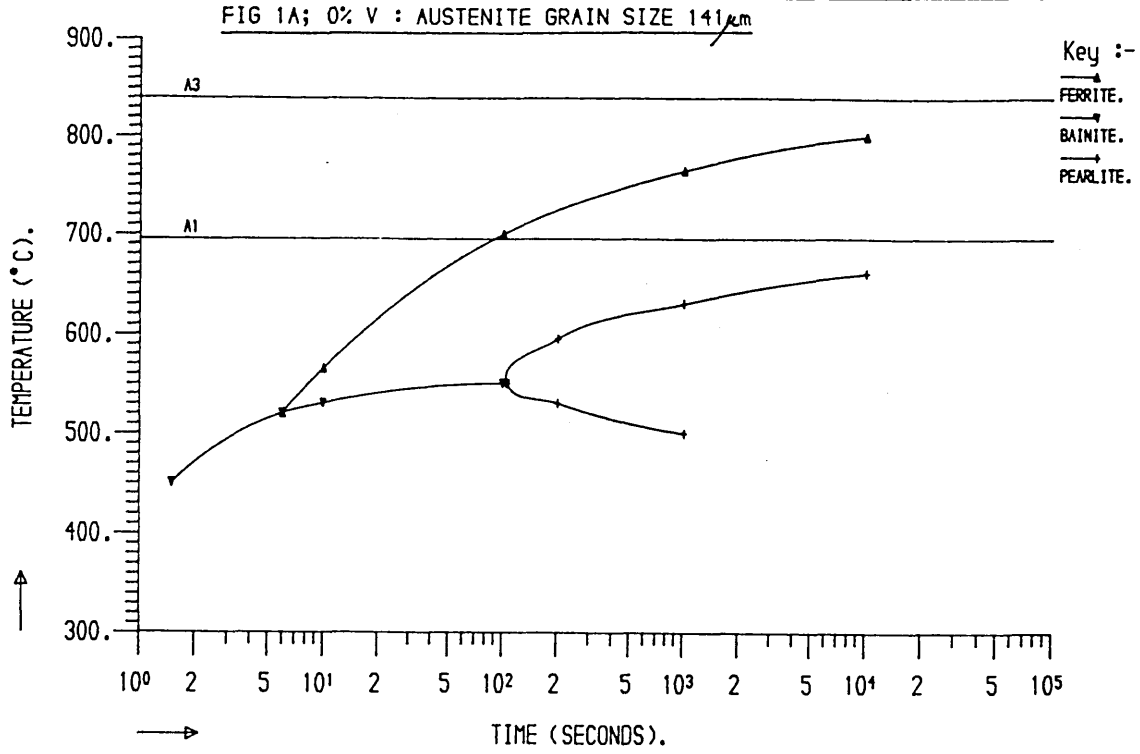
FIG 2;EFFECT OF VANADIUM ON THE C.C.T. DIAGRAM OF A LOW CARBON STEEL.
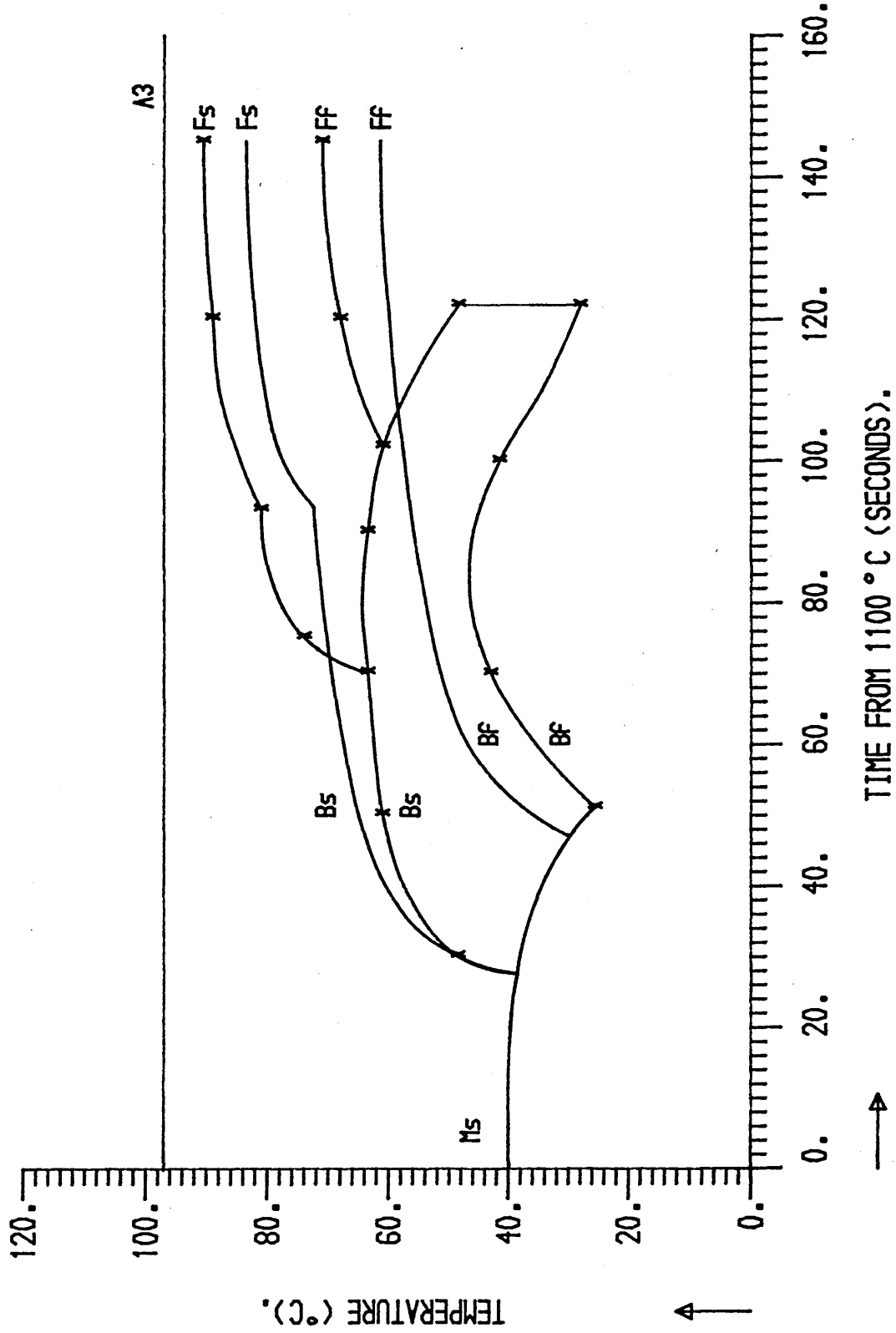
FIG 3;SCHEMATIC DIAGRAMS ILLUSTRATING THE MIGRATION OF AUSTENITE/FERRITE BOUNDARIES BY A LEDGE TYPE MECHANISM.(83)

AUSTENITE.

PARTIALLY COHERENT, IMMOBILE $(111)\gamma//(110)_\alpha$ INTERFACE.

CARBIDE.

MOBILE LEDGE.

FERRITE + CARBIDE.

PLANAR SHEETS OF CARBIDES.

AUSTENITE.

DISORDERED γ/α INTERFACE.

CARBIDE.

MOBILE LEDGE.

FERRITE + CARBIDE.

CURVED SHEETS OF CARBIDES.
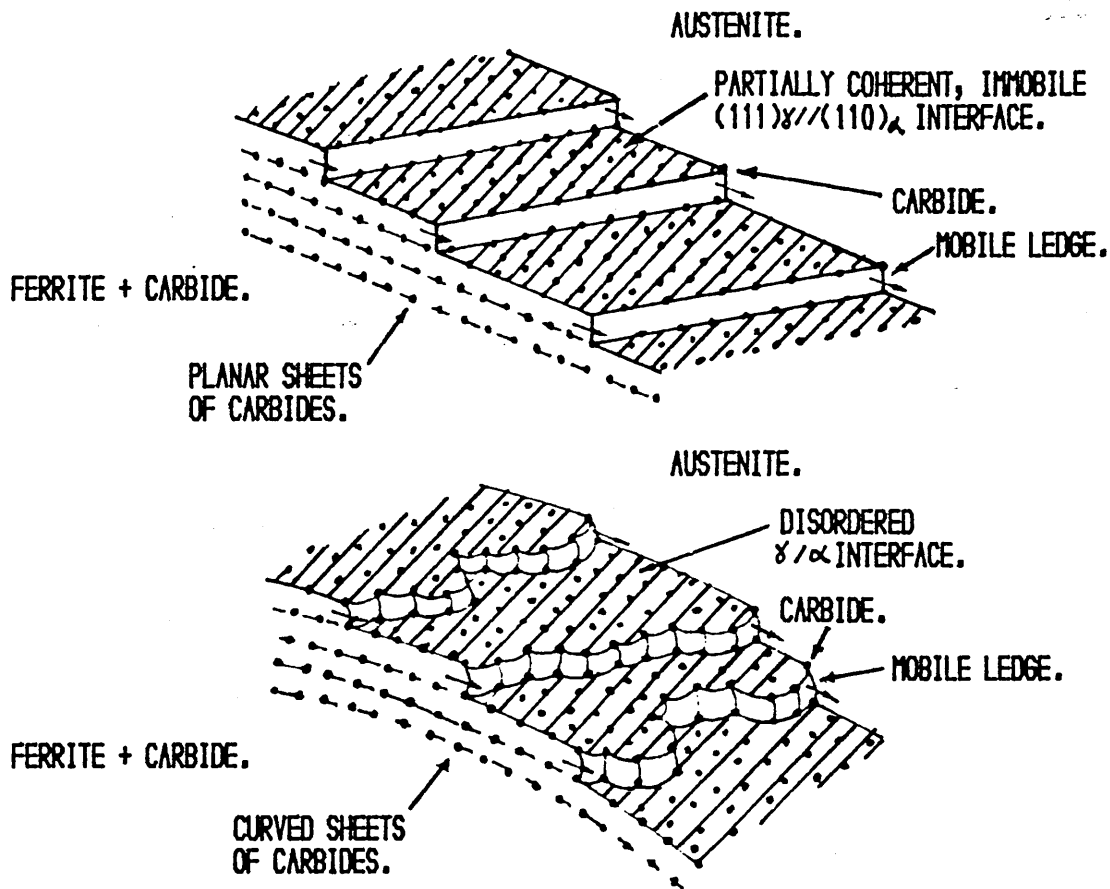
FIG 4;SCHEMATIC DIAGRAM ILLUSTRATING THE ESTABLISMENT OF A LEDGE TYPE MECHANISM FOR A PINNED INTERFACE.(83)

AUSTENITE.

FERRITE.

(1).

(2).

(3).

(4).

260
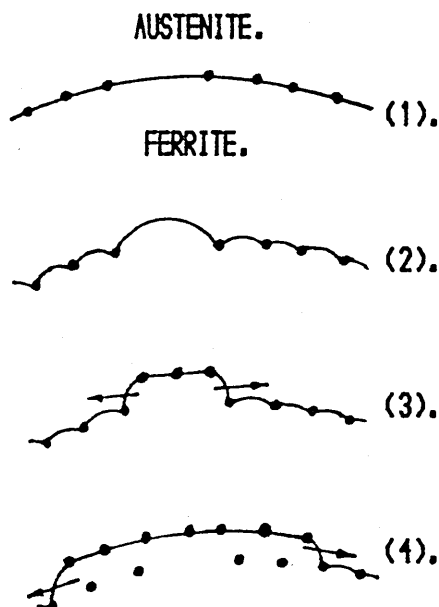
FIG 5;THE EFFECT OF CARBON ON THE HARDENABILITY OF STEELS.

FIG 5A;THE EFFECT ON THE 50% MARTENSITE HARDNESS.
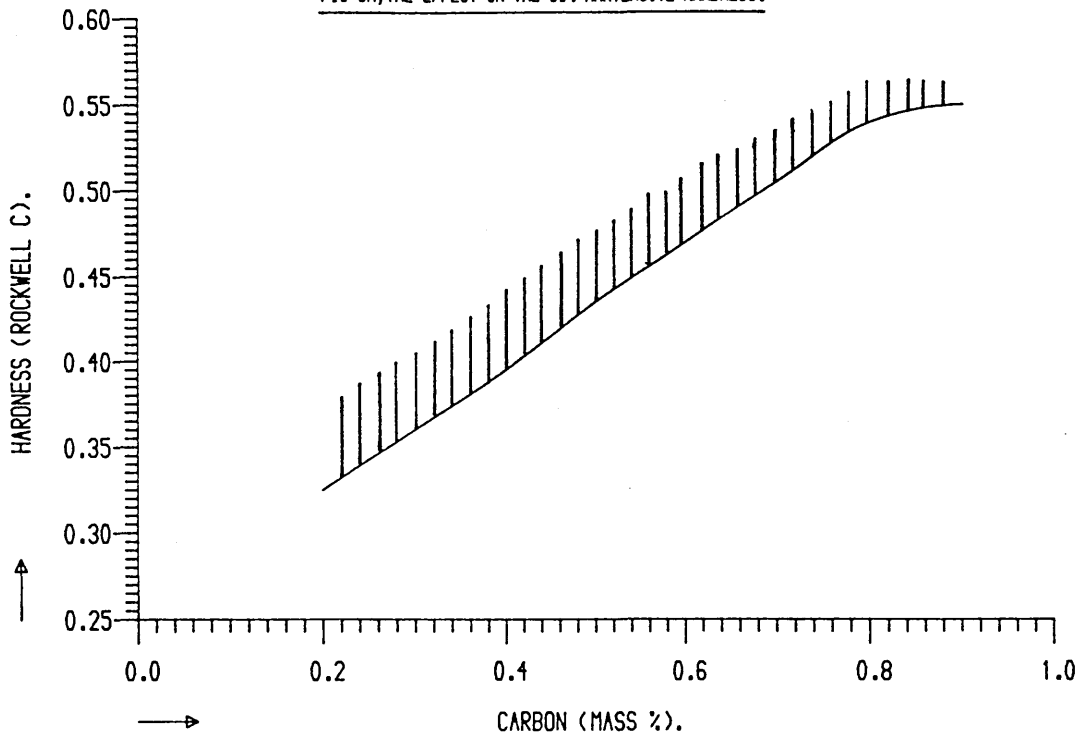
FIG 5B;THE EFFECT ON THE HARDENABILITY MULTIPLYING FACTORS.

Key :-
——▲ ASTM 4.
——▼ ASTM 5.
——+ ASTM 6.
——× ASTM 7.
——□ ASTM 8.
——◆ ASTM 9.
——● ASTM 10.

261
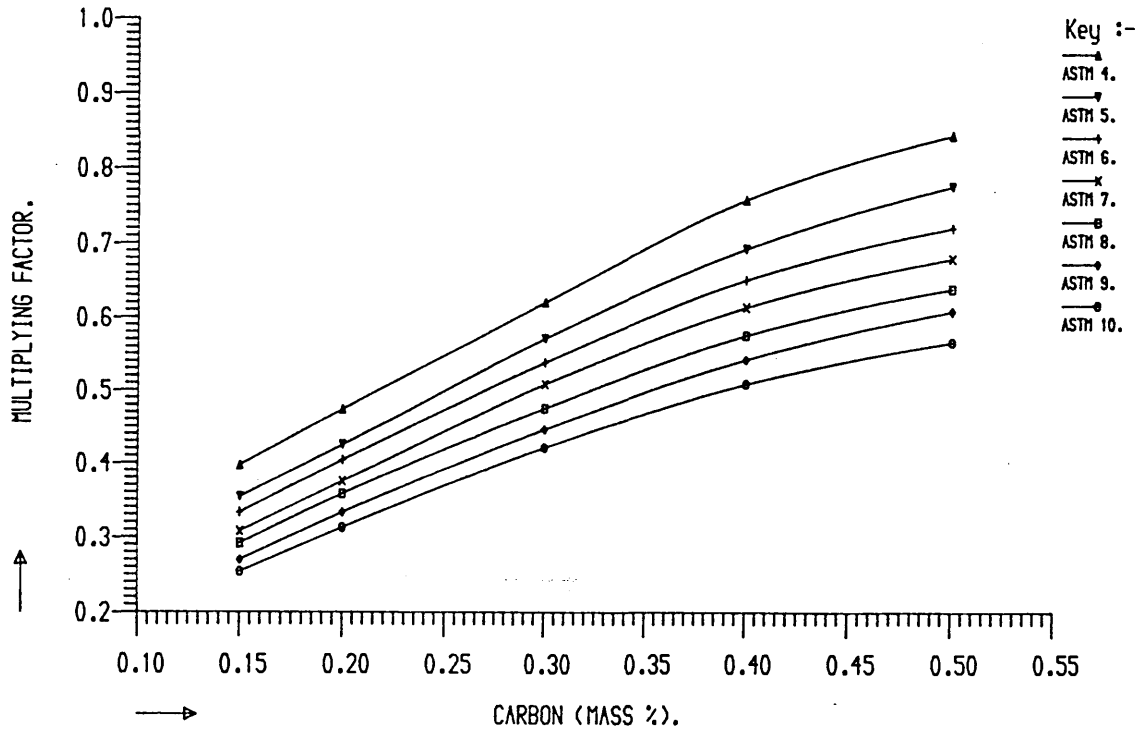
FIG 6;MULTIPLYING FACTORS FOR VARIOUS ALLOYING ELEMENTS (106).

FIG 6A;

FIG 6B;
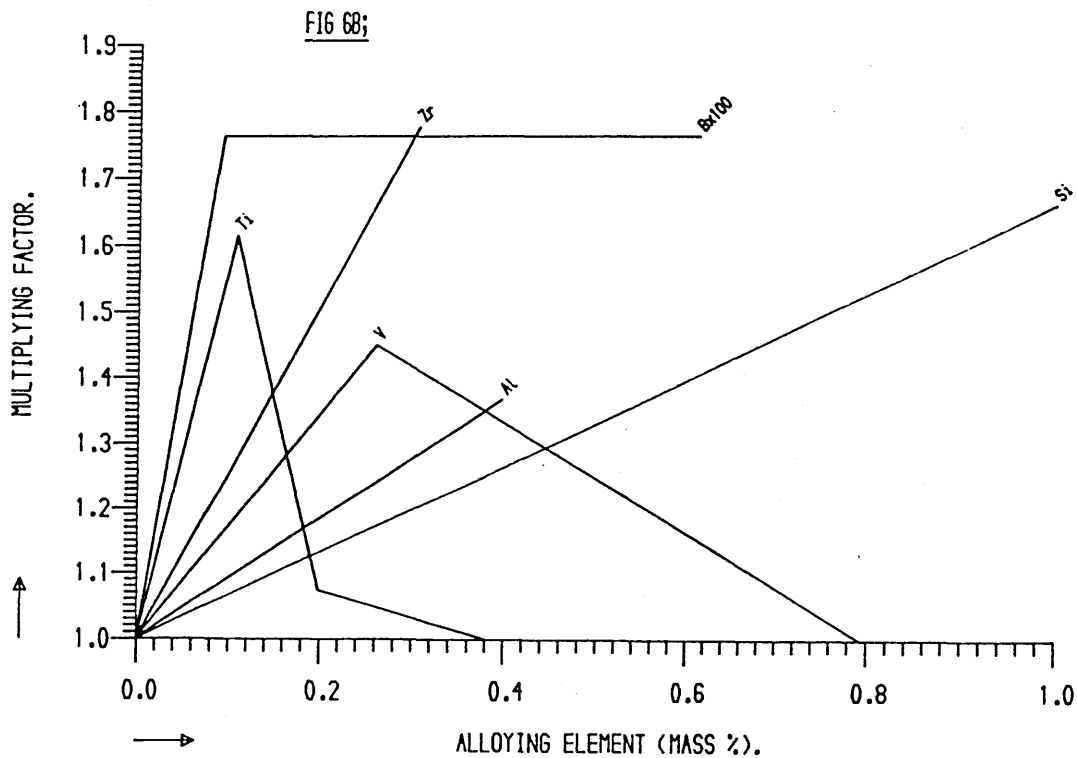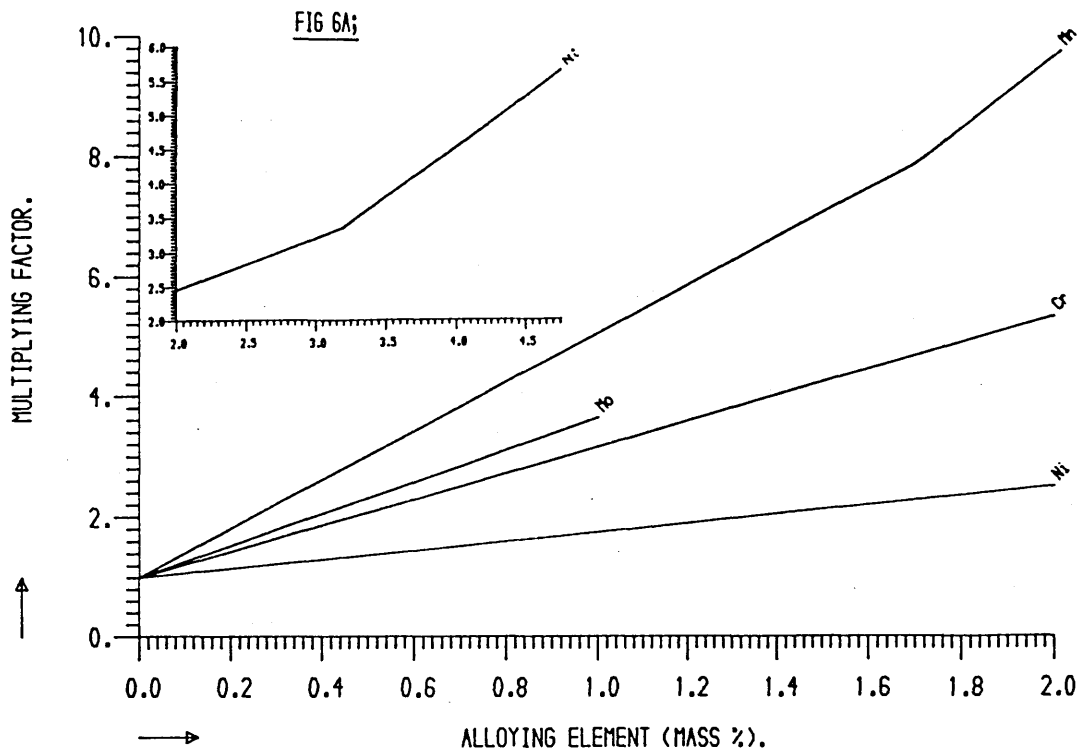
FIG 7; EFFECT OF VANADIUM ON HARDENABILITY.(101)
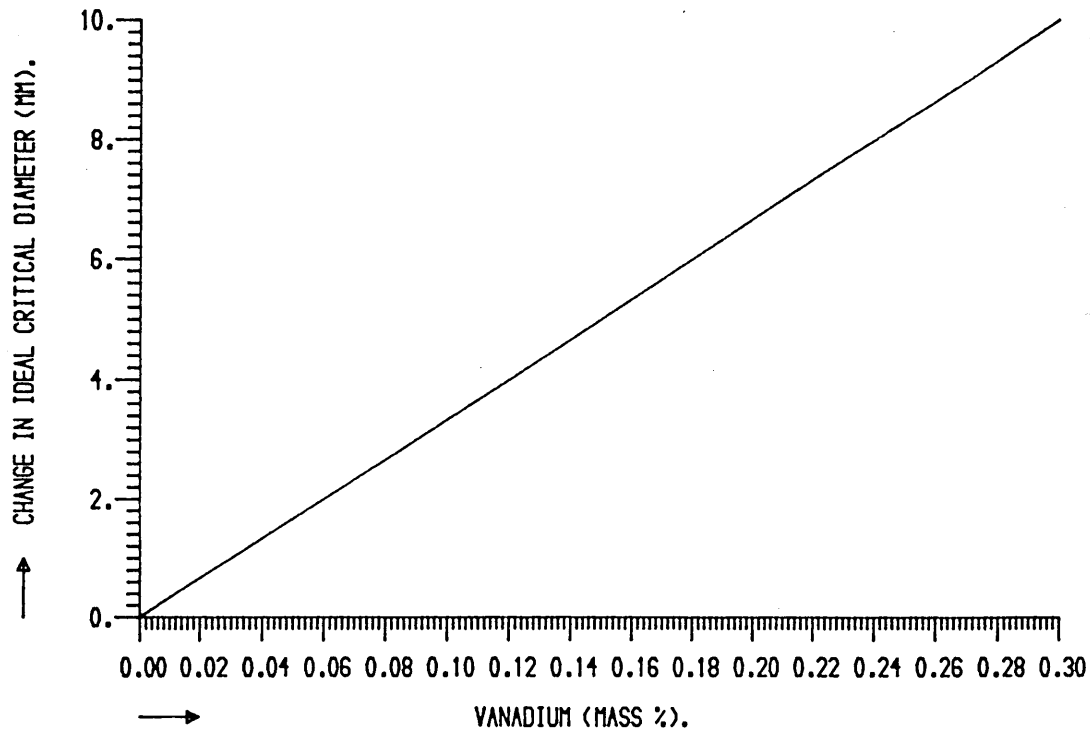
FIG 8; EFFECT OF VANADIUM ON HARDENABILITY MULTIPLYING FACTORS.

Key :-

REF.(104) 925°C

REF.(104) 815°C

REF.(99)

FIG 9; MULTIPLYING FACTORS FOR VARIOUS ALLOYING ELEMENTS (100).
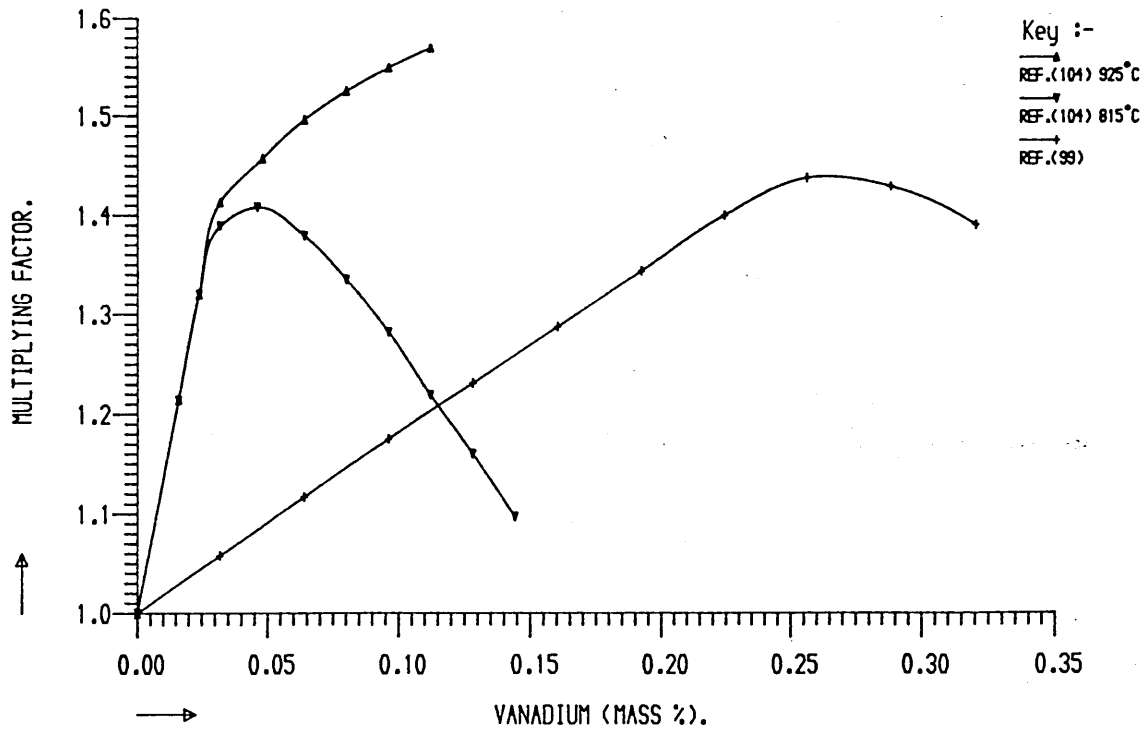
FIG 9; MULTIPLYING FACTORS FOR VARIOUS ALLOYING ELEMENTS (100).

FIG 10; EFFECT OF AUSTENITISING TEMPERATURE ON HARDENABILITY.

FIG 10; EFFECT OF AUSTENITISING TEMPERATURE ON HARDENABILITY.

264

| MARTE-NSITE. | MARTENSITE AND INCREASING AMOUNTS OF BAINITE. | FERRITE WITH A HIGH DISLOCATION DENSITY BUT NO PRECIPITATES. EASY NUCLEATION CONDITIONS DUE TO HIGH SUPERSATURATION AND MANY DISLOCATIONS. | FERRITE AND INTERPHASE PRECIPITATION. | FERRITE WITH NO PRECIPITATION AND A LOW DISLOCATION DENSITY. DIFFICULT NUCLEATION DUE TO DISLOCATION DENSITY. |

HARDNESS.

DISTANCE FROM QUENCHED END.
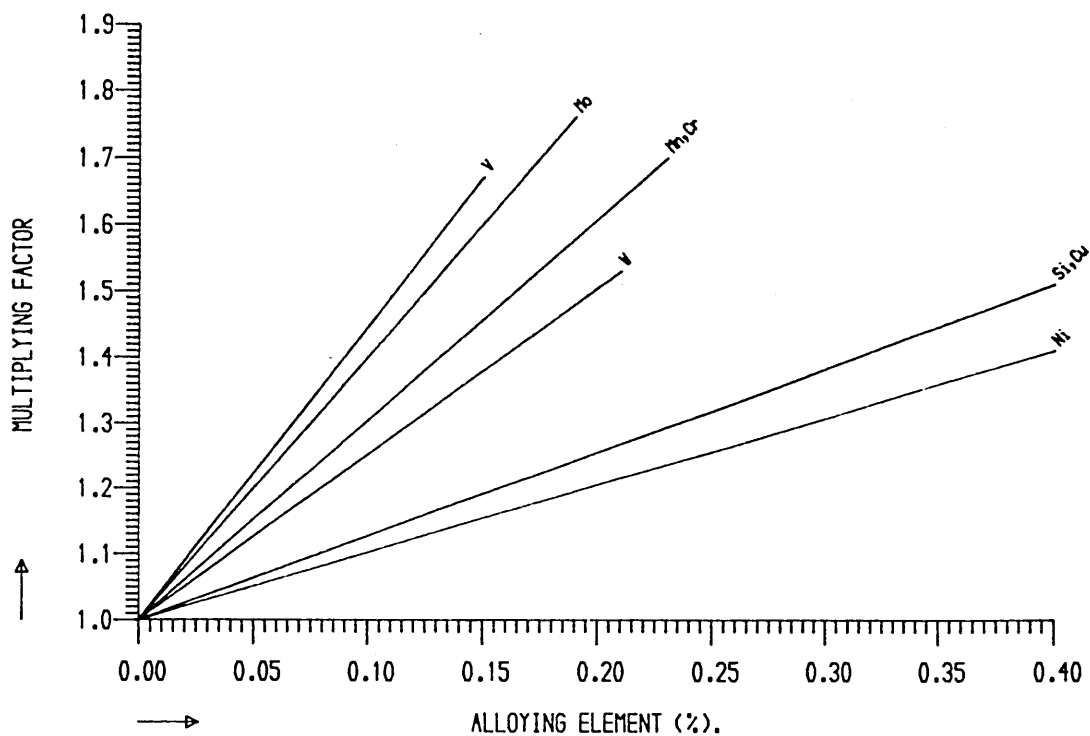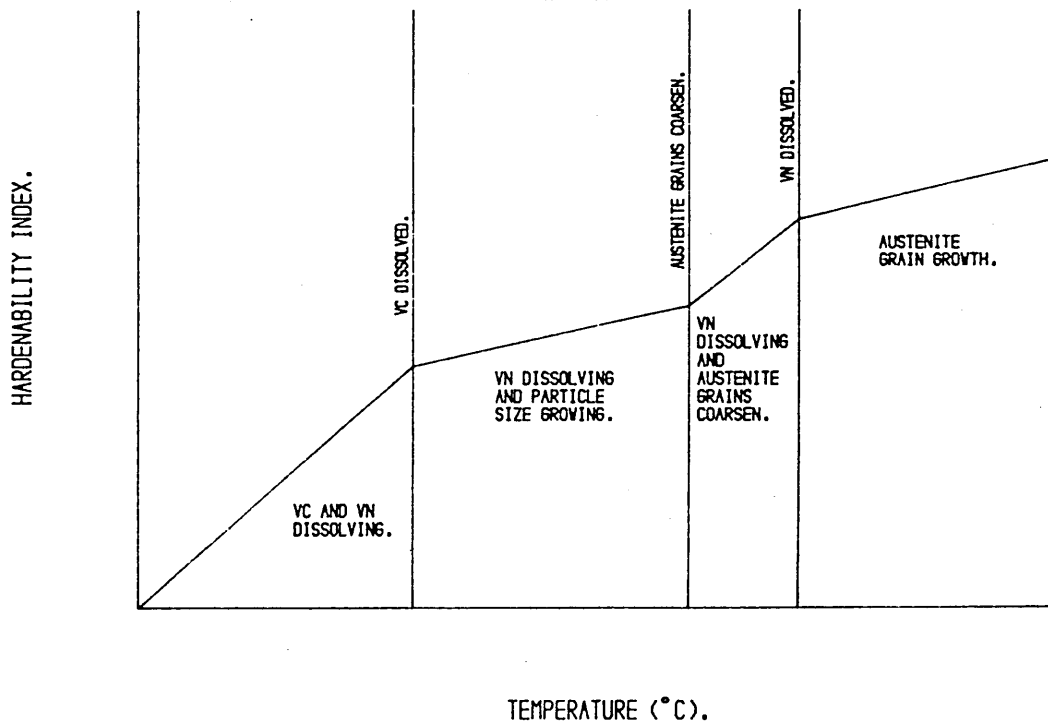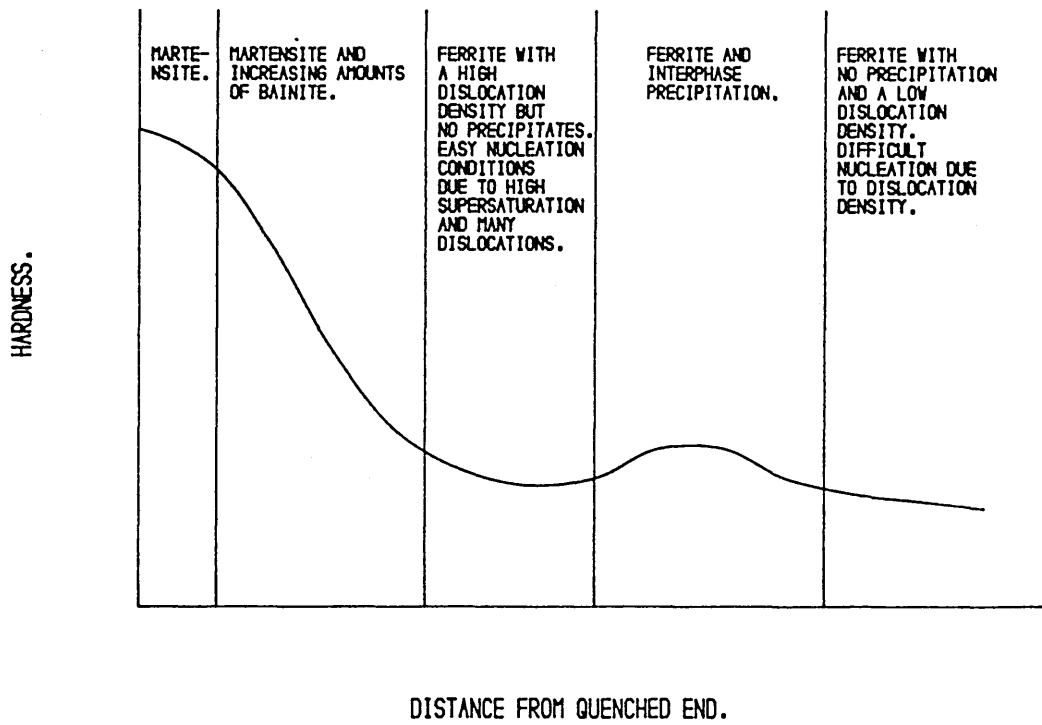
FIG 12;INCREASE IN HARDNESS DUE TO INTERPHASE PRECIPITATION IN A JOMINY SPECIMEN

$0.3\%C,1.7\%Ni,0.51\%Cr,0.24\%V,0.013\%N_2.$

$0.12\%C,1.5\%Mn,0.13\%V,0.010\%N_2.$

HARDNESS (ROCKWELL C).

DISTANCE FROM QUENCHED END (MM).

265
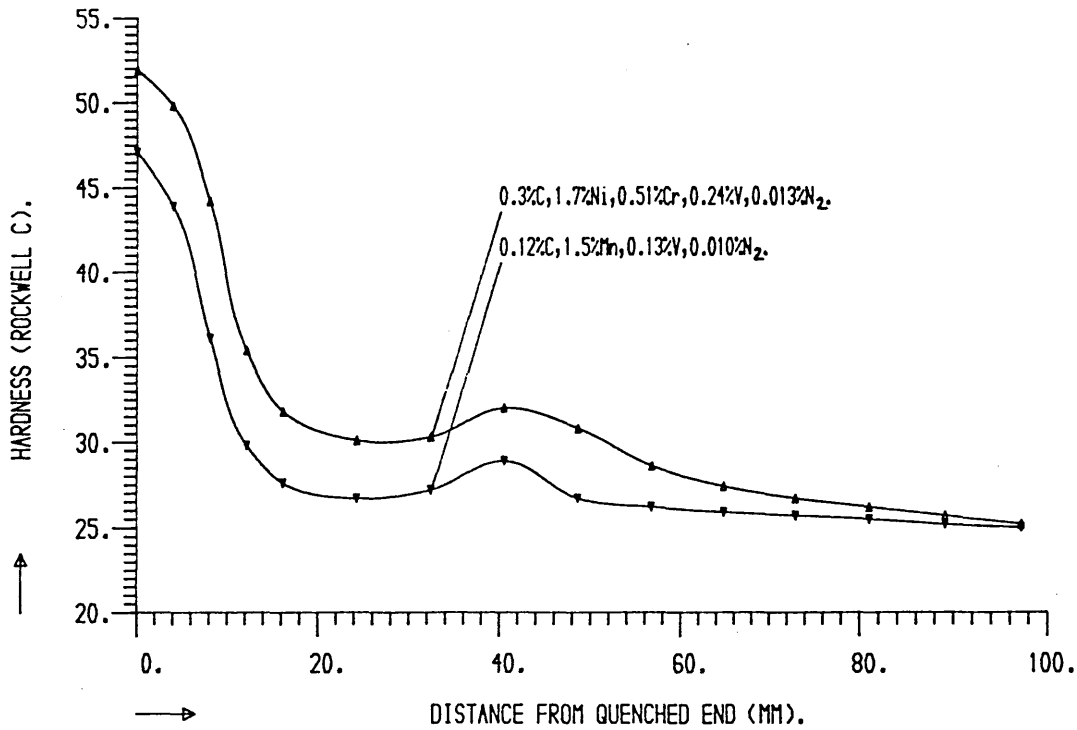
FIG 13;EFFECT OF TEMPERING ON JOMINY CURVE FOR A LOW CARBON,VANADIUM STEEL.

Key :-
AS QUENCHED.
T=550°C.
T=650°C.
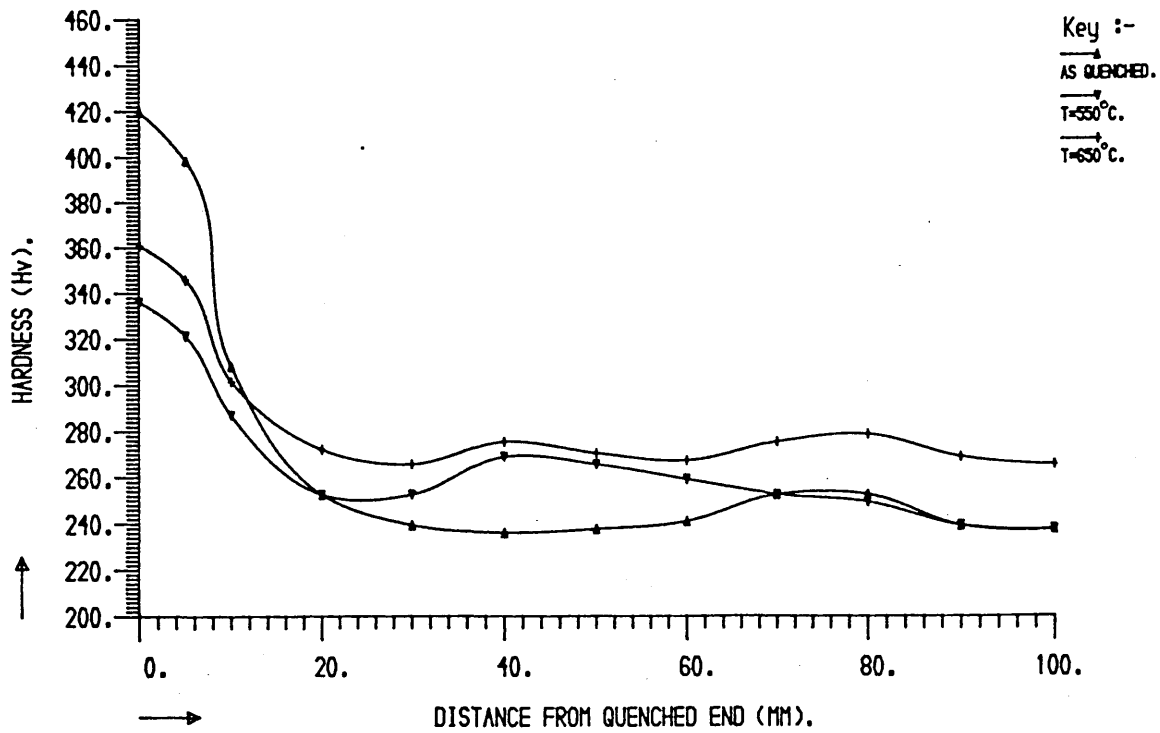
FIG 14;EFFECT OF ALLOYING ELEMENTS ON HARDENABILITY (ELDIS ET AL (7)).

AUSTENITISED AT 1200°C.

A.S.T.M. GRAIN SIZE: 2.

BASE CHEMICAL ANALYSIS:
0.10 w/o C,0.008 w/o N₂,
0.11 w/o Si,1.47 w/o Mn.

266
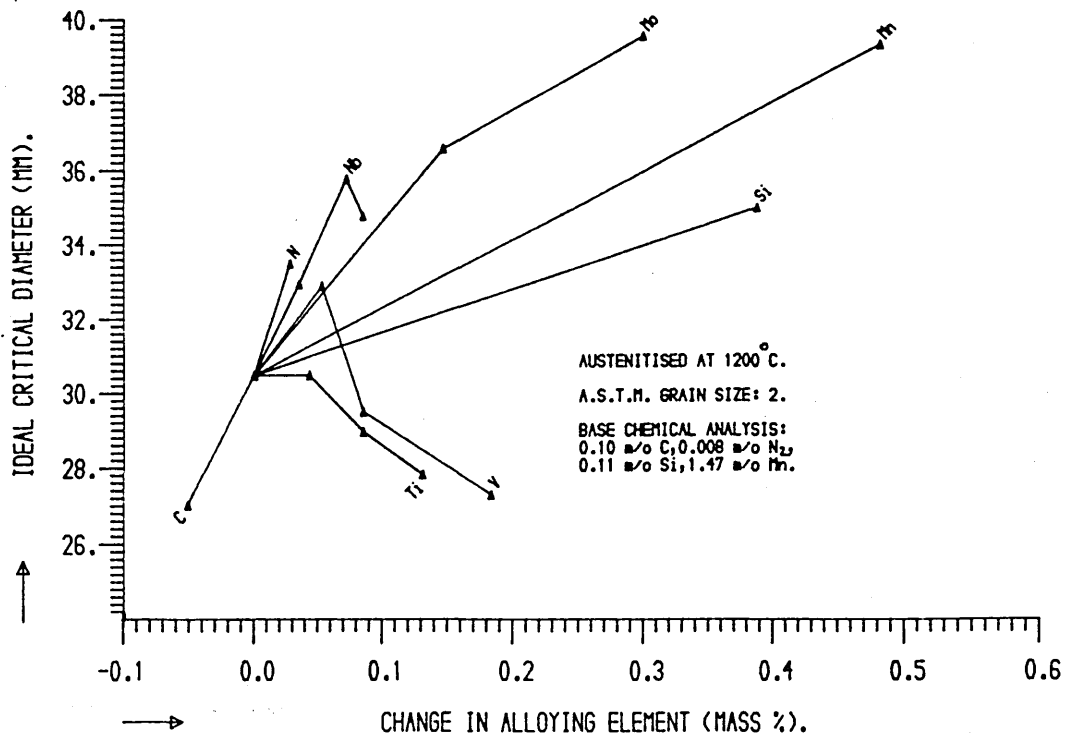
FIG 15; ISOTHERMALLY TRANSFORMED 'AS FORGED' BAR.
        MAGNIFICATION : X40.

FIG 16; ISOTHERMALLY TRANSFORMED 'AS CAST' STRUCTURE.
        MAGNIFICATION : X40.
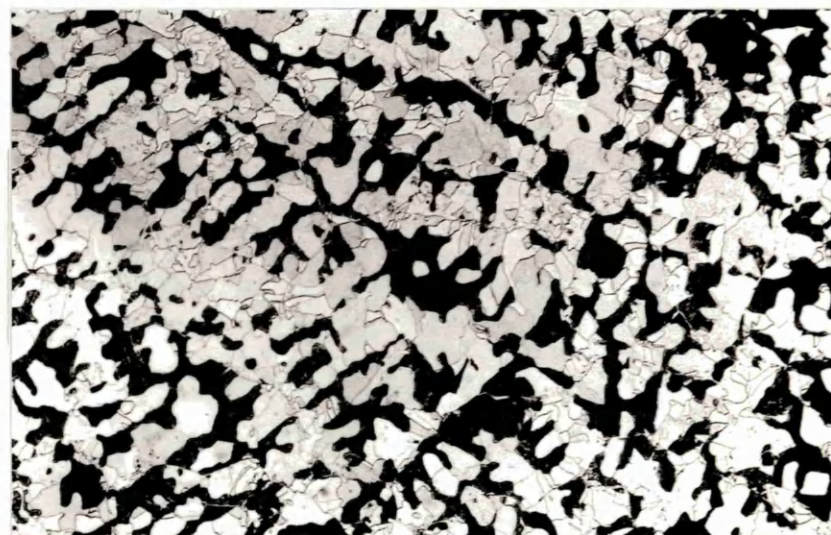
FIG 17;ISOTHERMALLY TRANSFORMED HOMOGENISED STRUCTURE.
MAGNIFICATION : X40.
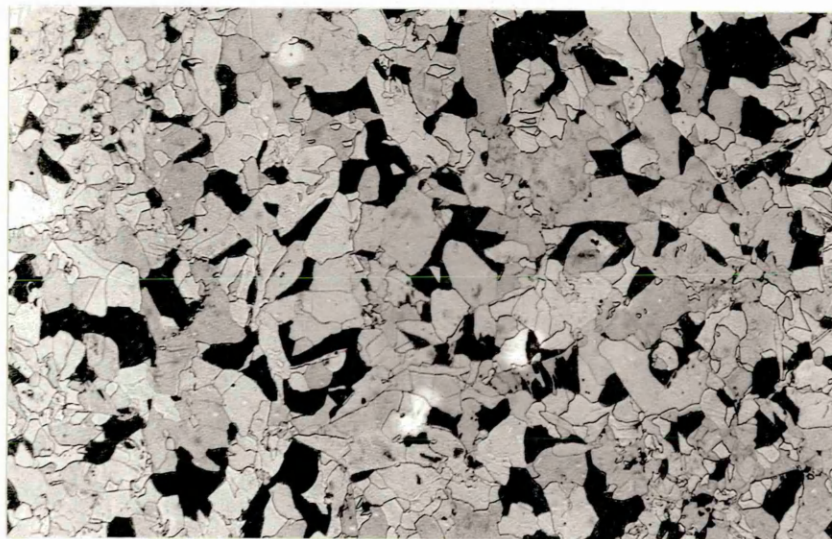
FIG 18; COOLING RATE AT CENTRAL AXIS OF BAR, QUENCHED IN VARIOUS MEDIUMS.

Key :-
WATER QUENCH.
OIL QUENCH.

AVE. RATE
TO 600°C:
12.7°C/SEC.

AVE. RATE
TO 600°C:
35°C/SEC.

TIME (SECONDS).

TEMPERATURE (°C).
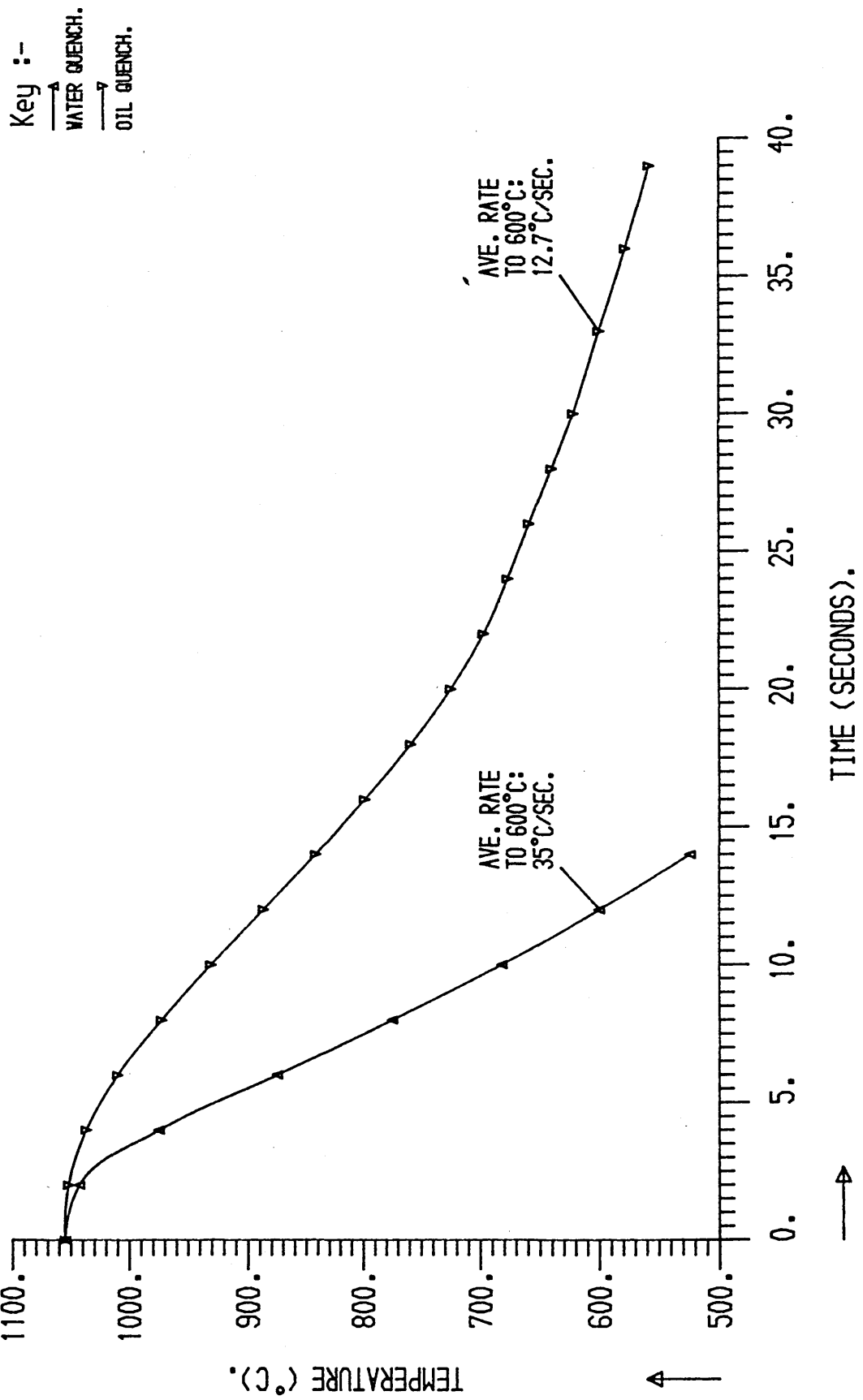
FIG 19;CHARPY TEST SPECIMEN. (BS 131: PART 2)

NOTE: ALL DIMENSIONS IN MM.
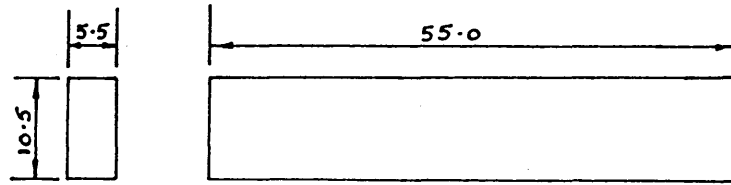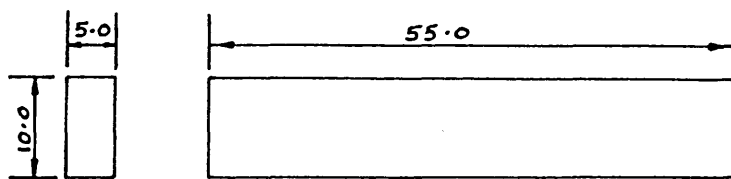
STAGE 1.

STAGE 2.

FIG 20;TENSILE TEST SPECIMEN. (BS 18: PART 2)

NOTE: ALL DIMENSIONS IN MM.
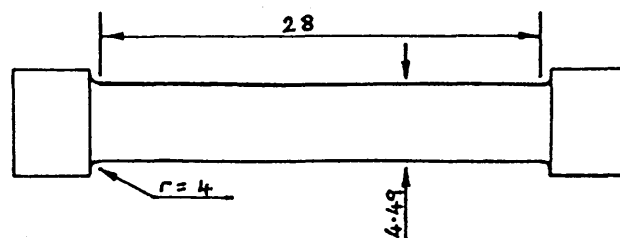
STAGE 1.

STAGE 2.
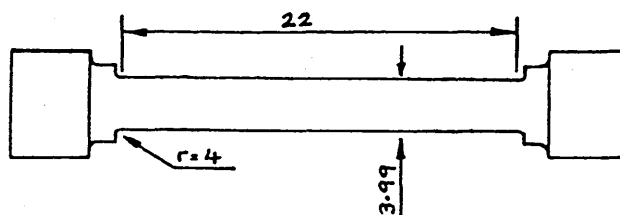
FIG 21;HEATING CURVES FOR JOMINEY SPECIMENS.

Key :-

1200°C

950°C.

TEMPERATURE (°C).

TIME (MINUTES).

271
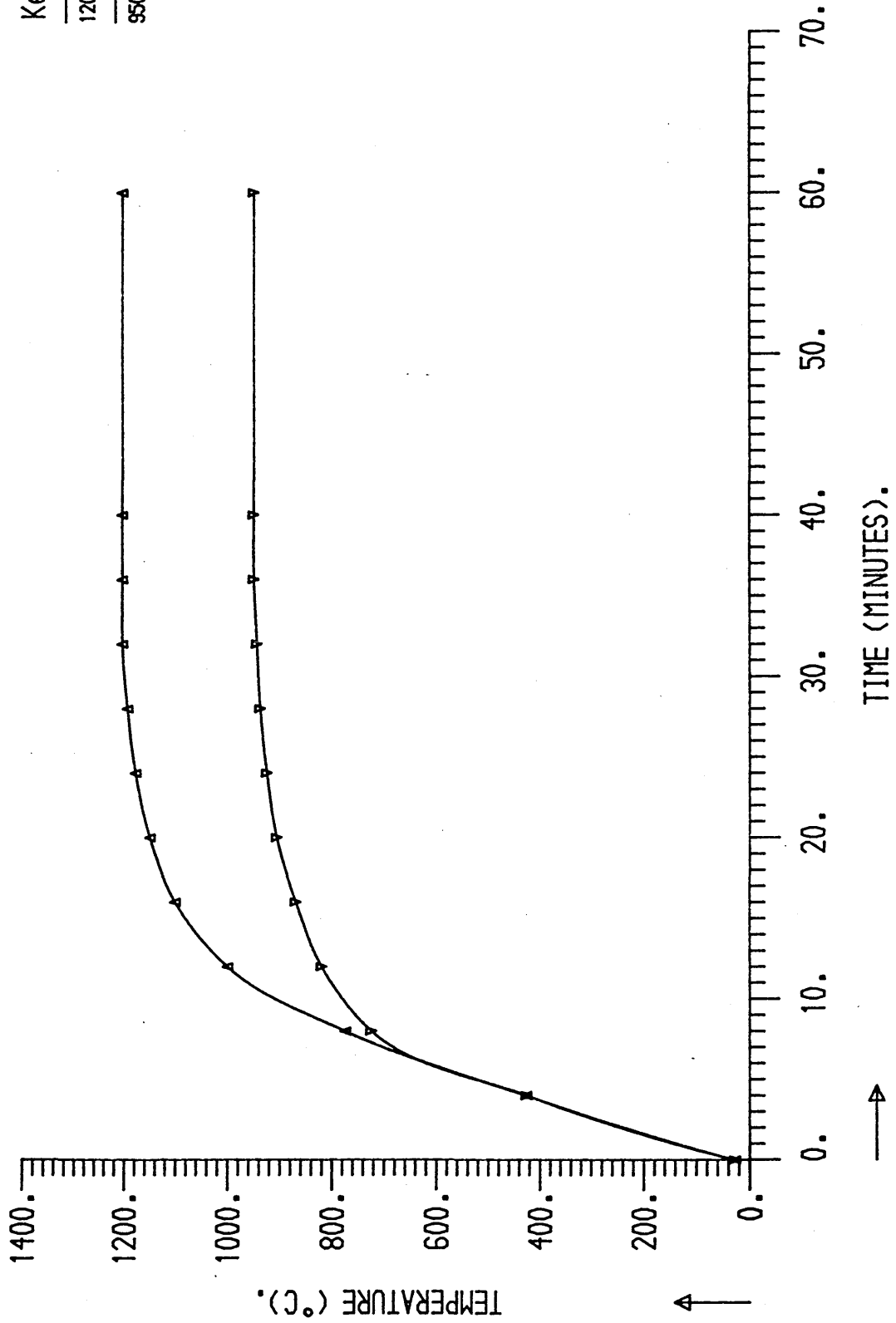
FIG 22:COOLING CURVES FOR A JOMINY SPECIMEN
END QUENCHED FROM 950°C.
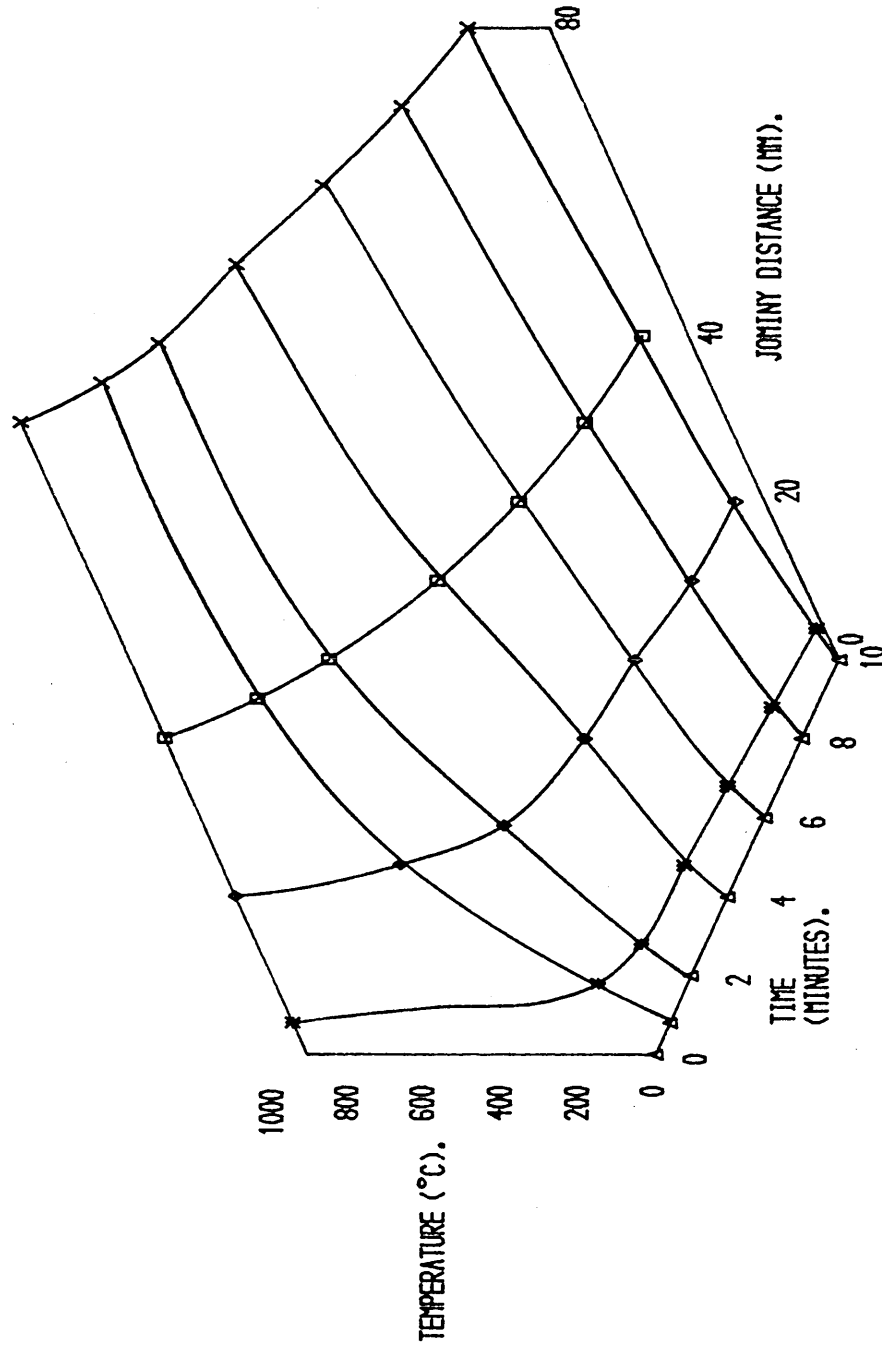
FIG 23;COOLING CURVES FOR A JOMINY SPECIMEN
END QUENCHED FROM 1200°C.
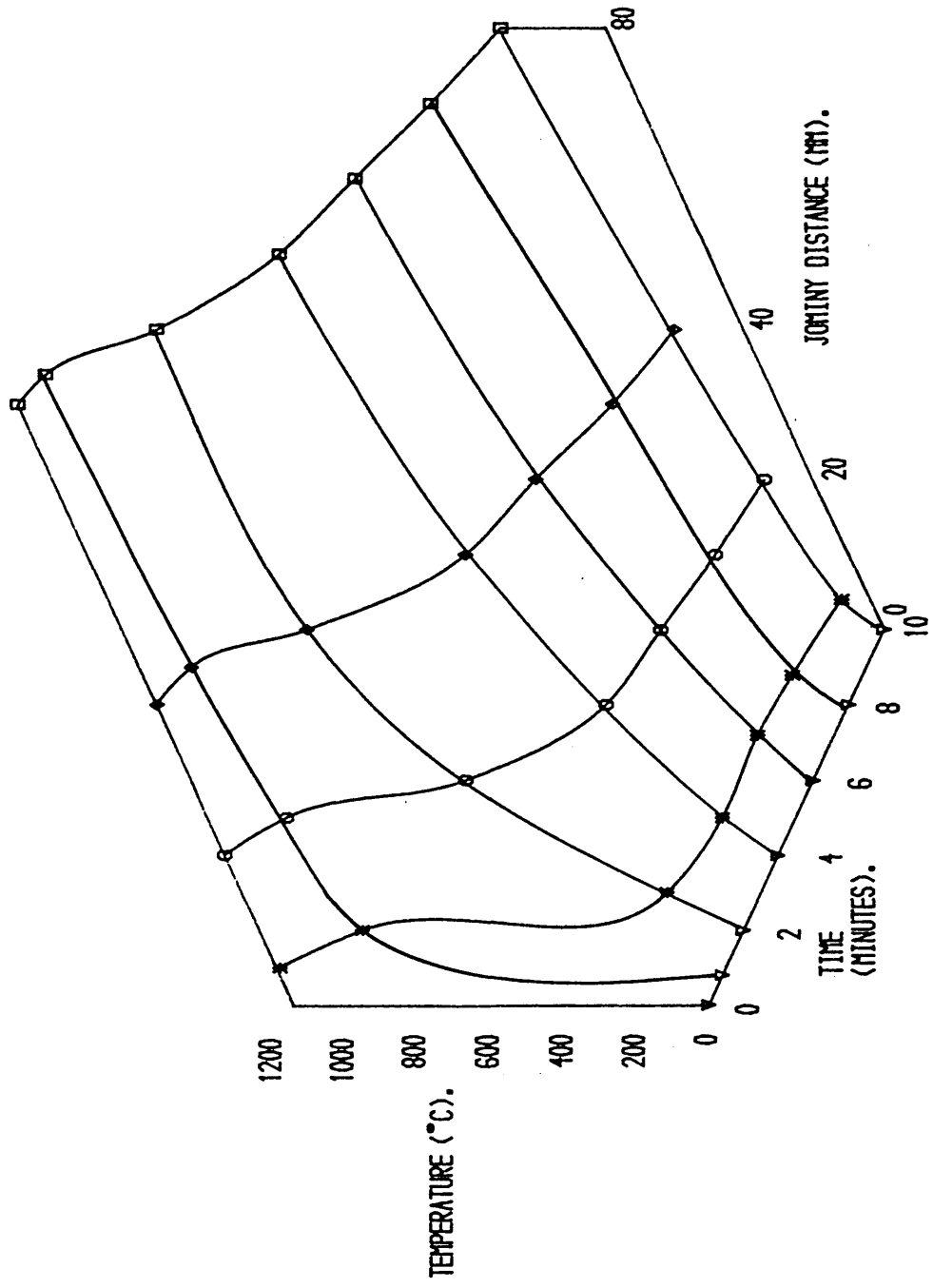
FIG 24; HEAT TREATMENT TO INVESTIGATE EFFECT OF COOLING RATE ON HARDENABILITY.
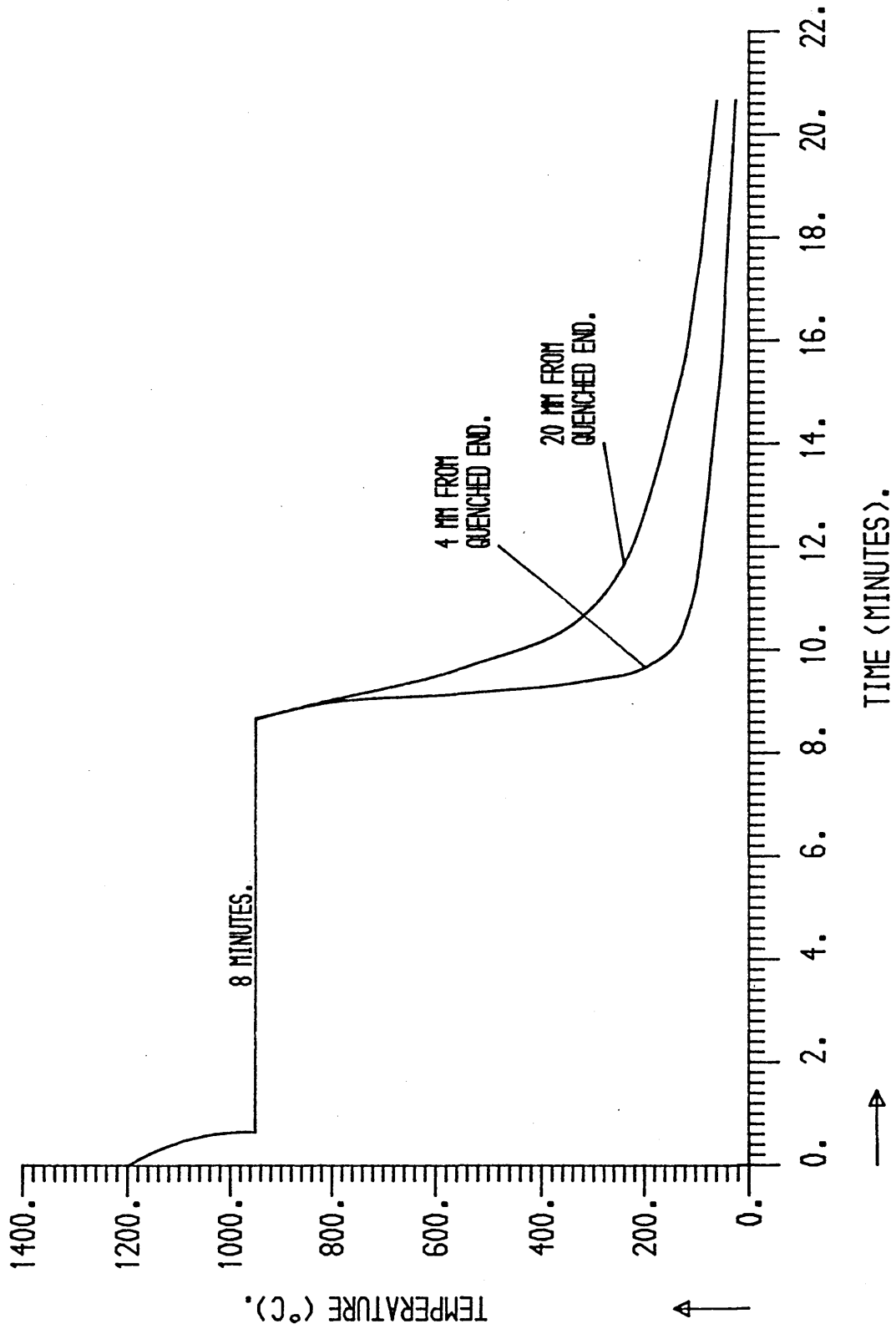
8 MINUTES.

4 MM FROM QUENCHED END.

20 MM FROM QUENCHED END.

TEMPERATURE (°C).

TIME (MINUTES).

FIG 25; EFFECT OF VANADIUM ON THE HARDENABILITY OF A LOW CARBON STEEL.

AUSTENITISED AT 950°C.

A.S.T.M. GRAIN SIZE: 10.

VANADIUM IN SOLUTION (MASS %).

IDEAL CRITICAL DIAMETER (MM).

FIG 26; EFFECT OF VANADIUM ON THE HARDENABILITY OF A LOW CARBON STEEL.

IDEAL CRITICAL DIAMETER (MM).

VANADIUM IN SOLUTION (MASS %).

AUSTENITISED AT 1200°C.

A.S.T.M. GRAIN SIZE: 2.

276
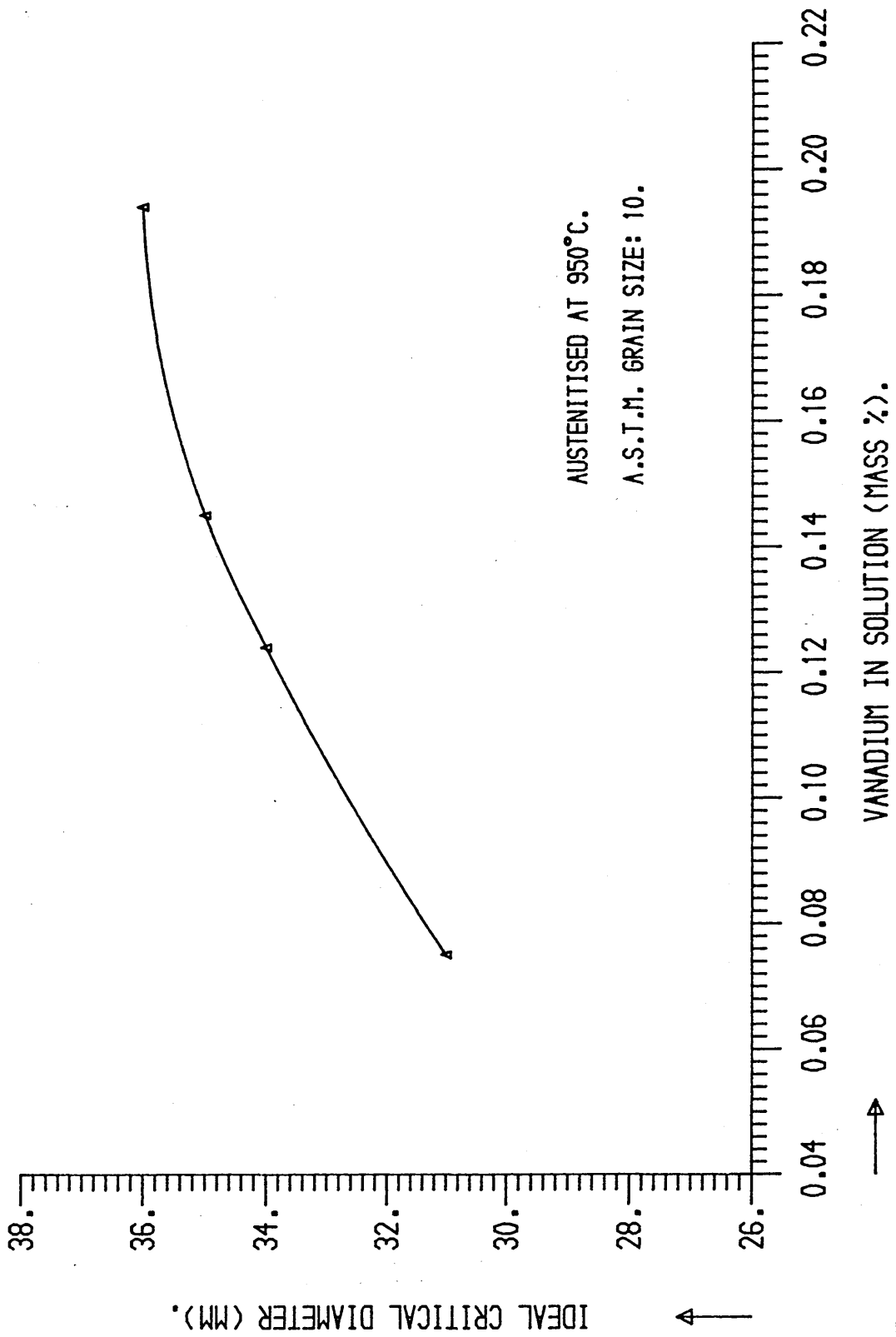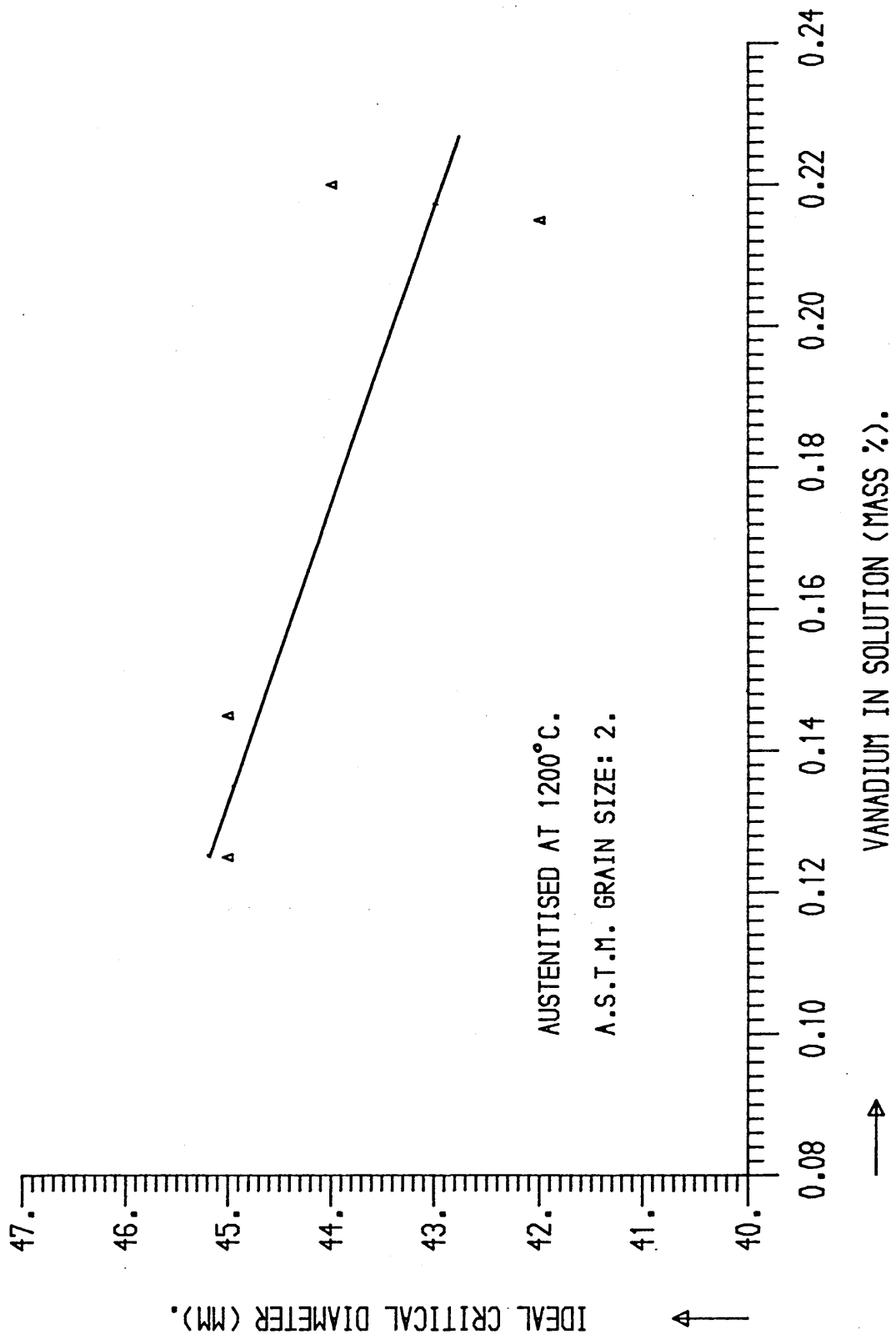
FIG 27; EFFECT OF VANADIUM ON HARDENABILITY AT A CONSTANT GRAIN SIZE (ASTM4).

Key :-
950°C
1200°C
1200/950°C

VANADIUM IN SOLUTION (MASS %).

IDEAL CRITICAL DIAMETER (MM).
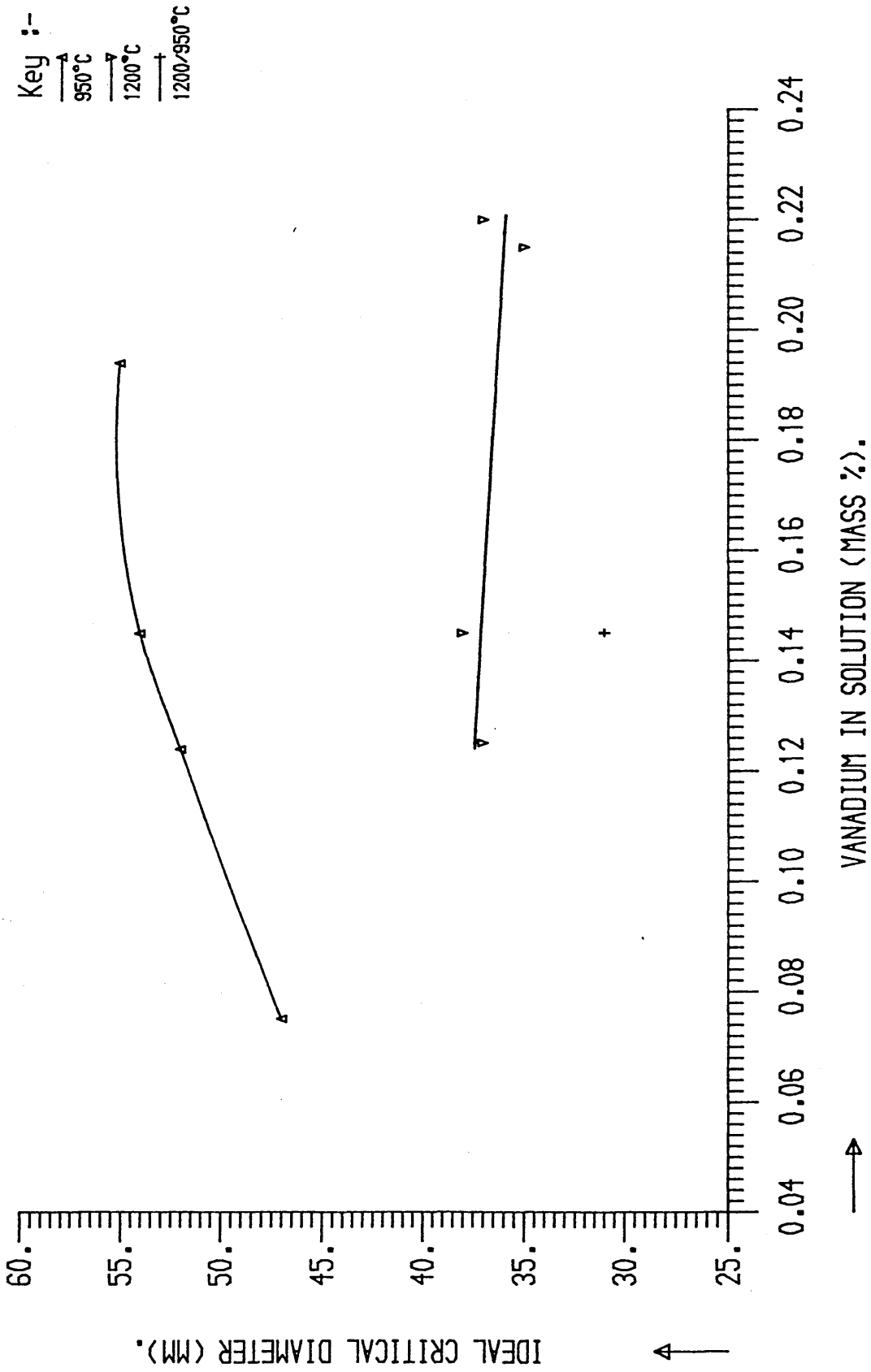
FIG 28;EFFECT OF TEMPERATURE ON THE HARDENABILITY OF LOW CARBON STEELS.
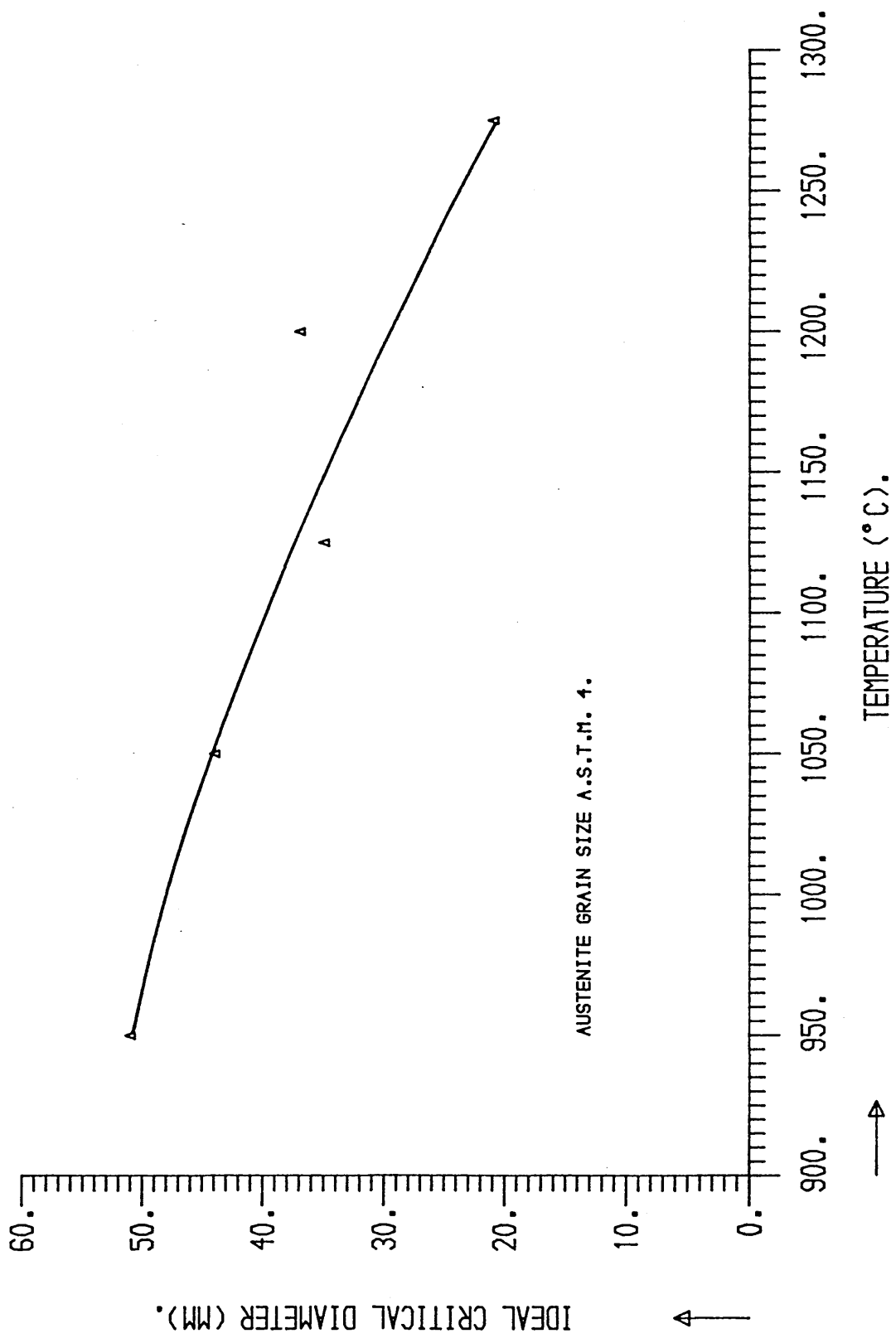
AUSTENITE GRAIN SIZE A.S.T.M. 4.

TEMPERATURE (°C).

IDEAL CRITICAL DIAMETER (MM).

278

FIG 29;EFECT OF AUSTENITISING TIME ON THE HARDENABILITY OF LOW CARBON STEELS.

Key :-
ALLOY 612.
ALLOY 619.
ALLOY 622

AUSTENITISED AT 950°C.
A.S.T.M. GRAIN SIZE; 10.

TIME AT TEMPERATURE (HOURS).

IDEAL CRITICAL DIAMETER (MM).
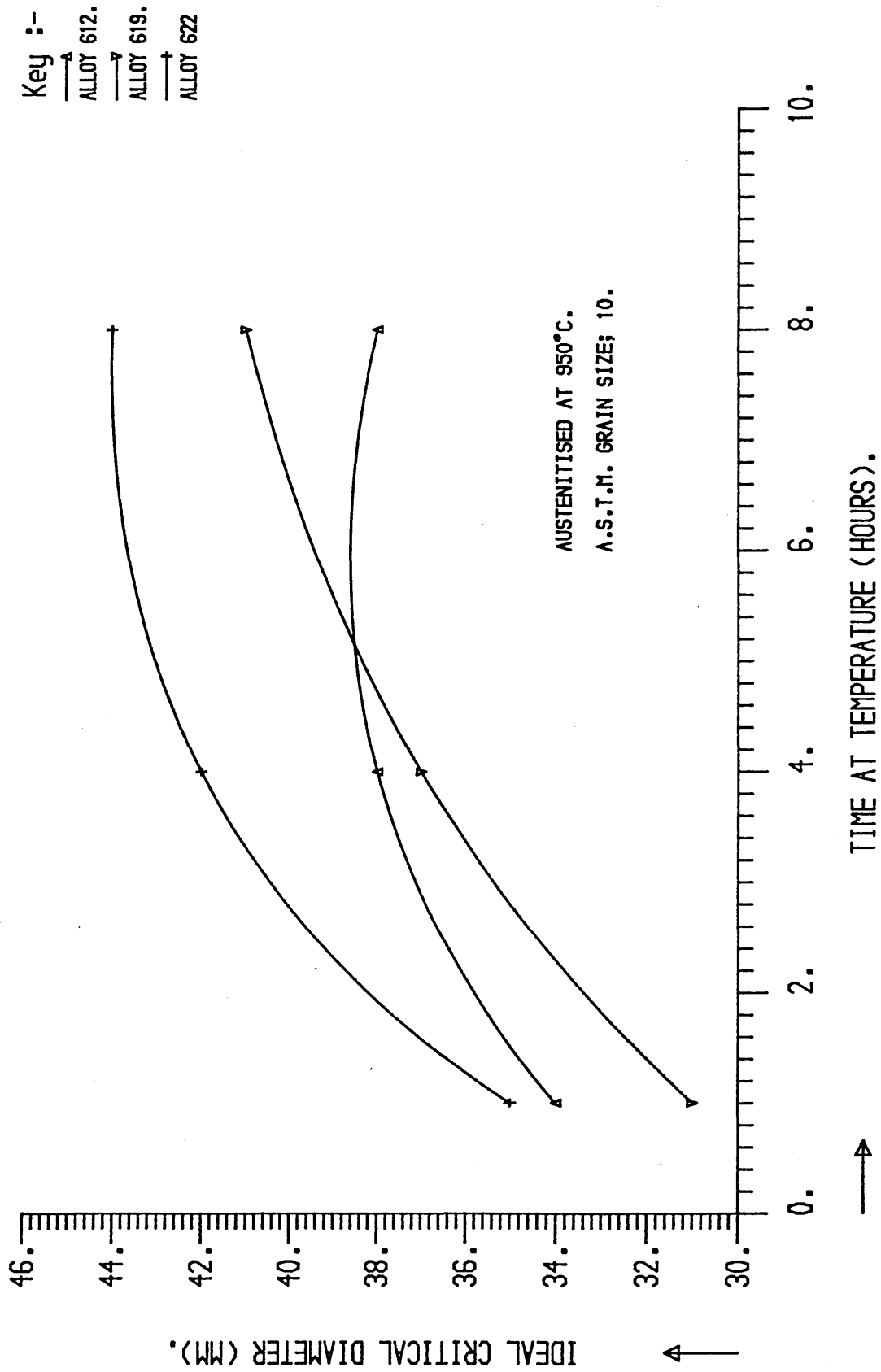
FIG 30; EFFECT OF VANADIUM ON HARDENABILITY AFTER VARIOUS AUSTENITISING TIMES.

AUSTENITISED AT 950°C.

A.S.T.M. GRAIN SIZE; 10.

Key :-
— 1 HOUR.
— 4 HOURS.
— 8 HOURS.

VANADIUM IN SOLUTION (MASS %).

IDEAL CRITICAL DIAMETER (MM).
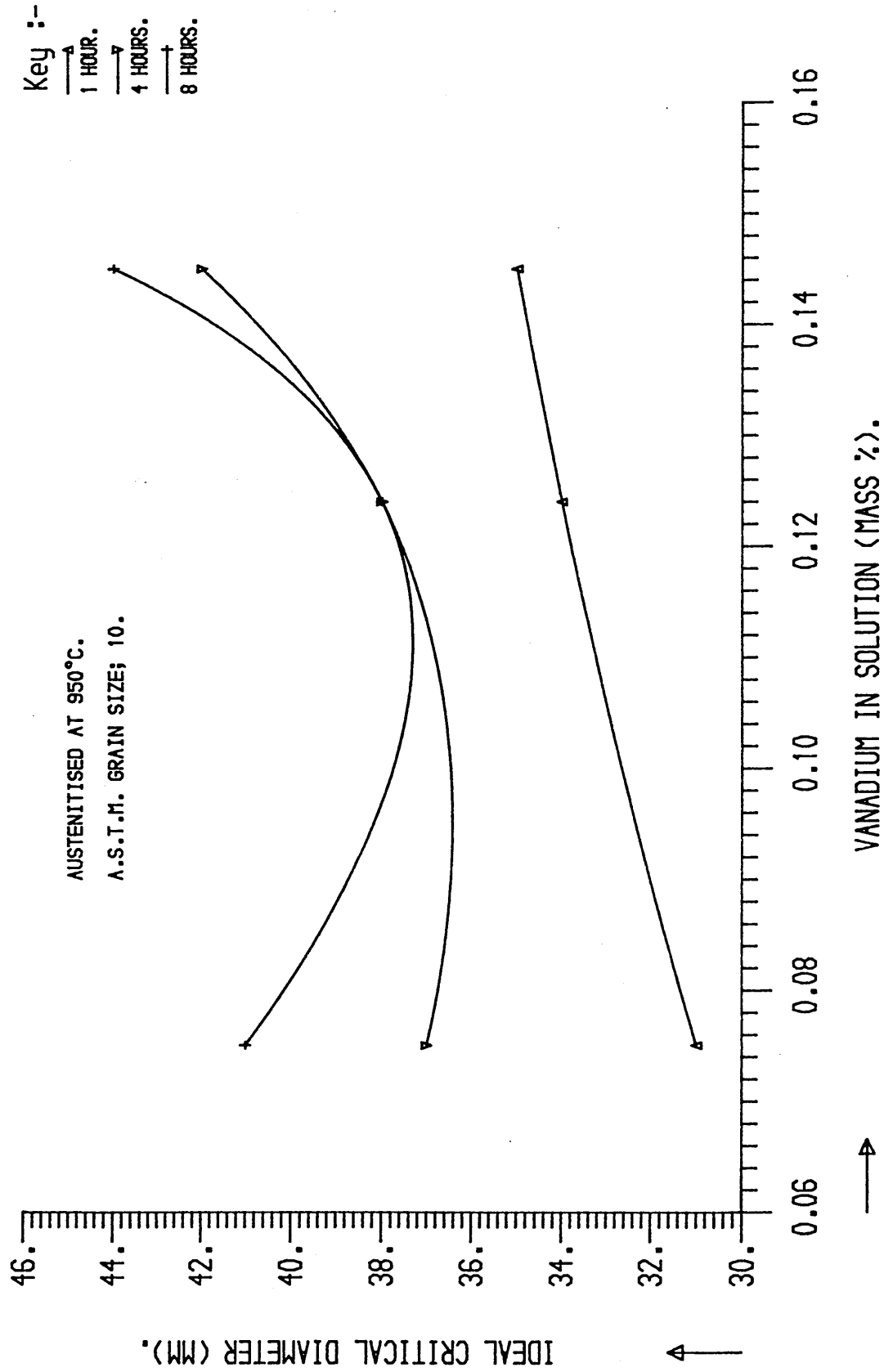
FIG 31; EFFECT OF PRECIPITATE MORPHOLOGY ON HARDENABILITY AT 950°C.

Key :-
AIR COOLED.
OIL QUENCHED.
HOMOGENISED

IDEAL CRITICAL DIAMETER (MM).

TIME AT TEMPERATURE (HOURS).

AUSTENITE GRAIN SIZE A.S.T.M. 10.

281

FIG 32;EFFECT OF ALLOYING ADDITIONS ON THE HARDENABILITY OF LOW C STEELS.

AUSTENITISED AT 950°C.

A.S.T.M. GRAIN SIZE: 10.

BASE CHEMICAL ANALYSIS:
0.080 m/o C,0.30 m/o Si,
1.54 m/o Mn,0.145 m/o V,
0.0083 m/o N_2.

CHANGE IN ALLOY CONTENT (MASS %)

IDEAL CRITICAL DIAMETER (MM)

282
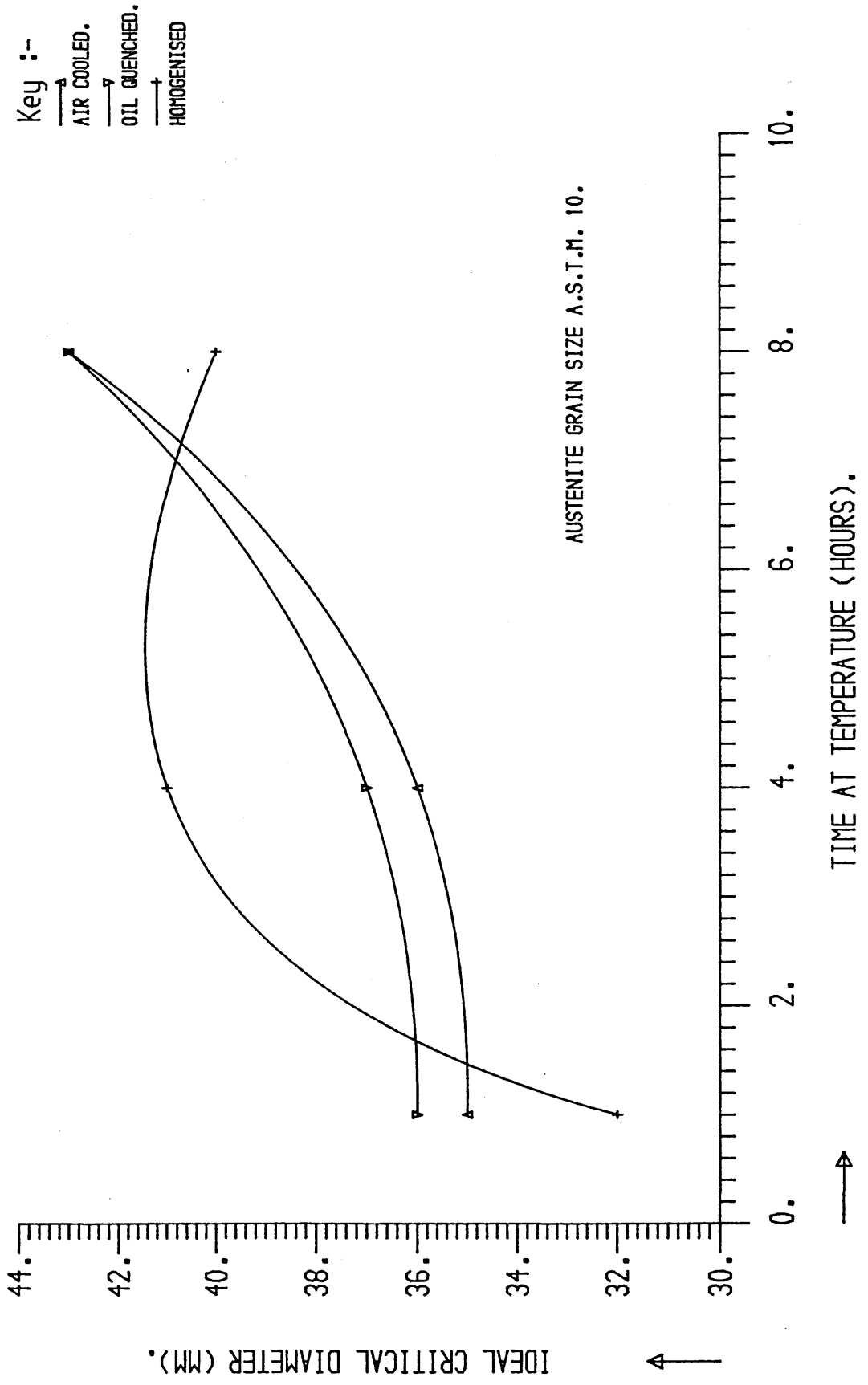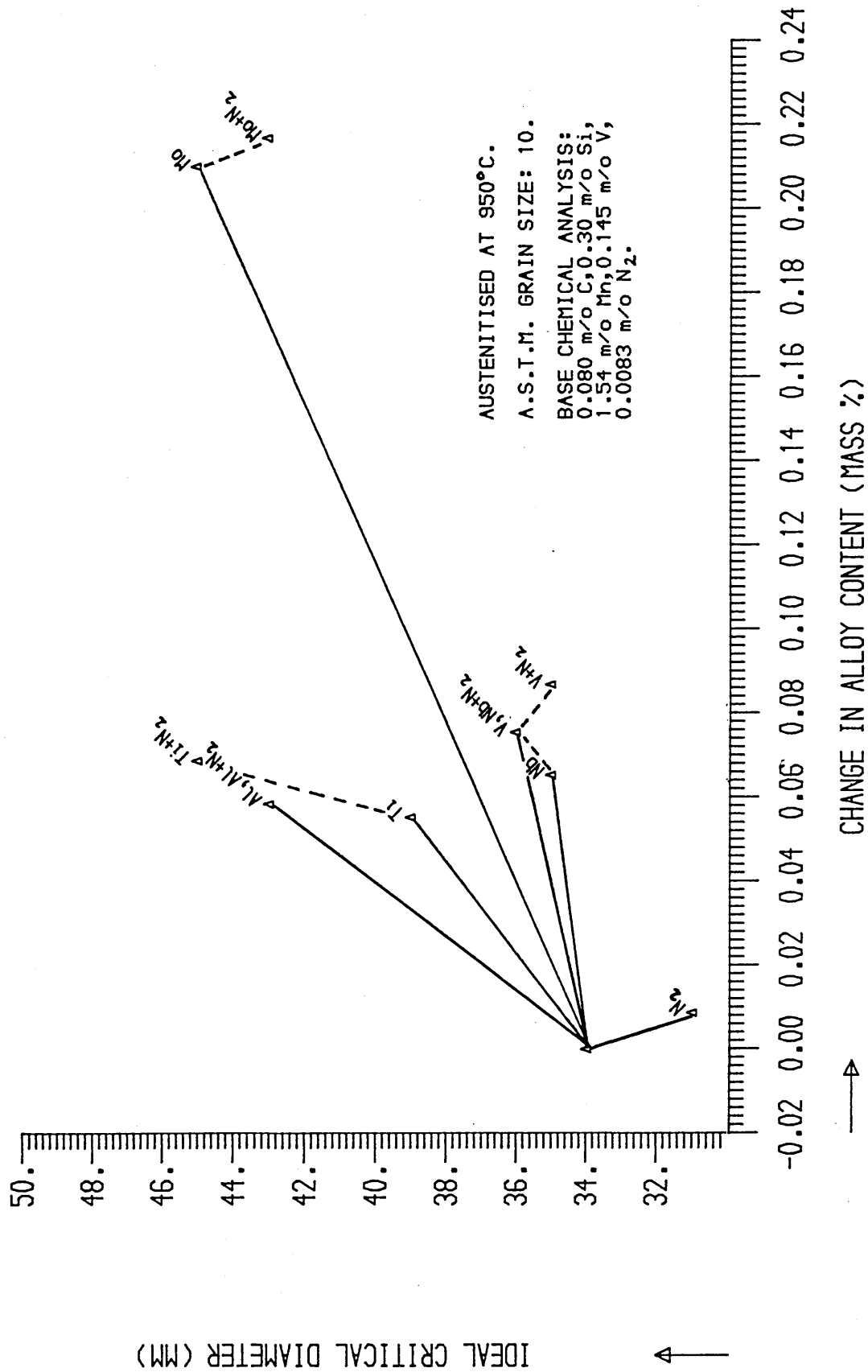
FIG 33;EFFECT OF AUSTENITISING TIME AT 950°C ON HARDENABILITY OF LOW C STEELS.
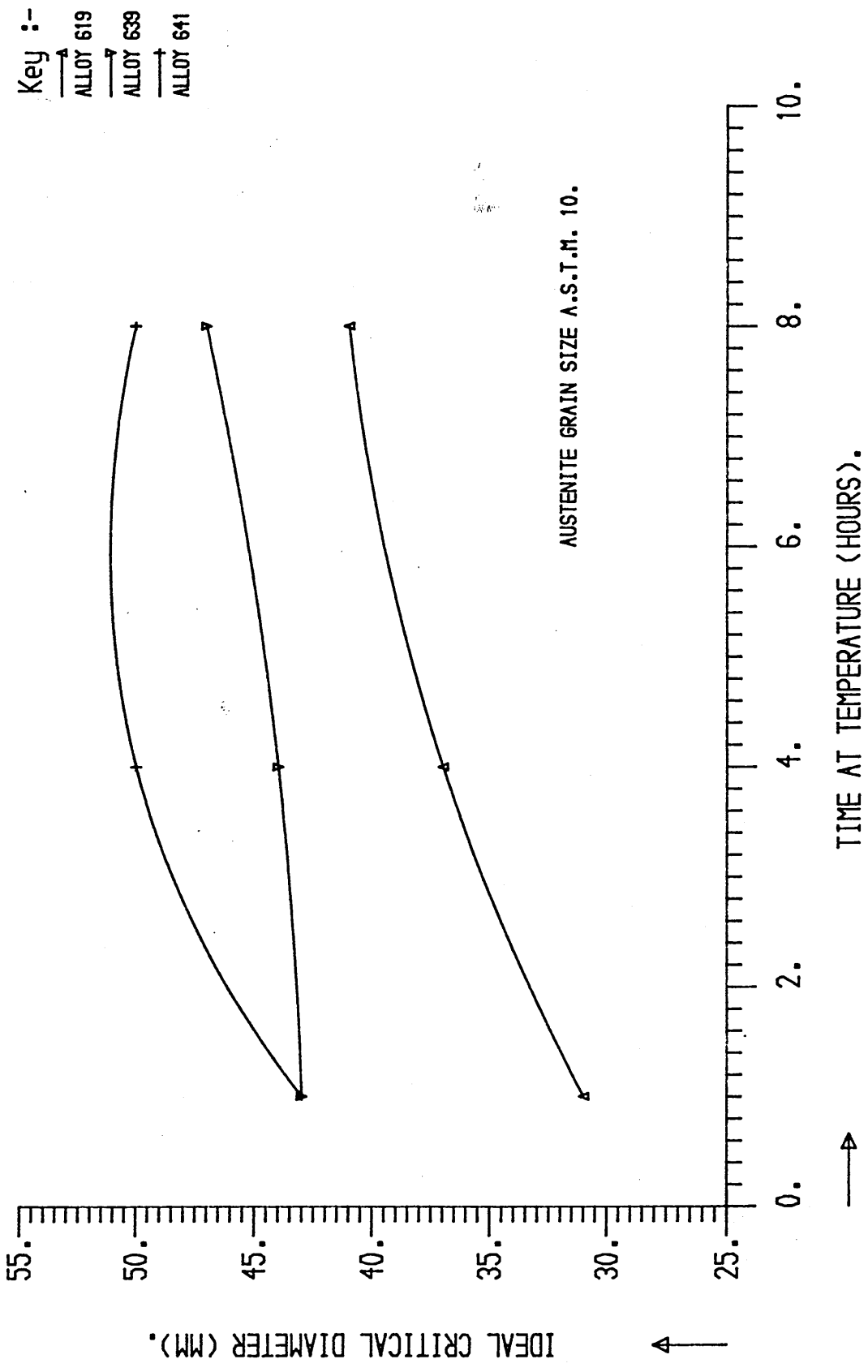
Key :-
ALLOY 619
ALLOY 639
ALLOY 641

AUSTENITE GRAIN SIZE A.S.T.M. 10.

TIME AT TEMPERATURE (HOURS).

IDEAL CRITICAL DIAMETER (MM).

FIG 34;EFFECT OF ALLOYING ADDITIONS ON THE HARDENABILITY OF LOW C STEELS.

AUSTENITISED AT 1200°C.

A.S.T.M. GRAIN SIZE: 2.

BASE CHEMICAL ANALYSIS:
0.080 m/o C,0.30 m/o Si,
1.54 m/o Mn,0.145 m/o V,
0.0083 m/o N_2.

FIG 35;EFFECT OF ALLOYING ADDITIONS ON THE HARDENABILITY OF MEDIUM C STEELS.

AUSTENITISED AT 950°C.

A.S.T.M. GRAIN SIZE: 10.

BASE CHEMICAL ANALYSIS:
0.390 m/o C,0.43 m/o Si,
1.57 m/o Mn,0.130 m/o V,
0.020 m/o N_2.

FIG 36; EFFECT OF ALLOYING ADDITIONS ON THE HARDENABILITY OF MEDIUM C STEELS.

AUSTENITISED AT 1200°C.

A.S.T.M. GRAIN SIZE: 2.

BASE CHEMICAL ANALYSIS:
0.390 m/o C, 0.43 m/o Si,
1.57 m/o Mn, 0.130 m/o V,
0.020 m/o N₂.

CHANGE IN ALLOY CONTENT (MASS %).

IDEAL CRITICAL DIAMETER (MM).
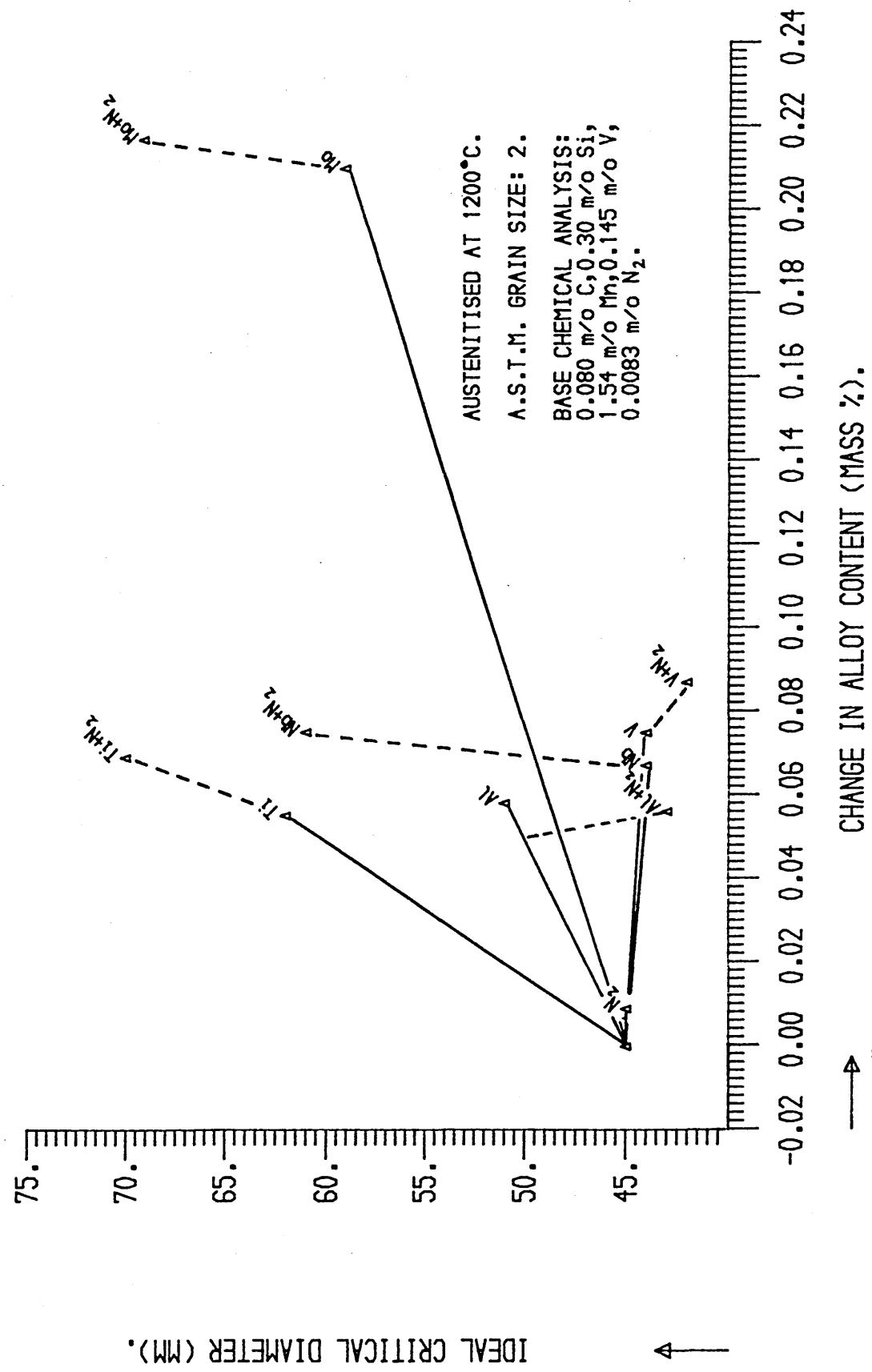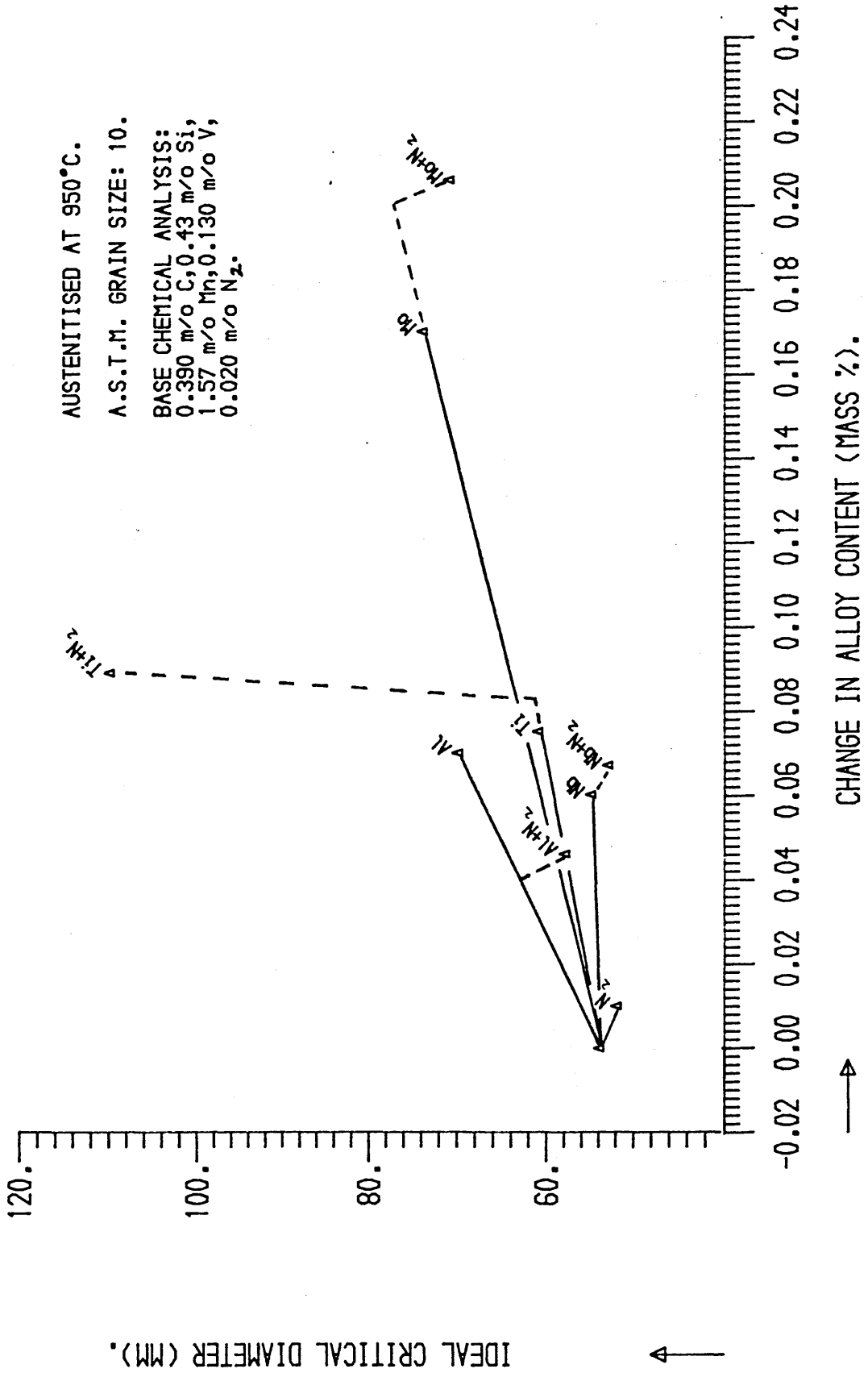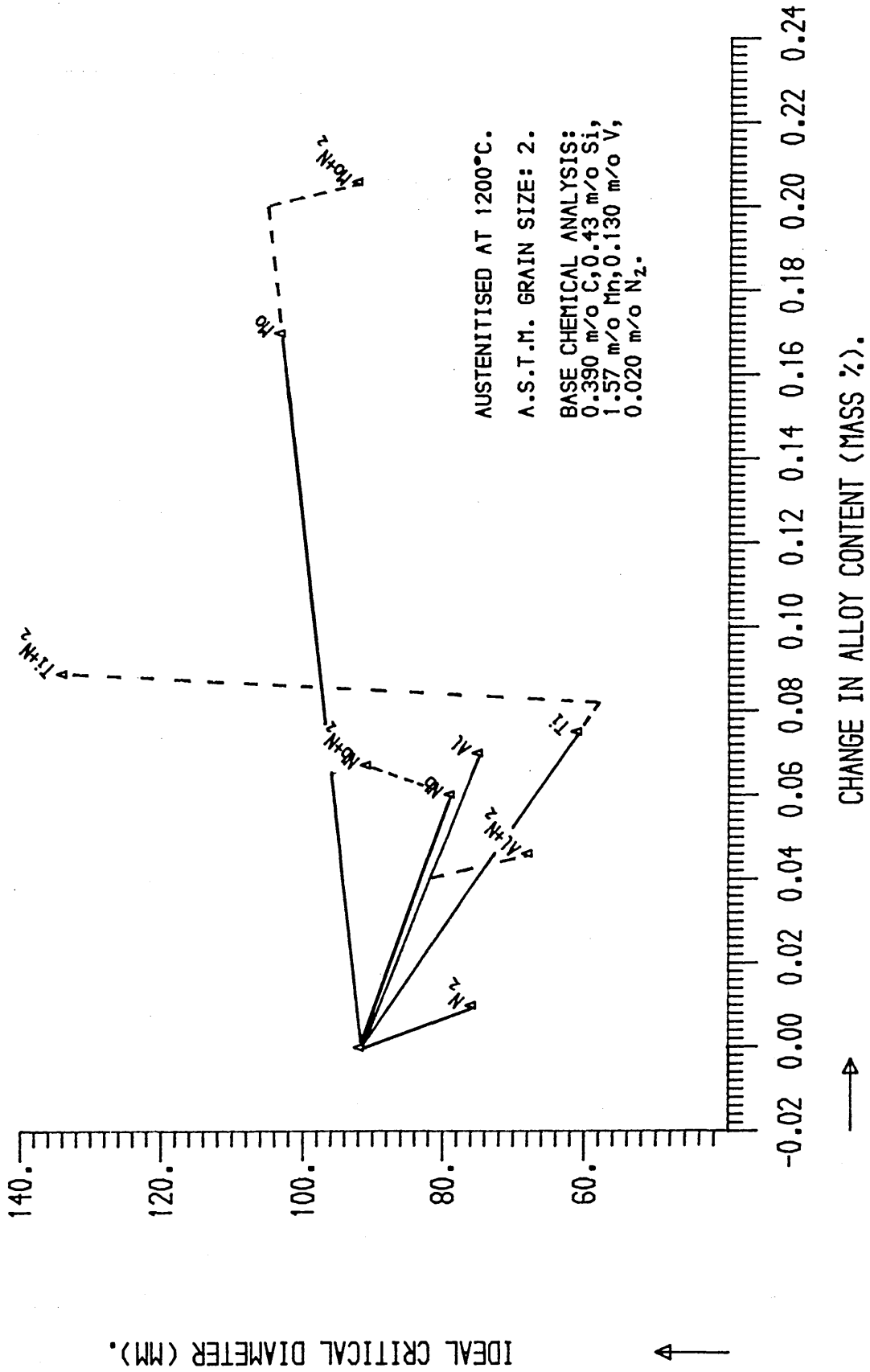
FIG 37; T.T.T. DIAGRAM FOR HIGH CARBON VANADIUM STEELS.

Key :-

	ALLOY 626 START
	ALLOY 626 END
	ALLOY 695 START
×	ALLOY 695 END
□	TREATMENT TIME.

TIME (SECONDS).

TEMPERATURE (°C).

287
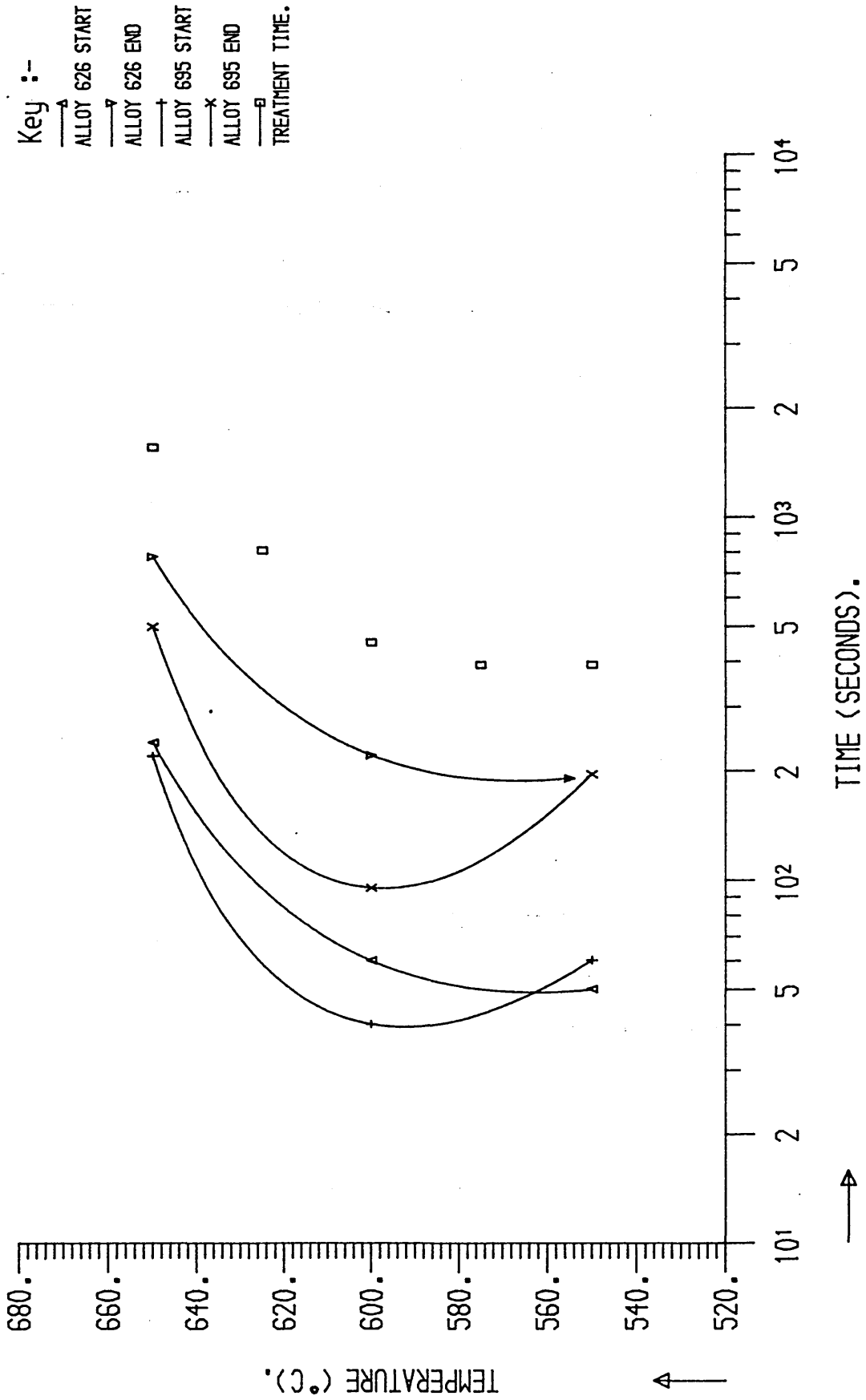
FIG 38;EFFECT OF TRANSFORMATION TEMPERATURE ON HARDNESS OF HIGH CARBON STEELS.

Key :-

△ ALLOY 626.

▽ ALLOY 695.

HARDNESS (HV30).

TRANSFORMATION TEMPERATURE (°C).
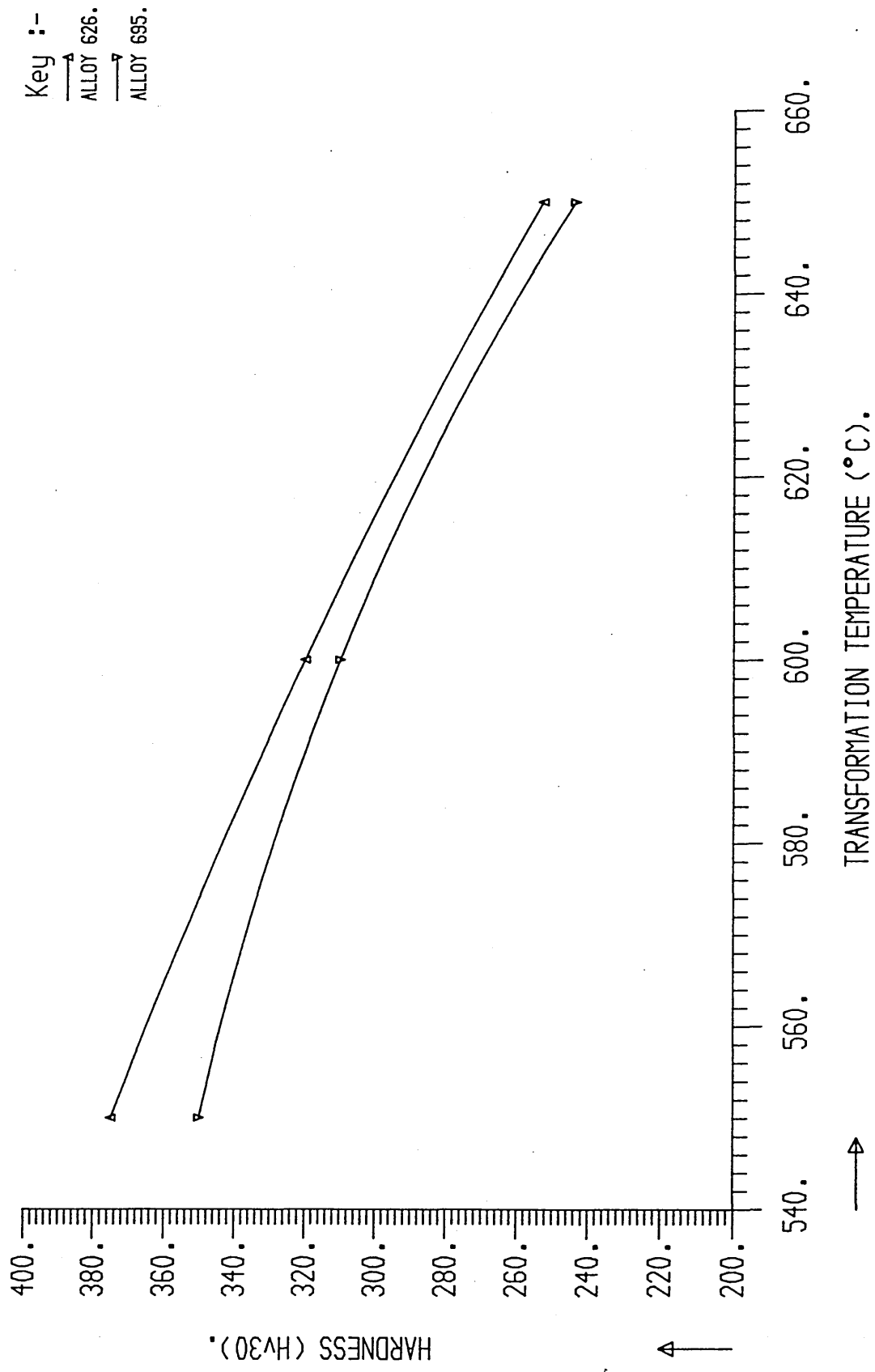
FIG 39;ALLOY 695 ISOTHERMALLY TRANSFORMED AT 650°C.
MAGNIFICATION : X3200.
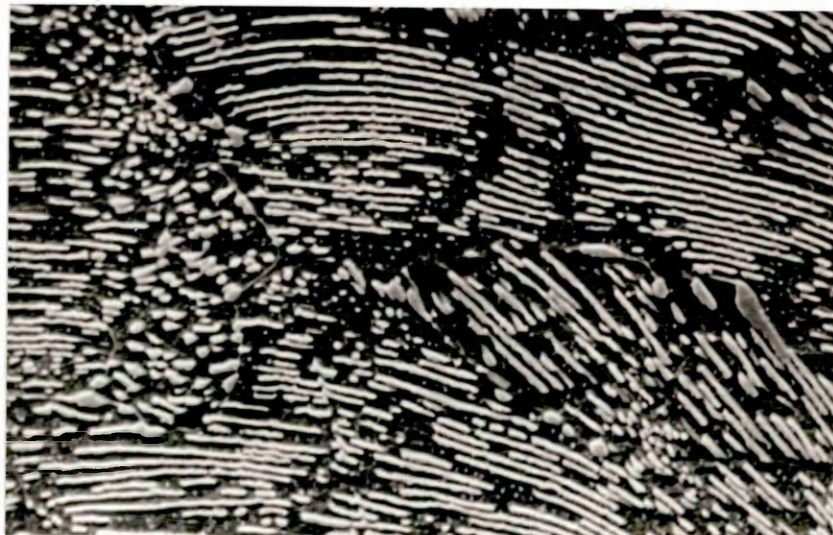
FIG 40;ALLOY 695 ISOTHERMALLY TRANSFORMED AT 650°C.
MAGNIFICATION : X6400.

FIG 41; ALLOY 695 ISOTHERMALLY TRANSFORMED AT 600°C.
     MAGNIFICATION : X3200.
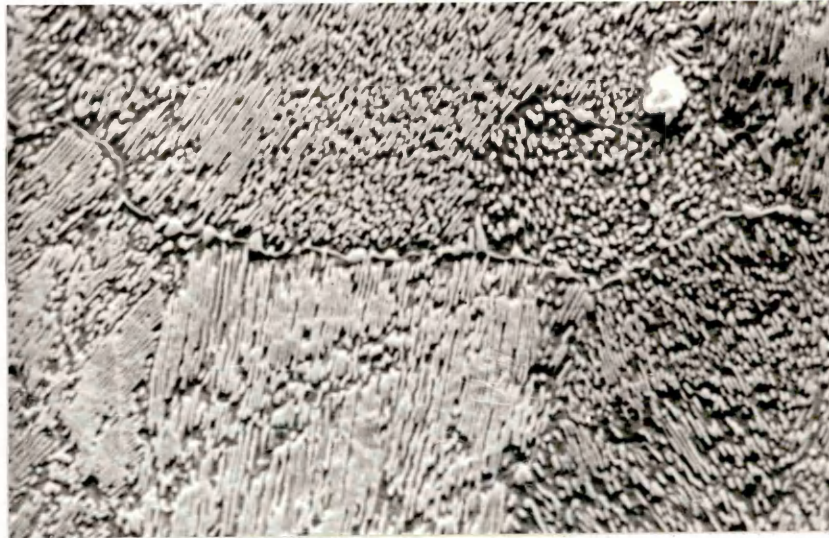
FIG 42; ALLOY 695 ISOTHERMALLY TRANSFORMED AT 600°C.
     MAGNIFICATION : X6400.
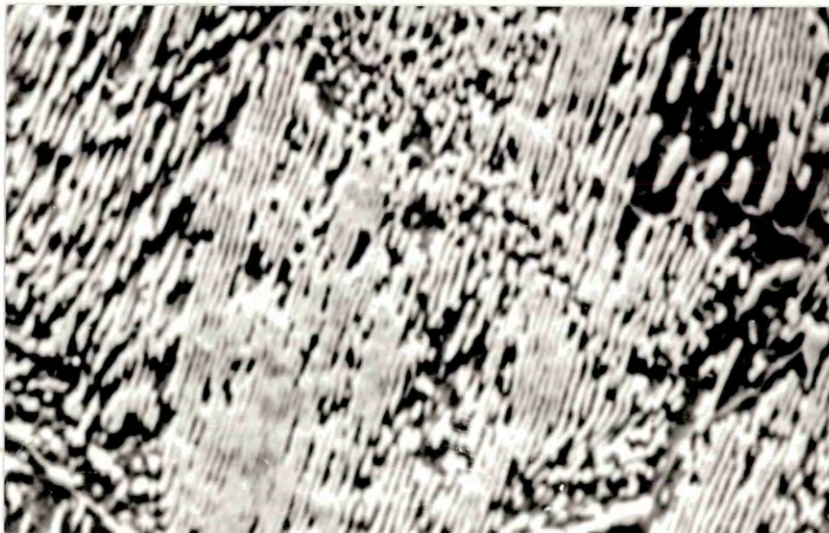
FIG 43;ALLOY 695 ISOTHERMALLY TRANSFORMED AT 650°C.
MAGNIFICATION : X3200.
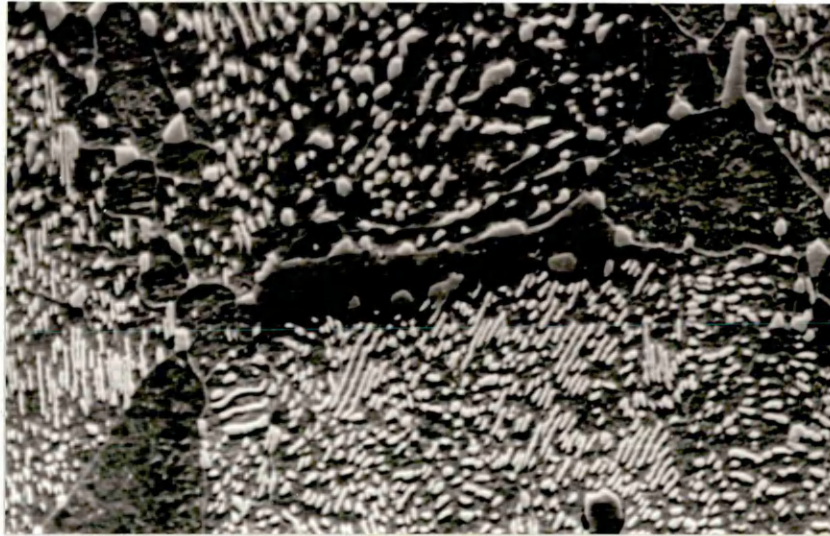
FIG 44;ALLOY 695 ISOTHERMALLY TRANSFORMED AT 650°C.
MAGNIFICATION : X3200.
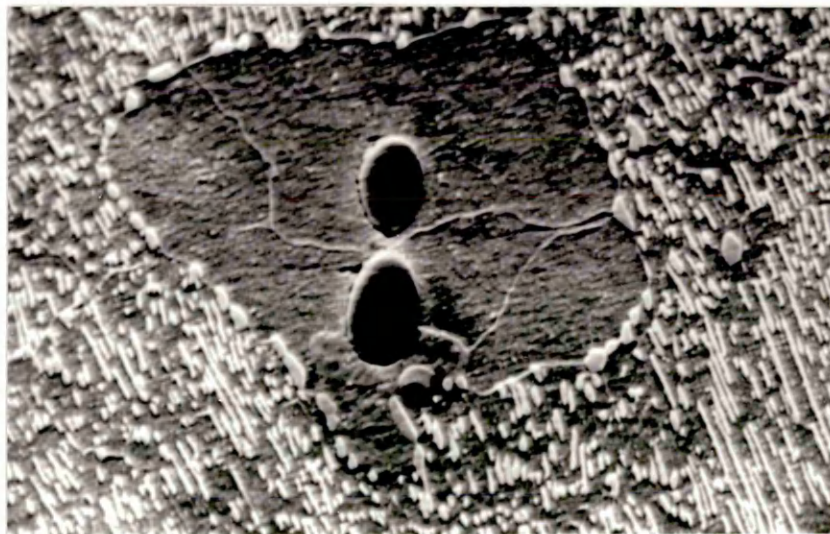
FIG 45;ALLOY 695 ISOTHERMALLY TRANSFORMED AT 650°C.
MAGNIFICATION : X6400.
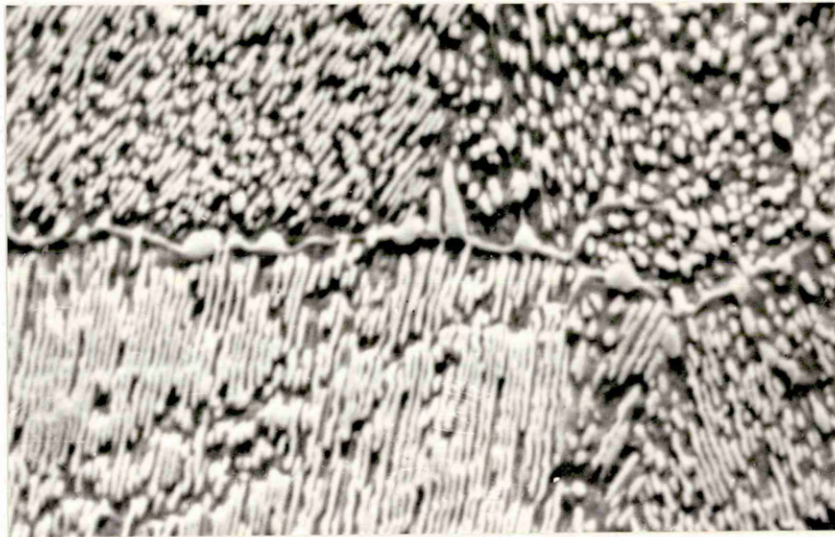
FIG 48;ALLOY 695 ISOTHERMALLY TRANSFORMED AT 650°C FOR 24 HOURS.
MAGNIFICATION : X50000.
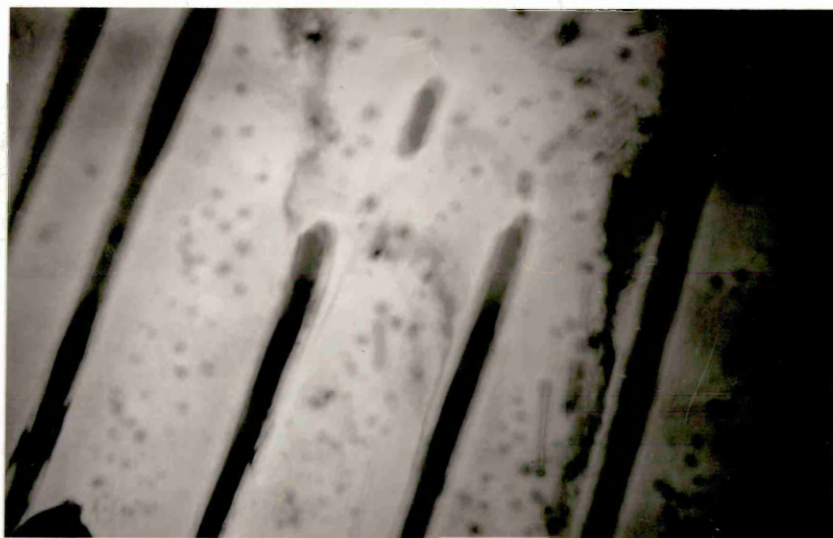
FIG 49;ALLOY 695 ISOTHERMALLY TRANSFORMED AT 650°C FOR 24 HOURS.
MAGNIFICATION : X50000.
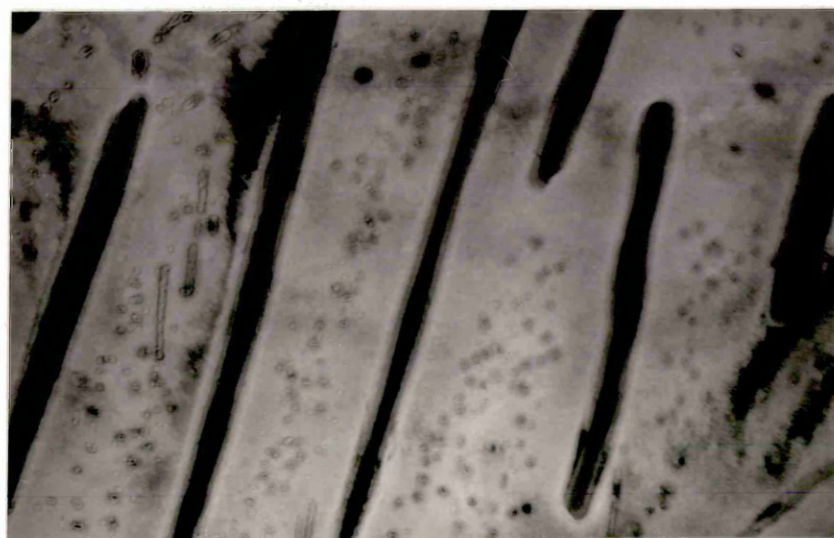
FIG 50;ALLOY 695 ISOTHERMALLY TRANSFORMED AT 650°C FOR 24 HOURS.
        MAGNIFICATION : X66000.
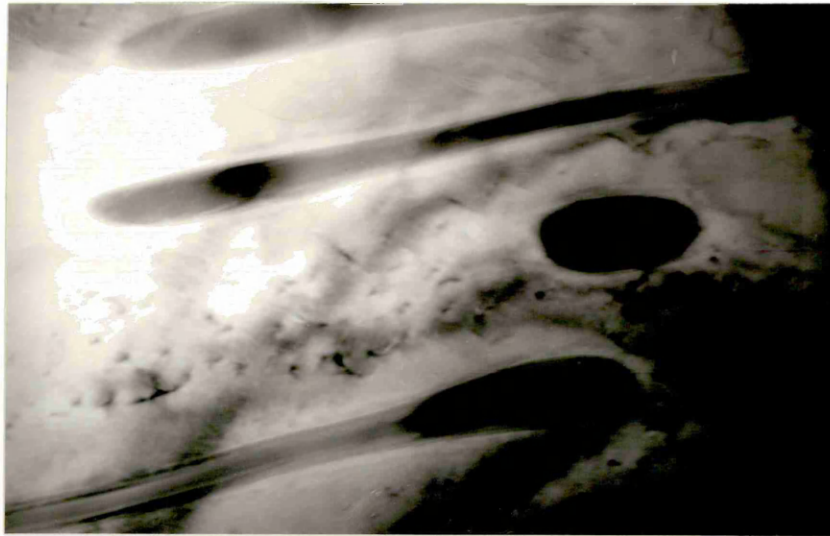
FIG 51;ALLOY 695 ISOTHERMALLY TRANSFORMED AT 650°C FOR 24 HOURS.
        MAGNIFICATION : X66000.
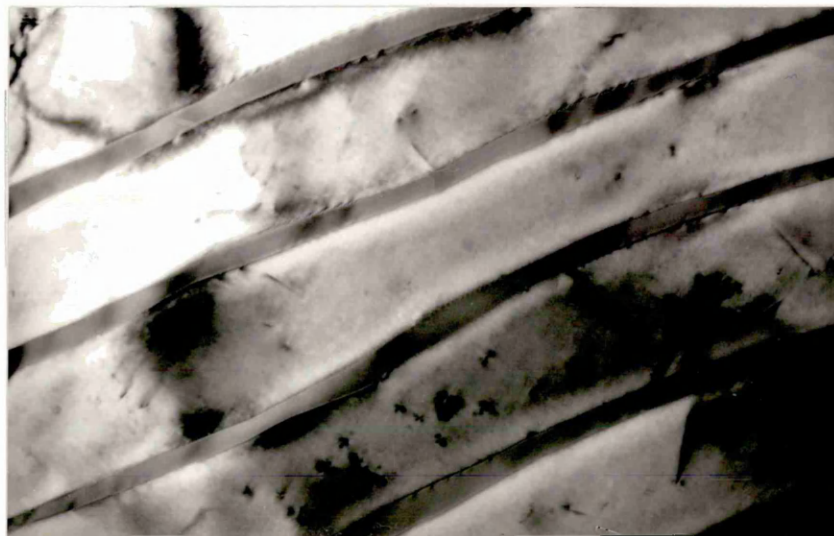
FIG 52;ALLOY 695 ISOTHERMALLY TRANSFORMED AT 650°C FOR 24 HOURS.
MAGNIFICATION : X50000.
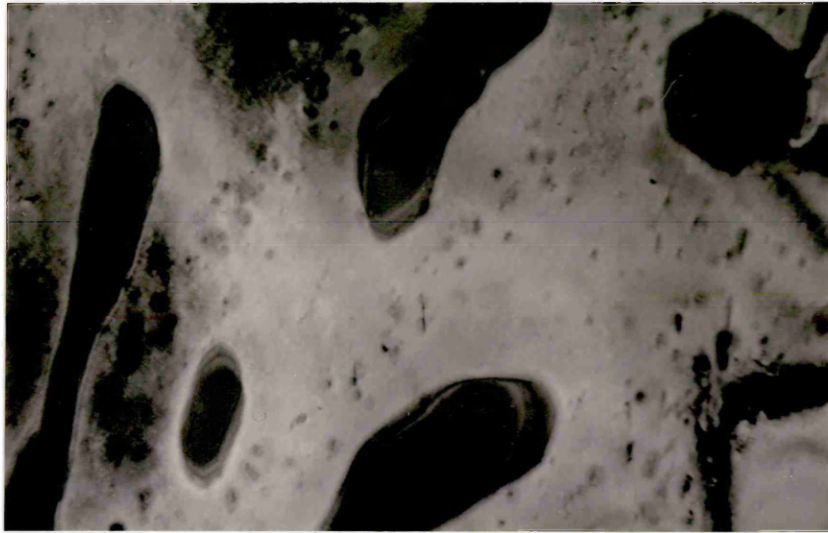
FIG 53;ALLOY 695 ISOTHERMALLY TRANSFORMED AT 650°C FOR 3 MIN. 40 SEC.
MAGNIFICATION : X130K.
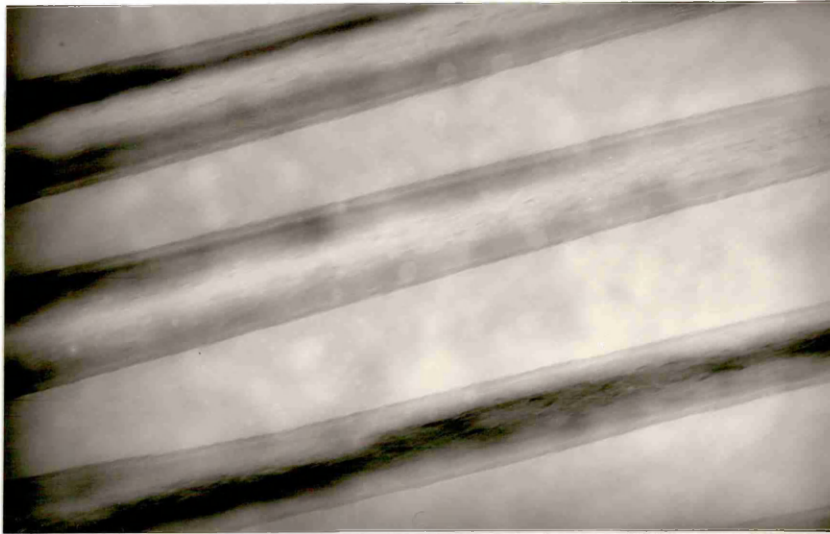
FIG 54;ALLOY 695 ISOTHERMALLY TRANSFORMED AT 650°C FOR 3 MIN. 40 SEC.
MAGNIFICATION : X160K.
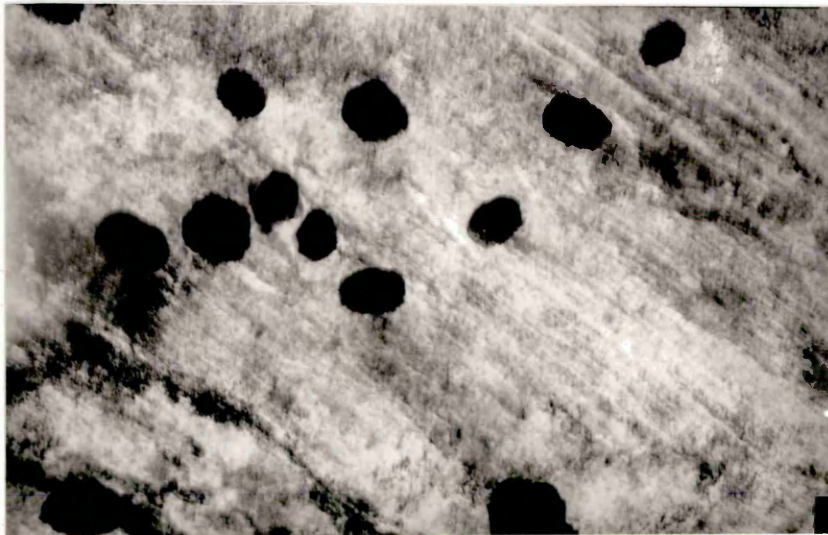
FIG 55;ALLOY 695 ISOTHERMALLY TRANSFORMED AT 650°C FOR 3 MIN. 40 SEC.
MAGNIFICATION : X130K.
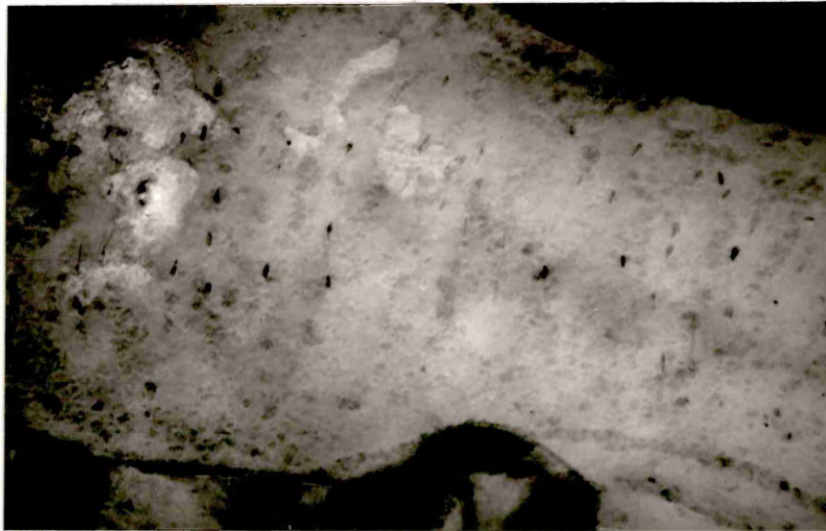
FIG 56;ALLOY 695 ISOTHERMALLY TRANSFORMED AT 650°C FOR 3 MIN. 40 SEC.
MAGNIFICATION : X250K.

298
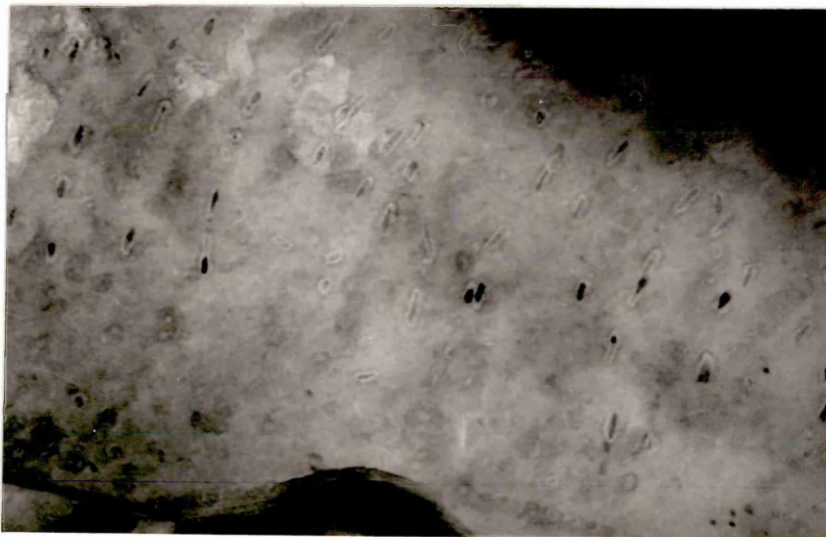
FIG 57; ALLOY 695 ISOTHERMALLY TRANSFORMED AT 650°C FOR 11 MIN. MAGNIFICATION : 100K.
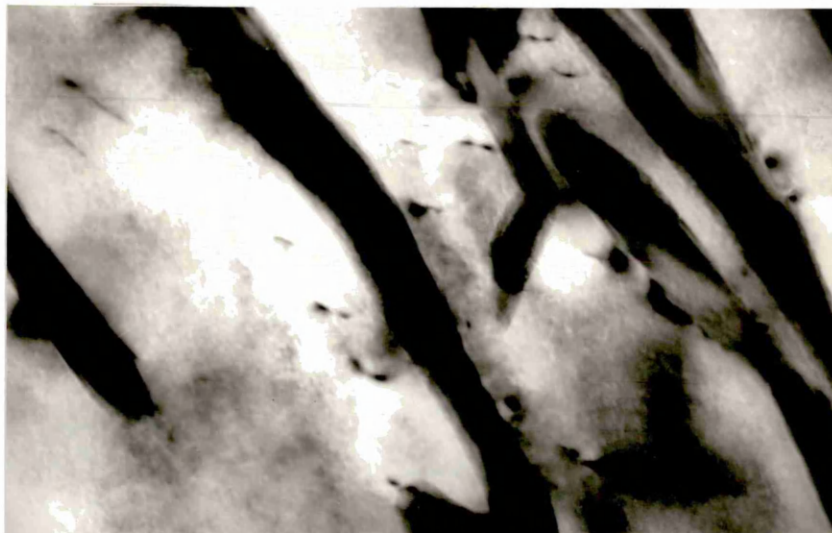
FIG 58; ALLOY 695 ISOTHERMALLY TRANSFORMED AT 650°C FOR 11 MIN. MAGNIFICATION : 130K.
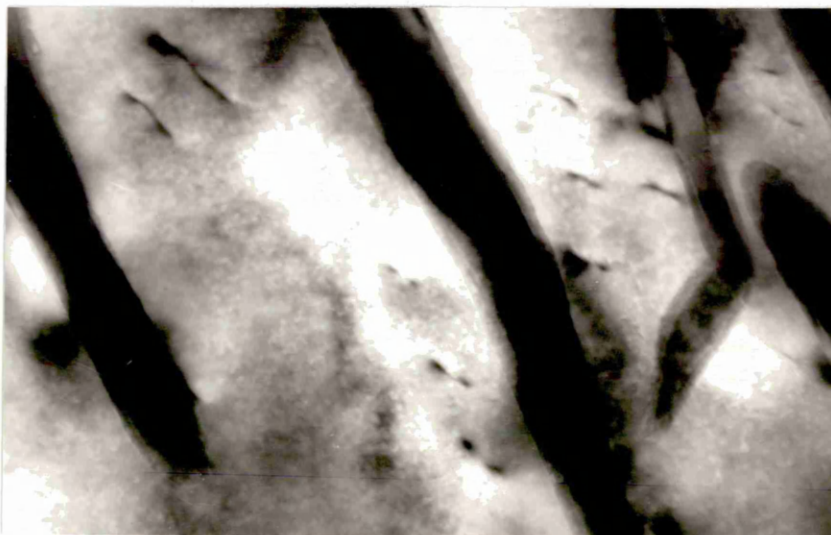
FIG 59; ALLOY 695 ISOTHERMALLY TRANSFORMED AT 650°C FOR 11 MIN.
MAGNIFICATION : 130K.
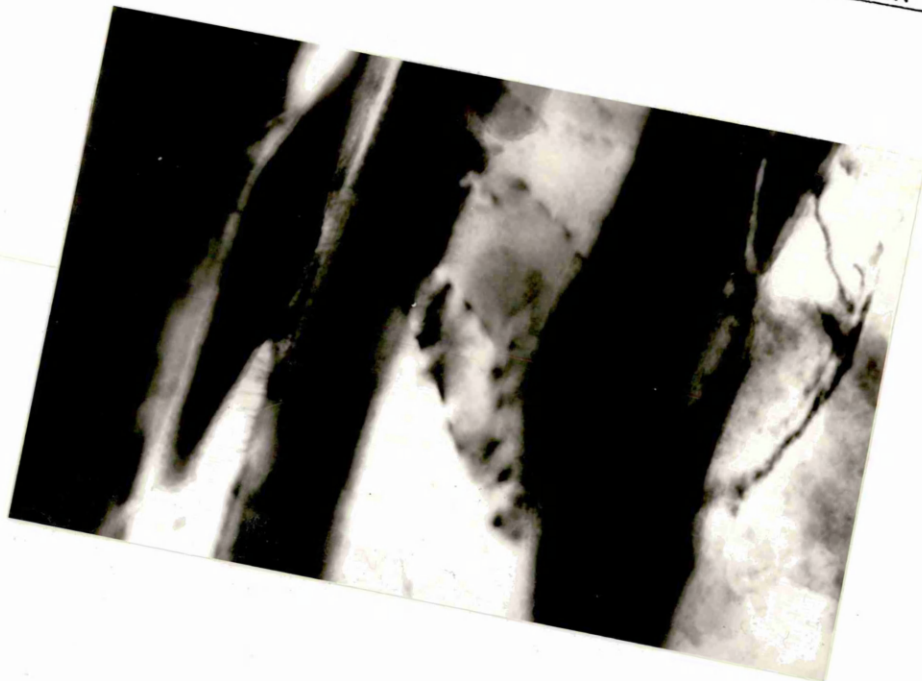
FIG 60; ALLOY 695 ISOTHERMALLY TRANSFORMED AT 650°C FOR 16 MIN.
MAGNIFICATION : 100K.
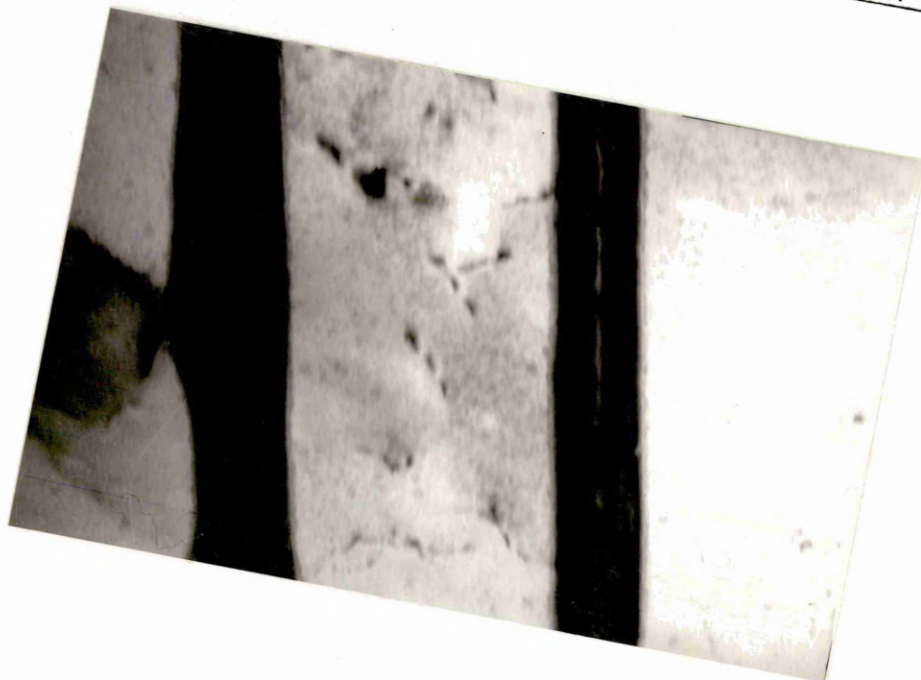
FIG 61;ALLOY 695 ISOTHERMALLY TRANSFORMED AT 650°C FOR 16 MIN. MAGNIFICATION : 130K.
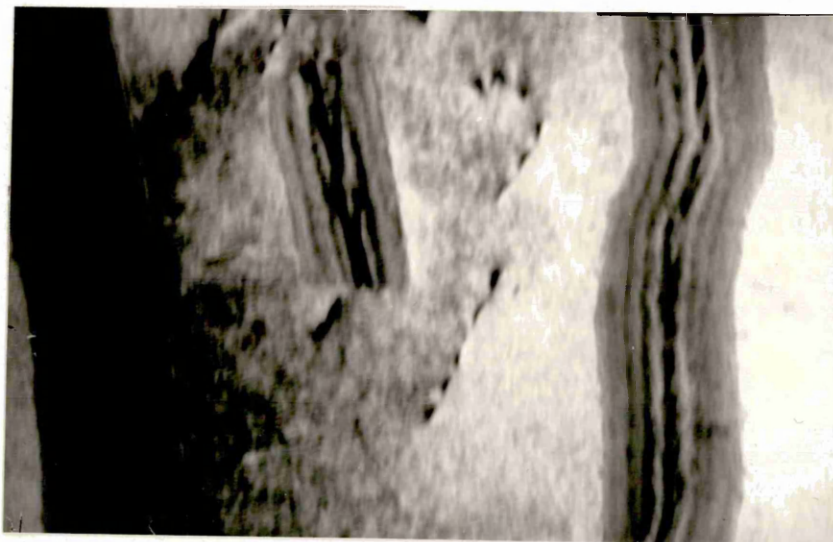
FIG 62;ALLOY 695 ISOTHERMALLY TRANSFORMED AT 650°C FOR 16 MIN. MAGNIFICATION : 100K.
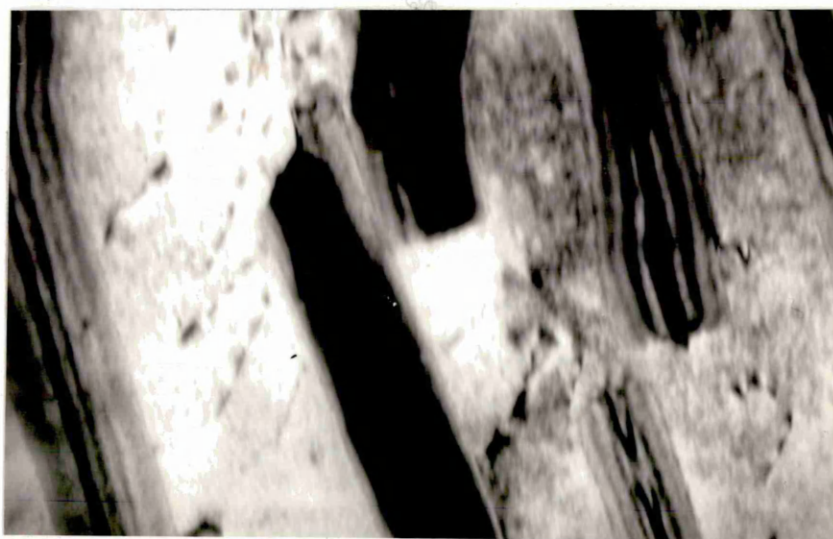
FIG 63; MECHANICAL PROPERTY DATA FOR HIGH CARBON VANADIUM STEELS.

Key :-

→ ALLOY626;UTS
→ ALLOY626;0.2%PS
→ ALLOY695;UTS
→ ALLOY695;0.2%PS

STRENGTH (MPa).

TRANSFORMATION TEMPERATURE (°C).

302
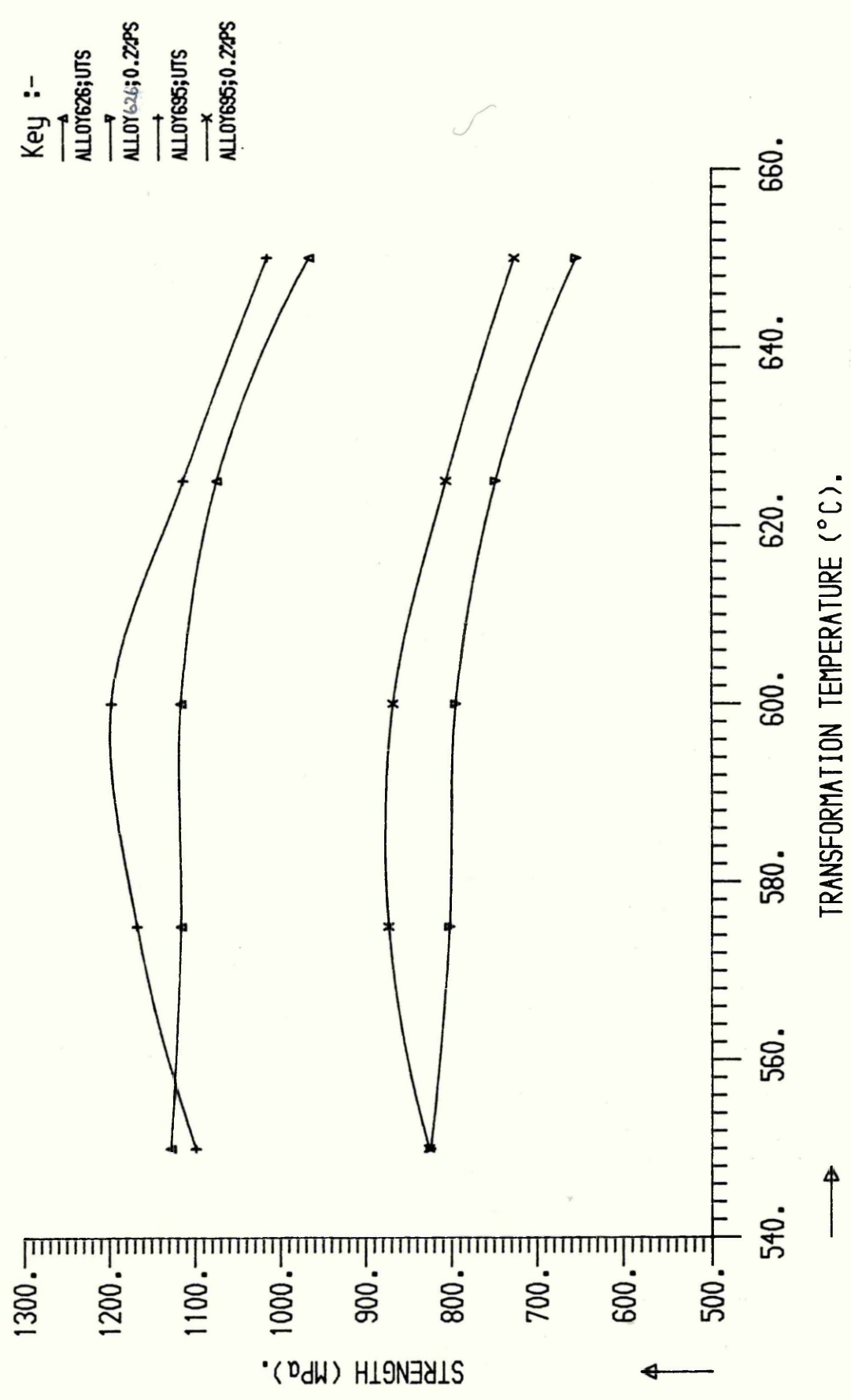
FIG 64;ELONGATION RESULTS FOR HIGH CARBON VANADIUM STEELS.
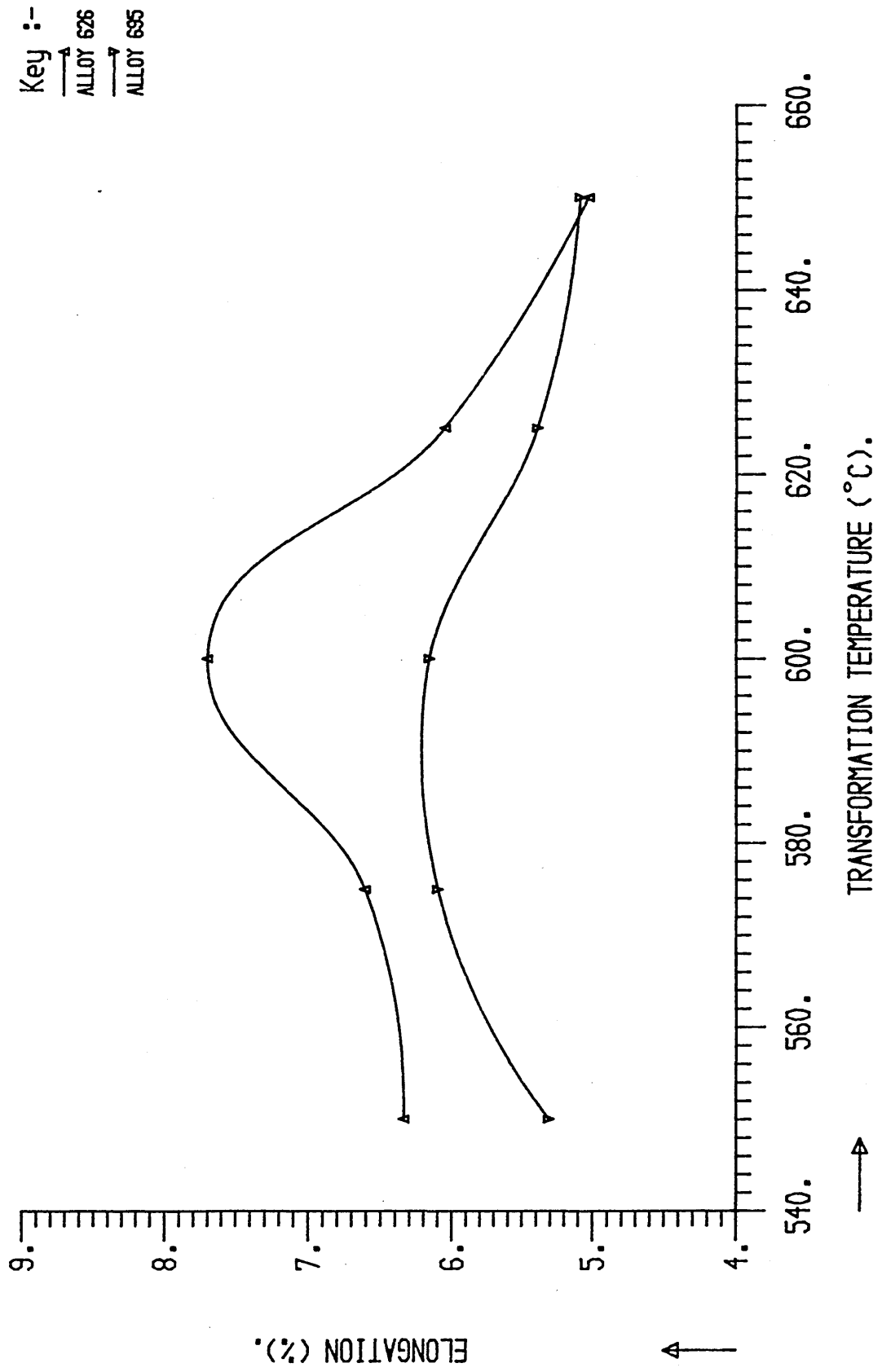
Key :-

ALLOY 629

ALLOY 695

TRANSFORMATION TEMPERATURE (°C).

ELONGATION (%).

303

FIG 65;CHARPY IMPACT DATA FOR HIGH CARBON VANADIUM STEEL 626.

Key :-
20°C.
100°C.
200°C.
250°C.

ENERGY ABSORBED (J).

TEST TEMPERATURE (°C).

304

FIG 66;CHARPY IMPACT DATA FOR HIGH CARBON VANADIUM STEEL 695.

Key :-
20°C.
100°C.
200°C.
250°C.

TEST TEMPERATURE (°C).

ENERGY ABSORBED (J).
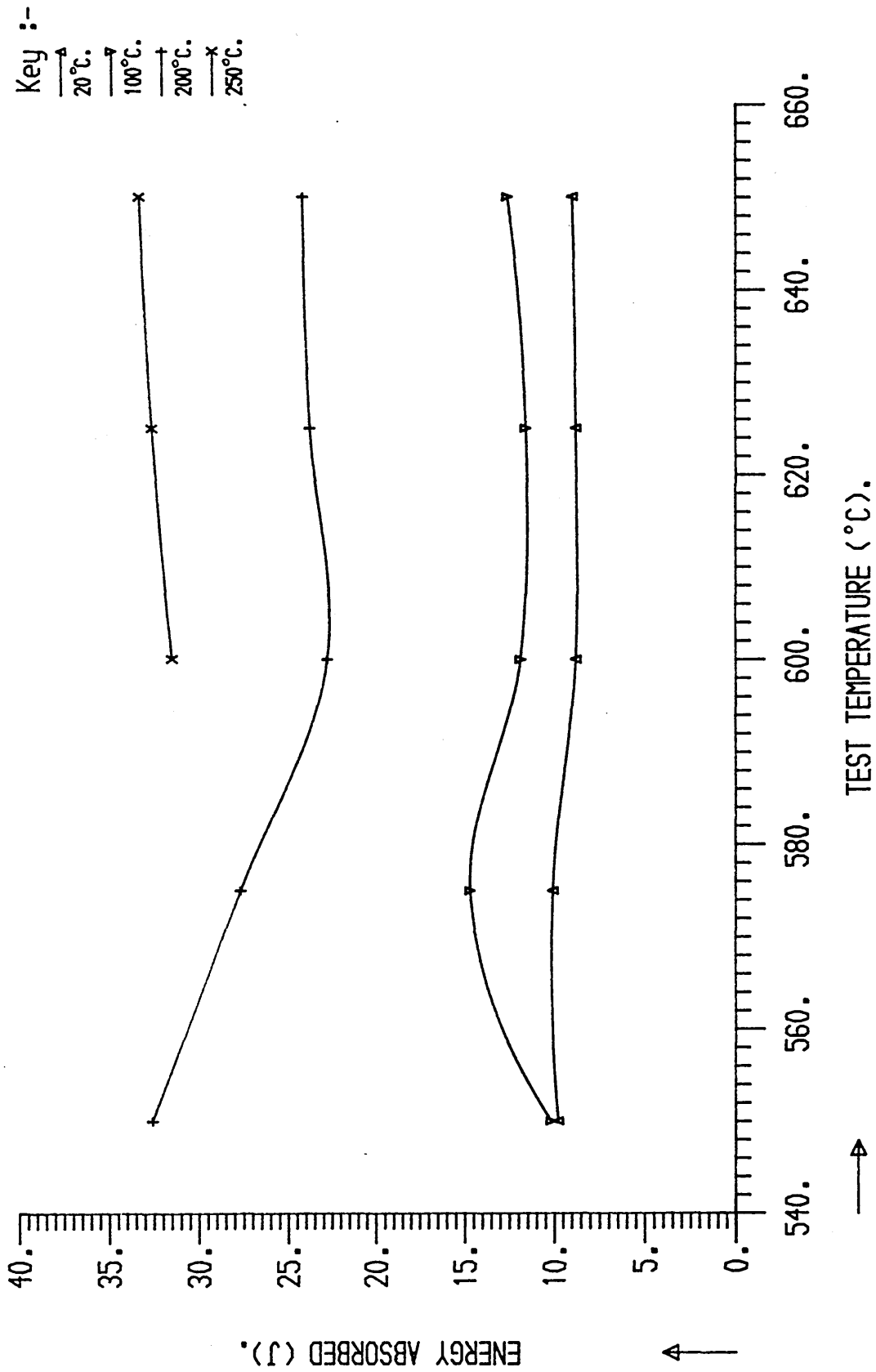
305

FIG 67; CHARPY IMPACT DATA FOR HIGH CARBON VANADIUM STEEL 626.

Key :-

△ I.T.T.550°C
▽ I.T.T.575°C
+ I.T.T.600°C
✕ I.T.T.625°C
□ I.T.T.650°C

TEST TEMPERATURE (°C).

ENERGY ABSORBED (J).
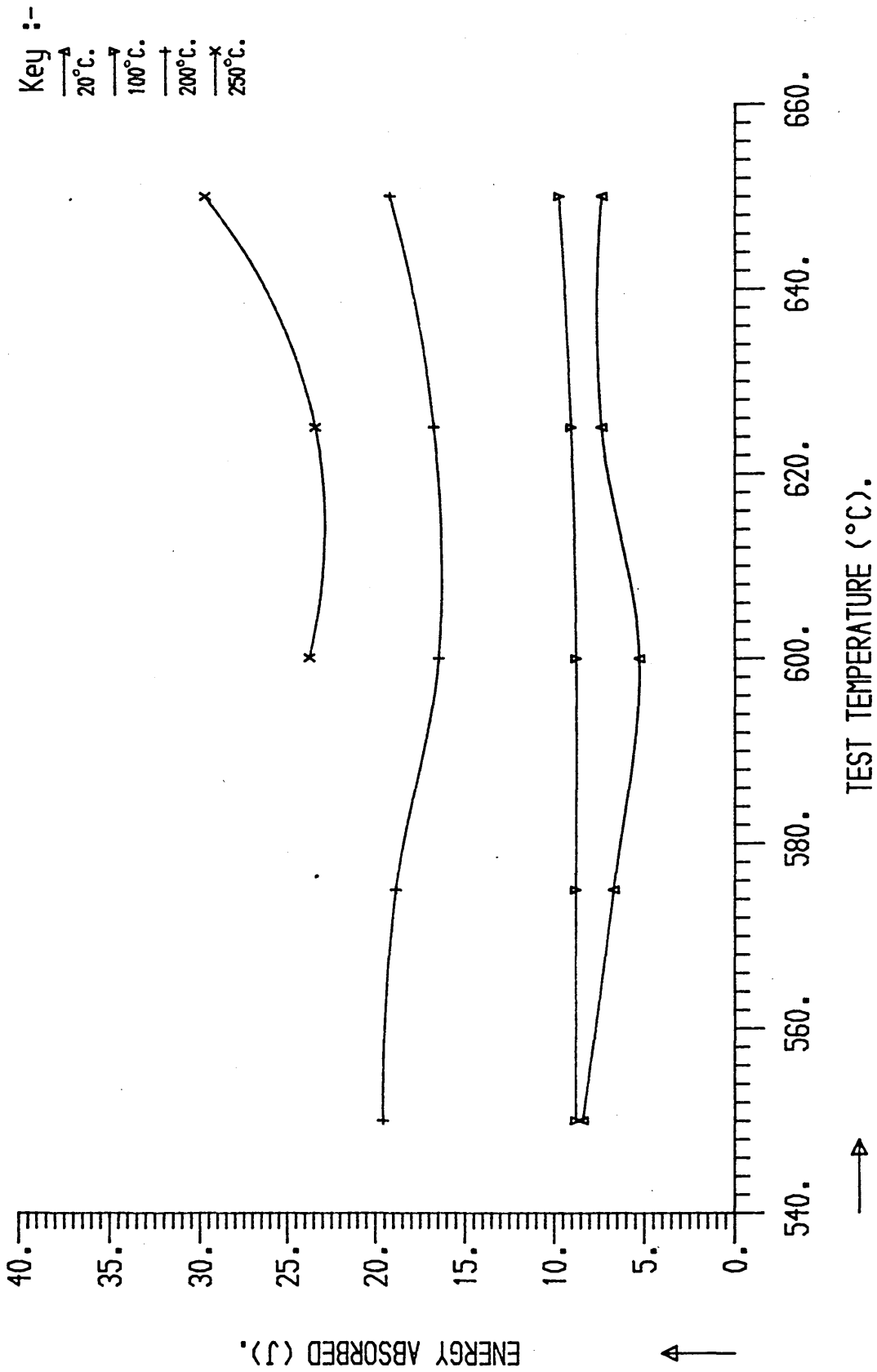
306

FIG 68;CHARPY IMPACT DATA FOR HIGH CARBON VANADIUM STEEL 695.

Key :-

I.T.T. 550°C.
I.T.T. 575°C.
I.T.T. 600°C.
I.T.T. 625°C.
I.T.T. 650°C

TEST TEMPERATURE (°C).

ENERGY ABSORBED (J),
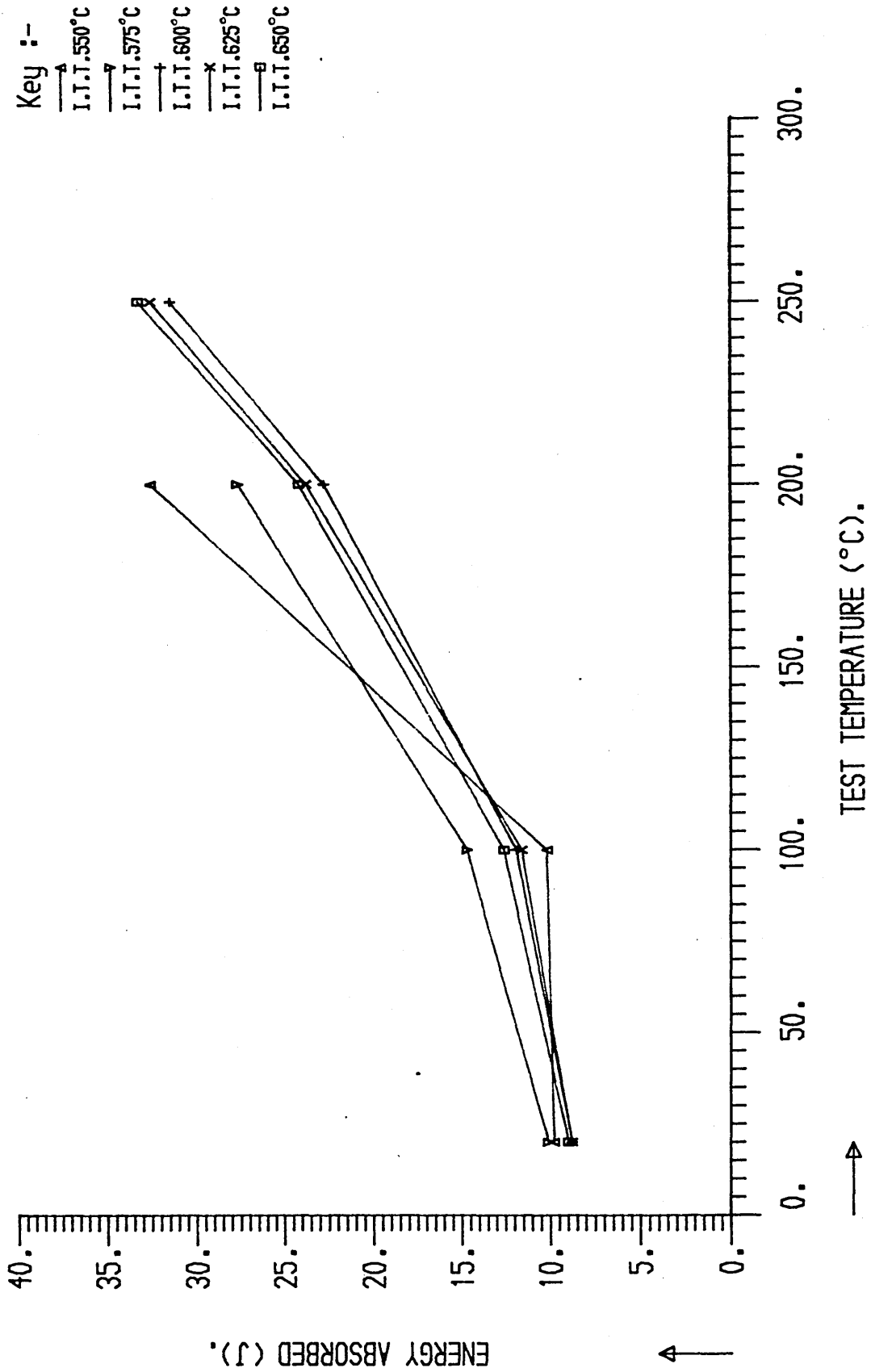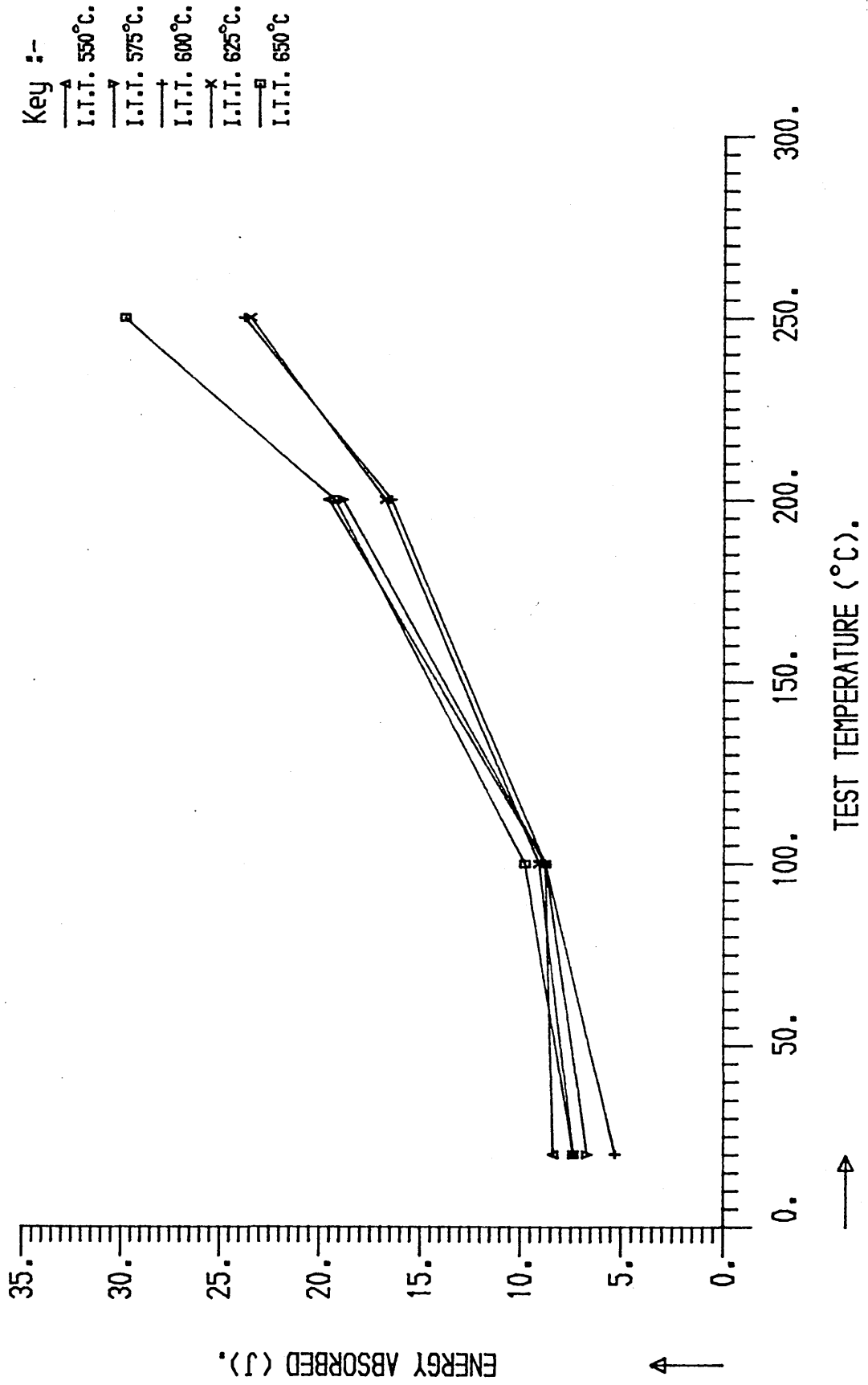
FIG 69; GRAIN COARSENING TEMPERATURE RELATIONSHIPS.

SOLUBILITY TEMPERAURE OF VC/VN.

GRAIN COARSENING TEMPERATURE.

CRITICAL RADIUS.

PARTICLE RADIUS DUE TO GROWTH.

UNDISSOLVED VC/VN PARTICLE RADIUS.

AUSTENITISING TEMPERATURE.

308
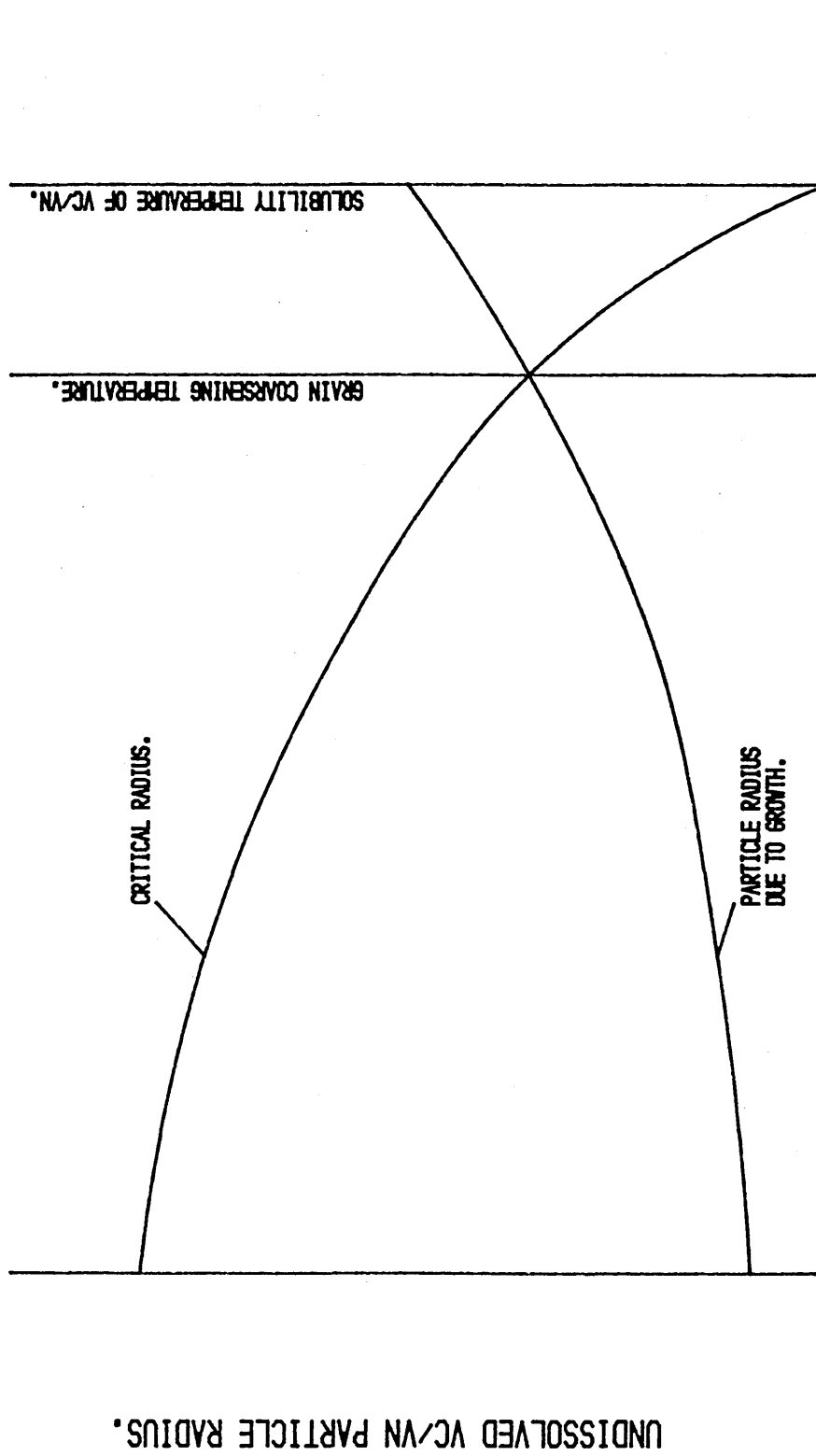
FIG 70;ALLOY 619 AT CALCULATED 50% MARTENSITE POSITION.
AUSTENITISED AT 950°C.
MAGNIFICATION : X400.

FIG 71;ALLOY 619 AT CALCULATED 50% MARTENSITE POSITION.
AUSTENITISED AT 950°C.
MAGNIFICATION : X1000.

FIG 72;ALLOY 624 AT CALCULATED 50% MARTENSITE POSITION.
AUSTENITISED AT 950°C.
MAGNIFICATION : X400.

FIG 73;ALLOY 624 AT CALCULATED 50% MARTENSITE POSITION.
AUSTENITISED AT 950°C.
MAGNIFICATION : X1000.

FIG 74;ALLOY 640 AT CALCULATED 50% MARTENSITE POSITION.
AUSTENITISED AT 950°C.
MAGNIFICATION : X400.

FIG 75;ALLOY 640 AT CALCULATED 50% MARTENSITE POSITION.
AUSTENITISED AT 950°C.
MAGNIFICATION : X1000.
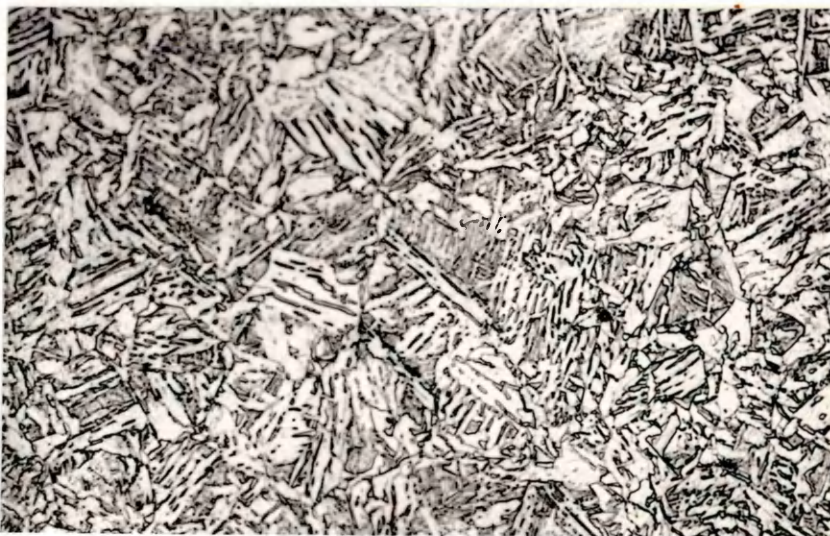
FIG 78;ALLOY 619 AT CALCULATED 50% MARTENSITE POSITION.
AUSTENITISED AT 1200°C.
MAGNIFICATION : X100.
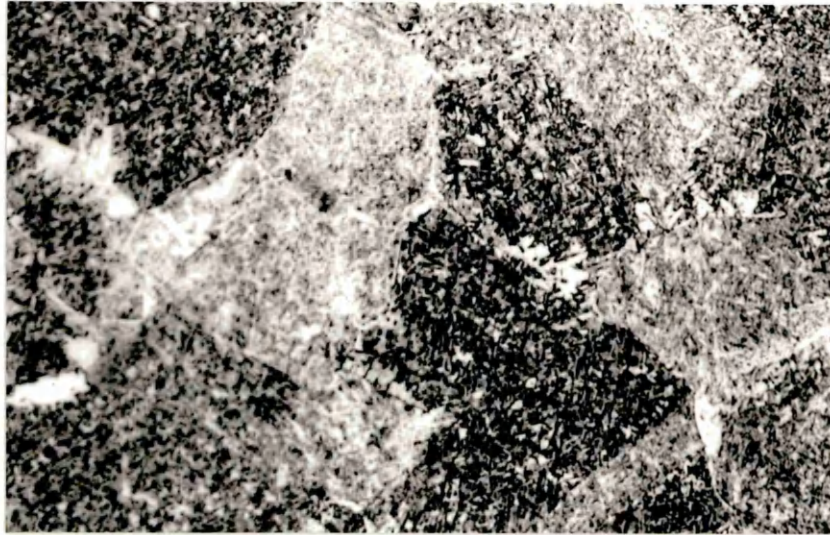
FIG 79;ALLOY 619 AT CALCULATED 50% MARTENSITE POSITION.
AUSTENITISED AT 1200°C.
MAGNIFICATION : X400.
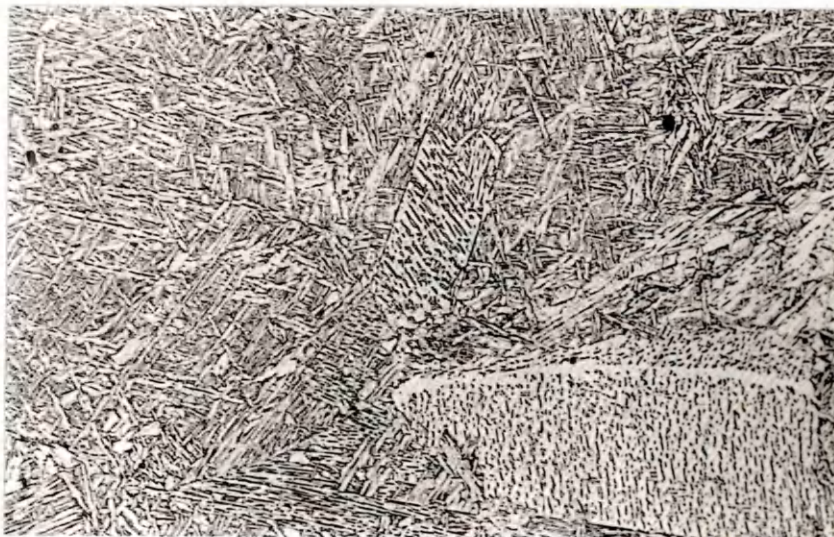
FIG 80;ALLOY 624 AT CALCULATED 50% MARTENSITE POSITION.
AUSTENITISED AT 1200°C.
MAGNIFICATION : X100.

FIG 81;ALLOY 624 AT CALCULATED 50% MARTENSITE POSITION.
AUSTENITISED AT 1200°C.
MAGNIFICATION : X400.

314

FIG 82;ALLOY 640 AT CALCULATED 50% MARTENSITE POSITION.
        AUSTENITISED AT 1200°C.
        MAGNIFICATION : X100.

FIG 83;ALLOY 640 AT CALCULATED 50% MARTENSITE POSITION.
        AUSTENITISED AT 1200°C.
        MAGNIFICATION : X400.

FIG 84;ALLOY 664 AT CALCULATED 50% MARTENSITE POSITION.
        AUSTENITISED AT 1200°C.
        MAGNIFICATION : X100.

FIG 85;ALLOY 664 AT CALCULATED 50% MARTENSITE POSITION.
        AUSTENITISED AT 1200°C.
        MAGNIFICATION : X400.
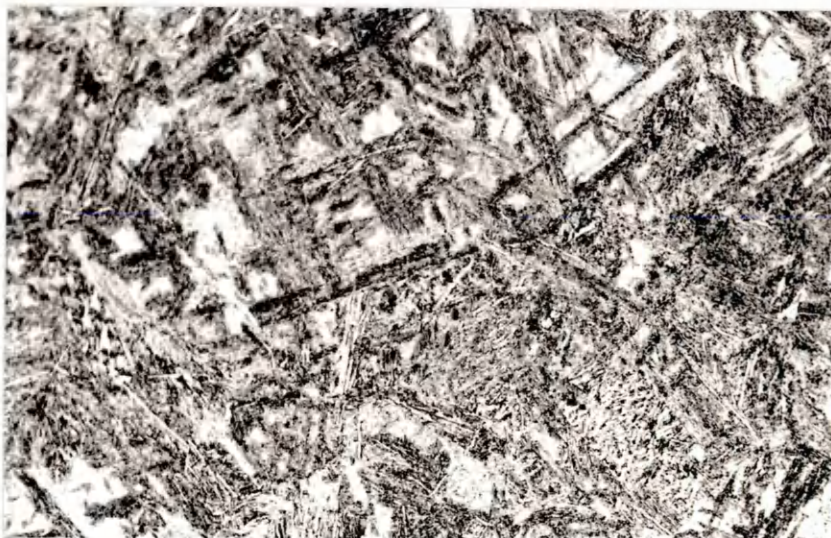
FIG 86; EFFECT OF ALLOYING ELEMENTS ON THE MULTIPLYING FACTOR AT 1200 °C.
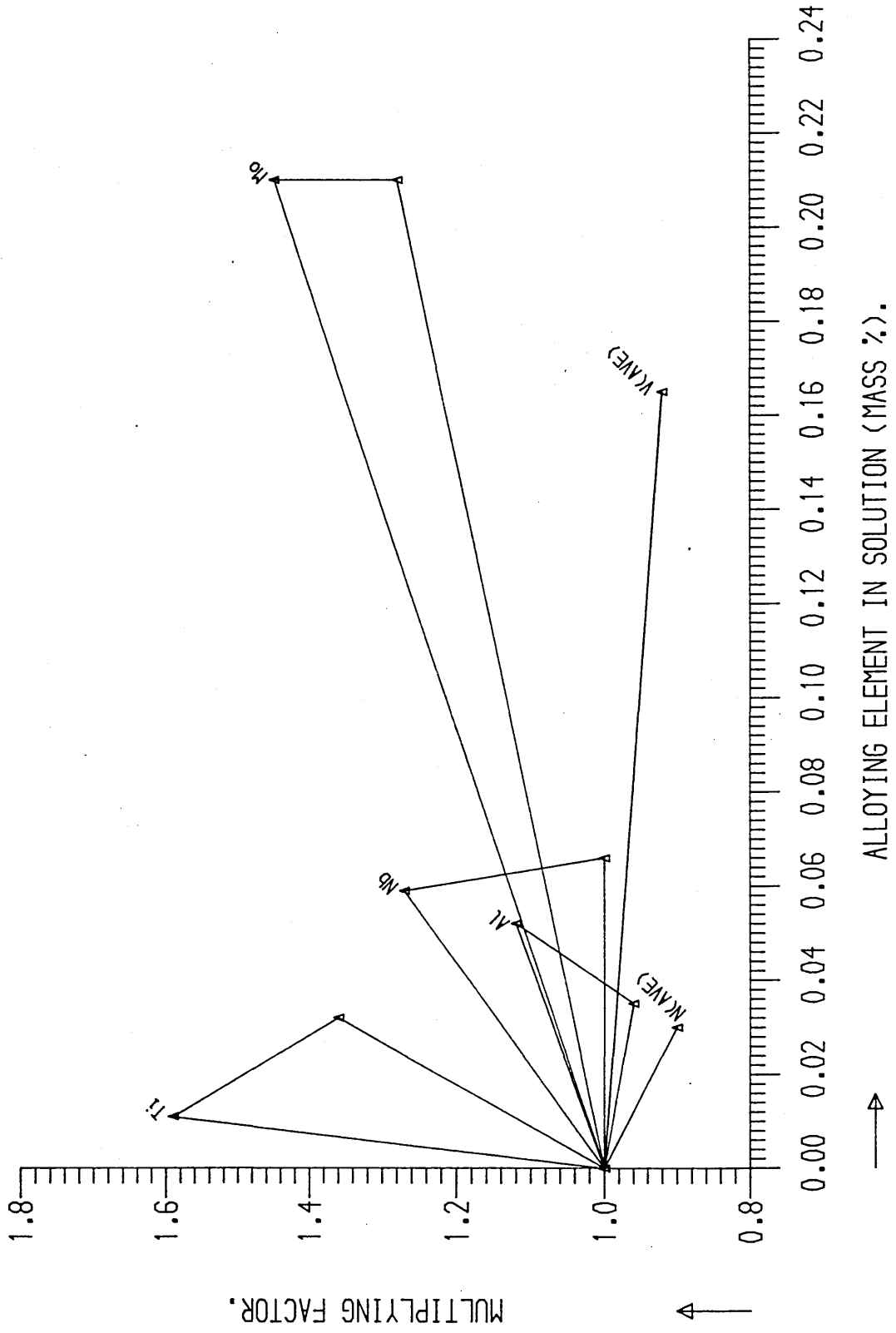
FIG 87;TENSILE PROPERTY DATA FOR HIGH CARBON VANADIUM STEELS.

Key :-

ALLOY626;UTS
ALLOY626;YIELD
ALLOY695;UTS
ALLOY695;YIELD
PC STEEL;UTS
PC STEEL;YIELD

STRENGTH (MPa).

TRANSFORMATION TEMPERATURE (°C).
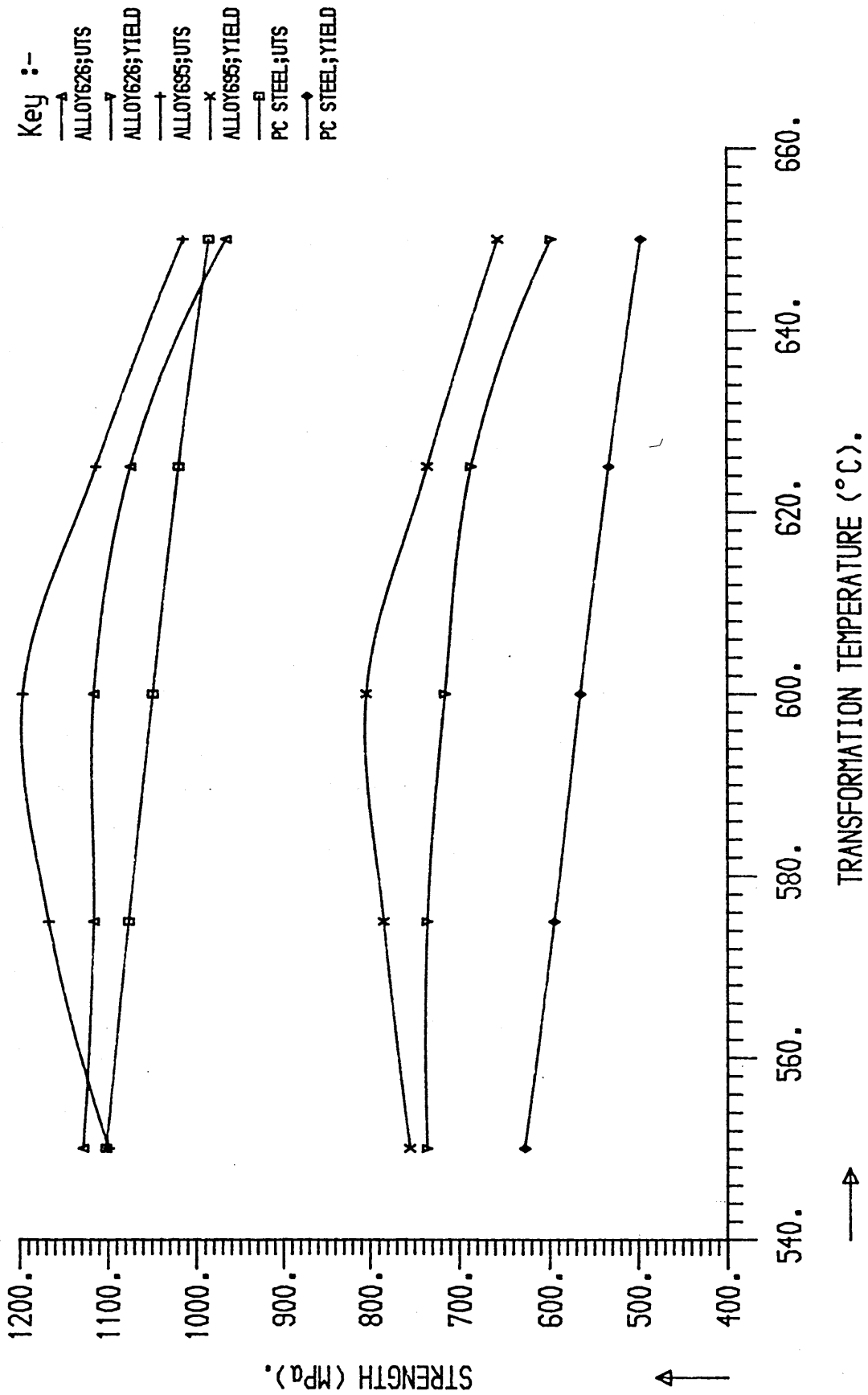
FIG 88; TEMPERATURE TO ACHIEVE SPECIFIED IMPACT ENERGY.

Key :-
ALLOY626;27J
ALLOY655;17J
PC STEEL;27J

TRANSFORMATION TEMPERATURE (°C).

CHARPY TEST TEMPERATURE (°C).

319
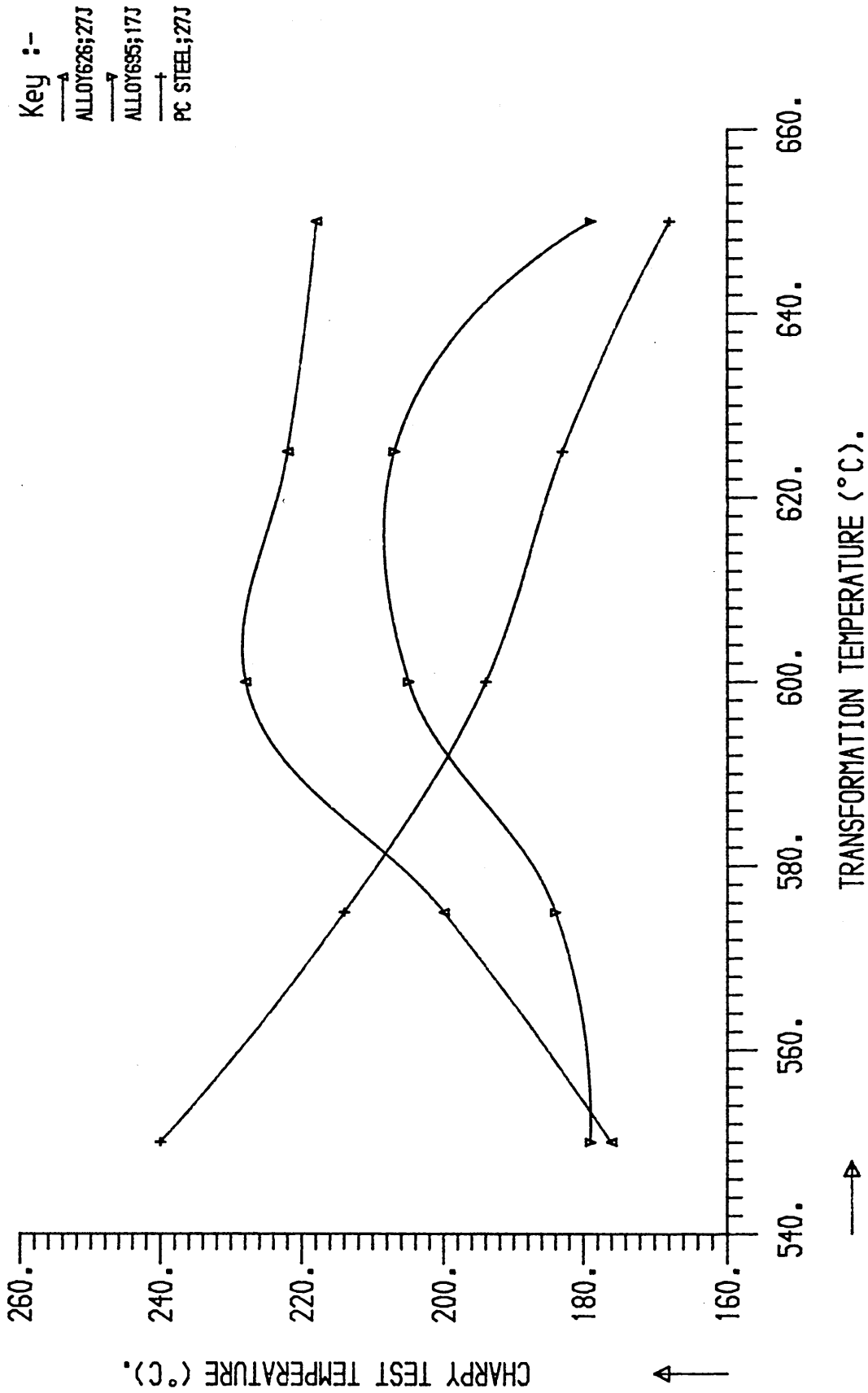
APPENDICES

APPENDIX A

Etching of Prior Austenite Grain Boundaries (48)

Prior austenite grain boundaries were electrolytically etched in a chromic/phosphoric acid solution, made up as follows:

10 grms of chromium trioxide is dissolved in distilled water and then 40 ml of phosphoric acid is added. The solution is then made up to 100 ml by the addition of distilled water.

A Stru ers Electropol system is used with the above electrolyte at a current density of 6 ma/mm .

APPENDIX B

All the work conducted by Eldis was on a 0.1%C
alloy, therefore it is possible to determine the
amount of microalloying element required to exceed
the alloy/carbon solubility limit at 1200°C.

(i)   vanadium

using $Log_{10}[V][C] = -\dfrac{9500}{T} + 6.72$ .... (8)

where T is in degrees Kelvin

% vanadium required is 18.65%

(ii)   titanium

using $Log_{10}[Ti][C] = -\dfrac{7000}{T} + 2.75$ .... (21)

% titanium required is 0.10%

(iii)   niobium

using $Log_{10}[Nb][C] = -\dfrac{7520}{T} + 3.11$ ... (22)

% niobium required is 0.10%

Consequently no reduction in hardenability due to
carbon removal should occur before 0.10% of
titanium, or niobium is added, and not before 18.65%
for vanadium. Therefore, the decrease in
hardenability above 0.05% alloy addition cannot be

caused by carbon removal as the alloy carbide.

Alternatively it can be calculated that the solubility temperature at which all the vanadium and carbon is taken into solution for the largest vanadium and carbon combination used by Eldis, i.e. 0.18%V, 0.1%C, using equation (8) above would be 850°C.